
Electronic Thesis and Dissertation Repository

4-16-2012 12:00 AM

On-Line Monitoring of Engine Health Through the Analysis of Contaminants in Engine Lubricant

Hamid R. Aghayan, *The University of Western Ontario*

Supervisor: Dr. Evgueni Bordatchev, *The University of Western Ontario*

Joint Supervisor: Dr. Jun Yang, *The University of Western Ontario*

A thesis submitted in partial fulfillment of the requirements for the Doctor of Philosophy degree in Mechanical and Materials Engineering

© Hamid R. Aghayan 2012

Follow this and additional works at: <https://ir.lib.uwo.ca/etd>



Part of the [Other Mechanical Engineering Commons](#)

Recommended Citation

Aghayan, Hamid R., "On-Line Monitoring of Engine Health Through the Analysis of Contaminants in Engine Lubricant" (2012). *Electronic Thesis and Dissertation Repository*. 528.

<https://ir.lib.uwo.ca/etd/528>

This Dissertation/Thesis is brought to you for free and open access by Scholarship@Western. It has been accepted for inclusion in Electronic Thesis and Dissertation Repository by an authorized administrator of Scholarship@Western. For more information, please contact wlsadmin@uwo.ca.

ON-LINE MONITORING OF ENGINE HEALTH THROUGH THE ANALYSIS OF CONTAMINANTS IN ENGINE LUBRICANT

(Spine title: On-line Monitoring of Engine Health through the Analysis of
Contaminants in Engine Lubricant)

Thesis format: Monograph

by

Hamid R. Aghayan

Graduate Program in Mechanical & Material Engineering

A thesis submitted in partial fulfillment
of the requirements for the degree of
Doctor of Philosophy

The School of Graduate and Postdoctoral Studies
The University of Western Ontario
London, Ontario, Canada

© Hamid R. Aghayan 2012

THE UNIVERSITY OF WESTERN ONTARIO
School of Graduate and Postdoctoral Studies

CERTIFICATE OF EXAMINATION

Joint Supervisors

Examiners

Dr. Evgueni Bordatchev

Dr. George K. Knopf

Dr. Jun Yang

Dr. Remus Tutunea-Fatan

Dr. Jesse Zhu

Dr. Qiyang Chen

The thesis by

Hamid Reza Aghayan

entitled:

**On-line Monitoring of Engine Health through the Analysis of
Contaminants in Engine Lubricant**

is accepted in partial fulfillment of the
requirements for the degree of
Doctor of Philosophy

Date

Chair of the Thesis Examination Board

Abstract

Monitoring automobile liquids, such as engine lubricants, has received increasing attention recently mainly due to environmental and safety legislation, cost saving measures, and customer demand.

Literature review in monitoring engine lubricant condition indicates systems approach, an intellectual discipline method to address complex problem, has never been used to monitor engine performance and health through the engine sub-systems such as lubricant system. The literature review also points toward deficiency in considering lubricant as a source of information for engine performance evaluation, and lack of understanding of engine lubricant as a medium with random properties.

Engine lubricant condition reflects the state of health of engine through its properties. Recognition and analysis of the correlation between engine lubricant system based on the lubricant properties and engine performance is crucial to provide insight into engine health.

The contribution of this research will be implementation of systems approach to monitor engine performance through engine lubricant using new methodologies of surface plasmon resonance, object shape based optical analysis and statistical optical analysis methodologies to monitor optical properties of lubricant with respect to aging process and contaminants in real time and on-line.

Degradation of engine lubricant causes variation in the optical properties of lubricant such as refractive index, absorption, statistical optical characteristics, shape parameters and *etc.* The purpose of using surface plasmon resonance (SPR) is to study the change in the reflectivity and incidence angle caused by variation in the refractive index and absorption of lubricant due to its degradation and presence of contaminants. Utilization of SPR measurement for characterization of engine lubricant will develop new knowledge which can be used for on-line condition monitoring of lubricant quality.

To investigate the variation in statistical optical characteristics of lubricant, this research also introduces two new methodologies. Statistical optic and object shape-based methodologies are based on the optical analysis of the distortion effect when an object image

is obtained through a thin random medium. In the object shape-based optical analysis, several parameters of an acquired object image are measured and compared. In the statistical optic analysis methodology, statistical auto and cross-characteristics are used for the analysis of combined object-lubricant images. Both proposed methodologies utilize the comparison of measured and calculated parameters for fresh and contaminated lubricants.

Proposed methodologies are verified experimentally showing ability to distinguish lubricant with different contamination individually and in a combined form. Capabilities of the proposed methodologies are extended to establish the linkage between accumulated travelled distance and the change in the optical statistical properties of the lubricant. Also, on board analysis to detect the presence of coolant, gasoline and water (1%-5%) are performed.

Keywords

Systems approach, Engine lubricant, Random medium, Lubricant properties, Optical properties, SPR, Object shape based analysis, Statistical optics analysis, Contaminants, Real time measurement, On board monitoring

Acknowledgments

First of all, I would like to express my deepest gratitude to my supervisors Dr. Evgueni Bordatchev and Dr. Jun Yang for being my guide and mentor throughout this project. Always open to discussions, supportive, and helpful in finding the right track.

I would like to thank NRC technical officers Hugo Reshef, Marco Zeman, Mike Meinert, for their continued technical support in this work. Also, I would like acknowledge NRC management support during this research work.

In addition, thanks to all my colleagues at the Department of Mechanical & Materials engineering, for making it an enjoyable place to be.

Last, but not least, thanks to my family and nearest friends for their support, patience, and friendship.

London, February 2012

Hamid R. Aghayan

Table of Contents

CERTIFICATE OF EXAMINATION	ii
Abstract.....	iii
Acknowledgments.....	v
Table of Contents	vi
List of Tables	xi
List of Figures	xii
List of Appendices	xix
Chapter 1	1
1 New Developments in Sensor Technologies and Measurement Methodologies for Engine Lubricant Condition Monitoring.....	1
1.1 Introduction.....	2
1.2 Lubrication ingredients and degradation	4
1.3 Sensing parameters and sensing methodologies for engine lubricant condition monitoring.....	6
1.3.1 Sensing of physical-mechanical properties.....	7
1.3.2 Sensing of electrical properties (conductivity, permittivity, magnetic susceptibility).....	15
1.3.3 Sensing of chemical properties	21
1.3.4 Sensing of optical properties (color, transparency, refractive index, absorbance)	29
1.3.5 Sensing contamination	32
1.4 New developments in sensors and sensing methodologies for engine lubricant conditions monitoring	46
1.5 Remaining challenges in the development of sensors and sensing methodologies for engine lubricant condition monitoring	46
1.6 Research objectives, scope and methodology.....	47
1.6.1 Research objective	49

1.6.2	Research scope.....	49
1.6.3	Research methodology.....	50
1.7	Summary and conclusions	54
Chapter 2.....		56
2	Systems Approach for Monitoring Engine Performance	56
2.1	Systems approach definition.....	56
2.2	Systems representation of internal combustion engine.....	57
2.3	Monitoring engine health through engine lubricant using systems approach.....	60
2.4	Analysis of engine lubricating oil	61
2.5	Summary	66
Chapter 3.....		68
3	Experimental Characterization of Contaminants in Engine Lubricants using Surface Plasmon Resonance Sensing.....	68
3.1	Application of SPR sensors for analysis of liquids.....	68
3.2	Surface plasmon resonance sensors	70
3.3	Experimental set-up and methodology	74
3.4	Results and discussion	77
3.4.1	SPR characterization of gasoline contamination	78
3.4.2	SPR characterization of coolant contamination.....	80
3.4.3	SPR characterization of water contamination.....	82
3.4.4	SPR-based Bayesian classification and monitoring of lubricant condition	84
3.5	Summary and conclusions	88
Chapter 4.....		91
4	Generalized Approach for Optical Analysis of Contaminated Engine Lubricant	91
4.1	Generalized approach for optical analysis of contaminated lubricants	91
4.2	Functional design of opto-microfluidic sensing system	94

4.3 Summary	98
Chapter 5	100
5 Object Shape Based Optical Analysis and System for Monitoring Contaminated Engine Lubricant	100
5.1 Object shape-based optical analysis methodology	100
5.2 Opto-microfluidic sensing system, experimental set-up and measurement methodology	101
5.3 Functional design of opto-microfluidic system	103
5.4 Experimental set-up	105
5.5 Preliminary image analysis and experimental methodology	106
5.6 Experimental verification.....	111
5.6.1 Analysis of coolant, gasoline and water contamination.....	112
5.6.2 Analysis of combined coolant and gasoline.....	120
5.6.3 Road test engine lubricant analysis.....	124
5.7 Summary and conclusion	128
Chapter 6	132
6 Statistical Optical Analysis Methodology for Monitoring Contaminated Engine Lubricant	132
6.1 Statistical optics analysis methodology	132
6.2 Opto-microfluidic sensing system, experimental set-up and measurement methodology	135
6.2.1 Functional design of opto-micro sensing system.....	137
6.2.2 Preliminary image analysis and experimental methodology	142
6.3 Experimental verification.....	146
6.3.1 Statistical optical analysis of coolant, gasoline, and water contaminated lubricant	146
6.3.2 Analysis of combined coolant and gasoline contamination.....	162
6.3.3 Statistical optics analysis of road test	170

6.4 Summary and conclusion	177
Chapter 7	182
7 On-line Monitoring Engine Lubricant Condition	182
7.1 On-line monitoring contaminated engine lubricant	182
7.2 Experimental set up.....	185
7.3 Testing procedure.....	186
7.4 Statistical optical analysis and system for on-line monitoring contaminated engine lubricant	188
7.4.1 Statistical optical analysis of coolant contaminated engine lubricant	188
7.4.2 Statistical optical analysis of gasoline contaminated engine lubricant ...	195
7.4.3 Statistical optical analysis of water contaminated engine lubricant	201
7.5 Object shape based optical analysis for on-line monitoring contaminated engine lubricant	208
7.5.1 Object shape based optical analysis of coolant contaminated engine lubricant	209
7.5.2 Object shape based optical analysis of gasoline contaminated engine lubricant	213
7.5.3 Object shape based optical analysis of water contaminated engine lubricant	217
7.6 Discussion.....	221
7.7 Summary and conclusion	223
Chapter 8.....	227
8 Conclusion	227
8.1 Summary of results	227
8.2 Thesis contribution.....	229
8.3 Suggestions for future work.....	230
Publication	231
References.....	232

Appendices.....	240
Curriculum vitae	254

List of Tables

Table 1 Sensing parameters vs. sensors and sensing methodology	45
Table 2 On-line on board engine lubricant monitoring procedure	187

List of Figures

Figure 1.1 Engine performance – lubricant condition functional interdependence.....	51
Figure 1.2 Lubricant condition as a source of information on engine performance.....	52
Figure 2.1 Schematic presentation of internal combustion engine sub-systems and their interrelationships.....	58
Figure 2.2 Lubricant condition as a source of information on engine performance.....	61
Figure 2.3 Basic optical system considered for optical analysis	64
Figure 2.4 Schematic presentation of systems approach to monitor engine performance.....	66
Figure 3.1 Kretschmann–Raether configuration of an SPR sensor	71
Figure 3.2 Experimental set up of SPR measurement	76
Figure 3.3 Schematics set up of SPR measurement.....	77
Figure 3.4 SPR measurements and characterization of gasoline contamination	79
Figure 3.5 SPR measurements and characterization of coolant contamination.....	81
Figure 3.6 SPR measurements and characterization of water contamination.....	83
Figure 3.7 SPR measurements and Bayesian classification of informational parameters θ_{SPR} and R_{min} with respect to the engine lubricant condition.....	87
Figure 4.1 Generalized schematic of optical analysis methodologies	94
Figure 4.2 Functional design of the opto-microfluidic sensing (measuring) system.....	96
Figure 4.3 Original object image with known periodical structure and its characteristics....	97
Figure 5.1 Generalized methodology for experimental optical analysis of contaminated lubricant	103

Figure 5.2 Functional design of the opto-microfluidic sensing (measuring) system.....	105
Figure 5.3 Experimental set-up and design of a microfluidic chip.....	106
Figure 5.4 Schematic of preliminary image analysis to obtain object's color cross-section	108
Figure 5.5 Typical image and color cross-sections and object shape parameters	109
Figure 5.6 Object shape-based optical sensing analysis methodology	110
Figure 5.7 Evolution of color cross-sections (OOI and DOI) with respect to coolant, gasoline, and water concentration.....	113
Figure 5.8 Evaluation of relative lubricant-object color index ΔC with respect to coolant, gasoline and water concentration.....	115
Figure 5.9 Evaluation of the non-uniformity coefficient of object width ΔW with respect to coolant, gasoline, and water concentration.....	117
Figure 5.10 $\{\Delta C, \Delta W\}$ information space wrt coolant, gasoline and water concentration .	119
Figure 5.11 Schematic presentation of coolant-gasoline combined contaminated engine lubricant proportional mixture	120
Figure 5.12 OOI and DOI color cross-section graph of coolant-gasoline contaminated engine lubricant	121
Figure 5.13 Evolution of coolant-gasoline combined contaminant in $\{\Delta C, \Delta W\}$ informational space.....	122
Figure 5.14 $\{\Delta C, \Delta W\}$ informational space of $C_{0\%-5\%}G_{0\%}$, $C_{0\%-5\%}G_{1\%}$, $C_{0\%-5\%}G_{2\%}$, $C_{0\%-5\%}G_{3\%}$, $C_{0\%-5\%}G_{4\%}$, $C_{0\%-5\%}G_{5\%}$	124
Figure 5.15 Color cross-section graph of road test engine lubricant analysis	125
Figure 5.16 Road test engine lubricant ΔC at different travelled distance	126
Figure 5.17 Road test engine lubricant ΔW wrt travelled distance	127

Figure 5.18 $\{\Delta C, \Delta W\}$ information space of road test engine lubricant	128
Figure 6.1 Generalized methodology for experimental optical analysis of contaminated lubricant	136
Figure 6.2 Functional design of the opto-microfluidic sensing (measuring) system.....	138
Figure 6.3 Original object image with known periodical structure and its characteristics..	140
Figure 6.4 Schematic of preliminary image analysis to obtain object's color cross-section	143
Figure 6.5 Generalized schematic of the statistical optical analysis methodology.....	145
Figure 6.6 Color cross-sections of the coolant, gasoline, and water contaminated lubricant	148
Figure 6.7 Auto correlation function of coolant, gasoline and water contaminated engine lubricant	150
Figure 6.8 Auto spectral function of coolant, gasoline, and water contaminated engine lubricant	152
Figure 6.9 Evaluation of change in W_{ASF} graph with respect to contaminants percentage ..	153
Figure 6.10 Evolution optical transfer function with respect to coolant, gasoline and water concentration.....	154
Figure 6.11 $\{C(T/2), \Delta H_{eff}\}$ informational space of coolant, gasoline, and water contaminated engine lubricant	157
Figure 6.12 Evaluation of $\{\Delta H_{eff}, W_{ASF}\}$ for coolant, gasoline and water	159
Figure 6.13 Evaluation of $\{C(T/2), W_{ASF}\}$ information space wrt coolant, gasoline and water concentration.....	161
Figure 6.14 Color cross-section graph of coolant-gasoline contaminated engine lubricant	163

Figure 6.15 Correlation function graph of coolant-gasoline contaminated engine lubricant	164
Figure 6.16 Spectrum density function plot of coolant-gasoline contaminated engine lubricant	165
Figure 6.17. Optical transfer function evaluation of coolant-gasoline contaminated engine lubricant	166
Figure 6.18 $\{C(T/2), \Delta H_{eff}\}$ information space of coolant-gasoline combined contaminated engine lubricant.....	167
Figure 6.19 2-D information apace $\{C(T/2), \Delta H_{eff}\}$ values for coolant-gasoline concentration (0%-5%).....	168
Figure 6.20 $\{\Delta H_{eff}, W_{ASF}\}$ for coolant-gasoline combined contaminated engine lubricant .	169
Figure 6.21 $\{C(T/2), W_{ASF}\}$ for coolant-gasoline combined contaminated engine lubricant	170
Figure 6.22 Color cross-section graph of Ford Taurus road test analysis	171
Figure 6.23. Auto correlation of road test analysis.....	172
Figure 6.24 Spectrum density function graph of road test analysis.....	173
Figure 6.25 Optical transfer function of road test analysis.....	173
Figure 6.26 $\{C(T/2), \Delta H_{eff}\}$ information space wrt accumulated travelled distance.....	175
Figure 6.27 $\{C(T/2), W_{AFS}\}$ of road test analysis	176
Figure 6.28 $\{W_{AFS}, \Delta H_{eff}\}$ information space wrt accumulated travelled distance	177
Figure 7.1 Color cross section graph of coolant contaminated engine lubricant.....	189

Figure 7.2 Evaluation of auto-correlation function of coolant contaminated engine lubricant with respect to coolant concentration	190
Figure 7.3 Evaluation of spectrum density function of coolant contaminated engine lubricant	191
Figure 7.4 Evaluation of optical transfer function of coolant contaminated engine lubricant	192
Figure 7.5 Evolution of coolant contaminant in $\{C(T/2), \Delta H_{eff}\}$ information space	193
Figure 7.6 Evolution of coolant contaminant in $\{W_{ASF}, \Delta H_{eff}\}$ information space.....	194
Figure 7.7 Evolution of coolant contaminant in $\{W_{ASF}, C(T/2)\}$ information space	195
Figure 7.8 Evolution of color-cross-sections (OOI and DOI) wrt gasoline concentration..	196
Figure 7.9 Evolution of auto-correlation function wrt gasoline concentration.....	197
Figure 7.10 Evolution of spectrum density function wrt gasoline concentration.....	197
Figure 7.11 Evolution optical transfer function wrt gasoline concentration	198
Figure 7.12 Evolution of gasoline contaminant in $\{C(T/2), \Delta H_{eff}\}$ information space	199
Figure 7.13 Evolution of gasoline contaminant in $\{W_{ASF}, \Delta H_{eff}\}$ information space.....	200
Figure 7.14 Evolution of gasoline contaminant in $\{W_{ASF}, \Delta H_{eff}\}$ information space.....	201
Figure 7.15 Evolution of color-cross-sections (OOI and DOI) with respect to water concentration.....	202
Figure 7.16 Auto-correlation function graph of water contaminated engine lubricant	203
Figure 7.17 Evolution of water contamination on spectrum density function.....	203
Figure 7.18 Evolution of water concentration on optical transfer function.....	205

Figure 7.19 Evolution of water contamination in $\{C(T/2), \Delta H_{eff}\}$ information space	206
Figure 7.20 Evolution of water concentration on the $\{\Delta H_{eff}, W_{ASF}\}$ in information space ..	207
Figure 7.21 Evolution of water contaminant in $\{C(T/2), W_{ASF}\}$ information space	208
Figure 7.22 Color cross sections (OOI and DOI) of coolant contaminated engine lubricant	210
Figure 7.23 Evaluation of relative lubricant-object color index ΔC with respect to coolant concentration.....	211
Figure 7.24 Evaluation of relative lubricant-object color index ΔW with respect to coolant concentration.....	212
Figure 7.25 Evolution of coolant contamination in $\{\Delta C, \Delta W\}$ information space.....	213
Figure 7.26 Color cross sections (OOI and DOI) of gasoline contaminated engine lubricant	214
Figure 7.27 Evaluation of relative lubricant-object color index ΔC with respect to gasoline concentration.....	215
Figure 7.28 Evaluation of non-uniformity coefficient of object width ΔW wrt gasoline concentration.....	216
Figure 7.29 Evolution of gasoline concentration in $\{\Delta C, \Delta W\}$ information space	217
Figure 7.30. Evaluation of color cross section of fresh and water contaminated engine lubricant	218
Figure 7.31. Evaluation of relative lubricant-object color index ΔC with respect to water concentration.....	219
Figure 7.32 Evaluation of non-uniformity coefficient of object width ΔW wrt water concentration.....	220

Figure 7.33 Evolution of water concentration in $\{\Delta C, \Delta W\}$ information space..... 220

List of Appendices

Appendix A: RGB gray scale MATLAB programming.....	241
Appendix B: Statistical optics analysis MATLAB programming	242
Appendix C: Object shape based optical analysis MATLAB programming.....	246

Chapter 1

1 New Developments in Sensor Technologies and Measurement Methodologies for Engine Lubricant Condition Monitoring

An internal combustion engine consists of several systems, such as intake and exhaust, fuel injection, ignition, engine cooling, engine lubricant, and engine control system. Each system's function affects the engine performance. The most important factors that can reduce the performance and life expectancy of the engine are related to the friction and wear which are controlled by the engine lubricant system. That's why monitoring engine lubricant condition has received increasing attention in the recent years. The experimental and theoretical research results obtained in the past decades and progressed in recent years by the present author and by others are reviewed. The goal of recent developments in lubricant sensors has shifted from "quantity" to "quality" and is focused mainly on condition monitoring through direct and indirect measurements of physical-mechanical, chemical, optical, electrical and other properties of engine lubricants. Sensors for measurement of physical-mechanical and electrical properties of engine lubricants, e.g., viscosity and permittivity, are very well developed and utilized acoustic wave-based and capacitance-based sensing methodologies to monitor dynamic viscosity, mass density and soot content. Since most engine lubricant decomposition products are acidic, measuring total acid number (TAN) or total base number (TBN) is a key index to monitoring engine lubricant condition. Typical sensing methodology for measurement of TAN and TBN is based on measuring electric current conducted through lubricant between gold-plated parallel electrodes. Capacitive sensors with temperature compensation can be also used to measure contaminants in engine lubricants. Several optical methods, such as, absorption measurement, near-UV absorption, scattering, interferometry, and fluorescence measurement were proposed to measure soot, chemical degradation, presence of solid particles, water contamination and coolant, respectively. With rapid developments in microfabrication of micro-opto-electro-mechanical systems, sensors for lubricant condition became multi-functional and therefore more complex. For example, multiwall carbon nanotubes were used to monitor engine lubricant degradation.

This chapter provides a very useful material for the engineers who are engaged in the design and also identified and discussed the future trends in this area. Analysis uncovers the lack of a systems approach for understanding of interrelation between lubricant condition and engine performance and proposes considering lubricants as a source of information for engine performance evaluation.

1.1 Introduction

Automotive liquids, such as, engine lubricant, coolant, fuel, transmission fluid, brake and battery liquids have been always essential and critical components of any vehicle. In particular, automotive engine lubricant as a complex combination of base lubricant and chemical additives plays a critical role in the engine performance providing lubrication between the moving parts and reducing friction and wear, transferring heat and energy, preventing corrosion, and cleaning engine internal compartments. Any degradation in the lubricant's properties due to introduction of contaminants, depletion of additives and breakdown of hydrocarbon chains caused by engine operation directly influences engine performance, efficiency, maintenance, and life expectancy.

Conventional maintenance routine consists of lubricant level monitoring and frequent, mileage-based lubricant change. This "quantity-based" approach is not sufficient anymore because nowadays demands by customers and government regulations for more efficient cars and engines instruct the ability to monitor lubricant condition on-line and the operator capability to replace the used lubricant at the optimum schedule or when unexpected high degradation rate is detected. Lubricant condition sensors become an essential component together with other automotive sensors and sensing systems to improve safety, environmental compliance, communications, and entertainment of modern vehicles [76, 39, 40].

Increasing lubricant drainage intervals and monitoring lubricant level were the main goals of initially developed engine lubricant sensors. New developments in microfabrication technologies, micro-mechatronics, and micro-opto-electro-mechanical systems are opening up completely new possibilities for development of intelligent, multi-functional, integrated sensing systems and technologies with enhanced

functionality, e.g. on-line measurement and instantaneous analysis and control. Developments in novel lubricant sensors has shifted from “quantity-based” to “quality-based” approach focusing mainly on lubricant condition monitoring through direct and indirect measurements of physical-mechanical, chemical, optical, electrical and other properties of engine lubricant.

Smolenski and Schwartz [104] have made the first attempt to classify lubricant analysis techniques and interpret changes in lubricant condition with respect to the source of contaminations. The results were summarized as following: lubricant thickening occurs due to the presence of insoluble materials (pentane and toluene), wear metallic products, and ethylene glycol (coolant) resulting in changing viscosity, total acid number (TAN), and total base number (TBN), using infrared (IR) spectroscopy for semi-quantitative information on species concentrations and using differential scanning calorimetry (DSC) to measure the oxidation induction time of an engine lubricant; lubricant thinning occurs due to fuel contamination and can be estimated through molecular weight distribution; wear of engine components can be estimated through presence of metal contaminants, insoluble materials, water, and glycol and by measuring viscosity, TAN, and TBN; presence of metallic deposits causing changes in TAN, TBN, and viscosity, and can be measured by IR spectroscopy; presence of corrosion of engine components is resulting in changes of TAN, TBN, and of metals, water, and glycol concentrations presence of low temperature sludge can be recognized through concentration of water, coagulated pentane insoluble materials, and glycol in lubricant.

In addition to primary analysis of viscosity, TAN, TBN, and contaminants as lubricant condition properties, main directions for development of lubricant analysis methodologies (e.g. specific gravity, density, Brookfield viscosity, pour point, flash point, distillation characteristics, sulfated ash, chlorine, sulfur, nitrogen, nickel, silver, other metals, and ferrographic analysis) and sensors (e.g. to measure conductivity, impedance, or dielectric properties, and to measure optical properties such as refractive index, visible light absorption) were identified.

Another very important statement was made by Smolenski and Schwartz [77] relating lubricant analysis to engine damage or impaired performance. It was shown that analysis of engine lubricant can provide useful information regarding condition of the lubricant and engine, and it can possibly detect the potential problems or failures and their causes.

This chapter attempts to analyze the development in sensor technologies and in sensing and signal processing methodologies, mainly during the past decade, and their merits and drawbacks have been investigated to identify the future trends and areas that need more investigations with regard to engine lubricant condition monitoring. Five main classes of lubricant properties namely physical-mechanical, electro-magnetic, chemical, optical and presence of contaminants are identified as being used as sensing parameters. For each class of sensing parameters, sensing methodologies are reviewed, and their applicability is analyzed. Finally, discussion and future trends in engine lubricant condition monitoring are presented.

1.2 Lubrication ingredients and degradation

Engine lubricant is formed from base oil and chemical additives. Depends on the application, lubricants are formulated differently; however the main characteristics of lubricants come from the base oil. Base oil mainly is consisted of hydrocarbons chains. Fresh base engine oils are nonpolar and provide zero conductivity. The base oils can be mineral or synthetic. The mineral base oils are distilled from crude oil while the synthetic oils are made in the lab. The synthetics based oils provide the advantage of lower oxidation rate, better lubricity, better thermal resistance, and extended life span in comparison to mineral oil base oils.

The base oil mostly shaped from long carbohydrate chains. Due to high temperature and excessive force exerted on the oil, the oxidation chain reaction initiates by breaking a hydrocarbon compound into a free radical. Then the free radicals can propagate the chain reactions and more free radical forms by breaking the oxygen bond in the hydroperoxidize molecules. The free radical formed at the above stage can combine and terminate the chain reaction. The presence of metal ions plays a catalyst role in

decomposing of hyperoxidize. Other by-products of combustion such as nitrogen can also react with the intermediate product and enhance the oxidation process.

A variety of chemicals are added to the base oil to modify lubricant performance. These chemical are called additives and the most common are as follow [68]:

Anti-oxidation Inhibitors: In an engine, lubricant oil works under harsh condition. High operating temperature, introduction of contaminants such as moisture and metallic debris accelerate the rate of degradation. Lubricant oxidation causes change in lubricant properties such as increased viscosity, increased acidity, increased darkness in color and formation of sludge. The common anti-oxidants are hindered phenols, zinc dithiophosphates, aromatic amines and alkyl sulphides. These products react with pro-oxidants, sacrifice themselves to produce stable by-products.

Rust inhibitors: They are polar molecules that are chemically attracted to steel and iron surfaces and have an oil soluble tail. The rust inhibitor forms a barrier film to repel water away from the surfaces of the iron or steel components, preventing them from corrosion.

Dispersant & Detergent: Dispersants are added to the lubricant oil to keep the soot particles small and finely divided. These additives are polar as well and envelope the soot and sludge molecules from agglomeration and deposition onto components surfaces. Detergents clean the high temperature surfaces, preventing the deposition of combustion by-products.

Anti-wear & Extreme Pressure Additives: In engine operation mechanical wear is unavoidable. Due to the relative motion of mechanical parts and acting forces, different types of wear happen. Anti-wear and extreme pressure additives can partially prevent some types of wears. These additives react with component surfaces to form a soft, soap-like oxide films under high pressure. These films can enhance the lubricity of the contact surfaces.

Viscosity Index Improvers: The viscosity of oil is a function of temperature. Viscosity index is defined to describe the relationship between oil viscosity and temperature. It is necessary to maintain a consistent lubrication capability in whole operation temperature

range. Viscosity index improvers are added to the oil to minimize the change of viscosity with temperature.

Foam Inhibitor: Foam is defined as a gas phase dispersed in the liquid. The existence of foam at the oil-air interface can accelerate the oxidation process of oil, cause pressure drop in the lubrication system and reduce the heat exchanger efficiency. The foam inhibitors or defoamants can prevent the formation of stable foam above the oil level in tanks, reservoirs and sumps, and improve the lubrication performance.

Pour Point Depressant (PPD): PPDs interfere with wax formation of the oil at low temperatures, therefore allow the use of lubricants in the low temperature.

Engine lubricant works in a very harsh environment. High temperature and excessive force exerted on the oil starts the degradation process. The degradation process starts with the breakdown of hydrocarbon compounds into smaller chain and form free radical. The additives also break down and loss their properties, while, contaminants accumulate in the lubricant. In general, engine lubricant degradation is the combination of base oil oxidation, additives depletion and addition of contaminants to the lubricant.

1.3 Sensing parameters and sensing methodologies for engine lubricant condition monitoring

Sensors and sensing of automotive liquid media conditions with a significant market potential in the future, are emerging a new class of sensing systems for automotive application and are still in the research and development stage according to Marek *et al.* [76] and Fleming [40]. However, engine lubricant condition sensors are already introduced into the market by Bosh [72], Delphi [28], Continental [23-25], Hella [49] corporations and sensors are being integrated into the engine performance management system. Gotch [46] even announced “End of a Black Art” in guess-based decision on engine lubricant change replacing it with total analysis of lubricant degradation. Nevertheless, development of new approaches for engine lubricant condition monitoring is only accelerated over the last decade mainly focusing on exploring different lubricant properties as new sensing parameters, developing new advanced and intelligent sensing

methodologies, increasing sensing capabilities through integration of different sensors into one multi-functional sensing system and finally targeting total cost reduction of the entire sensing system.

The search results show, only few (up to ten) papers focused on development of sensors for lubricant condition monitoring have been published before year 2000 although science of lubricants has over several centuries history. Starting in year 2000, number of research publications has significantly.

Four main classes of lubricant properties namely physical-mechanical (approximately 30% of papers), electro-magnetic (15%), chemical (22%), optical (3%) and contamination (30%) were identified in this review as being used as sensing parameters. Following analysis systemizes and classifies sensors and sensing technologies being mainly used during the past decade for lubricant condition monitoring with respect to lubricant properties.

1.3.1 Sensing of physical-mechanical properties

Physical-mechanical properties, such as, viscosity (including complex and dynamic viscosity) and specific density have been always a first choice for estimation of actual engine lubricant and lubricant condition monitoring starting in early 90th [94, 77]. By classical definition, viscosity is a measure of liquid inability to flow (resistance of fluid to flow) or in other words, it is an ability to resist to irreversible movement or deformation of a liquid mater under an applied shear, extensional and/or other type of stresses. There are two main parameters for definition of lubricant viscosity – kinematic and dynamic viscosity [86]. It is necessary to note that temperature significantly affects viscosity properties of any fluid including engine lubricants making fluid less viscous with temperature raise, and therefore viscosity parameters are always considered as a function of temperature. In engines, lubricant becomes too thin between functional surfaces due to the engine's heat and lubricant's functionality significantly decreases. To address this issue, additives are developed to keep viscosity parameters independent from high temperature.

1.3.1.1 Complex Viscosity

A frequency-dependent viscosity function determined during forced harmonic oscillation of shear stress. It is related to the complex shear modulus and represents the angle between the viscous stress and the shear stress. The complex viscosity function is defined as the difference between the dynamic viscosity and the out-of-phase viscosity, or imaginary part of the complex viscosity.

1.3.1.1.1 Sensing of complex viscosity using shear vibrations

Agoston *et al.* [3] proposed using microacoustic sensor to monitoring lubricant condition. The sensing principle was based on the phenomena that loading effect lead to an associated change in the electric parameters of the resonator depending on the viscosity (and density) of the liquid. Details of the sensor were presented in [77]. It had been shown with artificially aged lubricant samples, the sensor signal correlates with the measured TAN value. It was concluded that the sensor was potentially suited for the detection of the oxidation-induced viscosity changes caused by thermal deterioration of the lubricant.

Agoston *et al.* [1] studied the application of online monitoring biogas engine lubrication system aiming to determine the physical and chemical properties of lubricant. In this study an array of sensors consisted of microacoustic viscosity sensor, permittivity sensor, and a corrosion sensor was used. The microacoustic viscosity sensor indicated the viscosity increase of the base lubricant. Additionally the microacoustic sensor showed to be sensitive for the sedimentation of deterioration products. In the presented field test, the change in the permittivity sensor signal indicated water contamination. The corrosion sensor was introduced at the end of the field test. The results from corrosion sensor showed no significant corrosion problem during the tests.

Bode *et al.* [16] described a miniaturized high-shear rheometer using GaPO₄ resonators which allows the detection of the rheological behavior of Newtonian and non-Newtonian fluids. A combination of a torsional and a thickness-shear mode transducer was used to realize a micro-rheometer. This study concluded that the combination of torsional and a thick-shear mode transducer provide ability to determine the viscous and

the elastic parts of the viscosity from a non-Newtonian fluid.

Durdag [37,38] introduced a bulk acoustic wave (BAW) device, or more specifically an AT cut thickness shear mode (TSM) device, which can be used for liquid-based application to measure the change in the resonant frequency of liquid in contact with the sensing film. The sensor measurement was made by placing the quartz crystal wave resonator in contact with liquid. The oscillating surface generated plane-parallel laminar flow in the contacting liquid. The “viscously-entrained” liquid endured a phase lag that increased from the distance from the surface of the TSM device. Then by measuring series resonant frequency and shift in frequency as a function of the square root of the density-viscosity product, the change in the viscosity of liquid in contact with the sensitive film was measured. In this study, the sensor, commercially available, was tested in order to continuously monitor the condition of the lubricant as a function of the fuel dilution. This study concluded that the designed sensor is capable of monitoring lubricant condition at different fuel contamination concentration.

Jakoby *et al.* [54,56,57] introduced a viscosity sensor which was realized with microacoustic devices utilizing shear-polarized oscillation. Liquid loading of a device led to an entrainment of a thin liquid film. The entrainment led to an effective mass loading of the device causing a change in resonance frequency. The sensor measurements were compared to viscosity measurements performed by Ubbelode method, and the relationship between temperature and kinematics viscosity and the sensor output was studied.

1.3.1.1.2 Sensing of complex viscosity using mass-sensitive quartz crystal microbalance

Dickert *et al.* [29,30] explored the inclusion in imprinted porous phases technique to deposit sensitive material (ceramic sol-gel layers) directly on mass-sensitive quartz crystal microbalances (QCMs) to monitor the degradation process of engine lubricant. FTIR spectroscopy was used to study the effect of this technique on sensor layer exposed to fresh and used lubricant. This study concluded that imprinted ceramic sol-gel layers

increase the sensitivity of the sensor layer and suitable for monitoring engine lubricant degradation process.

1.3.1.1.3 Sensing complex viscosity using vibration, acoustic signal

A study by Albarbar *et al.* [9,8] was conducted aiming at engine lubricant condition monitoring and quality evaluation by analyzing engine block vibration caused by piston slap excitation and its induced noise. The vibration signal was measured using an accelerometer mounted on the thrust side of first cylinder of a diesel engine, and the noise was recorded using a microphone facing the cylinder. Vibration signals of engine, influenced by the change in lubricant level, lubricant temperature, engine load, lubricant type and engine speed, and band pass filtered and transformed to frequency domain. This experimental study concluded that the condition of engine lubricant has a noticeable influence on engine vibration and airborne acoustics signals. The peaks on the frequency ranged between 900 Hz to 2.7 kHz were found to be associated with lubricant condition or piston slap excitation. Reduction in the lubricant level, increase in the lubricant temperature, engine load and speed, and improper lubricant type increased the piston slap excitation or engine vibration.

1.3.1.1.4 Sensing complex viscosity using IR absorption

Scherer *et al.* [97] in his contribution to engine lubricant system management discussed the utilization of online lubricant condition monitoring for diesel engine application for detection possibilities for soot contamination and diesel dilution. This study proposed use of multifunctional sensor combining a standard lubricant capacitive level sensor with temperature, lubricant microacoustic viscosity sensor, and permittivity sensor. It also considered transmissive IR-sensing methods for fuel condition monitoring. This study demonstrated the feasibility of infrared sensing for the detection of added components to standard fuels as a reliable method to monitor automotive powertrain fluid.

1.3.1.1.5 Sensing complex viscosity using capacitive sensor

In response to need for sensors that respond to chemical and physical properties of engine lubricant, Saloka and Meitzler [94] have developed an experimental design of an engine-

mounted, capacitive sensor to monitor changes in the dielectric constant of the engine lubricant. The sensing element was a small, air-gap capacitor, mounted in a spacer ring that fit between the lubricant filter and the engine block. Experiments on test vehicles demonstrated that the sensor could monitor a change in dielectric constant of the lubricant as it aged. The lubricant dielectric constant tended to increase with accumulated mileage. This change covered a range of approximately 10% over 11,200 km. This study concluded that lubricant dielectric sensor alone was not adequate to alert the driver when to change the lubricant, the dielectric sensor data could be used to enhance the diagnostic capabilities of present lubricant monitoring systems.

Turner and Austin [109] reported a study in which changes to the dielectric and magnetic properties of the lubricant were assessed as methods of measuring the degradation of engine lubricant. The relationship between lubricant use, measured by accumulated mileage, and lubricant viscosity was also measured. A parallel plate capacitor was constructed which consisted of 10 interleaved 50 mm diameter, 1 mm thick brass discs with 1 mm separation on a nylon core. The air capacitance of this device was 170 pF. When lubricant was used as a dielectric this rose to around 400 nF. The meter used carried out all capacitance measurements at a fixed frequency of 100 kHz. The magnetic susceptibility balance reading was used to measure the changes in magnetic property of the lubricant. The conclusions from this work were that simple distance travelled (miles/kilometers) was not a good indicator of the state of a lubricant, as estimated by measuring its viscosity. The magnetic characteristics of lubricating oil (i.e. its magnetic permeability) do change as the lubricant degrades, but the measurements were poorly correlated with viscosity and did not seem to offer much promise as the basis of a lubricant monitoring system. The dielectric properties of lubricating lubricant were reasonably well correlated with viscosity, and it was proposed that this could form the basis of a useful sensing technique.

1.3.1.1.6 Sensing complex viscosity using electrochemical impedance spectroscopy

Every liquid is capable of passing current (I) when a voltage is applied to it. If the applied voltage (V) to the material is variable (AC), the ratio V/I is known as impedance.

If a measurement of impedance over a suitable frequency range is made, and the results are properly evaluated, it is possible to relate the results to the physical and chemical properties of materials.

Wang [116] proposed a model to correlate a.c. impedance sensor output to key engine lubricant parameters i.e. total acid number (TAN), and total base number (TBN). Based on this model, the sensor output measured from a degraded engine lubricant should be linearly proportional to the concentration of acidic decomposition products and inversely proportional to the viscosity. The model was verified using the sensor output measured either in-situ from dynamometer engine tests or in the lubricant samples collected from the dynamometer test. It was found that the model correlates the sensor output with key engine lubricant parameters as long as the lubricant sample viscosity does not exceed five times its value when the lubricant was still fresh. The verification of this model demonstrated that the increase of sensor output during the rapid increase of acidic decomposition products stage was indeed caused by the accumulation of acidic decomposition products in engine lubricant. If the viscosity had not increased during the rapid viscosity increase stage, the sensor output would continue to increase until the end of the test.

Wang [115] introduced the installation of a.c. impedance sensor in three vehicles to perform road test and correlate the sensor outputs with key engine lubricant parameters i.e. TAN, TBN, viscosity at different operating conditions. The sensor was installed inside the engine pan through lubricant drain plug and the data was collected on-line. Lubricant samples were collected periodically from the vehicles. Key parameters, such as viscosity, TAN, TBN, and oxidation induction time were measured for these samples to verify the performance of the sensor. The viscosity in centiStokes unit (cSt) was measured at two temperatures, 40°C and 100°C. Based on the sensor outputs collected from the road tests, the degradation of lubricant could be divided into three stages: (1) the additives in engine lubricant being consumed or transformed, (2) rapid increase of TAN due to the oxidation of lubricant, and (3) rapid increase of viscosity. The onset of the second and the third degradation stages could be detected by analyzing the trend of sensor outputs. For short trip and cold start service, the sensor could detect water

condensation in engine lubricant. Furthermore, the sensor outputs correlated with the amount of water existing in the engine lubricant. This study also indicated that lubricant condition sensor could also detect antifreeze contamination in engine lubricant.

1.3.1.1.7 Sensing complex viscosity using light detecting resistor

Kumar and Mukherjee [65] investigated the relationship between accumulated mileage and key engine lubricant parameters such as pH, viscosity, resistance, and transmittance, and proposed an optical methodology to monitor engine lubricant condition. The proposed method was based on the light intensity measurement of thin layer of lubricant and correlating the sensor reading to key engine lubricant parameters. This study showed the optical sensor was capable of measuring the change in the lubricant color, caused by operating hours and monitored the engine lubricant condition.

1.3.1.2 Dynamic viscosity

Dynamic viscosity (μ) is defined as a tangential force per unit area required to move one horizontal plane with respect to the other for a unit distance with a unit speed and it is measured in a unit of *mPa.s*, although the centipoises (*cP*) is commonly used. In contrary to dynamic viscosity, kinematic viscosity does not involve applied force and it is defined as the ratio of dynamic viscosity to density of fluid having a unit of mm^2/s , although the centiStokes (*cSt*) is used as well.

1.3.1.2.1 Sensing dynamic viscosity using tuning fork quartz resonator

Basu *et al.* [12] developed a lubrication sensor which can measure five independent lubricant parameters. The mechanical resonator, a so-called Tuning-Fork, consisted of piezo- electric materials and mono-crystal quartz, was capable to measure 4 independent physical parameters of a liquid, e.g. dynamic viscosity, density, permittivity and electrical conductance. In addition, the concept was capable of detecting the lubricant level continuously during normal engine operation. Also, the sensor included an intelligent Oil Condition Algorithm (OCA) which evaluated the incoming signals from the sensor and calculates the current oil quality considering additional information from the engine.

This study concluded that both the bench and the vehicle testing sensor outputs for the viscosity correlated well with the calculated viscosity and the oil analysis data.

1.3.1.2.2 Sensing dynamic viscosity using capacitive sensor

Kim *et al.* [60] proposed liquid dielectric constant measurement device to monitor the lubricant degradation using cross capacitance measurement. This study employed Thompson-Lampard theorem to design a capacitive sensor to measure the dielectric constant of lubricant with respect traveled mileage. This study showed that the dielectric constant of engine lubricant increased as a function of accumulated mileage and the proposed sensor was capable of monitoring the change in the sensing parameter.

1.3.1.3 Specific density

Specific density or density is the defined as the ratio of mass per unit volume. This property often is measured with viscosity and permittivity to monitor the condition of the media. The unit of measure density is kg/m^3 or g/cm^3 .

1.3.1.3.1 Sensing specific gravity using shear vibration

Martin *et al.* [77] examined the responses of smooth- and textured-surface thickness-shear mode (TSM) resonators in liquid. Smooth devices, which viscously entrain a layer of contacting liquid, exhibited a response that depended on the product of liquid density and viscosity. Textured-surface devices, which also trapped liquid in surface crevices, pores, *etc.*, exhibited an additional response that depends on liquid density alone. Combining smooth- and textured-surface resonators in a monolithic sensor enabled the liquid density and viscosity to be extracted simultaneously. This study demonstrated that quartz resonators with smooth surfaces could be operated in liquids to measure the density-viscosity product of a contacting fluid. Surface texture on the resonator caused fluid trapping and an additional response proportional to liquid density. Comparing the responses of a pair of resonators, one smooth and one textured, enables the liquid density to be extracted. Once the density was known, the response of a smooth device yielded the liquid viscosity.

1.3.1.3.2 Sensing specific gravity using tuning fork quartz resonator

Dobrinski *et al.* [33] performed a study to design a micro sensor based on a Tuning Fork quartz resonator, capable of measuring the dynamic viscosity, specific density, permittivity, conductance, and temperature of lubricant. The tuning fork offered a direct access to the dynamic viscosity and specific density of the liquid while thickness shear mode TSM resonators only provide the product of both values. A high temperature and chemical resistant coating ensured the long-term stability of the tuning fork and prevents absorption of particles suspended in the lubricant, as for example soot. The resonant curve of a tuning fork quartz resonator was converted into the equivalent electrical impedance. The current lubricant condition was calculated by a multi-parametric analysis and transferred to the electronic control unit (ECU) of the vehicle. The received data was used substantially to prolong frequencies of lubricant changes and prevent vehicle downtime caused by wear. The sensor was used for in lab and on vehicle measurements to monitor the all the sensing parameters. This study concluded that the proposed design was able to monitor engine lubricant condition off-line and on-line.

1.3.2 Sensing of electrical properties (conductivity, permittivity, magnetic susceptibility)

Lubricant consists of long-chain hydrocarbons. As lubricant ages, it oxidizes and undergoes a slow increase in polarity. Lubricant oxidation is a chain reaction initiated by appearance of colloidal carbon, giving rise to black coloration and solid deposits and by breakage of hydrocarbon compound, into a free radical due to high shear force between engine components. The two degradation mechanisms are expected to affect electromagnetic properties of lubricant such as permittivity, electrical conductivity, and magnetic susceptibility.

1.3.2.1 Permittivity

Permittivity or dielectric constant is a measure of the extent to which it concentrates electrostatic lines of flux. It is the ratio of the amount of stored electrical energy when a potential is applied, relative to the permittivity of a vacuum. The relative static permittivity is the same as the relative permittivity evaluated for a frequency of zero. The

exact effect of lubricant oxidation on dielectric constant is unclear. It has been suggested that the main effect may be to raise the dielectric constant, since the oxidized lubricant will acquire a dipole character. This process implies that a correlation between lubricant aging process and dielectric constant should exist.

1.3.2.1.1 Sensing permittivity using shear vibration

Jakoby *et al.* [55] described a multi-sensors device to measure the lubricant's viscosity, permittivity, temperature, and level. The viscosity sensor was a microacoustic device utilizing shear-polarized oscillations. In this study, the viscosity measurements of engine lubricant (fresh, used and contaminated) were compared to permittivity sensor reading for better understanding of correlation between physical properties of engine lubricant. Also, the lubricant viscosity was studied as a function of accumulated mileage and temperature signal. This study concluded that it is imperative to study more than one physical-mechanical property of lubricant to help evaluate the monitoring of lubricant condition.

1.3.2.1.2 Sensing permittivity using mass-sensitive quartz crystal microbalance

Duchowski and Ringholm [35] introduced a multi-sensor array, which consisted of mass-sensitive quartz crystal microbalance (QCM), resistance temperature detection (RTD), capacitor with polyimide dielectric and an inner digital capacitor sensor to measure relative viscosity, temperature, moisture and dielectric, respectively. The preliminary results indicated that the multi-sensor array was able to measure relative viscosity, temperature, dielectric constant and contaminants in the engine lubricant. However, the lack of response to characterizing aging processes in different fluid classes was considered to be the next step into the applicability of this sensor.

1.3.2.1.3 Sensing of permittivity using tuning fork quartz resonator

Furthermore, Dobrinski *et al.* [32] developed a combo-sensor capable of measuring several independent lubricant parameters continuously. It comprised an ultrasonic transducer for the lubricant level detection as well as a tuning fork mechanical resonator for the lubricant condition measurement. Both elements were realized as small multi-

chip modules, which are combined within a mechanical flange. The raw data was transmitted to an external electronic control unit (ECU) and a complementary software module provided the lubricant condition for user. This study concluded the proposed sensor was successful to fulfill its purpose to monitor the lubricant level and condition, and also to provide a lubricant management system for vehicle to provide lubricant change based on the operating condition and driving habit and for different types of vehicles.

1.3.2.1.4 Sensing permittivity using capacitive sensor

Na *et al.* [82] designed a capacitive sensor with interdigit structure to monitor changes in the dielectric constant of the engine lubricant and fabricated the sensor by using semiconductor fabrication technology. This study concluded that the dielectric constant change of engine lubricant resulted in the capacitance change of the sensor. It also stated that the dielectric constant of engine lubricant changed as it deteriorated and the fabricated sensor could measure the degree of deterioration.

Turner and Austin [109] reported a study in which changes to the dielectric and magnetic properties of the lubricant were assessed as methods of measuring the degradation of engine lubricant. The relationship between lubricant use, measured by accumulated mileage, and lubricant viscosity was also measured. A parallel plate capacitor was constructed using brass discs with 1 mm separation on a nylon core. The air capacitance of this device was 170 pF. The magnetic susceptibility balance reading was used to measure the changes in magnetic property of the lubricant. The conclusions from this work were that simple distance travelled (miles/kilometers) was not a good indicator of the state of a lubricant, as estimated by measuring its viscosity. The magnetic characteristics of lubricating oil (i.e. its magnetic permeability) do change as the lubricant degrades, but the measurements were poorly correlated with viscosity and did not seem to offer much promise as the basis of a lubricant monitoring system. The dielectric properties of lubricating lubricant were reasonably well correlated with viscosity, and it was proposed that this could form the basis of a useful sensing technique.

In a study by Zhang *et al.* [122] a chemical sensor which was consisted of bulk acoustic wave quartz resonator and a capacitor formed between a grounded quartz resonator electrode and an additional electrode was developed to monitor the soot content in the heavy-duty diesel engine. Two series of diesel lubricant samples, low and high soot concentration, were tested. The results showed that mass-sensitive quartz crystal microbalance (QCM) sensor was capable of detecting soot concentration in the samples regardless of its concentration or agglomeration, while the permittivity sensor exhibited different sensing pattern in detecting soot at higher concentration. It was also observed soot agglomeration had effect on the permittivity sensor reading.

1.3.2.2 Sensing electrical conductivity

Electrical conductivity or specific conductivity is a measure of a material's ability to conduct electric current. When an electrical potential difference is applied across a conductor, its movable charges flow, giving rise to an electric current. The conductivity is defined as the ratio of the current density to the electric field strength.

1.3.2.2.1 Sensing electrical conductivity using tuning fork quartz resonator

Bennett *et al.* [13] designed and fabricated a miniature, solid state lubricant condition sensor based on a crystal tuning fork. The sensor provided direct measurement of the critical physical properties of viscosity, density, dielectric permittivity, and AC conductance of lubricants. This study demonstrated the capabilities of a tuning fork flexural resonator based sensor to provide in-situ characterization of engine lubricant oil. The results compare favorably with those obtained through laboratory analysis.

1.3.2.2.2 Sensing electrical conductivity using capacitive sensor

In a study by Basu *et al.* [11] progress of development work to design a lubricant monitoring sensor was described. This study, capacitive sensor and impedance measurement methods were utilized to measure the TAN and TBN contents and also the lubricant level inside the lubricant pan on-line and correlate the sensing parameters to lubricant viscosity. Several laboratory and road tests were conducted and the preliminary

results indicated of capability of the proposed sensor to monitor engine lubricant condition using capacitive and impedance methodologies.

1.3.2.2.3 Sensing electrical conductivity using corrosion sensor

Agoston *et al.* [2] proposed a methodology to monitor the corrosion effect of engine lubricant as a measure to monitor the condition of lubricant in biogas-fuelled engines. The sensor was consisted of four copper resistive films with thickness of 100 nm, 300 nm, 600 nm, and 1000 nm to monitor the rate of corrosion. The rate of the corrosion depends on the current corrosiveness of the lubricant. The corrosive material loss was monitored electrically by the resistance of the copper films. This study identified two major corrosion mechanisms which takes place in biogas-fuelled engines lubricant: a quasi-uniform corrosion and a blotched type of corrosion. The first kind represents etch-type corrosion. The second type is often combined with surface depositions and chemical conversion of the copper layer to mechanically weak compounds, like copper sulfide. In case of the non-uniform, blotched corrosion, the applied resistive read-out method suffered from lacking reproducibility because corrosion blotches can lead to an unpredictable and early loss of electric contact due to their random distribution over the surface.

1.3.2.2.4 Sensing electrical conductivity using CNT

Moon *et al.* [81] have developed a new approach that examined the use of multiwall carbon nanotube (CNT) to monitor lubricant degradation. Oxidation of the engine lubricant in the internal combustion engine led to an increase in the electrical conductivity of CNTs used as a sensing parameter in this study. In this work, the correlation between TAN formed from the lubricant degradation and CNT sensor was used to monitor the life of the engine lubricant. This study concluded that the engine lubricant sensor output corresponded to TAN could withstand the maximum temperature of 160°C of engine lubricant. This study also showed the CNT sensor can be applied to other type lubricants.

1.3.2.3 Impedance

Electrical impedance, or simply impedance, describes a measure of opposition to alternating current (AC). Electrical impedance extends the concept of resistance to AC circuits, describing not only the relative amplitudes of the voltage and current, but also the relative phases. When the circuit is driven with direct current (DC) there is no distinction between impedance and resistance; the latter can be thought of as impedance with zero phase angle. Impedance is defined as the frequency domain ratio of the voltage to the current. In other words, it is the voltage–current ratio for a single complex exponential at a particular frequency ω . In general, impedance will be a complex number, with the same units as resistance, for which the SI unit is the ohm. For a sinusoidal current or voltage input, the polar form of the complex impedance relates the amplitude and phase of the voltage and current.

1.3.2.4 Sensing Impedance using electrochemical impedance spectroscopy

Lvovich and Smiechowski [73,74] examined the application of electrochemical impedance spectroscopy (EIS) for analysis of the electrochemical properties of industrial lubricants and focuses on establishing a relationship between lubricant chemical composition and EIS data. Theory on the planar interdigit electrode sensors was combined with experimental results to come to a better description of a sensor for highly resistive industrial fluid monitoring. The experiments were conducted on an impedance/dielectric analyzer. Electrochemical data were generated on several series of lubricant drains from engine field tests. Impedance spectra for lubricants were investigated over a range of temperatures, electrode geometries, potentials, and degradation states. Analysis of the spectra was divided into high, medium and low frequency regimes. The modeling and analysis of the EIS data as a combination of changes in bulk, adsorption, diffusion and charge transfer resistances, capacitances and constant phase element (CPE) parameters allowed studying the conditions of a lubricant. Experimental results demonstrated that the diffusive process could often be modeled as Warburg impedance with a finite double layer. The electrochemical structure of a typical industrial lubricant through the use of an equivalent circuit (EC) model was presented.

The study proposed the use of this model for analysis of the impedance results as a reflection of chemical composition and changes in the system.

1.3.3 Sensing of chemical properties

In all lubricating systems, organic compounds exposed to high temperatures and pressures in the presence of oxygen will partially oxidize. Carboxylic acids contribute to the acidity of the lubricant and deplete its basic reserve as neutralization takes place. The net effect of prolonged oxidation is that chemically the lubricant becomes acidic. Measuring change in chemical properties of engine lubricant such as total acid number (TAN) or total base number (TBN) is the key index to monitoring engine lubricant condition.

1.3.3.1 Measuring proton spin-lattice relaxation rate dispersion

Spin-lattice nuclear magnetic resonance (NMR) relaxation is a powerful technique that has been used extensively and successfully for the study of molecular dynamics in liquids, polymer melts, liquid crystals, surfactants and related materials. In particular, it is well known that the proton spin-lattice relaxation rate T_1^{-1} in liquids is governed mainly by two kinds of molecular motions: self-diffusion of individual molecules and rotations of the whole molecule or internal groups. NMR relaxometry, that is, the study of the Larmor frequency (ν) dispersion of the relaxation parameter, is particularly suitable for scanning the correlation times that characterize the underlying molecular dynamics. Since lubricant oil degradation is a process which takes place at the molecular level, spin lattice NMR relaxation can be employed to monitor the degradation in liquid with long polymer chains.

1.3.3.1.1 Sensing proton spin-lattice relaxation rate dispersion using nuclear magnetic resonance spectroscopy

Ballari *et al.* [10] investigated the use of nuclear magnetic resonance (NMR) relaxometry for lubricant analysis. This study investigated lubricant oil degradation at the molecular level. Aging effects, as reflected on the proton spin-lattice relaxation rate dispersion, were studied in two different lubricant engine lubricants. The proton field cycling

technique was used to scan relaxation of new and aged samples of monograde and multigrade lubricants. Relaxation dispersions were interpreted in terms of self-diffusion and molecular rotations. This study shows that proton T_1^{-1} could be very sensitive to degradation processes, especially at low Larmor frequencies. The analysis reveals a noticeable sensitivity of the involved correlation times.

1.3.3.2 Sensing total acid number (TAN)

Total Acid Number (TAN) is the weight in milligrams of base required to neutralize all the acidic constituents. The conventional method to quantify TAN in-vivo are colorimetric and potentiometer titration methods. TAN increases slowly over a long period of time in normal working condition of engine lubricant. The unit of TAN is mg KOH/gm of lubricant.

1.3.3.3 Sensing total acid number (TAN) using capacitive sensor

Lubricant degradation process causes change in the TAN and TBN content and variation in electrical and chemical properties of lubricant. Capacitive sensor methodology with accompany of other method such as impedance measurement has been utilized to capture the changes in TAN and TBN content of lubricant [11]. The changes in TAN and TBN content together with variation in permittivity were correlated to other lubricant properties such as viscosity.

1.3.3.3.1 Sensing total acid number (TAN) using carbon nanotube (CNT)

Moon *et al.* [81] have developed a new approach that examined the use of multiwall carbon nanotube (CNT) to monitor lubricant degradation. Oxidation of the engine lubricant in the internal combustion engine led to an increase in the electrical conductivity of CNTs used as a sensing parameter in this study. In this work, the correlation between TAN formed from the lubricant degradation and CNT sensor was used to monitor the life of the engine lubricant. This study concluded that the engine lubricant sensor output corresponded to TAN and capable of withstanding the maximum temperature of 160°C of engine lubricant. This study also showed the CNT sensor can be

applied to other type lubricants.

1.3.3.3.2 Sensing total acid number (TAN) using electrochemical impedance

Smiechowski and Lvovich [102] monitored the levels of acidity and basicity as the sensing parameters for industrial lubricant. The sensor was based on the electrochemical impedance methodology. Iridium oxide potentiometric sensor was developed to detect acidity and basicity in diesel engine lubricant. Two versions of sensor, a macro and MEMS configurations with iridium oxidized, were created to monitor pH, TAN and TBN of the lubricant. Results showed that the conventional iridium oxide sensors were more sensitive to changes in pH than MEMS sensors with reduction reaction occurring on the surface of working electrode. Tests of the sensors in diesel lubricant drains showed a good correlation between TAN and TBN and the voltage output of each sensor. Conventional IrO_x sensors showed a greater sensitivity to changes in TAN and TBN than the MEMS sensors. The sputter formed sensor demonstrated a better response to oxidative degradation of lubricant due to its higher sensitivity to ketones and carboxylic acids. The differences in reaction mechanisms between the iridium oxide and the components of the solution resulted in an opposite direction of response to changes in basicity in aqueous and non-aqueous systems. Long term stability tests showed that all three versions of the sensor were not stable in diesel lubricant over a 24 hours period.

Wang and Lee [112] developed in-situ lubricant-condition sensor to monitor total acid number as the sensing parameter. In this study, in-situ macro and micro lubricant-condition sensors was developed. The macro sensor was composed of two circular-shaped, gold-plated iron electrodes, while the micro sensor was made of aluminum and silicon layers deposited on top to silicon wafer. Bothe sensors were tested in two sets of engine-lubricant samples. It was found that after suppressing the high current associated with the fresh engine lubricant, the microsensor's output current correlates with the total acid number (TAN) of engine lubricant.

In another study Wang [117] proposed an alternative method to titration to measure TAN and establish a better correlation between engine lubricant condition

sensor's output and total acids number. Complementary electrochemical method applied potential waveform to two sensing electrodes submerged into the lubricant. The TAN of lubricant then determined by the amount of current passed through the lubricant. The results showed the correlation between sensor output and TAN could be improved if the scatter data generated by titration method was reduced. This study concluded that electrochemical method was more suitable way of measuring the TAN in the lubricant. This method helped to establish a better correlation between sensor readings and amount of TAN in the lubricant.

1.3.3.4 Sensing total base number (TBN)

Total Base Number (TBN) is defined as the milligram of acid, expressed in equivalent milligram of KOH, to neutralize all basic constituents. As oil ages, TBN tends to decrease as a result of the depletion of the oil's reserves alkalinity by combustion and oxidation of oil. Like TAN, TBN can be quantified by colorimetric or potentiometric titration methods.

1.3.3.4.1 Sensing total base number (TBN) using mass sensitive quartz crystal microbalance

Lieberzeit *et al.* [69] investigated the effect of molecular imprinting of organic and inorganic polymers nanostructured on the mass-sensitive quartz crystal microbalances (QCMs) to monitor the degradation process and presence of contaminants in the engine lubricant. By using of fresh and degraded engine lubricant as a template, the polymer was selectively adjusted to sense fresh or used lubricant. By the same strategy, sensitive material could be deposited to detect fuel or water contamination in the engine lubricant. This study showed that that sensing surfaces imprinted by fresh and used lubricant exhibits different behavior in Fourier transform infrared spectroscopy (FTIR) absorbance measurements. This was to confirm the lubricant imprinted sensitive surfaces were able to detect the degradation process in engine lubricant. FTIR measurements on bulk materials proved that the sensor responses, indeed, resulted from bulk effects, where the lubricant or its components are incorporated into the matrix. Additionally, the sensor data could be qualitatively and quantitatively correlated with changes in the lubricant TBN,

which was a standard laboratory parameter in engine lubricant chemistry. This study concluded that the nanopatterned systems were highly suitable to transform overall chemical changes in the lubricant caused by oxidative degradation into a single sensor parameter.

1.3.3.4.2 Sensing total base number using electrochemical impedance

Smiechowski and Lvovich [102] introduced an iridium oxide potentiometric sensor to monitor pH, TAN and TBN of the lubricant as the sensing parameters for industrial lubricant. The sensing principle was based on the electrochemical impedance measurement methodology. Two versions of sensor, a macro and MEMS configurations with iridium oxidized, were created. Tests of the sensors in diesel lubricant drains showed a good correlation between TAN and TBN and the voltage output of each sensor, however the conventional version was more sensitive to the change in pH.

1.3.3.5 Measuring pH

As lubricating oil ages, it oxidizes and undergoes a slow increase in polarity. The oxidation chain reaction initiates by breaking a hydrocarbon compound RH, into a free radical (R^*). These free radicals R^* can then propagate the chain reactions causing a significant increase in pH. Measuring the acidity of lubricating oil in association with TAN is a common practice when monitoring engine lubricant.

1.3.3.5.1 Sensing pH using light detecting spectroscopy

Kumar and Mukherjee [65] investigated the relationship between accumulated mileage and key engine lubricant parameters such as pH, viscosity, resistance, and transmittance, and proposed an optical methodology to monitor engine lubricant condition. The proposed method was based on the light intensity measurement of thin layer of lubricant and correlating the sensor reading to key engine lubricant parameters. This study showed the optical sensor was capable of measuring the change in the lubricant color, caused by operating hours and monitored the engine lubricant condition.

1.3.3.6 Oxidation index

The oxidation index measures the degree to which the lubricant has been oxidized and is a good indicator of lubricant degradation. A rapid increase in oxidation may indicate engine overheating or a depletion of the anti-oxidant additive in the lubricant due to an over extended lubricant drain period.

1.3.3.6.1 Sensing oxidation index using FTIR spectroscopy–IR absorption

Agoston *et al.* [5,9] proposed an infrared (IR) absorption sensor to measure oxidation index in the engine lubricant which was related to the change in absorption at a characteristic wavelength $\lambda=5.85 \mu\text{m}$. A sensor prototype setup consisted of an IR emitter, a narrow band IR filter, a fluid cell, and an IR detector to determine the absorption at $5.85 \mu\text{m}$ where the absorption was scarcely affected by oxidation. It was shown that a simple sensor setup realized with a broadband IR detector and fixed narrow-band IR filters was capable to measure a value, which correlates to the oxidation index. The sensor setup indicated of potentials which would allow a miniaturization to makes this concept utilizable for online monitoring of engine lubricant. This study suggested further application of this method to monitor the presence nitration index, soot, water and glycol content in the engine lubricant.

Kudlaty *et al.* [64] have described the use of an infrared sensor for on-line analysis of the deterioration stage of industrial lubricants. The developed sensor consists of a broad-band infrared light source, two collimating mirrors, an attenuated total reflection (ATR) crystal, a filter-chopper and a pyroelectric detector. The ATR technique provided the separation of sensitive sensor optics from the hazardous environment. The spatial distribution of the filters in the chopper provided different frequencies of the signal components corresponding to different wave numbers. The second filter transmitted at the wavelength at which $C=O$ absorptions of oxidation products of lubricants occur. In order to separate the reference and sample signals the detected signal was Fourier transformed. This study showed that the designed sensor was capable of on-

line analysis of engine lubricant. The quantitative results and accuracy were comparable to standard FTIR-ATR investigations of aged lubricants.

1.3.3.7 General chemical properties

General chemical properties sensing is referred to monitoring engine lubricant condition in a general sense and comparison with fresh lubricant. In this sensing category, methods such as FTIR spectroscopy, deposition of ceramic sol-gel material in mass-sensitive devices, electro chemical impedance spectroscopy, different optical methods, and time of mass spectrometer are used to monitor presence of contaminants i.e. water, coolant and gasoline, soot , TAN, and TBN in the lubricant.

1.3.3.7.1 Sensing general chemical properties using FTIR spectroscopy-IR absorbance

Kasberger *et al.* [58,59] have designed a fully integrated infrared absorption sensor, capable of determining chemical properties by investigating infrared absorption at selected distinct wavelengths in the mid-infrared region. A highly sensitive absorption element, a planar mono-mode waveguide was utilized which required an appropriate coupler to couple the infrared light into the waveguide. The employed grating couplers have been modeled in order to derive a design yielding the desired sensor performance. Kasberger in his study utilized the evanescent field of a single mode waveguide with high sensitivity in the mid-infrared region. Grating couplers were utilized for coupling broadband IR-radiation in and out of the waveguide, where the coupling angle was used for spectral separation. As the targeted wavelength was located in the mid-infrared region, a suitable infrared source or detector, respectively, was fabricated by thermal components.

1.3.3.7.2 Sensing general chemical properties using electrochemical impedance spectroscopy

Ulrich *et al.* [110] have studied the combination of Electrochemical Impedance Spectroscopy (EIS) and multivariate data analysis to simultaneously predict the concentrations of soot and diesel in engine lubricant. The impedance data was obtained with an LCR meter (Inductance (L), Capacitance (C), and Resistance (R)), using a frequency range of 20 Hz to 600 kHz and an oscillator level of 20 V_{rms}. A four terminal

pair configuration was used together with a coaxial/triaxial cable assembly to contact the electrodes. The resistance (R) and the reactance (X) were measured at 24 different frequencies. The electrochemistry cell used was consisted of two 1.0 cm thick stainless steel electrodes. The electrodes were separated by glass slides to create an effective electrode area. The measurement was done on engine lubricant (Exxon Mobil Delvac MX 15W40) with different amount of soot and diesel. The results showed that EIS is suitable for predicting different contaminations in engine lubricant; however a measurement set-up with temperature control and possibility to use lower frequencies would improve the results.

In a study by Wang and Lee [114] an electrochemical sensor, which was composed of two gold-plated iron electrodes, was developed to differentiate two-stroke-engine lubricant from four-stroke-engine lubricant. Since the electrical conductivity of engine lubricant was low, the two electrodes were placed closely (0.015 mm). Then a triangle waveform was applied between the electrodes (± 5 V). Seven two-stroke-engine lubricants were tested at 0°C, 23°C, and 50°C. Three four-stroke-engine lubricants were also tested for comparison. This measurement was based on the fact that the additives percentage in the two-stroke-engine lubricant was considerably less than four-stroke-engine lubricant, therefore the electrochemical system formed within a two-stroke-engine lubricant should be much less reactive than that formed with a four-stroke-engine lubricant. The results indicated that the sensor was capable of detecting metallo-organic detergent, ZDP's, and ashless detergent. The sensor read higher output in four-stroke-engine lubricant as to two-stroke-engine lubricant.

1.3.3.7.3 Sensing general chemical properties using time of flight mass spectroscopy

Sepcic *et al.* [99] introduced time of flight mass spectrometer (TOF MS) and sensor arrays a method for determination of the volatile compounds present in new and used lubricant. The identification of the new and used lubricants was based on the abundance of volatile compounds in headspace above the lubricants. Multivariate analysis based on principal component analysis (PCA), and hierarchal cluster analysis was used to evaluate the degradation compounds found in used engine lubricant. The gas phase of new and

used petroleum lubricants was analyzed using a time of flight mass spectrometer (TOF MS) and sensor arrays. The samples included used engine lubricant, up to 35,500 miles. The principal components identified by PCA were volatile constituents of the lubricants. New and used lubricants were also differentiated using multivariate analysis of the results from these gas phase detection methods. The identification of the origin of volatile samples in the used lubricants has been studied by spiking newer lubricant samples with a complex mixture of volatile compounds. These samples were then analyzed with the sensor array. Results from the spiked samples correlated better with the older, more used lubricant samples, confirming that the previously identified volatile compounds can be used to classify new and used engine lubricants. Using chemometrics, the used lubricants were differentiated into categories using metal oxide semiconductor (MOS) and quartz crystal microbalance (QCM) sensor arrays or mass spectrometry. The QCM sensors were able to better differentiate the new and used lubricant samples compared to the metal oxides. In the mass spectrometry and sensor array analysis the new lubricants were clustered into groups and separated by mileages. The older, more used lubricants were clearly distinguished from the newer lubricants.

1.3.4 Sensing of optical properties (color, transparency, refractive index, absorbance)

The optical properties of engine lubricant are the most apparent properties that can be used to distinguish used lubricants from new lubricant. These properties include color, transparency, reflection, refractive index, and absorbance.

Fresh engine lubricant color is brown. This color comes from the base stock and additives. As lubricant ages, the color darkens. The intensity of color has a direct relationship with the oxidation of lubricant. Increase in the color darkness indicates the aging process of it. Fresh engine lubricant transfers light through. As lubricant degrades this transparency decreases due to introduction of particles to the lubricant. Like lubricant color, change in lubricant transparency is an indication of lubricant oxidation. Refractive index (or index of refraction) of a medium is a measure for how much the speed of light (or other waves such as sound waves) is reduced inside the medium. The refractive index of a medium is defined as the ratio of the light velocity of a wave

phenomenon such as light or sound in a reference medium to the phase velocity in the medium itself. In spectroscopy, the absorbance is defined as the logarithmic ratio of the intensity of light at a specified wavelength that has passed through a sample (transmitted light intensity) and the intensity of the light before it enters the sample or incident light intensity.

1.3.4.1 Absorbed light intensity

In spectroscopy, the absorbance is defined as the logarithmic ratio of the intensity of light at a specified wavelength that has passed through a sample (transmitted light intensity) and the intensity of the light before it enters the sample or incident light intensity. Absorbance measurements are often carried out in analytical chemistry, since the absorbance of a sample is proportional to the thickness of the sample and the concentration of the absorbing species in the sample. As lubricant ages, the color darkens. The intensity of color has a direct relationship with the oxidation of lubricant. Lubricant color intensity can not quantify the oxidation level, but increase in the color darkness indicates the aging process of it.

1.3.4.1.1 Sensing absorbed light intensity using FTIR spectroscopy

Dahmani and Gupta [27] have investigated the infrared absorption spectroscopy (IR) and acousto-optic tunable filter (AOTF) technology combined to develop a portable spectrophotometer for use in engine lubricant analysis to identify and quantify lubricant contaminants and residue products. Preliminary measurements were taken with a field-portable AOTF-based spectrometer (2 to 4.5 μm) and an FTIR spectrometer (2 to 25 μm) for comparison. Absorption spectra of used and unused lubricant samples were measured and compared to determine absorption changes between the various samples resulting from lubricant degradation and any chemical reactions that might have taken place during high-temperature engine lubrication. These preliminary results indicated that IR spectroscopy can be used for lubricant quality monitoring in automotive engines, which will help predict and prevent engine failure and degradation.

1.3.4.1.2 Sensing absorbed light intensity using light detecting resistor

Kumar and Mukherjee [65] investigated the relationship between accumulated mileage and key engine lubricant parameters such as pH, viscosity, resistance, and transmittance, and proposed an optical methodology to monitor engine lubricant condition. The proposed method was based on the light intensity measurement of thin layer of lubricant and correlating the sensor reading to key engine lubricant parameters. This study showed the optical sensor was capable of measuring the change in the lubricant color, caused by operating hours and monitored the engine lubricant condition.

1.3.4.1.3 Sensing absorbed light intensity using optical sensing

Scott *et al.* [98] discussed the design, manufacturing, and evaluation of a robust optical microsystem for measuring general chemical properties of engine lubricant such as soot, solid particles, water, coolant, using optical sensing methodology. Bulk fused silica was used as the substrates for sensor. A three-dimensional micro fluidic circuitry was incorporated side-by-side with three-dimensional wave guided optical networks. The manufacturing of the optical waveguides were completed using a direct-write process based on the use of femtosecond laser pulses to locally alter the structure of the glass substrate at the nano-level. The microfluidic circuitry was produced using the same femtosecond laser based process, followed by an anisotropic wet chemical etching step. The proposed lubricant-condition monitoring sensors measure the optical characteristics of engine lubricant, and correlate these optical properties to the physical and chemical properties of lubricant. The sensors were designed to constantly monitor the lubricant while the engine was operating. The sensor system was consisted of several optical methods such as absorption measurement, near-UV absorption, scattering, interferometry, and fluorescence measurement to monitor soot, chemical degradation, presents of solid particles, water contamination and coolant, respectively. The author concluded that the online vehicle lubricant condition monitoring is far from a mature technology and requires more investigation.

1.3.5 Sensing contamination

There are a wide variety of by-products produced during the combustion process such as ketones, esters, aldehydes, carbonates and carboxylic acids. These compounds are dissolved by the lubricant or remain suspended owing to the dispersive additives in the oil. The net effect of prolonged oxidation is that chemically the oil becomes acidic causing corrosion whilst physically an increase in viscosity occurs. Besides the oxidation of base oil and depletion of additives, contaminants also change the condition of the lubricant entering from the atmosphere or subsystems of engine. Contamination is the scourge of hydraulic and lubricated mechanical systems. Contamination, by definition, is anything in the lubricant that should not be there. Contaminants reduce the life of mechanical components and lubricant. Micro-particles, moisture, gasoline, soot, coolant and air are the most common fluid contaminants for engine lubricant.

1.3.5.1 Particle contamination

Abrasive particles are responsible for much of the wear that leads to mechanical failure. The amount of damage inflicted by particles depends upon their size, shape, hardness and chemistry. Abrasive particles must be controlled in any system deemed critical to operation or expensive to repair. Many particles enter the lubricant at those points where the machine interfaces with its environment while others are generated from within. Particle ingress sources may be vents and breathers, ineffective or damaged seal, new lubricant, and full or defective filter. Particles, especially catalytic metal particles like copper, iron, and lead increase the rate at which oxidation occurs. Particles also strip the lubricant of its polar additives, including anti-wear additive, extreme pressure additives, rust inhibitors and dispersants. Also, numerous very small particles in stable suspension can cause the lubricant's viscosity to increase. Abrasive particles are responsible for much of the wear leading to premature failure of mechanical components. Under sliding conditions, clearance-sized particles enter the lubricant film between surfaces and cut away material. Under rolling contact conditions, particles transfer concentrated load between two surfaces in relative motion, resulting in surface fatigue, pitting, and spalling.

1.3.5.1.1 Sensing presence of micro-particles using light scattering method

The content of micro-particles in light lubricant products was studied and investigated by Bilyi *et al.* [15] using an optical sensor. The sensor design was based on the optical absorption spectroscopy to monitor the contamination of light lubricant product used in aircraft turbine gas. The lubricant used in this study was TN-210A absorption spectrum in 25000-21000 cm^{-1} region. The sensor was based on the principle of light scattering in a flowing cell. The counting zone in cell was formed by lightening scheme based on using of the monochromatic light source which wave length exceeded the bound of absorption band of testing lubricants. The analyzed liquid with the help of automatic bin crossed the counting zone causing the impulsive change of light flow proportionally to the particles dimension. Light impulses were converted into electric ones by photo detector and then were registered by the amplitude detector in six parallel memory bands depending to their dimension. The concentration of particles was determined by medium frequency of impulse appearance in memory band.

1.3.5.1.2 Sensing presence of micro-particles using capacitive sensor

Raadnui *et al.* [89] have reported the development of a low cost condition monitoring sensor for used lubricant. The sensor was designed for direct measurement of overall quality of lubricant as to compare to unused lubricant. The system detected the relative variation of lubricant degradation i.e. degradation of physical/chemical properties, suspended wear particles and ingested contaminants, by using the grid capacitance sensor configuration. The system consisted of grid sensing unit and a multitude of small holes (1 mm in diameter) between each parallel sensing grid. The system worked on a principle of measuring for the relative variation of the dielectric constant of lubricant caused by contaminants such as water, fuel dilution, wear debris, etc. The sensor developed in this work could distinguish the relative variation of lubricant quality caused by simulated contaminants such as ferrous particles, water contamination and SiO_2 particles with significant degree of confident.

1.3.5.1.3 Sensing presence of micro-particles using image analysis methodology

Michael *et al.* [78] performed a study to monitor the effect of base lubricant and additives selection in the appearance of phantom count in the engine and hydraulic lubricant. Automatic particle counters were used to verify the cleanliness of these systems. Filtered Group I and Group III paraffinic base oils lubricants were doped with the components of an engine lubricant formulation. Particle levels were monitored before and after filtration using an on-line automatic particle counter. The results showed that base lubricant selection had minimal bearing upon appearance of phantom counts while additive selection was a significant factor. Results from three different particle counters were compared. Two laser particle counters that operate by the light-blockage principle were found to produce phantom counts from polydimethylsiloxane antifoam additives. A direct-imaging laser particle counter classified antifoam particles as water droplets and was less susceptible to phantom particle interferences from silicone antifoam additives.

In a study by Podeszwaa *et al.* [87] the dependency between amounts of rub products gathered in lubricating oil and current wear condition of engine was studied. The ferrographic method was used to monitor the presence of micro-particle in the lubricant. Images were taken from sample and magnified by fiberscope, and then converted by charge-coupled device (CCD) camera into digital. Then the captured images were analyzed by computer software, using fast Fourier transform (FFT). Based on the results from the analysis the images were classified in one of the four diagnostics levels.

1.3.5.1.4 Sensing presence of micro-particles using optical sensing method

Yonghui *et al.* [120] investigated a systematic method for analyzing wear particles in the lubricant used in a diesel engine, in a laboratory setting. This study proposed an integrated on-line lubricant monitoring system, which combined an inductive transducer with a fiber optic transducer. The inductance transducer, whose operation was based on an inductive measurement technique, could detect large ferrous and non-ferrous wear debris. The fiber optic transducer detected small particles and was used for inspection of lubricant contamination levels. The integrated lubricant monitoring system included two

transducers. The inductance transducer distinguished the ferrous and nonferrous wear particles and the particle material properties reflect the particle origins; the frequency was used for estimating wear particle size. The fiber optic transducer detected small particles and be used for monitoring the lubricant contamination levels. This study concluded that the proposed monitoring system required further improvement to accurately monitor wear and lubricant conditions in industrial equipment.

1.3.5.2 Presence of water in engine lubricant

Water contamination is the second amongst most destructive contaminants. The source of water in the lubricant can be from atmosphere, condensation, or the leakage from the coolant. Water can coexist with lubricant in three forms: dissolved, emulsified, and free. When un-dissolved water is presented in the engine, it is fragmented into small sizes particles and remains suspended in a stable state in the lubricant. The emulsified water creates a hazy, cloudy or milky appearance changing optical and physical properties. Water also affects the lubricant by forming some chemically aggressive by-products and it can act as a catalyst to accelerate the oxidation process. Water in free or emulsified form interferes with lubricant and weakens the strength of lubricant film. The weakened lubricant film makes the machine more susceptible to abrasive, adhesive and fatigue wear.

1.3.5.2.1 Sensing presence of water using shear vibration method

Jakoby and Vellekoop [53] proposed the use of viscosity and permittivity sensors to detect the present of contaminants such as water in the engine lubricant. Permittivity measurement was based on the Maxwell–Garnett (MG) theory, using a coaxial probe, while for viscosity microacoustic viscosity sensor was used. This study concluded that microacoustic viscosity sensor was capable to evaluate the viscosity of the base liquid (lubricant) independently of apparent water contamination.

1.3.5.2.2 Sensing presence of water using tuning fork quartz resonator method

Dobrinski *et al.* [32] developed a multi-sensor capable of measuring several independent lubricant parameters (viscosity, density, permittivity, conductance, level, temperature) continuously. It comprised an ultrasonic transducer for the lubricant level detection as well as a tuning fork mechanical resonator for the lubricant condition measurement. Both elements were realized as small multi-chip modules, which were combined within a mechanical flange. The raw data was transmitted to an external ECU and a complementary software module provided the lubricant condition for user. This study investigated the effect of water in lubricant to dynamic viscosity, density, and permittivity. It conclude the proposed sensor was successful to fulfill its purpose to monitor the lubricant level and condition, and also to provide a lubricant management system for vehicle to provide lubricant change based on the operating condition and driving habit and for different types of vehicles.

1.3.5.2.3 Sensing presence of water using capacitive sensor method

Duchowski and Ringholm [35] introduced a multi-sensor array consist of mass-sensitive quartz crystal (QCM), resistance temperature detection (RTD), capacitor with polyimide dielectric and an inner digital capacitor sensor to measure relative viscosity, temperature, moisture and dielectric, respectively. The preliminary results indicated that the multi-sensor array was able to measure relative viscosity, temperature, dielectric constant and contaminants in the engine lubricant. However, the lack of response to characterizing ageing processes in different fluid classes was considered to be the next step into the applicability of this sensor.

1.3.5.2.4 Sensing presence of water using electrochemical impedance spectroscopy method

Byington *et al.* [18] have developed an on-line sensor with analog and digital electronics enabling to perform fluid interrogation, operate contaminant classifier algorithms, trend specific estimated contaminant, implement higher level of communication protocol, and

enable prognostics of future lubricant quality or contaminant level. The sensor employed a low-powered, broadband electrochemical impedance spectroscopy (EIS) coupled with multi-sensor fusion and a model based analysis package designed to be capable of predicting fluid quality and degradation for a range of fluid systems. Classifier architecture selected for the identification of fuel, water, and soot within diesel lubricant. The results from the proposed sensor were compared to the measurements provided by conventional laboratories.

1.3.5.2.5 Sensing presence of water using photoacoustic spectroscopy

Foster [41] has demonstrated the feasibility of non-destructively analyzing trace level of water in petroleum-based transmission and hydraulic oil and in synthetic poly ester engine lubricant oil using photoacoustics spectroscopy (PAS). In this study the fresh lubricant of US army vehicle were used. A known amount of water was added to the samples. FTIR specimen was used with fluid cell [100 micron path length, ZnS (IRTRAN) windows]. The spectra were collected in mid-infrared region with 2 cm^{-1} resolution. This study concluded that PAS was able to detect the presence of water in transmission, engine and hydraulic lubricant, exceeding the current detection level using conventional methods.

1.3.5.3 Presence of fuel in engine lubricant

Gasoline contamination reduces the lubricant's performance by promoting early oxidation, thinning viscosity, dilution of the lubricant's additive, and increases the sulfur build-up in the lubricant. Adversely, gasoline dilution increases the wear of machine components, and increase corrosion. Hence, the presence of gasoline in engine lubricant can deteriorates the properties of lubricant much faster than any other degradation process. The contamination by unburned gasoline becomes the first and most dominant cause of degradation of engine lubricant.

1.3.5.3.1 Sensing presence of fuel using shear vibration

Durdag [37,38] introduced an AT cut thickness shear mode (TSM) device used for liquid-based application to measure the change in the lubricant condition at different fuel contamination concentration. The oscillating surface of quartz crystal in contact with liquid generated plane-parallel laminar flow. By measuring series resonant frequency and shift in frequency as a function of the square root of the density-viscosity product the change in the viscosity of liquid in contact with the sensitive film was measured. This study concluded that the designed sensor is capable of monitoring lubricant condition at different fuel contamination concentration.

1.3.5.3.2 Sensing presence of fuel using FTIR spectroscopy IR absorption method

Scherer *et al.* [97] in his contribution to engine lubricant system management discussed the utilization of online lubricant condition monitoring for diesel engine application for detection possibilities for soot contamination and diesel dilution. This study proposed use of multifunctional sensor combining a standard lubricant capacitive level sensor with temperature, lubricant microacoustic viscosity sensor, and permittivity sensor. It also considered transmissive IR-sensing methods for fuel condition monitoring. This study demonstrated the feasibility of infrared sensing for the detection of added components to standard fuels as a reliable method to monitor automotive powertrain fluid.

1.3.5.3.3 Sensing presence of fuel using HS-SPME/GC/MS and sensor array

Capone *et al.* [20,22] developed a method to detect the presence of unburned diesel fuel in used diesel fuel engine lubricant. The method was based on the use of an array of different gas microsensors based on metal oxide thin films deposited by sol gel technique on Si substrates. The sensor array, exposed to the volatile chemical species of different diesel fuel engine lubricant samples contaminated in different percentages by diesel fuel, resulted to be appreciable sensitive to them. Principal component analysis (PCA) applied to the sensor response data-set gave a first proof of the sensor array ability to discriminate among the differently diesel fuel diluted lubricating oils. Moreover, in order to get

information about the headspace composition of the diesel fuel-contaminated engine lubricants used for gas-sensing tests, the engine lubricant samples were analyzed by Static Headspace Solid Phase Micro Extraction/Gas Chromatograph/Mass Spectrometer (SHSSPME/ GC/MS).

In another study by Capone *et al.* [21] a system based on metal oxide gas micro-sensors to estimate diesel or gasoline contamination in different engine oil samples was proposed. The gas-sensing layers (undoped, Pt, Pd, Rh-doped SnO₂, In₂O₃ and mixed In₂O₃-SnO₂) were synthesized by the sol-gel method and deposited by spin-coating onto 2 mm x 2 mm silicon substrates equipped by Pt heater on the back and Pt interdigitated electrodes on the front. The sensor array was exposed to no-used and used commercial engine oil samples contaminated with different amounts of unburned fuel. The results of data analysis (DWT-based feature extraction, PCA and Gaussian mixture model (GMM) classifier) showed that different fuel contaminated used engine lubricants can be discriminated and successfully classified by the sensor array.

1.3.5.4 Presence of soot in engine lubricant

Soot is a natural by-product of combustion. Extended lubricant drain or poor combustion leads to abnormal soot accumulation that has harmful effect upon the lubricant and the machine. New environmental regulation (EPA) requirement to control atmospheric soot and nitrous-oxide (NO_x) emission using exhaust gas recirculation (EGR) will lead to increased soot loading in crankcase. Soot enters the lubricant as blow-by with combustion gases and is caused by the low compression, high fuel/air ratio, cold air temperature, lugging, and excessive idling. Soot absorbs dispersant additive molecules, causing a rapid decrease in dispersancy performance leading to a premature lubricant failure. Soot also absorbs anti-wear additives molecules, rendering them unavailable to protect machine components. Soot suspended in the lubricant increase the lubricant viscosity. The effect of soot on the machine includes filter plugging, increasing abrasive wear, and deposition formation, slug and blockage.

1.3.5.4.1 Sensing presence of soot using tuning fork quartz resonator method

Dobrinski *et al.* [32] were able to develop miniaturized measurement systems for lubricant level, lubricant condition, and lubricant temperature. The oil level sensor made use of an ultrasonic transducer to compute the oil level with a runtime measurement via a correlation process. The oil condition sensor, a Tuning Fork quartz resonator was capable of measuring the dynamic viscosity, specific density, permittivity, electrical conductance, and the temperature of the oil via the examination of the measured electrical impedance curve. In this study, the effect of soot on the dynamic viscosity and permittivity was investigated.

1.3.5.4.2 Sensing presence of soot using FTIR spectroscopy IR absorption method

Scherer *et al.* [97] investigated the exploitation of online oil condition monitoring for diesel engine application. In particular, this study showed the detection possibilities for soot contamination and diesel dilution. Transmissive IR-sensing methods for fuel condition monitoring were considered. It was demonstrated the feasibility of infrared sensing for the detection of added components to standard fuels. Based on these results, an onboard detection of fuel quality with high precision seemed possible in the future.

1.3.5.4.3 Sensing presence of soot using electrochemical impedance spectroscopy

Byington *et al.* [18] described the Smart Oil Sensor technology that employed broadband spectroscopy approaches, electrochemical techniques, and advance multi-sensor data fusion methods to present a near real-time, inline oil analysis device. The results demonstrated that the sensor was capable of detecting the level of lubricant contamination due to fuel, water and soot.

Ulrich *et al.* [110] explored the electrochemical impedance spectroscopy and multivariate data analysis to simultaneously predict the concentrations of soot and diesel in engine oil. It was found that diesel had a larger influence at lower frequencies as to compare to soot. Partial least squares modelling was used to simultaneously predict the concentrations of both soot and diesel in engine oil. Also, the influence of the oil

temperature was investigated in a preliminary experiment. This study was a part of the development of an electrochemical on-board sensor for real-time monitoring of engine oil.

1.3.5.5 Sensing coolant in engine lubricant

Coolant, always present and flowing, is a constant threat to leak into the lubricant, especially in crankcase applications. When coolant leaks into lubricant, it forms gels and emulsions and increases the viscosity of the lubricant. Coolant also increases the oxidation rate and reduces the pH to acidity region. Coolant contamination increases the wear on the machine parts by forming glycol emulsion and starvation of lubricant to the components due to increased viscosity. It also increases the corrosion effect on the part due to increase in acidity of the lubricant. However, coolant in the lubricating oil can oxidize, polymerize, esterify, evaporate, and be absorbed by lubricant filters.

1.3.5.5.1 Sensing coolant in engine lubricant using capacitive sensor method

In an attempt to determine the actual condition of the engine lubricant online, an oil-condition sensor was developed and tested by Lee *et al.* [67]. The sensor had two gold-plated parallel electrodes with a 150 μm gap between them. The performance of this sensor was based on the detection of reactivity of chemical species in the lubricant/electrode interfacial regions combined with the conductivity of charge carriers in the bulk layer of engine lubricant. With an a.c. sawtooth waveform voltage source applied to the electrodes, an oil-condition-dependent current can be collected by the sensor. The sensor fabrication was done by growing SiO_2 on a silicon wafer, followed by silicon nitride deposition, polycrystalline silicon deposition and then aluminum evaporation. Three different engine oils were tested and the output was collected every hour. To perform physical and chemical analysis, oil samples were taken every 8 hours to correlate the sensor output to the key physical and chemical properties of oil. This study concluded that the sensor showed promise for in-situ lubricant condition sensing in engine.

1.3.5.5.2 Sensing coolant in engine lubricant using electrochemical impedance spectroscopy method

Wang *et al.* [113] have made the attempt to detect glycol contamination in the engine lubricant by studying the a.c. impedance technique to measure the bulk-layer resistance of engine oil containing glycol. A current flow induced in the glycol-contamination sensor reflects not only the electro-chemical reactivity of the electrode-oil interfacial region but also the resistance of the bulk oil layer. The a.c. impedance technique can be used to measure the electrical properties of the three regions. A sinusoidal voltage was applied to the electrodes and the sinusoidal current response was measured. In this study the impedance of engine lubricant was measured over the wide range of frequencies (0.001 to 1000 Hz) at 100°C. A commercial-grade ethylene glycol and two commercial SAE 5W30, API SG engine oils, A and B were used. It was found that the bulk-layer resistance declines abruptly as the glycol concentration increased from 50 to 150 ppm. This technique suggests that the early stage of glycol leakage into the oil can be detected. It also observed that the measured bulk-layer resistance was not affected by formation of micelles between glycol and detergents/dispersants.

Wang and Lin [118] proposed utilization of lubricant condition sensor from previous work [113] and a new sensing algorithm to detect un-dispersed antifreeze. In order to detect un-dispersed antifreeze, the sensor was mounted at the bottom of the oil pan. This work demonstrated that the changes of engine lubricant resistance should provide opportunity to detect antifreeze during the early stage at a concentration of 0.5% for used engine lubricant or as low as 0.25% for fresh lubricant. This study concluded that add-on feature would not only offer more flexibility in mounting the sensor, but it would also enable the sensor to send out warning signals during early stage of antifreeze leakage.

1.3.5.6 Sensing lubricant oxidization by measuring capric acid

Carboxylic acid is an organic compound whose molecules contain carboxyl group and have the condensed chemical formula $R-C(=O)-OH$ in which a carbon atom is bonded to an oxygen atom by a solid bond and to a hydroxyl group by a single bond), where R is a

hydrogen atom, an alkyl group, or an aryl group. The first character of carboxylic acid is acidity due to dissociation into H^+ cations and $RCOO^-$ anions in aqueous solution. The two oxygen atoms are electronegatively charged and the hydrogen of a carboxyl group can be easily removed. The presence of electronegative groups next to the carboxylic group increases the acidity. In industry, higher ester of capric acid chain compounds are used as components in metalworking fluids, surfactants, lubricants, detergents, oiling agents, emulsifiers, wetting agents textile treatments and emollients. They are also used as intermediates for the manufacture of a variety of target compounds. Capric acid is an optimal model compound for oxidized engine lubricant compounds. Its chain length of ten carbon atoms turned out to be a good model for oxidized base oil components.

1.3.5.6.1 Sensing capric acid in lubricant using mass-sensitive quartz crystal microbalance

In a study by Lieberzeit *et al.* [71,70] the concept of molecular imprinting into sol–gel materials and extension from thin films to nanoparticles with different dimensions have been described. Titanate sol–gel layers imprinted with midchain carbonic acids proved highly useful for detecting engine lubricant degradation processes owing to selective incorporation of oxidized base oil components. This study showed depositing titanate MIP nanoparticles of 200–300 nm diameter on a transducer surface of QCM sensor increased the reuptake of capric acid by a factor of two and also showed a substantially extended dynamic range of the respective sensors. In engine lubricants, these sensors also exhibited two times larger effects towards waste lubricant than the corresponding sol–gel films. Preliminary measurements indicated that the increase in capric acid uptake depends on the diameter of the particles in the layer. Cross-linking the particles with a gluing layer consisting of a titanate sol resulted in very robust sensor materials.

1.3.5.7 Sensing air in lubricant

Lubricant aeration is defined as the ratio of the volume of free air to the total volume of air and lubricant. The presence of air in the engine lubricant system can adversely affect the lubrication and hydraulic functions; in some cases, severe aeration leads to hardware failures (e.g., loss of lubrication in the rotating components). The degree of aeration is

especially severe at high engine speeds because of the increased level of air ingestion into the lubricant, and because of the shorter residence time in the sump for the air bubbles to rise and escape from entering the lubricant pump inlet. The solubility of air in the engine lubricant is governed by the Bunsen coefficient or Henry's constant. The amount of air dissolved in the lubricant is proportional to the system pressure. Thus if the aeration is high at the lubricant pump inlet, it will be substantially lower when the fluid is pressurized by the pump since more air will dissolve in the lubricant. However when the pressure is released, for example, in a rotating bearing due to the centrifugal force, air will be significantly desorbed and will have an adverse effect on the system performance. Therefore, it is of interest to inventory the flow of free air into the lubricant pump inlet.

1.3.5.7.1 Sensing air in lubricant using light detecting resistor method

Manz and Cheng [75] investigated a method to measure the flow of free air to the sump pump inlet from the return oil flows in a V-6 spark-ignition passenger car engine under motoring condition using X-ray absorption method. Measurements were made at different locations in the sump representing the state of the lubricant at the pump inlet, the head return, and the timing chain return. The aeration of the block return was estimated from these measurements. At a fixed engine speed, the aeration (in % volume of air) of the head return and the chain return were about the same, and they were approximately twice the value found in the block return. This distribution did not change with engine speed. When weighted by the flow rate, however, the block return contributed to 55% of the aeration at the pump inlet; the total contribution of the head return and the chain return was 45% (36% from head return and 9% from chain return). Further aeration observations were made by comparing the cases with and without the oil sump windage tray in place. When the tray was removed, aeration at the pump inlet was found to increase by less than 30% for all speeds. Table 1 summarizes sensing parameters and sensing methodology used to monitor engine lubricant condition described in this chapter.

Table 1 Sensing parameters vs. sensors and sensing methodology

Sensing parameters		Sensor and Sensing Methodology																					
		shear vibration	mass-sensitive quartz crystal microbalance	vibration, acoustic signal	tuning fork quartz resonator	FT-IR spectroscopy	IR absorption	light scattering	capacitive sensor	corrosion sensor	CNT-based variable resistor	magnetic susceptibility balance	nuclear magnetic resonance spectroscopy	electrochemical impedance spectroscopy	HS-SPME/GC/MS and sensor array	photoacoustic spectroscopy	light detecting resistor	X-ray absorption	image analysis	optical sensing	time of flight mass spectrometry	Inductance sensing	
Physical-mechanical	complex viscosity	77,3, 7,4, 1,16 37,38 55,54 56,57 53	29 30 35 69	9, 8		69 97		11 94 105						115 116		65							
	dynamic viscosity				12 13 33 32		60, 109																
	specific density	77			12 13 33 32																		
	Electro-magnetic	permittivity	1, 55 53	35		12 13 33 32	97		1, 35 109 82 122														
		electrical conductivity				12 13		11 60	2	81													
		Impedance													73 74								
		magnetic susceptibility										105											
	Chemical	proton spin-lattice relaxation rate dispersion											10										
		total acid number (TAN)						11				81		102 111 115 117 67									
		total base number (TBN)		69				11						102									
		pH												102			65						
		oxidation index					5, 9, 64	5 9															
		general chemical properties					30 58 58								110 114					98 99			
	Optical	absorbed light intensity				27											65			98 98			
		index of refraction																		98			
	Contamination	Micro particles						15	89										78 87	120		98, 120	
		water, humidity	53	35 69		32			35, 89						18		41			98			
		unburned fuel	37 38	69		32	97								18, 110	20 21 22							
		soot				32	97								18, 110					98			
		coolant (glycol)							67						115, 118, 113								
capric acid			71 70																				
air (aeration)																75							

1.4 New developments in sensors and sensing methodologies for engine lubricant conditions monitoring

There are a variety of methods for determining the condition of lubricants, but most of these techniques fall under one of three main categories: quality, debris or elemental. A direct result of indirect measurement of a lubricant's quality can be based on additive depletion, oxidation, thermal breakdown or other physical or chemical properties. The goal of debris monitoring is to determine the presence, size and possible origin of both metallic and nonmetallic lubricant debris. Elemental monitoring uses precision equipment to determine the presence of foreign elements in the fluid system. It can also be used to measure the amount of desirable elements present (i.e. additives). In addition to the nature of lubricant analysis techniques, one must be aware of the various positions in which lubricant monitoring can occur. Lubricant monitoring can occur in three possible positions: off-line, on-line or in-line. In off-line monitoring a portion of the lubricant is sampled and analyzed away from the engine. A disadvantage of off-line monitoring is that it may be affected by a variety of influences during sampling, transport and/or testing. On-line monitoring is where a portion of the lubricant is sampled and analyzed by direct connection to the lubrication system. It has little impact on system flow, provides direct results and has little outside influence. However, like off-line monitoring, on-line monitoring can be misrepresentative of the system if the portion sampled is small relative to the system flow. In-line monitoring is where all the lubricant that passes is analyzed giving immediate results, with no outside influence. In-line monitoring can be difficult to implement and can influence the system. Note that on-line or in-line monitoring is required for real time lubricant analysis.

1.5 Remaining challenges in the development of sensors and sensing methodologies for engine lubricant condition monitoring

In the past, lubricant monitoring has predominantly been used to determine when the lubricant should be changed; however, it is now known that lubricant monitoring can also provide important information on the condition of the engine itself. Lubricant analysis

has proven to be an effective tool for determining failure modes for both equipment and the lubricant. The foremost goal of a lubricant analysis system is the early detection of lubricant degradation, contamination and machinery wear. This early detection can bring about several important benefits. Improved safety, early detection and warning of machinery failure can ensure a safer work environment. Additionally, early detection and control of the causes of lubricant degradation, contamination and wear can substantially reduce the occurrence of damage to machinery. And, early detection can result in increased equipment availability or effectiveness.

There is an increasing pressure on the auto manufacturers to provide ability to detect the degradation process taking place in the lubricant on-line or in-line. Consumer demands, government regulations, and merging new technologies are the driving force behind this demand. Within last 10 years monitoring engine lubricant has gained a significant attention. The proposed monitoring systems had used the lubricant properties, i.e. physical-mechanical, electromagnetic, chemical and optical to monitor the condition of lubricant. Physical-mechanical and chemical properties were the most popular choice and optical the least. Despite the high accuracy in optical methods, optical properties of the lubricant had not been used in full capacity to detect the state of lubricant. It is shown that changes in the optical properties are directly linked to the state of lubricant degradation and ultimately to the performance of engine. Monitoring the change in optical characteristics of engine lubricating oil such as refractive index, statistical characteristics and shape parameters have never been used. This information can be extracted from the lubricant easily by using SPR device, opto-microfluidic device with micro object. These techniques can be used as on-line optical methods to provide accurate information about the state of lubricant degradation and engine health.

1.6 Research objectives, scope and methodology

A review on the literatures indicates physical-mechanical properties of the engine lubricant are the most popular properties used to monitor the condition of engine lubricant. Researchers take advantage of correlation between physical-mechanical

properties of engine lubricant and other major key indexes such as wave propagation, impedance, or permittivity and design a monitoring system.

With respect to chemical methods, generally they are not very popular due to aging and drifting of the sensor, however chemical based methods usually use other key index such as impedance or permittivity to monitor the concentration of chemical components in the engine lubricant. These methods are mostly focused on the formation or deterioration of combustion products or additives.

Electrical properties based methods are generally inexpensive and relatively easy to design. Sensing surfaces can be chemically enhanced to increase the sensitivity of the detectors. Disadvantages of this methodology particularly with respect to engine lubricant is their lack of accuracy in high viscosity media, longevity issue, highly dependability of sensor output to the lubricant temperature, and requirement for correlation to other key index of lubricant.

Optical properties based systems usually are very accurate and reliable in their findings. Methods based on the properties such as color intensity, refractive index, and transparency are required correlation with other key indexes, while some other optical methods such as absorbance can be used directly. The ease of technology has provided the opportunity to implement some of the optical methods such as color intensity, and transparency for on-line monitoring, however, method like absorbance or transmittance are not fully implemented due to lack of technological development with hardware.

There is a great need to establish the relationship between engine performance and engine lubricant condition. It is believed engine lubricant conditions such as lubricant contamination, lubricant aeration, high viscous lubricant, low pH/corrosive lubricant and *etc.* indicate the engine health and influence engine overall performance. Engine operating condition, such, as engine load, cold starts, city/highway driving, *etc.* influences the engine lubricant condition in the span of its life. The lubricant oil reflects the performance of engine through its properties, while condition of lubricant oil can affect the performance of engine as well. This interrelationship between engine

performance and engine lubricant is an important diagnostic tool to evaluate the engine health and performance.

It is critical to identify the interrelationship between engine performance and lubricant condition. Previous studies mostly emphasis on engine lubricant condition and how to monitor the changes in its properties. Lubricant has been considered as an isolated entity and efforts have been directed toward monitoring the change in characteristics of lubricant as it deteriorates. The interrelationship between engine lubricant and engine performance has been neglected and lubricant oil has not been used as a source of information for engine health and performance.

1.6.1 Research objective

The objective of this research is to implement systems approach to monitor engine performance through engine lubricant system using new optical methodologies to detect the presence of coolant, gasoline and water in the engine lubricant and relate those findings and information to the state of engine lubricant system and eventually to the performance and health of engine. Surface plasmon resonance (SPR), statistical optical analysis and object shape-based sensing are the three optical methodologies proposed in this research. The detection of contaminants in the lubricant is based on the quantitative comparison of input and output optical signal using optical transfer function method. Presence of coolant, gasoline, and water in the lubricant can be a sign of mechanical issues in an engine. Detecting presence of these elements inside of the engine lubricant at an early stage can help to identify the state of engine health before a catastrophic failure happens. The application of this research can be extended to any mechanical system which benefits from a lubrication system i.e. CNC machines, pumps and hydraulic systems and *etc.* This research can help many industries such as auto industry in their maintenance program to perform an accurate monitoring job on machinery equipment with lubrication systems.

1.6.2 Research scope

The scope of this research will be to propose a systems approach for engine performance and health evaluation through lubricant condition monitoring based on engine

performance-lubricant condition functional interdependency and considering lubricant as a source of information on engine performance and health. The interrelationship between engine performance and engine lubricant condition suggests the application of systems approach to evaluate engine performance and health. In this approach engine lubricant system is considered as a sub-system of engine and the lubricating oil is studied as a sub-sub-system. Optical transfer function (OTF) approach is used to characterize the variation of lubricant optical properties and relate that information to the performance of the whole system. This research will introduce new optical based methodologies to detect the presence of coolant, gasoline, and water in the engine lubricant. The proposed methodologies will be verified experimentally in real time, online, and on board showing an ability to distinguish lubricant with contamination. Detecting the presence of contaminants in the lubricant is an indication of engine components defect and directly relates to the health of engine.

1.6.3 Research methodology

Lubricant performance is considered as a one of the major factors influencing engine overall performance. Main function of engine lubricant system is to provide lubrication on the moving parts to reduce friction and wear, transferring heat from mechanical components, preventing corrosion, transferring energy, contamination control by sealing engine components, engine internal cleanliness, and reduce environmental risk. It is believed that engine lubricant condition such as lubricant contamination, lubricant aeration, high viscous lubricant, low pH/corrosive lubricant etc. influence the engine overall performance. Engine operating condition such as engine load, city/highway driving, *etc.* influences the engine lubricant condition in span of lubricant life. The lubricant oil reflects the performance and health of engine through its properties, while condition of lubricant oil can affect the performance of engine as well. This interrelationship between engine performance and engine lubricant is an important diagnostic tool to evaluate the engine condition. Engine performance – lubricant condition functional interdependence is shown in Figure 1.1.

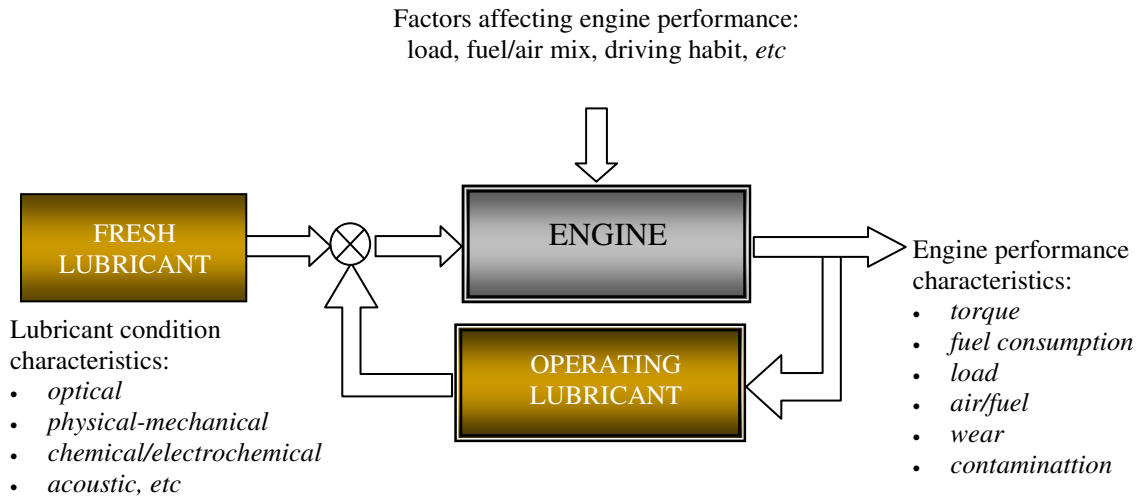


Figure 1.1 Engine performance – lubricant condition functional interdependence.

Engine lubricant can be considered as a source of critical information for engine performance and health evaluation. This information can be obtained through monitoring the variation in lubricant characteristic in relation with engine operating condition. Using engine lubricant as a source of information and monitoring lubricant condition in-situ to evaluate the performance and health of engine is an easy, inexpensive and practical method to evaluate engine performance and indicate proactive maintenance tasks. Figure 1.2 represents how lubricant condition can be used as a source of information on engine performance.

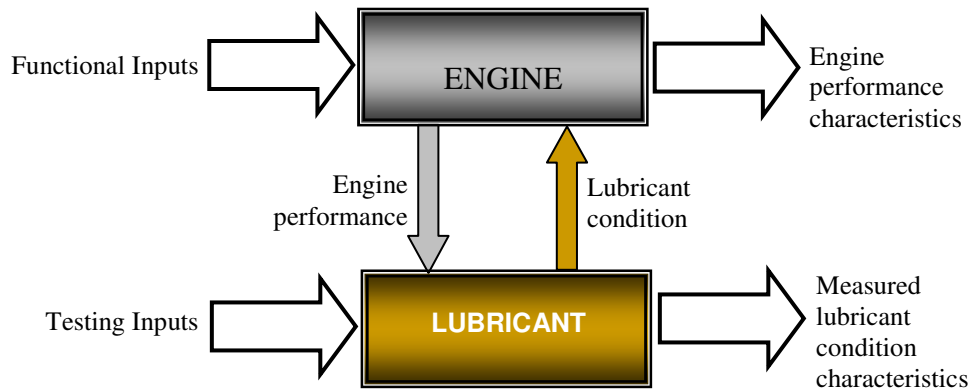


Figure 1.2 Lubricant condition as a source of information on engine performance

Characteristics of internal combustion engine and its interdependency with its sub-systems make a good application for systems approach to study the overall performance of engine in connection with lubricant system and lubricating oil at the sub and sub sub-system level. Studying the variation in engine lubricant optical characteristics provides insight into the state of lubricant system and engine health overall. Lubricant system is a closed loop system inside the engine. Lubricating oil is the working fluid inside of this closed loop system which its properties vary in an unpredictable fashion. Therefore, lubricant can be modeled as a dynamic optical medium with random characteristics. The random characteristics of medium imply the use of optical transfer function (OTF) analysis for quantitative measurement of optical properties variant in the lubricant based on the changes in input and output optical signals.

Surface plasmon resonance (SPR) measurement, Statistical optical sensing, and object shape-based optical sensing are three optical methodologies used in this research. In all these methodologies lubricant with random properties will affect and transform the characteristics of optical input. What causes the transformation of input to output signal is a distortion transformation factor imposed by the lubricant. In a case when input and output information are known or measurable, the distortion operator or the actual optical properties of the medium can be identified by removing known properties of the input

signal from the output signal.

Surface plasmon resonance (SPR) measurement has been widely used for dynamical analysis of molecular affinity and then drug screening due to its high sensitivity to the change of the refractive index of tested objects including liquid media. The effect of change in optical properties (e.g. transparency, absorption, and refractive index) of engine lubricants caused by the introduction of contaminants on the surface plasmon resonance characteristics can be investigated experimentally. Introduction of gasoline, water and coolant into the lubricant and the normal aging process affects the optical properties of liquid medium, such as transparency, absorption, and refractive index. In SPR measurement, variations in both the refractive index and absorption cause changes in the dependence of reflectivity versus incidence angle (SPR curve). This optical performance of engine lubricants can be expected and but it was never studied. The change in optical properties of engine lubricant as a liquid medium, caused by introducing contaminants and by the aging process, on the SPR characteristics will be studied. The SPR characteristics (e.g. refractivity) of engine lubricant contaminated by gasoline, water and coolant at different concentration will be measured as a function of resonance angle and analyzed with respect to different concentration of contaminants.

Statistical optical methodology is based on the theory of imaging in presence of randomly inhomogeneous media. Based on this theory, this analysis will explore the effects of light waves propagation through the lubricant acting as a random screen on the image quality.

In the methodology, an object with a known periodic shape will be introduced behind a thin film of the lubricant. A microfluidic chip will be designed, and light will be delivered into microfluidic channel where lubricant engine flows through. A CCD camera will capture the images of the known object and medium. In this case, an acquired image represents a combined lubricant-object optical appearance, where an a priori known periodical structure of the object is distorted by a contaminated lubricant. Statistical optical analysis i.e. statistical auto and cross characteristics will be used for the

analysis of combined object-lubricant images to compare the measured and calculated statistical parameters for lubricant samples.

The next proposed sensing methodology, object shape-based optical sensing methodology is based on the measurement and comparison of a set of parameters which defines the true shape of a deterministic object placed behind a thin layer of lubricant with random properties. Comparison between the extracted parameters from fresh and contaminated object-lubricant images leads to estimate and monitor the presence of contaminants in the lubricant. This approach also benefits from the theory of effect of random medium (e.g. engine lubricant) on the image quality to explain the evolution of the object caused by the random medium. In this approach, the goal is to study the geometrical properties of a deterministic object under evolution and its embedded context or medium. The embedded context or the medium which surrounds the shape is considered to be random and responsible for the evolution of the shape. In this condition, the changes in the medium directly influence the object's geometrical properties and study the pattern of change in the shape and comparing to the geometrical properties of the deterministic object enables to monitor and identify the variation in the medium.

1.7 Summary and conclusions

Monitoring automobile liquids, such as engine lubricants, has received increasing attention over last years. Sensors for automotive liquids, such as engine lubricant, can be used to detect the quality of refilled liquid, increase drain interval, reduce the environmental impact, and evaluate the performance of engine. Although functional prototypes of sensors to monitor engine lubricant properties, i.e. viscosity and soot, have been recently developed, further development of sensors lubricant condition monitoring is crucially required demanding increased functionality, durability, accuracy and applicability along with fabrication cost reduction. Also, recent developments in design, fabrication and integration of optical, electrical, mechanical, microfluidic systems open new horizons for automotive sensors applications including engine performance and lubricant condition monitoring, diagnostics, control and optimization.

Engine performance and operating condition influence the properties of engine lubricant and its degradation process. Lubricant reflects the state of health of engine at any instant through its properties. Therefore recognition and analysis of the interrelationship between engine lubricant condition through its properties and engine performance is crucial to provide an in-depth insight into the state of engine health.

The contribution of this research will be the implementation of systems approach, an intellectual discipline method to attack complex problem, for engine health evaluation through analysis of engine lubricant using optical property of engine lubricant. The optical properties of lubricant will be measured using optofluidic device which represents the use of advanced microfluidic devices to increase the functionality of photonic devices. This research will utilize surface plasmon resonance measurements, statistical optical properties and object shape statistical parameters measurement of lubricant to monitor the variation lubricant optical characteristics with respect to normal aging process and introduction of contaminants individually and combined in-vitro in real time and in-situ on-line. It is also necessary to note that this research opens a new scientific direction in engine performance evaluation through lubricant condition monitoring based on systems and statistical analysis of engine lubrication as a random media.

Chapter 2

2 Systems Approach for Monitoring Engine Performance

This chapter introduces systems approach, its characteristics and applicability for solving complex, large-scale problems in an objective, logical, complete, and thoroughly professional way. It also describes the internal combustion engine, a complex machine consisted of several sub-systems with complex interaction amongst them. The characteristics of internal combustion engine strongly suggest the application of systems approach to monitor the health of engine through monitoring engine sub-system such as lubricant system. Systems approach envisions engine lubricant system as a sub-system which its properties reflect the condition and performance of whole system. This approach tackles lubricating oil as a sub sub-system and proposes to monitor the properties of the lubricant using optical methodologies and related the obtained information to the condition and health of the engine.

2.1 Systems approach definition

In general, system approach [91] starts by definition of goals and ends with a description of a harmonious, optimum ensemble of the required humans and machines with such a significant network of flow of information and materials will cause this system to operate to solve the problem and fill the need. The approach includes use of sophisticated techniques for assembling and processing the necessary data, comparing alternative approaches as to their relative benefits and shortcomings, making sensible compromises, producing quantitative analyses and predictions where they are appropriate, seeking out judgments from experience of the past, and introducing creative innovations where they are indicated.

In particular, in the systems approach, concentration is on the analysis and design of the whole, as distinct from total focus on the components or the parts. The approach insists upon looking at a problem in its entirety, taking into account all the facets, all the intertwined parameters. It seeks to understand how they interact with one another and how they can be brought into proper relationship for the optimum solution of the

problem. This approach grasps the system and its details in many levels, decomposes a subsystem into sub-subsystems, and so on, to the last details, and changes focus to view different levels so the mind is not overwhelmed by complexity. To focus on a task, system approach abstracts and hides information, simplifies the system by treating its parts as black boxes except their interfaces. This approach in its methodology makes a complex system more tractable. This provides the opportunity to study or design a part of a systems with minimal interference from other parts or sub system.

2.2 Systems representation of internal combustion engine

The motor vehicle engine is basically a device for converting the internal energy stored in its fuel into mechanical energy. It is classified as an internal combustion engine by virtue of this energy conversion taking place within the engine cylinder.

From 1860 when Lenoir built the first engine until now, engine or internal combustion engine has evolved substantially. The Lenoir's engine was a simple two power strokes system with basic fuel, ignition and exhaust sub-systems. Today an internal combustion engine is viewed as a complex system incorporating several sub-systems, such as intake and exhaust, fuel injection, ignition, engine cooling, engine lubricant and engine control system. Each of the sub-system works in relation with other sub-system and influences the performance of the engine overall. Figure 2.1 illustrates the interrelationship amongst combustion engine sub-system and their effect on the engine outputs.

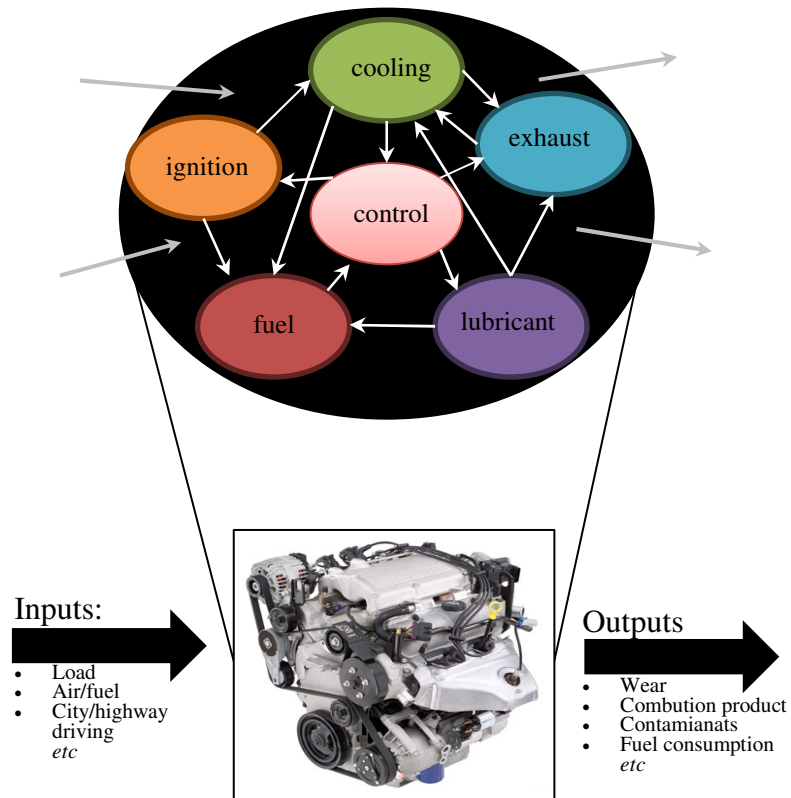


Figure 2.1 Schematic presentation of internal combustion engine sub-systems and their interrelationships

This interrelationship is more obvious in some sub-systems such as lubricant system. Engine lubricant system is a closed loop system which is responsible to reduce friction and wear, transfer heat from mechanical, prevent corrosion, transfer energy, control contamination, keeping the engine clean, and reduce the environmental risk. Engine lubricant system influences the performance of the engine and gets affected by engine performance. The main factors that can reduce the performance and life expectancy of the engine and other parts of the motor vehicle are the closely related phenomena of friction and wear, which is controlled by engine lubricant, while operating conditions, such as engine load, cold starts, driving habits, *etc.* influence the properties of engine lubricant and its degradation process. Lubricant system reflects the state of health of engine at any instant through its properties.

In engine, the beginning of a breakdown occurs thousands of miles or hundreds of hours before the breakdown itself. Sign of potential trouble usually appears first in the lubricant, the engine bloodline. Just as a human blood samples can reveal much about an individual's health, lubricant monitoring can afford critical insight not only on the optimum point at which lubricants should be changed, but when repairs might be necessary as well.

As lubricant degrades, contaminants such as water, fuel and coolant are accumulated into the lubricant. The source of water in the engine lubricant can be from a diffusion of vapor water from the atmosphere, water condensation promoted by cyclic variation of temperature, and aging of the lubricant. Diffusion and condensation of water can be enhanced due to poor crankcase ventilation, excessively worn piston rings, dramatic occurrence of water concentration, blow engine head gaskets, seal failure, or cracked water jacket. Water plays a detrimental roll to lubrication both physically and chemically.

Fuel contamination decreases the viscosity of lubricant, and this is typically leads to increased engine wear. Presence of fuel in the lubricant can be caused by leaking/defective injectors, excessive idling, incomplete combustion, worn liner/rings, and poor fuel quality.

Presence of coolant in the lubricant is an indication of mechanical failure in the cooling system. When coolant leaks into lubricant, it forms gels and emulsions and increases the viscosity of the lubricant, oxidation rate and reduces the pH to acidity region. Coolant contamination increases the wear on the machine parts by forming glycol emulsion and starvation of lubricant to the components due to increased viscosity. It also increases the corrosion effect on the part due to increase in acidity of the lubricant.

It is evident that the capability to continuously monitor engine lubricant could enable to evaluate the state of engine health.

2.3 Monitoring engine health through engine lubricant using systems approach

In previous section it was stated that engine is a complex system involving several sub-systems. The sub-systems influence the performance of engine and simultaneously interact with each other. This character provokes the idea of monitoring the engine performance through monitoring of engine sub-system such as engine lubricant system using systems approach. It was demonstrated that engine lubricant system has a strong interrelationship with performance and health of the engine. Figure 2.2 illustrates the relationship between engine performance and lubricant characteristics and how lubricant characteristics can be used as a source of information for monitoring engine performance. Engine functional inputs and engine physical states can cause variation in the properties of engine lubricant. Reversibly, lubricant with poor condition can not protect the engine and it eventually affects the performance and health of the engine. A close look at the lubricant system and lubricating oil to obtain information on the lubricant properties and relates the changes observed in the lubricant characteristics to the performance of the engine provides insight into engine performance and health state. Based on the systems approach, the engine function or performance can be considered as the whole and engine lubricant system and lubricating oil to be decomposed into sub and sub sub-system level for quantitative and objective analysis to extract information related to engine health and performance. The quantitative analysis at the sub sub-system level will provide accurate information on the lubricant characteristics which can be relayed to the engine health and performance.

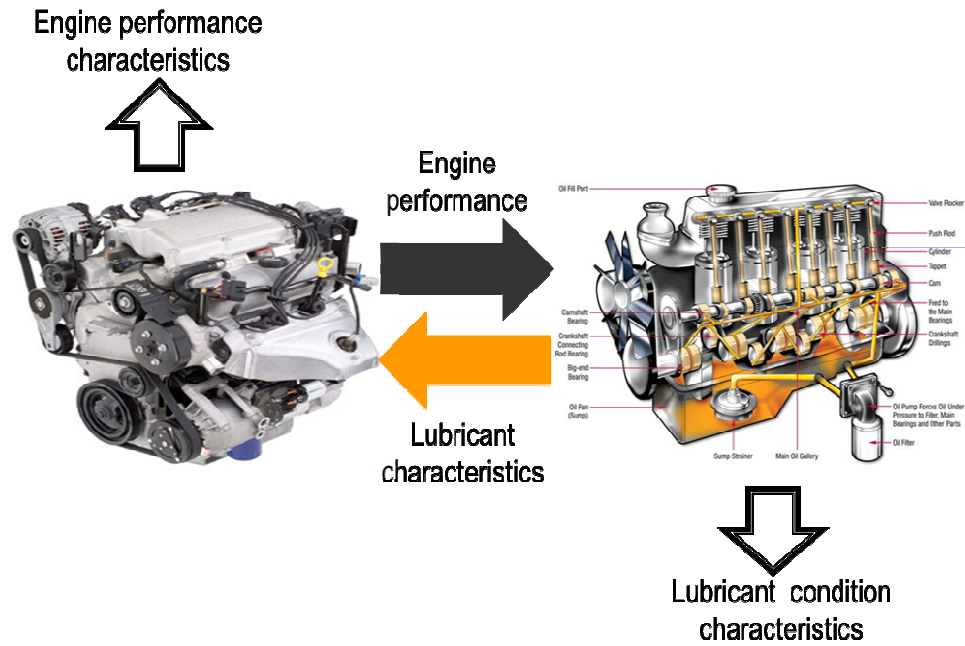


Figure 2.2 Lubricant condition as a source of information on engine performance

2.4 Analysis of engine lubricating oil

There is an increasing pressure on the auto manufacturers to be able to detect the degradation process taking place in the engine lubricant on-line. Consumer demands, government regulations, and merging new technologies are the driving force behind this demand. Within last 10 years monitoring engine lubricant has gained a significant attention [40]. The proposed monitoring systems had used the lubricant properties i.e. physical-mechanical, electromagnetic, chemical and optical to monitor the condition of lubricant. Physical-mechanical and chemical properties were the most popular choice and optical the least. Optical properties of the lubricant, despite their high precision and accuracy, had not been used in full capacity to detect the state of lubricant. It is shown that changes in the optical properties of lubricant are directly linked to the state of lubricant degradation. The obtained information from lubricant state can be directly used to evaluate the performance and health of engine. Based on the described relationship systems approach can be adopted for engine monitoring through engine lubricating oil.

Adapting systems approach allows representation of engine performance (EP) and health as a function of its sub-systems.

$$EP = f(\text{Sub-System}_{\text{intake \& exhaust}}, \text{Sub-System}_{\text{fuel injection}}, \text{Sub-System}_{\text{ignition}}, \text{Sub-System}_{\text{cooling}}, \text{Sub-System}_{\text{lubricant}}, \text{Sub-System}_{\text{control}}) \quad (1)$$

In this approach for more tractability, the relationship between engine performance and engine sub-systems can be simplified further by treating the other sub-systems as a black box without disregarding their interfaces with each other and the whole system. This provides the opportunity to study a part of the systems with minimal interference from other sub system.

$$EP = f(\text{Sub-System}_{\text{lubricant}}) \quad (2)$$

At the sub-system level, engine lubricant system's condition mainly depends on the lubricating oil characteristics flowing inside the system. This relationship allows representing the engine lubricant system condition as a function of engine lubricating oil.

$$\text{Sub-System}_{\text{lubricant}} \text{ Condition} = f(\text{Lubricating Oil}) \quad (3)$$

Lubricating oil's deterioration causes variation in the lubricant optical characteristics. Engine operating condition i.e. city or highway driving, driving habit, number of cold starts and engine condition or health are mainly responsible for lubricant characteristics variation. These factors influence the oxidation rate of lubricant directly and negatively resulting in reducing lubricant functionality life span.

$$\text{Lubricant Characteristics} = f(\text{Oxidation of Base Oil, Depletion of Additives, Contaminants}) \quad (4)$$

Equation (2), (3) and (4) illustrate how the engine performance is related to the lubricant deterioration process, therefore Equation (2) can be re-written to:

$$EP = f(\text{Oxidation of Base Oil, Depletion of Additives, Contaminants}) \quad (5)$$

Equation (5) can be further simplified to just focus on one aspect of lubricant oxidization process i.e. presence of contaminants.

$$EP = f(\textit{Presence of Contaminants}) \quad (6)$$

Equation (6) represents the relationship between engine performance and the lubricant deterioration process and in particular the presence of contaminants in the engine lubricant. In this research, coolant, water and gasoline are the three contaminants analyzed through engine lubricant to monitor engine performance.

Internal combustion engine must be provided with a system of cooling, so that it can be maintained at its most efficient practicable operating temperature. Excessive high operating temperatures would cause breakdown of the lubricating oil films, resulting in undue wearing and possible seizure of the working parts. Engine cooling system is a group of interrelated components to affect the transfer of heat. Antifreeze solution or coolant is the working fluid in the cooling sub-system. It travels through all the components of cooling sub-system to maintain the most efficient operating temperature. Conversely, coolant can be a constant threat to leak into the lubricant, especially in crankcase applications. Coolant can leak into the engine lubricant either from water jacket or engine cylinder head. Presence of coolant into lubricant is indication of engine cooling sub-system malfunction which potentially leads to deterioration of engine operation condition.

The purpose of the fuel supply system for a petrol engine is to store, transfer and filter the petrol required by fuel injection sub-system. Fuel supply system comprises of a fuel tank with pump, fuel filters and necessary pipelines to connect these services to their point of delivery. Likewise, gasoline is the working fluid in this sub-system. Presence of gasoline in the engine lubricant has a high destructive effect on the lubricating oil properties and can cause undue wearing of the working parts in the engine. The source of gasoline into the engine lubricant can be from a defected fuel supply sub-system, worn liner, or incomplete combustion process managed by central control sub-system.

Water is the second most destructive contaminant for the engine lubricant.

Presence of water into the engine lubricant can be from defected cooling system (water jacket), excessive worn piston ring, poor crankcase ventilation or seal failure. Presence of coolant, gasoline and water in the engine lubricant can be a sign of mechanical failure of engine sub-systems or components which can push the engine out of its optimum operating condition rapidly and lead to a catastrophic failure. The above facts describe the detailed technical interrelationship between engine performance and presence of coolant, water and gasoline in the lubricant and how equation (6) can be used for monitoring of engine health.

This research will use optical methods to monitor the variation in optical properties of lubricating oil. To do this, a simple optical system geometry represented in Figure 2.3 shall be adopted. In this basic set up, a transmitter with known characteristics described by intensity distribution radiates incoherently and sends optical inputs ($\mathbf{X} = const$) through lubricant. Lubricant with random properties ($\mathbf{h} = var$) will affect and transform the characteristics of optical outputs ($\mathbf{Y} = var$). The transformed/distorted optical outputs described by intensity distribution will be captured by a receiver located on the other side of passing lubricant. This basic optical configuration illustrates the foundation of optical measurement used in this research, however, the setup can be modified to measure different characteristics i.e. refractive index, statistical optical characteristics, shape parameters, intensity and *etc.*

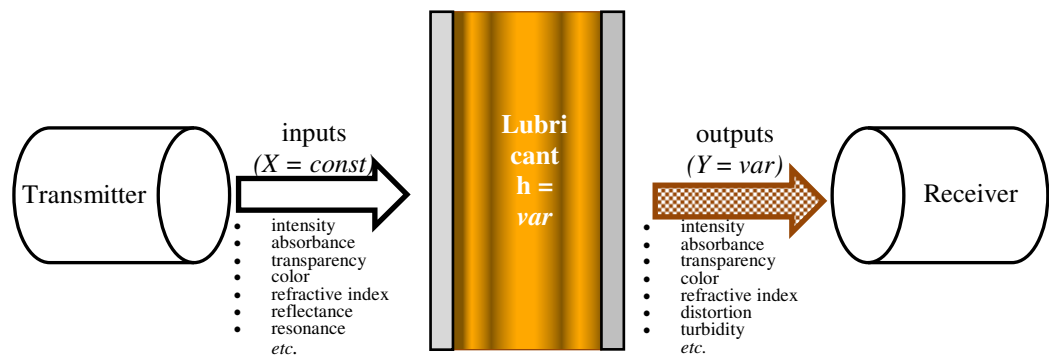


Figure 2.3 Basic optical system considered for optical analysis

In general, what causes the transformation of input signal ($\mathbf{X} = const$) to output signal ($\mathbf{Y} = var$) is a distortion transformation factor ($\mathbf{h} = var$) imposed by the lubricant. In a case when input ($\mathbf{X} = const$) and output information ($\mathbf{Y} = var$) are known or measurable, the distortion operator ($\mathbf{h} = var$) or the actual optical properties of the medium can be identified. By knowing the input signal, variations of the distortion operator can be fully described by the variations of the output signal. In general sense, by removing known properties of the input signal from the output signal, properties of the distortion operator can be obtained that will fully characterize an actual condition of the engine lubricant. The distortion operator can be described mathematically by multiplicative amplitude transmittance and it is correspondingly called a modulation transfer function of random media.

Monitoring the change in refractive index, variation in statistical optical characteristics and evolution in shape parameters have never been used to characterize engine lubricant. This information can be extracted from the lubricant easily by using SPR measurement to detect the change in reflectance or resonance angle, and applying the theory of imaging in presence of inhomogeneous medium to calculate the statistical auto and cross characteristics and shape parameters of object. These techniques can be used to provide accurate information about the state of lubricant degradation leading to monitor the performance of engine. Figure 2.4 illustrates the systems approach at the systems, sub-system and sub sub-system level.

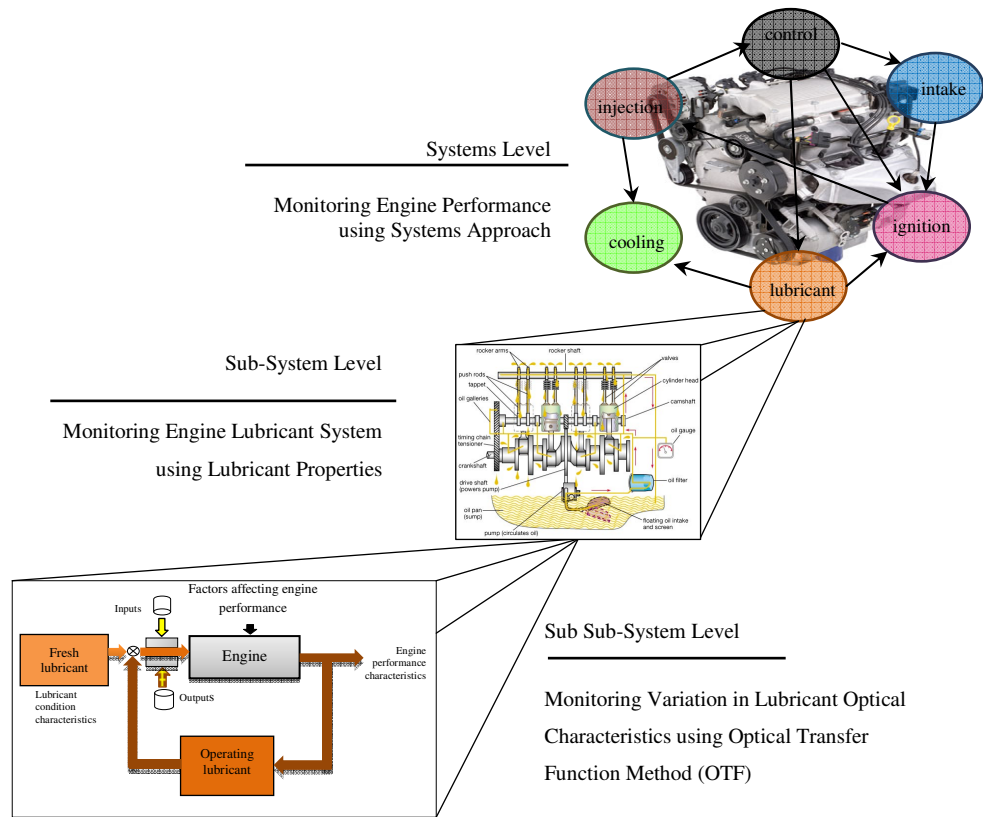


Figure 2.4 Schematic presentation of systems approach to monitor engine performance

2.5 Summary

Systems approach encompasses both the holistic and modular views. It grasps the arching features of the whole system, analyzes it into parts with proper interfaces, and synthesizes knowledge about the parts to understand the whole. This approach grasps the system and its details in many levels, decomposes a subsystem into sub-subsystems to simplifying the complexity of the problem and provides focus approach to different levels.

Internal combustion engine is a complex machine consisted of several sub-systems. Each sub-system interacts with engine and other sub-systems. The performance of the engine as whole is influenced by performance of each sub-system while, in some cases the sub-system becomes affected by engine operation. Engine lubricant system is

an important sub-system which controls the friction and wear of engine components. The life span of engine lubrication oil becomes affected by the operation condition of the engine as well. This interrelationship between engine health and engine lubricant's performance strongly suggests the application of systems approach to monitor the health of engine through analysis of lubricating oil. In this research the variation in optical characteristics of engine lubricant i.e. refractive index, statistical optical characteristics, and shape parameters will be monitored using optical transfer function (OTF) analysis. A distortion transformation factor imposed by lubricant causes the transformation of input signal to output signal. In a case when input and output information are known or measurable, the distortion operator or the actual optical properties of the medium can be identified. In general sense, by removing known properties of the input signal from the output signal, properties of the distortion operator can be obtained that will fully characterize an actual condition of the engine lubricant.

Chapter 3

3 Experimental Characterization of Contaminants in Engine Lubricants using Surface Plasmon Resonance Sensing

The purpose of this study is to develop new knowledge in experimental characterization of contaminants in engine lubricants using surface plasmon resonance (SPR) sensing that can be applicable for on-line condition monitoring of lubricant quality and engine health. The effect of change in optical properties (e.g. transparency, absorption, and refractive index) of engine lubricants caused by the introduction of contaminants, such as gasoline, coolant, and water, on the surface plasmon resonance characteristics is analyzed experimentally. In SPR measurement, variations in both the refractive index and absorption cause changes in the SPR curve, which is the dependence of reflectivity versus incidence angle. The knowledge generated in this study lays the informational basis to further develop an on-line system for engine lubricant condition monitoring using miniaturized SPR sensors fully suitable for on board applications.

3.1 Application of SPR sensors for analysis of liquids

In principle, SPR sensors are thin-film refractometers that measure changes in the refractive index occurring at the surface of a metal film supporting a surface plasmon. A surface plasmon excited by a light wave propagates along the metal film, and its evanescent field probes the medium (sample) in contact with the metal film. A change in the refractive index of the dielectric gives rise to a change in the propagation constant of the surface plasmon, which through the coupling condition alters the characteristics of the light wave coupled to the surface Plasmon (e.g., coupling angle, coupling wavelength, intensity, and phase).

The interacting molecules of the sample can be presented to the surface of a metal film in form of gaseous, aqueous, or solid. Among them, the aqueous samples provide the advantage of real time detection. The recent development in SPR sensing application has shown a substantial potential and applications in aqueous biological measurements. SPR affinity biosensors are sensing devices used in biosensing application. These

devices consist of a biorecognition element that recognizes and is able to interact with a selected analyte and an SPR transducer, which translates the binding event into an output signal. The biorecognition elements are immobilized in the proximity of the surface of a metal film supporting a surface plasmon. Analyte molecules in a liquid sample in contact with the SPR sensor bind to the biorecognition elements, producing an increase in the refractive index at the sensor surface, which is optically measured. The change in the refractive index produced by the capture of biomolecules depends on the concentration of analyte molecules at the sensor surface and the properties of the molecules. SPR biosensors are devices that are suitable for analysis of aqueous samples. Therefore, in order to detect target analyte in different real-world matrices (e.g. meat, tissue, soil and air) the analyte has to be transformed into liquid state.

SPR biosensors have been applied in numerous important fields including food safety and security, medical diagnostics, and environmental monitoring. As the acceptance of SPR biosensor technology in food analysis continues to increase, the number of publications on SPR biosensors for the detection of analytes related to food quality and safety increases. The targeted analytes include pathogens [14], toxins [84,83], drug residues [47], vitamins [19], hormones [42,42], antibodies [60], chemical contaminants [95], allergens [80], and proteins [36].

Another important field in which SPR biosensor technology has been increasingly applied is testing for veterinary drug residues (e.g., antibiotics, \hat{a} -agonists, and antiparasitic drugs) in food. Fast, sensitive, and specific detection of molecular biomarkers indicating normal biologic processes, pathogenic processes, or pharmacologic responses to a therapeutic intervention presents an important goal for modern bioanalytics. SPR biosensors have been demonstrated to hold promise for the detection of analytes related to medical diagnostics such as cancer markers [48], allergy markers [92], heart attack markers [31], antibodies [66], drugs [111], and hormones [119].

Analytes of environmental concern targeted by SPR biosensors include, in particular, pesticides [79], aromatic hydrocarbons [44], heavy metals [85], phenol [106], polychlorinated biphenyls [105], and dioxins [100]. These elements have been specifically detected by SPR biosensor.

Since the first demonstration of surface plasmon resonance for the study of processes at the surfaces of metals and sensing of gases in the early 1980s, SPR sensors have made vast advances in terms of both development of the technology and its applications. SPR biosensors have become a central tool for characterizing and quantifying biomolecular interactions. Aqueous sampling technique with its fast, sensitive, and specific detection in real time has made the SPR biosensors a promising technology for the detection of a variety of chemical and biological analytes. This technology will benefit numerous important sectors such as medical diagnostics, environmental monitoring, and food safety, security.

Application of SPR sensor can be extended into new fields such as automobile liquid sensing, machinery equipment maintenance or any mechanical system which requires liquid monitoring system. In such an application SPR sensor could be utilized to monitor the condition of liquid media i.e. lubricant, detect the presence of liquid contaminants such as coolant, gasoline and water. Application of SPR sensor into automotive liquid sensing would provide an alternative to the traditional methods of monitoring liquid media, detecting aqueous contaminants in a faster and less expensive way.

3.2 Surface plasmon resonance sensors

Surface plasmons (SP) are the electromagnetic waves within an visible and infra-red wavelength range propagating on the surface of a thin metal film at its interface with a dielectric sample (e.g. liquid media such as a lubricant). In general, an SPR sensor is an optical sensor for the detection and measuring of small changes in the refractive index of dielectric sample using the attenuated total reflection (ATR) method [90]. Typical SPR sensor with classical Kretschmann–Raether configuration consists of a high refractive index prism functioning as a light-plasmon coupler and located on a planar metal-dielectric interface as it is shown in Figure 3.1 [90]. In this configuration, when an incident light wave as a transverse magnetic (TM) polarized collimated beam with a wave vector $\mathbf{k} = k_x + k_z$ and amplitude of A_i from an excitation source propagates through the prism, one portion of the light reflects back and other portion propagates in the metal in the form of an inhomogeneous electromagnetic wave. The surface plasmon

(SP) waves (resonance oscillations) occur at the thin metal film (less than 100 nm) when the electron plasma partially absorbs the energy from the excitation source resulting in a sharp decrease in the reflected light amplitude, A_R , and it depends on the incident angle, θ , light wavelength, λ , and refractive index of the dielectric medium, which changes the propagation constant of the surface plasmon. It is also necessary to note that during SPR measurements the incident light does not propagate through the dielectric medium of the bulk sample minimizing the light absorption and scattering. Therefore SPR sensor is a highly effective tool for the measurement and on-line monitoring of the optical properties of a dielectric medium adjacent to a thin metal film.

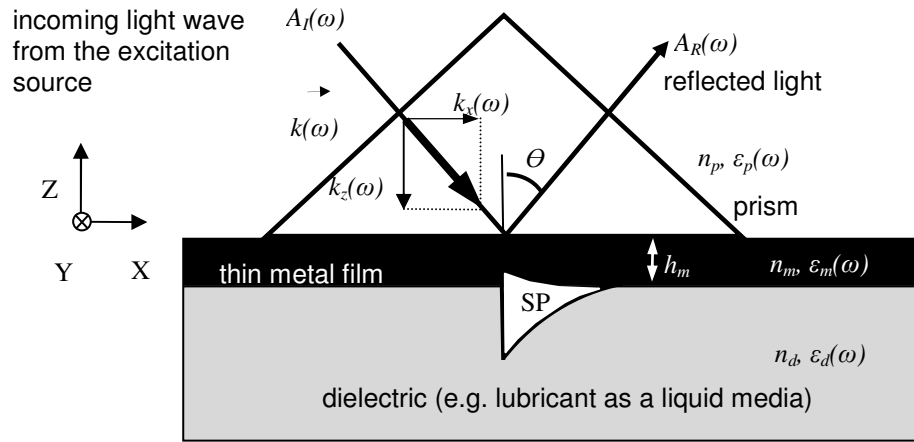


Figure 3.1 Kretschmann–Raether configuration of an SPR sensor

The linear time-invariant transformation of the incoming incident light wave, $A_I(\omega)$ into the reflected light wave, $A_R(\omega)$ by a three-layer system (prism-metal-dielectric waveguide) represented by a transfer function $W(j\omega)$ changing the amplitude and the phase angle of the incoming light wave, $A_I(\omega)$, as follows [90]:

$$A_R(\omega) = W(j\omega)A_I(\omega) = |W(j\omega)|e^{j\varphi(\omega)} \quad (1)$$

$$|W(j\omega)| = |A_I(\omega)|/|A_R(\omega)|$$

$$\varphi(\omega) = \arg(A_R(\omega)) - \arg(A_I(\omega)) = \arg(W(j\omega))$$

where ω is the angular frequency of the incident light and $j = \sqrt{-1}$ is the imaginary unit. Note that the transfer function $W(j\omega)$ can be understood as a total amplitude reflection coefficient of the prism-metal-dielectric system, $r_{pmd}(j\omega)$, and reflectivity (power reflection coefficient) for TM-polarized light wave, R , is then [50]:

$$R(\omega) = |r_{pmd}(j\omega)|^2 \quad (2)$$

The SPR measurement results are represented by an SPR curve, which is a function of the reflectivity, R versus incidence angle, θ and its form depends on variations in both the refractive index and the absorption characteristics of the sample medium. A minimum of the SPR curve $R(\theta)$ is an SPR point, $\{R_{\min}, \theta_{SPR}\}$ which is due to the maximum of energy absorption and corresponds to the SPR occurrence location. The SPR effect can be described by use of Maxwell's equations for a three-layer system [63,90] consisting of a glass prism (with a constant dielectric permittivity ε_p and refractive index n_p), a thin metal film (usually gold with complex dielectric permittivity $\varepsilon_m = \varepsilon'_m + j\varepsilon''_m$, refractive index n_m , and a thickness h_m), and a sample dielectric (medium with complex dielectric permittivity $\varepsilon_d = \varepsilon'_d + j\varepsilon''_d$ and refractive index n_d). It is assumed that two media adjacent to the metal film are semi-infinite. In practice, in order to understand the physical meaning and quantify the effect of the medium optical absorption, the following approximations are assumed: $\varepsilon'_m \gg \varepsilon''_m$ and $\varepsilon'_d \gg \varepsilon''_d$. Taking all these assumption into account, the reflectance of TM-polarized light wave in Kretschmann–Raether configuration based SPR sensor can be calculated as [63]:

$$r_{pmd}(j\omega) = \frac{r_{pm}(\omega) + r_{md}(\omega) \exp(2jk_{xm}(\omega)h_m)}{1 + r_{pm}(\omega)r_{md}(\omega) \exp(2jk_{xm}(\omega)h_m)} \quad (3)$$

with the Fresnel reflection coefficients:

$$r_{pm}(\omega) = \frac{\varepsilon_p(\omega)k_{xm}(\omega) - \varepsilon_m(\omega)k_{xp}(\omega)}{\varepsilon_p(\omega)k_{xm}(\omega) + \varepsilon_m(\omega)k_{xp}(\omega)} \quad (4)$$

$$r_{md}(\omega) = \frac{\varepsilon_m(\omega)k_{xd}(\omega) - \varepsilon_d(\omega)k_{xm}(\omega)}{\varepsilon_m(\omega)k_{xd}(\omega) + \varepsilon_d(\omega)k_{xm}(\omega)} \quad (5)$$

where wavenumbers at the material interfaces are

$$k_{xm}(\omega) = \sqrt{\varepsilon_m(\omega)\left(\frac{\omega}{c}\right)^2 - k_z^2(\omega)} = \sqrt{\varepsilon_m(\omega)\left(\frac{2\pi}{\lambda}\right)^2 - k_z^2(\omega)} \quad (6)$$

$$k_{xp}(\omega) = \sqrt{\varepsilon_p(\omega)\left(\frac{\omega}{c}\right)^2 - k_z^2(\omega)} = \sqrt{\varepsilon_p(\omega)\left(\frac{2\pi}{\lambda}\right)^2 - k_z^2(\omega)} \quad (7)$$

$$k_{xd}(\omega) = \sqrt{\varepsilon_d(\omega)\left(\frac{\omega}{c}\right)^2 - k_z^2(\omega)} = \sqrt{\varepsilon_d(\omega)\left(\frac{2\pi}{\lambda}\right)^2 - k_z^2(\omega)} \quad (8)$$

$$k_z(\omega) = n_p \frac{\omega}{c} \sin \theta = n_p \frac{2\pi}{\lambda} \sin \theta \quad (9)$$

and c is the speed of light (about 3×10^8 m/s).

Presented above mathematical description of the SPR effect lays an important foundation for the deep understanding and comprehensive interpretation of the experimental results and their physical meaning. The extensive results on numerical simulation and experimental analysis of SPR phenomenon [90,51,96] clearly highlight two main variables, a medium dielectric permittivity ε_d and thickness of the metal film h_m , that critically affects the signature of the SRP curve, $R(\theta)$, and location of the SPR point, $\{R_{\min}, \theta_{SPR}\}$. In general, the SPR angle of incidence, θ_{SPR} decreases with an increase in the metal film thickness h_m approaching a theoretical value of $\bar{\theta}_{SPR}$, when the finite thickness of the metal film $h_m \rightarrow 0$. The SPR reflectivity R_{\min} (depth of the reflectivity dip) also depends on the metal film thickness h_m having a minimum value at certain h_m . This criterion is usually used for optimization of the SPR sensor design with respect to the optimum metal film thickness h_m , which in practice is about 50 nm. A change in the medium dielectric permittivity ε_d is causing a parallel shift of the SPR curve, $R(\theta)$ along

the incidence angle axis θ . In particular, the SPR angle of incidence, θ_{SPR} shifts to the right with an increase in the medium dielectric permittivity ϵ_d . The width and asymmetry of the reflectivity curve around the SPR point, $R(\theta_{SPR} \pm \Delta\theta)$, also increases with a decreasing metal film thickness h_m . All mentioned above specific signatures of the SPR curve, $R(\theta)$, can be effectively used in the understanding how an experimentally measured reflectivity at the SPR point, $\{R_{min}, \theta_{SPR}\}$, and refractive index, R , represented by the intensity of the reflected light correlate to and describe the optical properties and the light absorption of a liquid dielectric medium (e.g. engine lubricant).

3.3 Experimental set-up and methodology

The experimental set-up used for SPR characterization of liquid medium consisted of an SPR measuring system, pumping syringe, and sample cell connected by Tygon plastic tubing with an internal diameter of 1.27 mm. The experimental set-up and schematics of SPR measurements are shown in Figure 3.2 and Figure 3.3. The SPR system (BIOSUPLAR 6, model 321) was used to measure reflectivity as a function of resonance angle obtaining optical properties of liquid medium in a view of SPR curve (reflectivity as a function of incidence angle) with resolution of 0.001° . The pumping syringe was used to deliver contaminated lubricant to the sample cell placed at SPR system. The sample cell was made of poly (methyl methacrylate) (PMMA) plastics with in-let and out-let tubes. Positioning the sample cell on top of a rubber seal formed a sample cavity, which withheld the pumped sample for SPR measurement. During measurements, contaminated lubricant was flowing through the sample cell at a low flow rate.

In general, SPR measurements are based on SPR effect when SPR measurements were performed using a laser beam ($\lambda = 632.8$ nm) passing through a glass plate serving as a semi-transparent mirror. Two photodiodes (photodiode 1 and 2, see Figure 3.3) were located adjacent to the glass plate to control the laser beam power. The polarized light beam entered the measurement prism (F1 Glass prism with 90° corner reflector with the angle 65°) mounted on the rotating drive. The right face of the prism was covered with a reflecting coating. At the end, the polarized beam was reaching the sensor chip which

consisted of the glass slide 1 mm thick with plasmon supporting coating (Au) placed upon the working surface of the prism. A drop of immersion oil (Cargille Labs, $n=1.6100\pm 0.0002$, $T = 25^{\circ}\text{C}$) between the working surface of the prism and coated glass was always applied to direct the light to the sample. A rubber seal was placed on top of the sensor slide to form a measuring cavity for sample and prevent leaks. The flow cell was placed on top of the chip and clamped.

During measurement, the angle was changing quasi-continuously over a pre-set range of 17° by a motorized prism drive. The reflected polarized light from the sensor slide was aimed at the surface of the sensor chip hitting the 90° prism wall and the mirror. Finally, the beam hit the photodiode 3, measuring the reflected beam intensity (see Figure 3.3). As a result of measurements, angular dependence of the reflected light intensity, the so-called resonant curve, was recorded. A typical measured SPR curve is shown in Figure 3.3.

The SPR curve was determined by 640 data points in the vicinity of the dip and fitting these points to a polynomial of third order and provided for visualization and data analysis by a software associated with the SPR measuring system. In general, the SPR curve had one minimum (SPR point) corresponding to the conditions where surface plasmon resonance phenomena takes place.

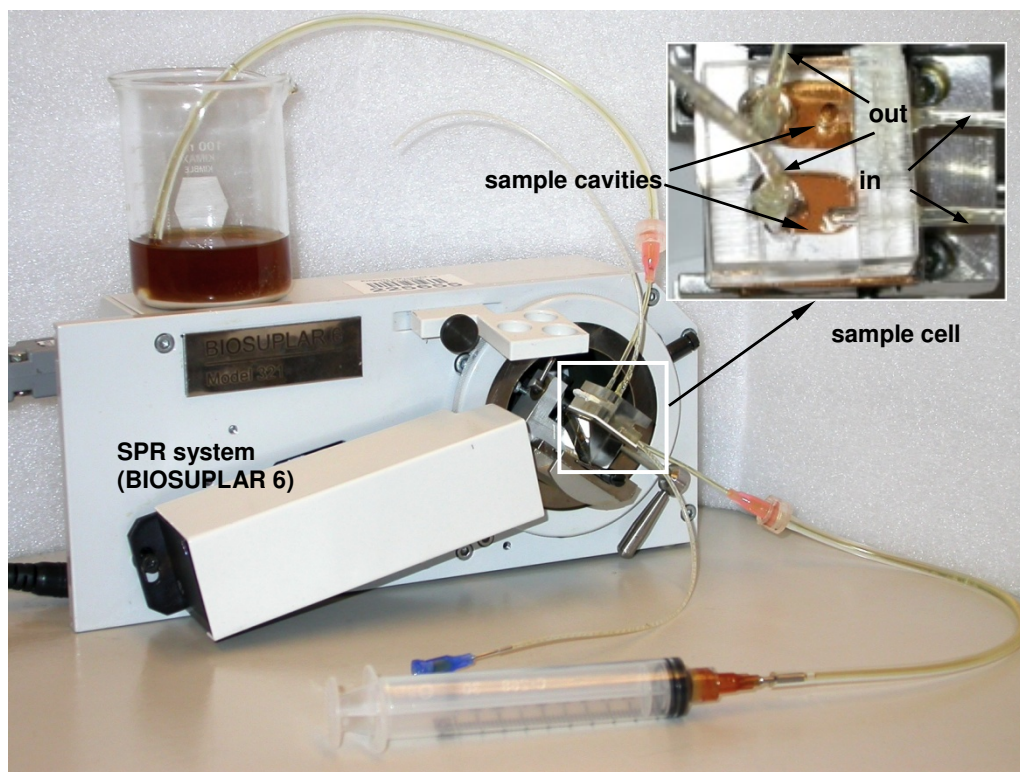


Figure 3.2 Experimental set up of SPR measurement

The preliminary experiments have shown that both coordinates of the SPR point, resonance angle θ_{SPR} and minimum reflectivity R_{min} , are sensitive to the change of optical properties of contaminated lubricant. Therefore, these two coordinates, R_{min} and θ_{SPR} , were chosen as informational parameters to study the dependence of optical properties of liquid medium (contaminated lubricant) with respect to contamination rate. The resonance angle θ_{SPR} was measured in degrees while reflectivity minimum R_{min} was reflectivity reading with arbitrary unit (r.u.). Also, having two informational parameters allowed use of Bayesian classification and pattern recognition analysis in two dimensional informational space $\{R_{min}, \theta_{SPR}\}$.

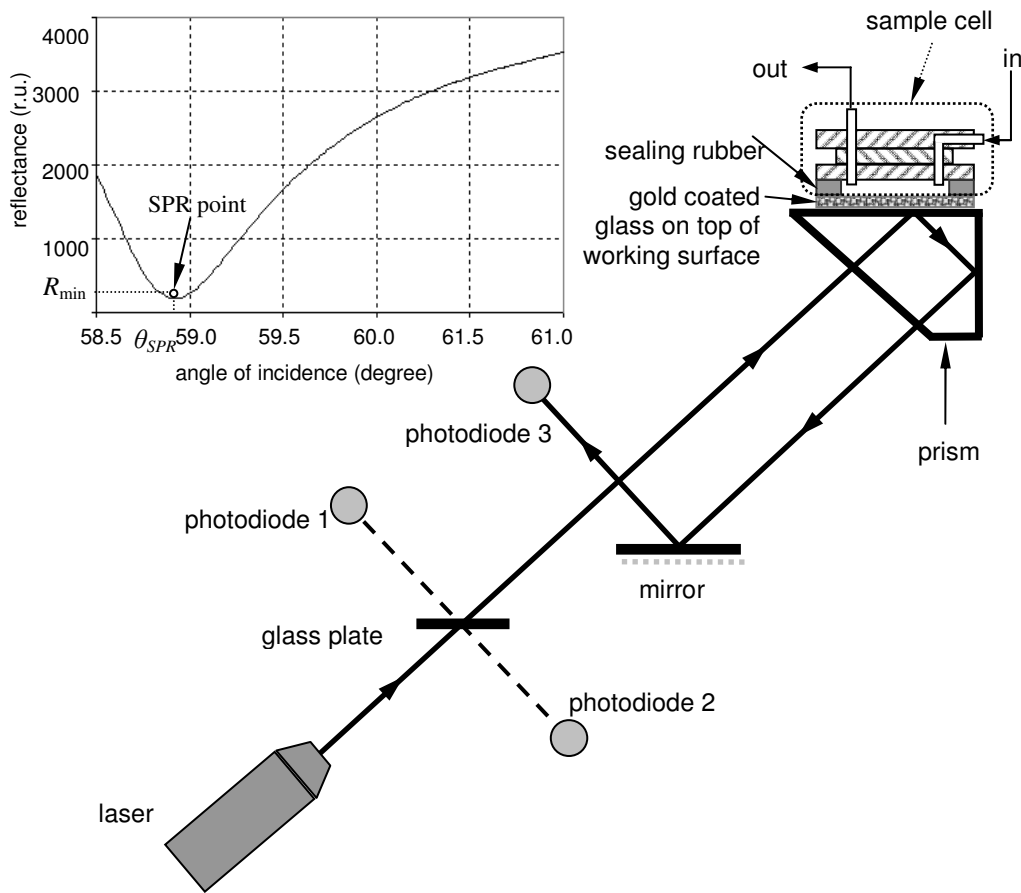


Figure 3.3 Schematics set up of SPR measurement

3.4 Results and discussion

To demonstrate the capability of SPR sensor to characterize contaminated lubricant and monitor the change in lubricant optical properties, fresh lubricant (Pennzoil 5W30) was mixed with the three fluid contaminants: gasoline, coolant, and water. In each case, 10 samples with a concentration of 1% to 10% were prepared prior to SPR measurements conducted at room temperature. For each contaminant, measurements were started with fresh lubricant, followed by the lowest to the highest contaminant concentration. Each SPR experiment was repeated five times and in order to confirm statistically the validity of the measured data standard uncertainty analysis was applied calculating 95% confidence limit. A mean value, standard deviation and confidence limit were calculated

for each R_{\min} and θ_{SPR} measurement and graphically presented as a solid line for mean value and dashed lines for 95% confidence limits.

3.4.1 SPR characterization of gasoline contamination

Figure 3.4 shows the SPR measurements and characterization of gasoline contamination in engine lubricant. In particular, changes R_{\min} and θ_{SPR} values with respect to gasoline contamination were analyzed in detail. Accumulation of gasoline in the engine lubricant causes dilution and changes lubricant color, transparency, and absorption. As a general trend, introduction of gasoline into the lubricant immediately changes its optical properties, and the SPR point is shifted to the larger angle (see Figure 3.4a) causing an increase of the R_{\min} and θ_{SPR} values.

Figure 3.4b shows the influence of gasoline contamination on the resonance angle θ_{SPR} as measured over the gasoline concentration. While concentration of gasoline was increased from 0% to 10%, the SPR resonance angle θ_{SPR} shifted from 58.859° to 59.155° (difference of 0.296°) causing average increase of θ_{SPR} value by 0.017° per 1% of gasoline contamination. Figure 3.4c illustrates the effect of gasoline concentration on the reflectivity minimum R_{\min} of the lubricant. As the gasoline concentration was increased, the reflectivity minimum R_{\min} shifted from 79.0 r.u. to 100.2 r.u. (difference of 21.2 r.u.) resulting in average increase of R_{\min} value by 1.8 r.u. per 1% of gasoline contamination. However, it is necessary to note that the most significant increase of θ_{SPR} and R_{\min} values took place due to initial introduction of gasoline. An increase of 0.049° and 5.0 r.u. was observed in θ_{SPR} and R_{\min} values at the introduction of 1% of gasoline, respectively. Above 1% gasoline contamination, θ_{SPR} and R_{\min} values increase more consistently with respect to gasoline concentration. These results also indicate that the resolution, accuracy and precision of the utilized SPR system is sufficient for reliable measurements of 1% contamination and can be used for measuring contaminants with a concentration even below 1%.

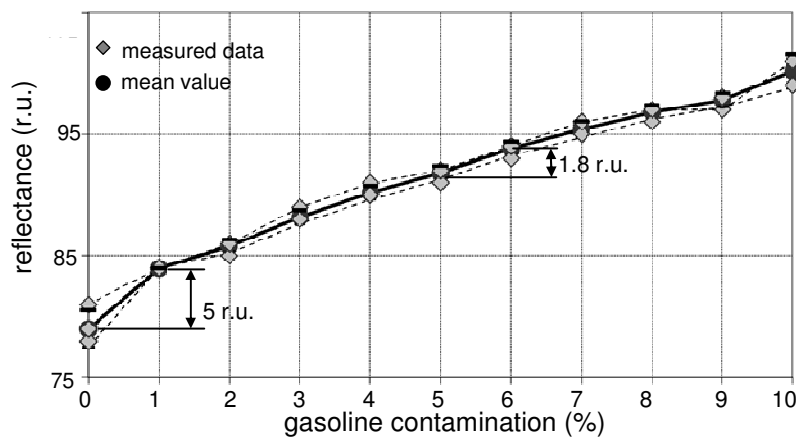
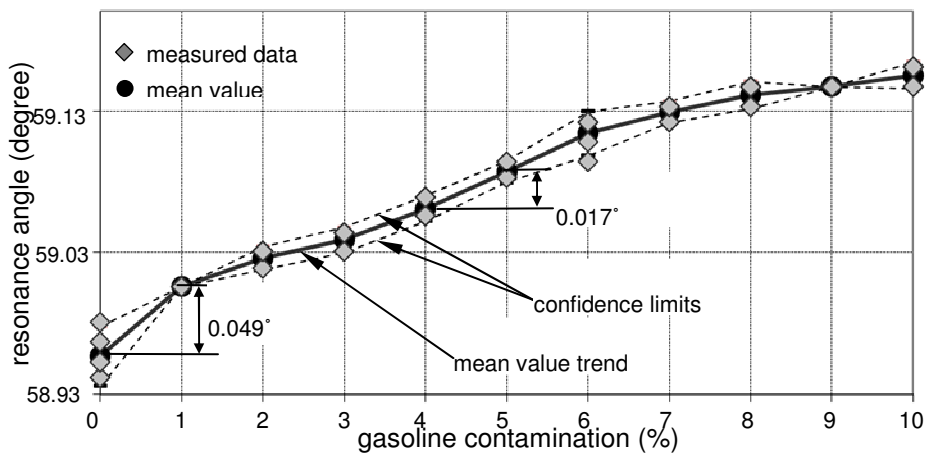
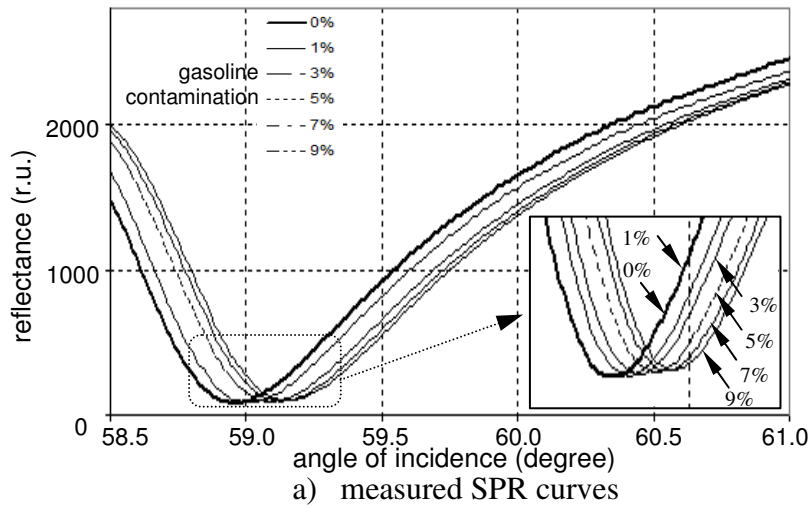


Figure 3.4 SPR measurements and characterization of gasoline contamination

3.4.2 SPR characterization of coolant contamination

The SPR measurements and characterization of coolant contamination are shown in Figure 3.5. Addition of coolant to the lubricant forms coolant emulsion particles causing changes in color, transparency, and light absorption of the lubricant. In general, the changes in the relative angular shift in the position of the SPR minimum can be ascribed to the concentration of coolant. Increase in the concentration of coolant in the sample provides a shift in angular position of the minimum of the SPR curve. Figure 3.5b represents the effect of coolant concentration on the resonance angle θ_{SPR} showing that introduction of coolant into the lubricant did not induce significant change in the θ_{SPR} values. While, as the concentration of the coolant was increased up to 10%, the resonance angle θ_{SPR} showed a shift from 58.909° to 59.038° (difference of 0.129°) having a fairly stable increase in θ_{SPR} value of 0.0129° per 1% of coolant contamination. This linear increase can be approximated by a linear equation with very high degree of correlation (see Figure 3.5b).

The effect of coolant contamination on the reflectivity minimum R_{min} is illustrated by Figure 3.5c. In general, the reflectivity minimum R_{min} is increased from 75.4 r.u. to 183.0 r.u. (difference of 107.6 r.u.) by the increase in the concentration of coolant up to 10%. However, the trend of this increase is not linear. It was observed, that before 7% coolant contamination R_{min} value is steady increased by an average rate of 4.16 r.u. per 1% increase of coolant contamination. From 7% to 10 %, the R_{min} value is changing at a much higher rate of 16.05 r.u. per 1% of coolant contamination increase.

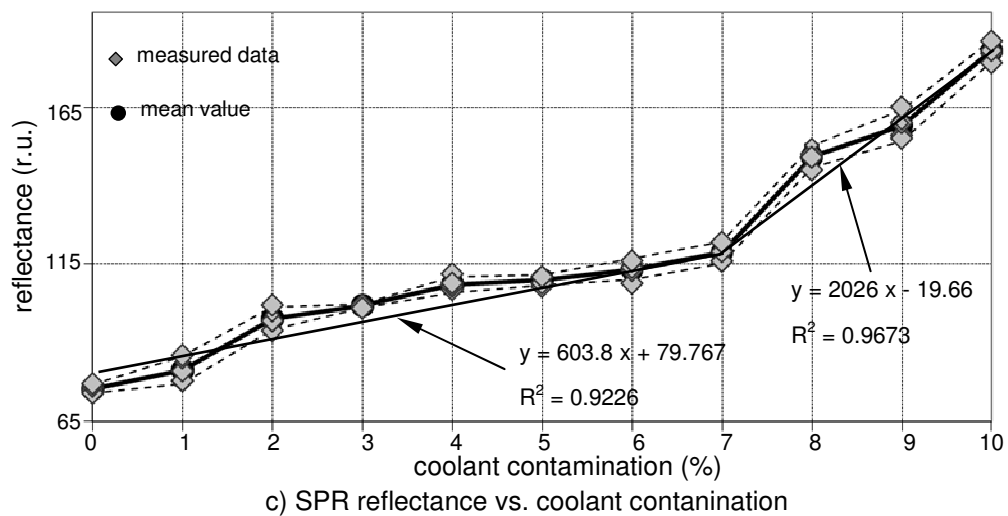
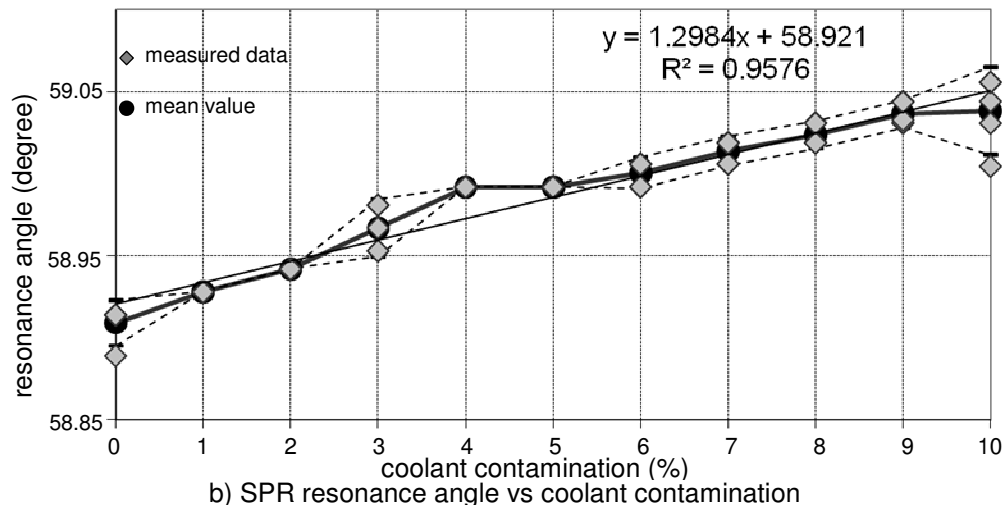
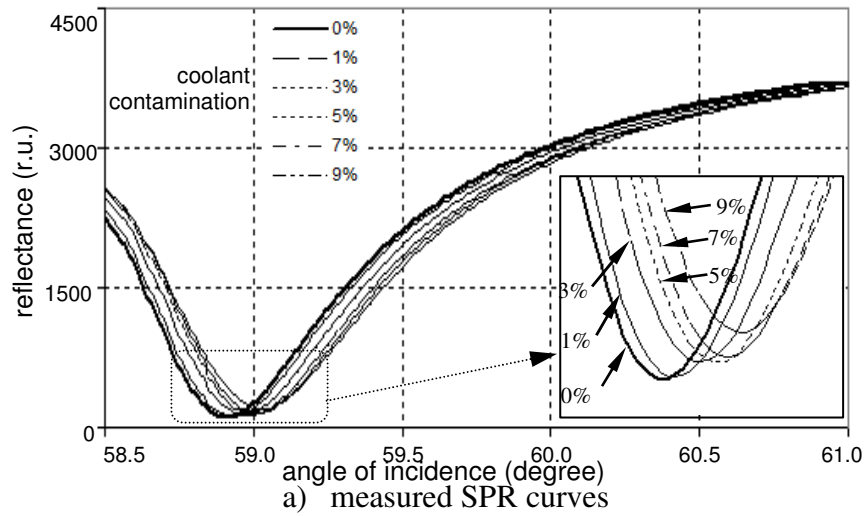


Figure 3.5 SPR measurements and characterization of coolant contamination

3.4.3 SPR characterization of water contamination

Introduction of water to the lubricant produced emulsified, hazy, cloudy appearance, which created an obvious change in the lubricant optical properties such as transparency. Figure 3.6 shows the SPR measurements and characterization of water contamination in the engine lubricant. Similar to the introduction of gasoline and coolant contaminations, water contamination also increases SPR resonance angle θ_{SPR} and reflectivity minimum R_{min} . In total, adding 10% of water contamination, the resonance angle θ_{SPR} value is increased from 58.984° to 59.117° (difference of 0.133°) and reflectivity minimum R_{min} value is increased from 78 r.u. to 107.6 r.u. (difference of 29.6 r.u.). Figure 3.6b shows the influence of water concentration between 0% and 10% on the resonance angle θ_{SPR} . It can be observed that the initial introduction of 1% of water contamination produces a most significant θ_{SPR} increase of 0.0346° with respect to a stable average rate of 0.0098° per 1% increase of water above 1% water contamination.

Figure 3.6c shows how the water contamination affects the reflectivity minimum R_{min} forming a distinct “step” phenomenon. As water contamination increases from initial introduction up to 4%, the reflectance value has very insignificant average increase of 0.64 r.u. per 1% of water contamination comparing to an average rate of 1.8 r.u. and 4.16 r.u. per 1% of gasoline and coolant contamination, respectively. However, as concentration of water increases from 4% to 6%, a significant increase in the reflectivity minimum R_{min} value of 19.4 r.u. was observed giving a significant increase of 8.7 r.u. per 1% of water contamination. For the range of water contamination from 6% to 10%, the R_{min} values were increased with an average of 1.72 r.u. per 1% water contamination. This experiment was repeated seven times and the “step” phenomenon was observed in each experiment.

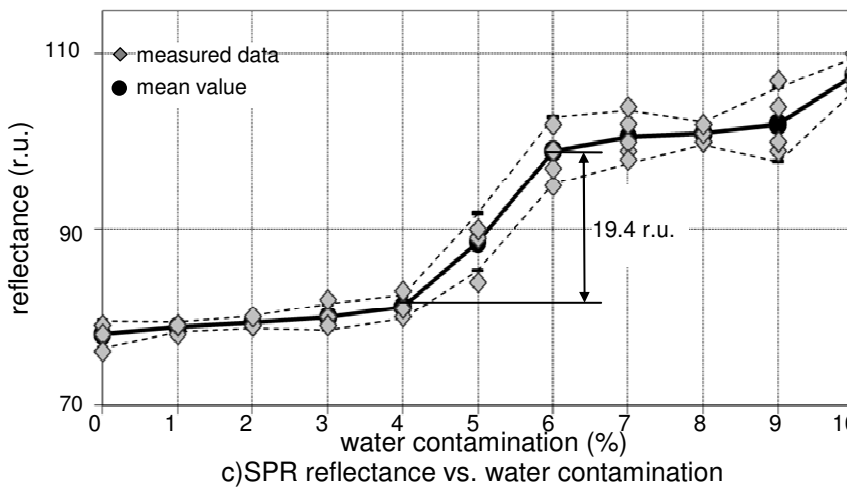
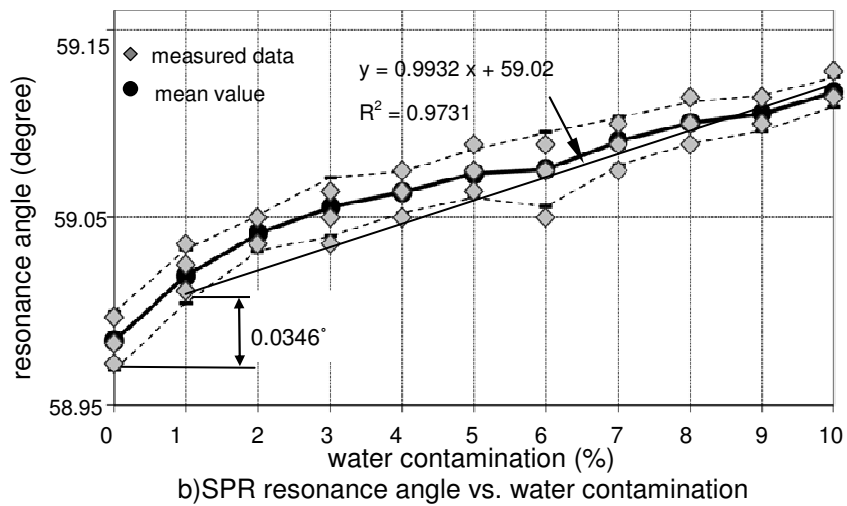
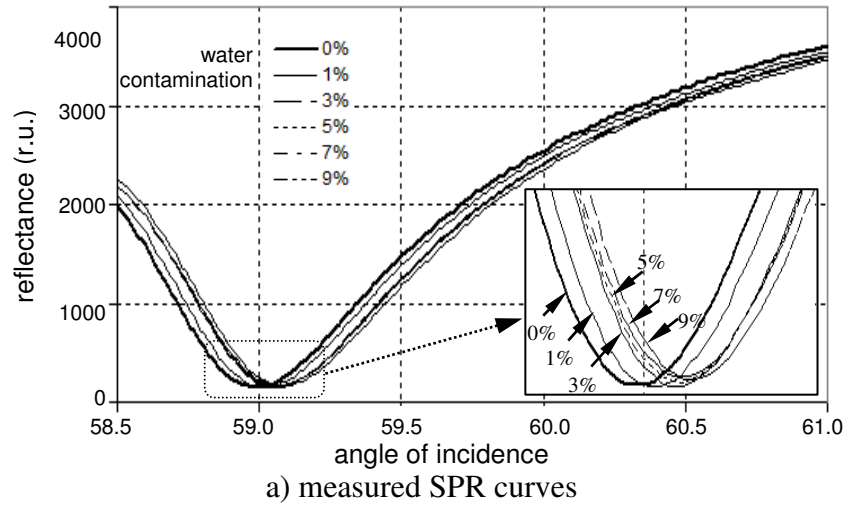


Figure 3.6 SPR measurements and characterization of water contamination

It is a general trend in all three cases of the introduction of gasoline, coolant and water contaminants that the R_{\min} and θ_{SPR} values have been increased in the accordance with a particular contaminant concentration. Taking into account the fundamentals of the SPR sensing described in Section 3.2, a physical meaning of the experimentally obtained results can be uncovered and justified. In particular, an introduction of contaminants increases the dielectric permittivity ε_d of a contaminated lubricant, which is represented by a shift of the SPR curve to the right. These results are in accordance with the experimental results obtained by Raadnui and Kleesuwan [89], where a dielectric constant of the contaminated-by-water lubricant was measured using a capacitive sensor. In addition, the introduction of contaminants shifts the SPR point upward causing an increase in the R_{\min} value. According to Eq. 3 and textbooks [90,50,96] increase in R_{\min} value is an indication of an increase of the metal film thickness h_m which is a design parameter of the SPR sensor.

3.4.4 SPR-based Bayesian classification and monitoring of lubricant condition

As for practical applications, it is very important to measure on-line actual condition and to estimate expected health of the engine lubricant. Therefore, in order to evaluate the applicability of SPR measurements for practical applications, samples of fresh (right after oil change) and used (after approximately 5000 km) lubricant (SAE 5W30) were collected from a Chevy Uplander and SPR characterization of samples was performed. The test started with the measurement of the fresh sample and followed by the used sample. Figure 3.7 shows the SPR measurements of fresh and used engine lubricant where it can be noticed that the position of the SPR resonance point shifts with respect to changes in the lubricant condition from fresh to used. In particular, the SPR resonance angle θ_{SPR} shifts from 58.8696° to 58.8796° (difference of 0.01°) the reflectivity minimum R_{\min} changes from 115.6 r.u. to 148.0 r.u. (difference of 32.4 r.u.). It is necessary to note that for an analyzed sample, the difference in θ_{SPR} values was 10 times

better than a θ_{SPR} sensitivity of 0.001° . In contrast, the difference between R_{min} values was 324 times better than a R_{min} resolution of 0.1 r.u.. As the SPR curve for a used lubricant is shifted to the right up with respect to a fresh lubricant's SPR curve and the R_{min} and θ_{SPR} values are increased (see Figure 3.7a), this indicated that the dielectric permittivity ε_d of a used lubricant is higher than for a fresh lubricant. This result obtained through the analysis of lubricant optical properties is clearly concurred with a dielectric constant-viscosity-mileage correlation measured by a capacitive sensor [109].

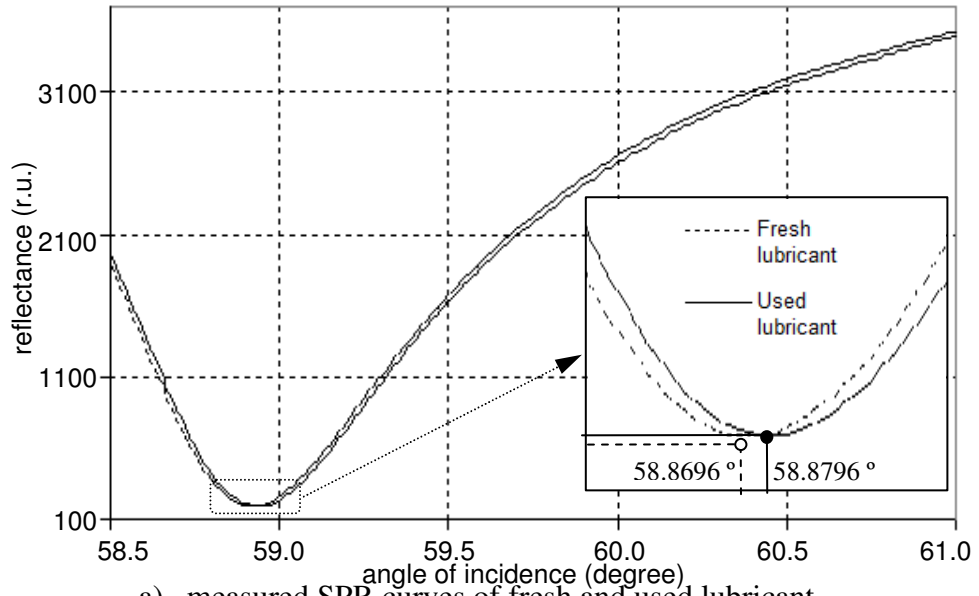
In order to analyze statistically the difference between SPR measurements of fresh and used lubricants presented by informational parameters θ_{SPR} and R_{min} , classic pattern recognition analysis [107] was applied. In general terms, pattern recognition analysis is based on the linear discriminant theory and makes it possible to separate data within n -dimensional informational space into clusters with specific and unique properties. Decisions for the separation obey strict mathematical rules called linear decision functions, which are calculated using Bayesian classifications (Bayes decision functions) and do not involve human concern or preference. Each informational parameter θ_{SPR} or R_{min} can not be used individually for proper estimation and prediction of the engine lubricant condition because the experimental data is particularly overlapped with respect to the concentration (see Figure 3.4, Figure 3.5, and Figure 3.6).

In order to implement the Bayesian classification methodology, the experimental data was re-organized into a two-dimensional informational space $\{R_{min}, \theta_{SPR}\}$ having resonance angle θ_{SPR} and reflectivity minimum R_{min} as informational coordinates. Then the ISODATA algorithm [107] was applied for automatic data separation with respect to fresh and used lubricant. The coefficients of the equation of the Bayesian classifier (Bayes decision function) were calculated with a quality of classification of 88.1% as follows:

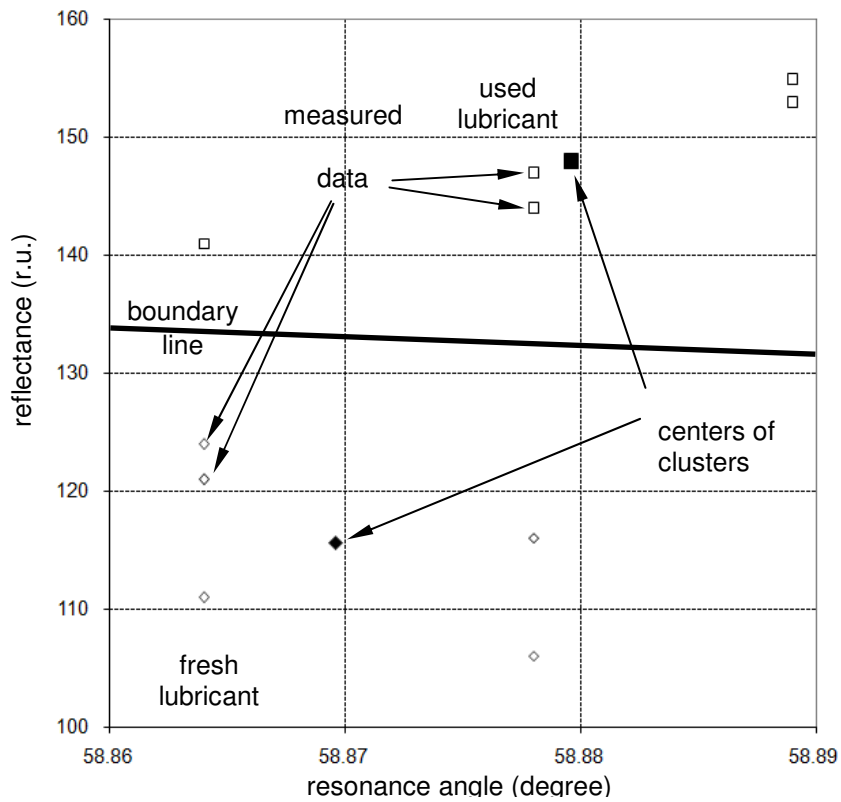
$$\begin{aligned} d_1(x_1, x_2) &= -1863539.625 * x_1 + 527.503 * x_2 + 54822428 \\ d_2(x_1, x_2) &= -1863562.205 * x_1 + 525.674 * x_2 + 54824000 \end{aligned} \quad (10)$$

where x_1 is the resonance angle θ_{SPR} (degree), and x_2 is the reflectivity minimum R_{min} (reflectance unit). In theory [107], each Bayes decision function is a function of a minimum distance pattern classifier. This means that $d_i(\cdot)$ estimates the distance between an analyzed point and the center of the i -th cluster. For practical applications, such as condition monitoring of actual engine lubricant, initially, a Bayesian classifier (e.g. Equation 10) will be developed, lubricant samples parameters θ_{SPR} and R_{min} will be placed into Bayesian classifier and distances $d_i(\cdot)$ will be calculated. Therefore, the minimum, $min(d_i(\cdot))$, indicates a cluster to which analyzed point with coordinates $\{R_{min}, \theta_{SPR}\}$ belongs and an appropriate decision is made if whether current condition is associated to fresh or used lubricant.

Figure 3.7b shows the Bayesian classification of informational parameters θ_{SPR} and R_{min} with respect to the engine lubricant condition, e.g. fresh and used lubricant. The solid thick line on the on Figure 3.7b is a boundary line calculated using Bayesian classifier (Equation 10) and it separates informational space $\{R_{min}, \theta_{SPR}\}$ in two sub-areas – upper (used lubricant) and lower (fresh lubricant). This separation can be used for practical application of engine lubricant condition monitoring. For example, a conclusion on if current lubricant is still fresh or already used can be made by placing a point with coordinates θ_{SPR} and R_{min} measured of any given time into Figure 3.7b. If a placed point is located above the boundary line (within upper sub-area) than lubricant condition is not satisfactory for optimal engine performance. In this regard, this approach can be used to predict and detect whether it is time for a lubricant change.



a) measured SPR curves of fresh and used lubricant



b) Bayesian classification of fresh and used engine lubricant

Figure 3.7 SPR measurements and Bayesian classification of informational parameters θ_{SPR} and R_{min} with respect to the engine lubricant condition

On board application of proposed measuring technique and data analysis methodology can be also economically justified by using SPR microsensors integrated with microcontrollers, e.g. single optical fiber based SPR microsensor Slavík *et al.* [101], that can be placed directly inside the engine and in this case the temperature effect on optical properties of engine contaminants will be taken into account. Use of modern SPR-based microsensors already widely used for biomedical applications [51] can significantly reduce device cost and measurement complexity providing alternative reliable, quick and inexpensive technical solution on evaluation/decision of engine lubricant condition, useful lifetime and time to change the lubricant. An additional advantage of the proposed approach over available sensors for oil change interval is in potential ability of monitoring and identification of each contaminant presented in the mixtures and recognizing of the source of engine performance degradation.

3.5 Summary and conclusions

In this study the effect of changes in the optical properties of engine lubricants caused by the introduction of contaminants, such as gasoline, coolant and water on the surface plasmon resonance (SPR) characteristics was analyzed conveying new scientific findings and analysis results which were not available before. The SPR characteristics (e.g. refractivity) of contaminated engine lubricant were measured as a function of resonance angle and analyzed with respect to different contaminant concentration (1%-10%). Also, pattern recognition analysis between fresh and used engine lubricants was performed to show applicability of Bayesian classification methodology for on-line monitoring and prediction of engine lubricant condition. From the results obtained, the following conclusions can be drawn:

- 1) It was shown experimentally that attenuation of surface plasmons due to introduction of contaminants to the engine lubricant leads to a noticeable increase in the resonance angle θ_{SPR} and reflectivity minimum R_{min} values due to an increase in the dielectric permittivity ε_d .

- 2) Introduction of gasoline into lubricant immediately changed its optical properties causing an increase in the R_{\min} and θ_{SPR} values. The most significant change in R_{\min} and θ_{SPR} was due to initial introduction of 1% gasoline to the lubricant. Above 1% of gasoline contamination, the R_{\min} and θ_{SPR} values increased more consistently with respect to gasoline concentration.
- 3) Introduction of coolant into engine lubricant did not cause any sudden increase in the R_{\min} and θ_{SPR} values. Increase in coolant concentration showed a steady increase in resonance values. The similar results were observed in reflectivity values up to 7% of concentration. From 7%, the reflectivity values were increasing at a higher rate.
- 4) Addition of 1% water into the lubricant brought a sharp increase in resonance θ_{SPR} value. Above 1% of water concentration, the θ_{SPR} value was increasing consistently. Also, the R_{\min} values were increasing at a constant rate up to 4% of concentration. From 4% to 6%, reflectivity increased dramatically forming a “step” phenomenon, and then became consistent.
- 5) Comparing the effect of different contaminations on SPR characteristics and parameters of the engine lubricant, it was found that that most significant change of the resonance angle θ_{SPR} of 0.299° , which is only 0.34% of θ_{SPR} of the fresh lubricant, was caused by the gasoline contamination and due to an increase in the dielectric permittivity ε_d . In comparison, the change in reflectivity minimum R_{\min} values was much more noticeable, e.g. 107.6 r.u. or 142.7% with respect to the fresh lubricant, when coolant was added to the lubricant. Overall, reflectivity minimum, R_{\min} is a more sensitive parameter than the resonance angle θ_{SPR} .
- 6) Although SPR measurements are reported on the detection of single contaminant, proposed approach and methodology can be applied for monitoring and identification of each contaminant presented in the mixtures.

- 7) The scientific contribution of this work was the application of systems approach, an intellectual discipline to monitor the health of engine through analysis of contaminants in the engine lubricant using SPR measurement. It was shown SPR measurement can monitor the presence of contaminants in the lubricant and this information can be related to health of engine.
- 8) The knowledge generated in this study lays the informational basis to further develop an on-line system for engine lubricant condition monitoring using miniaturized SPR sensors, e.g. single optical fiber based SPR microsensor (Slavík *et al.*, 2002), fully suitable for on board applications.

Chapter 4

4 Generalized Approach for Optical Analysis of Contaminated Engine Lubricant

This chapter describes the generalized approach for optical analysis of contaminated engine lubricant for two new methodologies for the quantitative and qualitative analysis of the presence of contaminants in the engine lubricants and the functional design of opto-microfluidic sensing device which allows to perform optical analysis on the engine lubricant on-line. The new methodologies, object shape-based optical analysis and statistical optical analysis, are based on the optical analysis of the distortion effect when an object image is obtained through a thin random optical medium (e.g. engine lubricant). The novelty of the new proposed methodologies is in introduction of an object with a known periodic shape behind a thin film of the contaminated lubricant. In this case, an acquired image represents a combined lubricant-object optical appearance, where an *a priori* known periodical structure of the object is distorted by a contaminated lubricant. In the object shape-based optical analysis, several parameters of an acquired optical image are measured. Variations in the contaminant concentration and use of different contaminants lead to the changes of these parameters measured on-line. In the statistical optical analysis methodology, statistical auto- and cross-characteristics are used for the analysis of combined object-lubricant images. Both proposed methodologies utilize the comparison of measured parameters and calculated object shape based and statistical characteristics for fresh and contaminated lubricants.

4.1 Generalized approach for optical analysis of contaminated lubricants

Physical phenomena are usually measured in terms of an amplitude-versus-time function, referred to as a time history record. The amplitude of the record may represent any physical quantity of interest. The time scale of record may represent any independent variable. Depends on the nature of phenomena, in some cases specific time history records of future measurement can be predicted with certain accuracy. However, many physical phenomena of engineering are not predictable, that is, each experiment produces

a unique time history record which is not likely to be repeated and can not be accurately predicted in detail. Such data and physical phenomena are called random. In such cases, the resulting time history from a given experiment represents only one physical realization of what might have occurred. To fully understand the data, one should conceptually think in terms of all time history records that could have occurred. This collection of all time history records which might have been produced by the experiment is called the ensemble that defines a random process describing the phenomenon. Random process or random media's properties are randomly distributed in time and space. In optics, random media has a distorting effect on the propagation of electromagnetic waves. This effect has been studied in various literatures in the past, however the effect of such a distortion on the image and characterization of the effect statistically is the subject of interest in this study.

In practice, the resolution achievable in an imaging system is limited by inherent aberrations from optical system and frequently medium through which the waves must propagate. In such a condition, the optical system may achieve actual resolutions that are far poorer than the theoretical diffraction limit. Classical optical and image analysis methods [17,121] are usually focused on the reconstruction of a true object image \mathbf{X} and recondition of characteristics and identification of parameters of an object from an observed image \mathbf{Y} . In general, only a distorted image \mathbf{Y} instead of an ideal image \mathbf{X} can be observed that can be represented by a distortion (random or deterministic) transformation $\mathbf{Y} = \mathbf{h}\mathbf{X}$. Formally, the distortion operator \mathbf{w} is defined as a digital filter to be inversely applied to restore unknown ideal/true image \mathbf{X} . Usually, the distortion operator \mathbf{h} does not have a physical meaning and it is an abstract mathematical operator that does not represent statistical properties of the actual distortion process.

However, if an object is placed behind (or into) a thin film of a random medium (e.g. lubricant) and an object image obtained, the obtained object image will be distorted by the media acting as a distortion operator. In this case, quality of the distorted object image (DOI) will mainly depend on the quality (actual condition) of the lubricant. Taking into account complex optical processes accompanying propagation of the light through the random liquid medium [45], a transformation/distortion operator \mathbf{h} gains a

mathematical notation as an optical transfer function (OTF) that represents a transformation of the original object image (OOI) into DOI. In addition, \mathbf{h} gains a physical meaning representing an optical ability of the lubricant to deliver an object image. The actual condition of the lubricant will be accountable for causing distortion, diffusion, blurring and other image quality degradation processes.

It is obvious that the distortion operator \mathbf{h} can be only identified in a case when OOI \mathbf{X} and DOI \mathbf{Y} are known. In this case, this approach for an identification of the distortion operator \mathbf{h} can be applicable for identification of the actual optical properties of the media (e.g. engine lubricant). An additional advantage of this approach is that the OOI \mathbf{X} is already known and it is a deterministic object ($\mathbf{X} = const$). Therefore, an evolution of the actual optical properties of the engine lubricant media represented by variations of the distortion operator \mathbf{h} ($\mathbf{h} = var$) can be fully described by the variations of the DOI \mathbf{Y} ($\mathbf{Y} = var$). In a general sense, by “removing” known properties of the OOI \mathbf{X} from the DOI \mathbf{Y} , properties of the distortion operator can be obtained that will fully characterize an actual condition of the engine lubricant. Another way to estimate an evolution of the actual condition of the lubricant during engine functioning is to compare the current DOI \mathbf{Y} properties with the properties of known OOI \mathbf{X} .

When DOI \mathbf{Y} is acquired through the random liquid medium (e.g. lubricant), the acquired image will contain a complex combination of original object and a liquid medium images. Therefore, the acquired image (which is the DOI) and its parameters become functionally depended on interrelated optical parameters of the object shape and media. In this case, statistical analysis of characteristics and parameters of the DOI \mathbf{Y} can be successfully applied to determine two outcomes – a) identify parameters that characterize only object and media and b) identify a functional interdependence of the known object parameters and unknown parameters of the lubricant as an image-distorting liquid medium. This is why two methodologies (*object shape-based* and *statistical optical analysis*) are necessary to be developed as an addition to each other in order to measure and analyse two afore-mentioned types (outcomes) of the complex object-liquid image parameters. *Object shape-based optical analysis methodology* is targeted to analyze the parameters of an object image distorted by the lubricant, and *statistical*

optical analysis methodology is focused on the identification of cross-correlation characteristics (e.g. OTF) of mentioned above functional interdependence that represents the distorting effect. Figure 4.1 shows a generalized schematic of two proposed methodologies for optical analysis of contaminated lubricants.

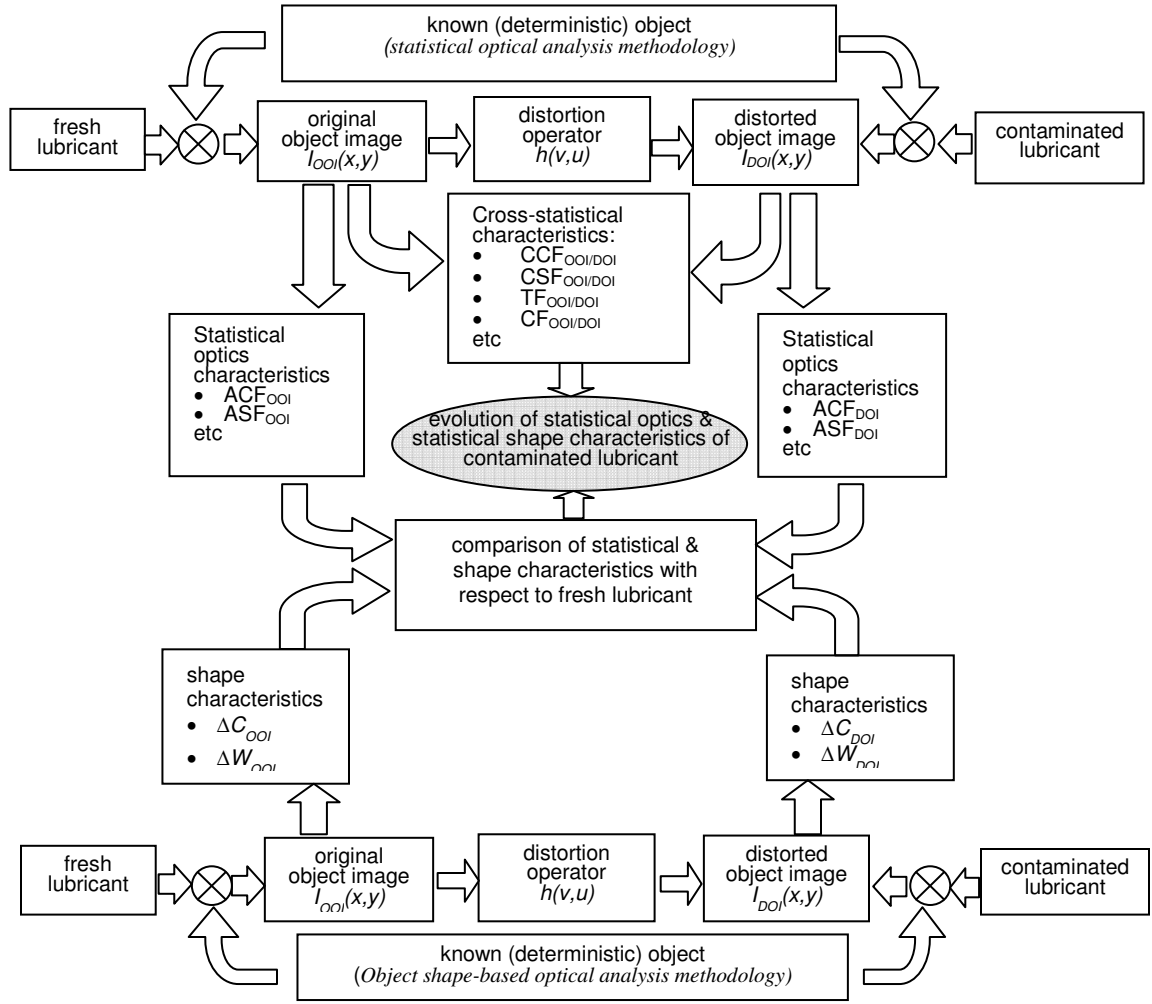


Figure 4.1 Generalized schematic of optical analysis methodologies

4.2 Functional design of opto-microfluidic sensing system

Opto-microfluidic is described as devices in which optics and fluidics replaced in a miniaturized device are used synergistically to synthesize novel functionalities. Opto-microfluidics represents the use of advanced optical elements to increase the functionality of microfluidic devices or the use of advanced microfluidic devices to increase the

functionality of photonic devices. Such integration represents a new approach to dynamic manipulation of optical systems with many applications in different fields of science. Fluidic replacement or modification leads to reconfigurable optical systems, whereas the implementation of optics through the microfluidic toolkit gives highly compact and integrated devices.

In this work implementation of optics in to a microfluidic device designed to replace a dynamic and random medium such as engine lubricant synthesizes a novel function to monitor the characteristics of the engine lubricating oil on-line and relay the obtained information to the state of engine health. The proposed are based on functional design of the opto-microfluidic sensing (measuring) system shown in Figure 4.2. In the system, the OOI is represented by an object vector $\mathbf{X} = (\xi, \eta)$ and it is described by an intensity distribution $I_{OOI}(\xi, \eta)$ radiated in a spatially incoherent fashion in the object plane. The radiation from this object propagates through and being distorted by a random media (e.g. contaminated engine lubricant). A distorted (blurred) image of the object DOI is represented by an object vector $\mathbf{Y} = (u, v)$ appeared in the (u, v) plane and it is also described by the intensity function $I_{DOI}(u, v)$. It is important to assume that the media located in the plane (x, y) is sufficiently thin that rays entering at coordinates (x, y) also leave at essentially the same coordinates. In this case, a thin liquid media can be considered as a random screen and statistical optic analysis can be applied [45,52]. Therefore, a distortion operator can be described mathematically by a multiplicative amplitude transmittance $\mathbf{h}(x, y)$, which is also called a modulation transfer function of a random media [52].

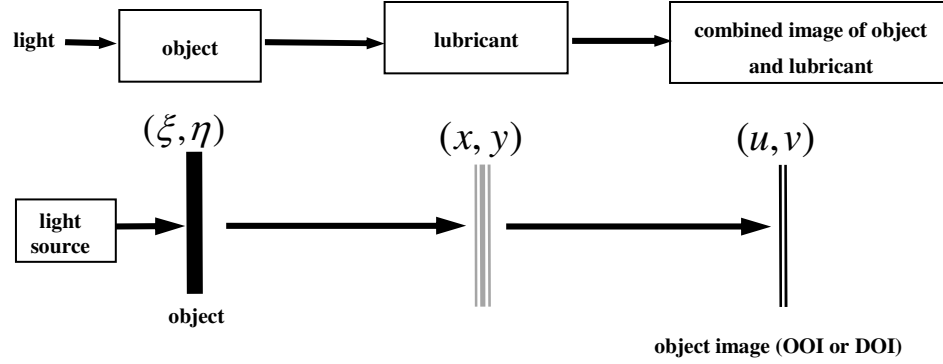


Figure 4.2 Functional design of the opto-microfluidic sensing (measuring) system

In the spatial domain, a transformation of the OOI $I_{OOI}(\xi, \eta)$ into a DOI $I_{DOI}(u, v)$ by the distortion operator $\mathbf{h}(x, y)$ can be described in general by a convolution integral:

$$I_{DOI}(u, v) = h(x, y) * I_{OOI}(\xi, \eta) = \iint h((u, v), (\xi, \eta)) I_{OOI}(\xi, \eta) d\xi d\eta \quad (1)$$

assuming that all intensity contributions in a point (u, v) add up. From the statistical optics point of view [45,52], $h((u, v), (\xi, \eta))$ is the response at a point (u, v) to a unit signal at (ξ, η) . Unfortunately, this straightforward mathematical definition of the distortion process leads to practical measurement and analysis complications. Therefore, a spatial frequency domain is more suitable after applying a Fourier transform to this convolution integral:

$$S_{DOI}(\omega, \psi) = |H(j\omega, j\psi)|^2 S_{OOI}(\omega, \psi) \quad (2)$$

where $S_{DOI}(\omega, \psi)$, $S_{OOI}(\omega, \psi)$, and $H(j\omega, j\psi)$ are the 2D Fourier transforms of $I_{DOI}(u, v)$, $I_{OOI}(\xi, \eta)$ and $h((u, v), (\xi, \eta))$, respectively. In frequency domain, $H(j\omega, j\psi)$ is called as 2D optical transfer function (OTF).

It is important to note that all statistical characteristics $S_{DOI}(\omega, \psi)$, $S_{OOI}(\omega, \psi)$, and $H(j\omega, j\psi)$ are 2D functions and therefore they are not fully suitable for real time calculations and on-line analysis. An alternative solution for these difficulties is proposed here by reducing a 2D dimension formulation (Eqs. 1 and 2) into 1D dimension case. This is possible when the OOI will have distinguished geometrical features along only one coordinate, e.g. ξ . Figure 4.3 shows an object with known periodical structure, e.g. vertical lines with a constant width τ and period T .

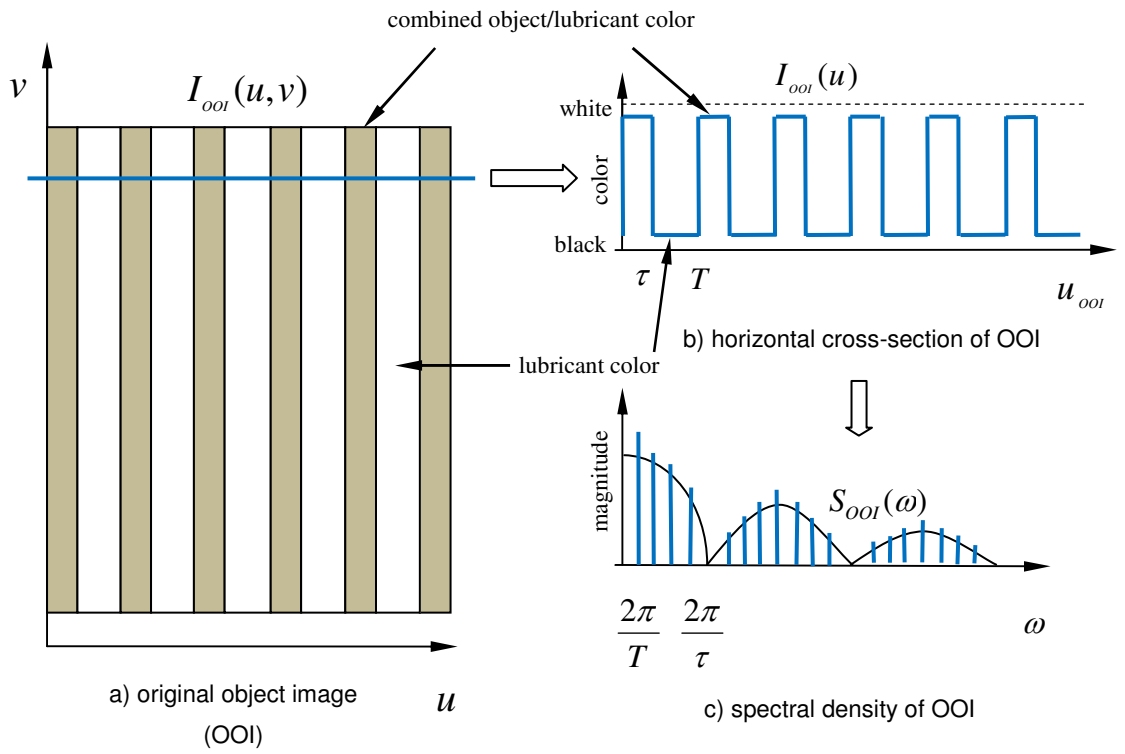


Figure 4.3 Original object image with known periodical structure and its characteristics

Such dimension reduction simplifies Equation 2 as

$$S_{DOI}(\omega) = |H(j\omega)|^2 S_{OOI}(\omega) \quad (3)$$

without losing any physical meaning and valuable information about OOI, DOI and distortion process. This also enables less complicated 1D analysis of statistical properties and characteristics of the OOI, DOI and distortion operator h .

This is a novelty of the proposed methodology consisting in introduction of an object with known periodic structure behind the optical medium, e.g. engine lubricant. In this case, an acquired image contains a synergetic effect of combined lubricant-object optical appearance, where known periodical structure of an object is distorted by a lubricant. Introduction of an object with known periodic structure significantly simplifies further medium condition monitoring through the analysis of lubricant-object combined image. This arrangement is very similar to a classic task of identification of a dynamic system with known input and output. The known periodic structure of object represents a deterministic signal with known statistical characteristics. Therefore, by measuring statistical characteristics of acquired image and comparing them with initial image, the difference in characteristics represents properties of the lubricant and it can be analysed with respect to changes in the lubricant condition providing accurate and precise estimation of contaminant presence.

4.3 Summary

Presence of contaminants such as coolant water and gasoline in the engine lubricant has a deterioration effect on the optical properties of the engine lubricant. Presence of these elements in the engine lubricant usually is a sign of mechanical failure within the engine. In this chapter, two new methodologies of object shape-based analysis and statistical optics analysis methodologies to monitor the condition of contaminated lubricants was introduced. The originality of the proposed methodology comprises of obtaining and analysis of an optical image that combines an object with known periodic shape and a thin film of the contaminated lubricant. Introduction of an object with a priori known periodical structure allowed reduction of 2D into 1D optical analysis, suitable for on-line application. The proposed sensing system utilizes the comparison of measured parameters and statistical characteristics for fresh and contaminated lubricants.

Developed statistical optical analysis and object shape-based analysis methodologies used in the proposed sensing system is a novel approach for analysis of a synergetic effect of combined lubricant-object optical appearance. It opens new opportunities for on-line monitoring, diagnostics and control of engine lubricant condition and engine performance.

In this work implementation of optics in to a microfluidic device designed to replace a dynamic, random medium such as engine lubricant synthesizes a novel function to monitor the characteristics of the engine lubricating oil on-line and relate the obtained information to the state of engine health. This functional characteristic of sensing system makes possible to implement the systems approach to monitor the health of combustion engine through analysis of contaminants in the engine lubricant.

Chapter 5

5 Object Shape Based Optical Analysis and System for Monitoring Contaminated Engine Lubricant

Presence of contaminants in the engine lubricant indicates mechanical failure within the engine and significantly reduces lubricant quality. This chapter describes a novel sensing system, its methodology and experimental verifications for analysis of the presence of contaminants in the engine lubricants. The sensing methodology is based on the object shape based analysis methodology utilizing optical analysis of the distortion effect when an object image is obtained through a thin random optical medium. Estimation of contaminant presence and lubricant condition was performed by comparison of shape parameters for fresh and contaminated lubricants. The novelty of the proposed sensing system lies within the integration of optics and microfluidic device and its functional characteristics used to obtain information on a periodic object shape placed behind a thin film of lubricant.

5.1 Object shape-based optical analysis methodology

The field of statistical shape analysis involves methods for studying the geometrical properties of random objects invariant under translation, scaling and rotation [34,26]. It is often extremely useful to measure, compare and categorize the shape of objects in a wide variety of disciplines, ranging from code recognition to medicine, archaeology, and geology. The main goal of shape analysis is the description of the mean shape of a random object and the analysis of its stochastic fluctuation. Shape analysis studies how shape changes during growth, or during evolution. This is achieved by bringing the set of shape into a frame of reference and then describing variation within the frame. Statistical-geometrical techniques are employed to study and describe the patterns of change in a shape. Applications of shape analysis are indeed concentrated in the fields of biology, geology and medicine, however, the theory and techniques can be applied to appropriate configuration matrices regardless of the discipline from which they arise.

The proposed methodology, object shape-based optical sensing methodology, is influenced by the statistical shape analysis methodology. In classical shape analysis method, the focus is to study the geometrical properties of a random object invariant under translation, scaling and rotation despite of the context which the shape is embedded in, while in the proposed methodology in this study, the goal is to study the geometrical properties of a deterministic object under evolution caused by its embedded context or medium. The embedded context or the medium which surrounds the shape is considered to be random and responsible for the evolution of the shape. In this condition, the changes in the medium directly influence the object's geometrical properties and study the pattern of change in the shape and comparing to the geometrical properties of the deterministic object enables to monitor and identify the variation in the medium. In chapter 4 the effect of random medium on the shape has been explained in details.

By knowing the effect of random medium on the shape, the next step is to define a set of parameters and then describing variation within the defined parameters amongst the set of data. Generally, selection of parameters to describe the shape is a crucial task which potentially alters the outcome of the study. Depends on the field of study these parameters can be different. In particular, to differentiate between the original object image and distorted object image, object/lubricant color parameters and shape width related parameters at object and lubricant level were selected as the defining parameters. The afore-mentioned steps require initial image processing, such as, cross-sectioning, color normalization *etc.* making optical images and data more suitable for further statistical-geometrical analysis. Performing quantitative and qualitative analysis on the shape parameters (color of lubricant and object, object shape width at object and lubricant levels, object relative color, and object width non-uniformity coefficient) of OOI and DOI provides accurate and precise estimation of medium condition $H(j\omega)$.

5.2 Opto-microfluidic sensing system, experimental set-up and measurement methodology

In this work integration of optics in to a microfluidic device designed to replace a dynamic, random medium such as engine lubricant synthesizes a novel function to

monitor the characteristics of the engine lubricating oil on-line and relay the obtained information to the state of engine health. The proposed opto-microfluidic measuring system is composed of an object located behind of a microfluidic channel with flowing contaminated lubricant and optical image acquisition system. An object with known periodic shape is placed behind liquid medium, e.g. automotive engine lubricant, and shape and statistical parameters of the acquired optical image are examined as the properties of the optical medium varies.

Generalized methodology for experimental optical analysis of contaminated lubricants is shown in Figure 5.1. Initially, the light is sent through a lubricant and object with periodic structure and a combined optical image is recorded. According to the proposed logic for further comparison, initially, optical image of a medium without distorting ingredients, e.g. fresh engine lubricant or lubricant right after oil change, will be acquired. Such an image from the undistorted optical medium and object represents the initial state or condition of the optical medium. Image from the undistorted optical medium and object represents the initial state or condition of the optical medium. As engine runs lubricant degradation process occurs leading to breakdown of hydrocarbon chains, depletion of additives, and addition of contaminants. Optical images with operating lubricant and unchanged periodical object are acquired further delivering optical information with respect to degradation of lubricant condition. Optical image analysis for both fresh and used engine lubricants consists of extraction of certain statistical characteristics and their consecutive comparison. The acquired optical data from images requires initial image processing, such as, cross-sectioning, color normalization *etc.* making optical images and data more suitable for further statistical analysis, such as object shape-based. Final step of the experimental analysis methodology is focused on a quantitative and qualitative analysis of contaminant presence and analysis of lubricant condition evolution using object shape related parameters of DOI. Comparison of these parameters and characteristics provides accurate and precise estimation of the contaminant presence. In this methodology, the object shape related parameters of the OOI for a fresh lubricant (without contaminants) are considered as a benchmark from which the evolution of the object shape related

parameters and statistical characteristics of the DOI due to the introduction of contaminants is analysed.

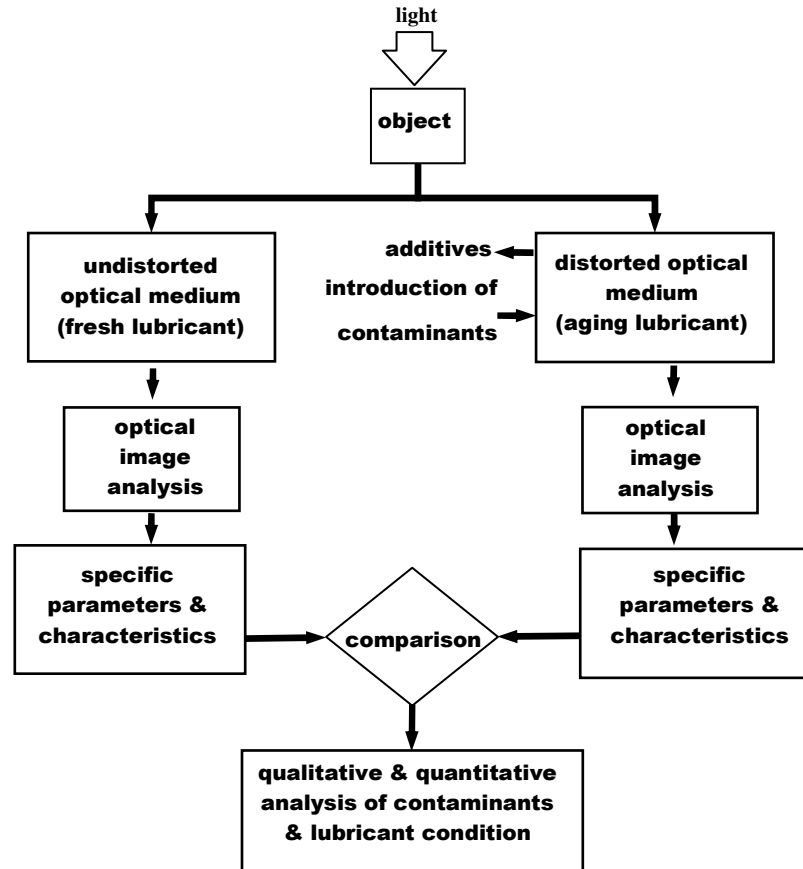


Figure 5.1 Generalized methodology for experimental optical analysis of contaminated lubricant

5.3 Functional design of opto-microfluidic system

Functional design of the opto-microfluidic measuring system (see Figure 5.2) specifies what functionalities the system should be able to perform and what design elements are necessary to have in order to perform these functions. A major function of the proposed opto-microfluidic system is the extraction of optical information for reliable

characterisation of the lubricant condition. However, analysis of the color intensity alone will not be capable of characterising the lubricant condition completely. When light propagates through the lubricant, due to the complex mixture of different contaminants, additives and wear particles, the optical properties of the lubricant, e.g. color, transparency, refractive index, absorbance, *etc.* change in a very complex manner. The introduction of gasoline can be considered as an example of this complexity, where gasoline has a diluting effect on the lubricant properties and will not alter the color sufficiently to allow detection and measurement.

A thin layer of the lubricant can be considered as a randomly inhomogeneous liquid medium and the theory of statistical optics [45,52] can be applied to fully characterize the statistical optical properties of the lubricant. This can be achieved by a functional design when light propagates through an object and random media (e.g. lubricant) and an image of the object distorted by the random media is acquired as shown in Figure 5.2. Each acquired object image, e.g. OOI and DOI, represented by an intensity distribution $I(x, y)$, has an optically valuable physical meaning. It determines that its values are proportional to the energy radiated by a physical source process (e.g. electromagnetic waves). As a consequence, every object image contains combined information of optical properties, such as illumination $i(x, y)$ and reflectance $r(x, y)$ components as $I(x, y) = i(x, y)r(x, y)$.

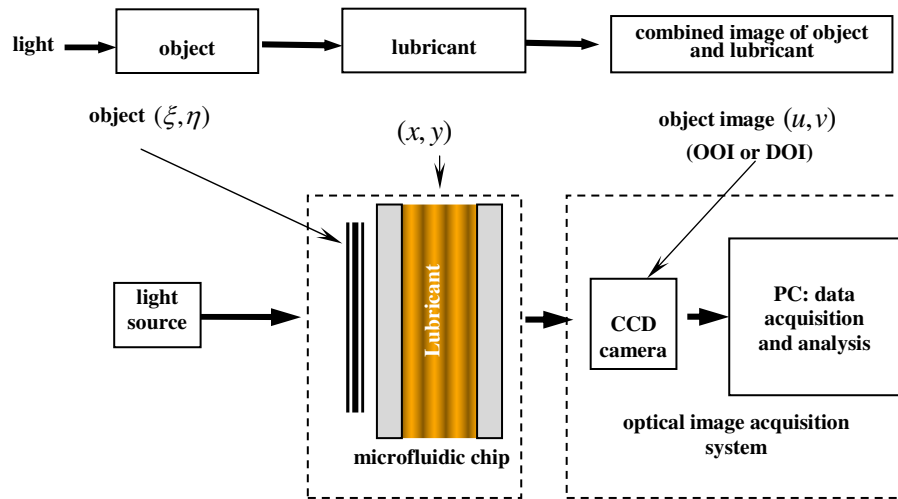


Figure 5.2 Functional design of the opto-microfluidic sensing (measuring) system

5.4 Experimental set-up

The experimental set-up used for analysis of engine lubricant consisted of a data acquisition system, micro fluid channel with in-let and out-let connections, detectable object, pumping system, and illumination source. The experimental set-up and design of a microfluidic chip are shown in Figure 5.3. The optical data acquisition system was composed of a CCD camera (Lumenera Infinity 1, Canada) with a zoom lens (Keyence, USA) of 35-245 mm focal length, mounted on an optical bench. The camera was connected to a PC equipped with imaging software (Infinity capture software, Lumenera). The CCD camera allowed capturing images from an object placed behind a medium passing through the channel with a magnification of 245x providing an overall optical magnification scale of around 2.25. The images from the camera were acquired as 8-bit 640 x 480 pixel digital bitmap files and they were digitized at 256 grey scale. The microfluidic channel was made of PMMA plastics with thickness of 1.5 mm with dimension of 170 μm deep, 500 μm wide and 50 mm long. The device was fabricated using a micro mold and hot press technique. The microfluidic channel provided a passage for the contaminated engine lubricant positioned between CCD camera and light

source. The pumping syringe was used to deliver lubricant to the microfluidic channel. The detectable object used in this set up was a 10 mm x 10 mm stainless still woven wire cloth (Tech-Met-Canada) with a mesh size of 0.065 mm x 0.065 mm and a circular wire diameter of 0.033 mm. The purpose of stainless steel woven cloth was to introduce a periodic grid into the image suitable for object shape-based and statistical optical analysis. The object was intentionally placed behind the microfluidic channel on opposite side of the CCD camera to avoid distortion of the laminar flow by the periodic structure. The visible light source (Stocker Yale, Model 21AC) with wavelength of 380-750 nm used in this study illuminated the object using two fiber light guides.

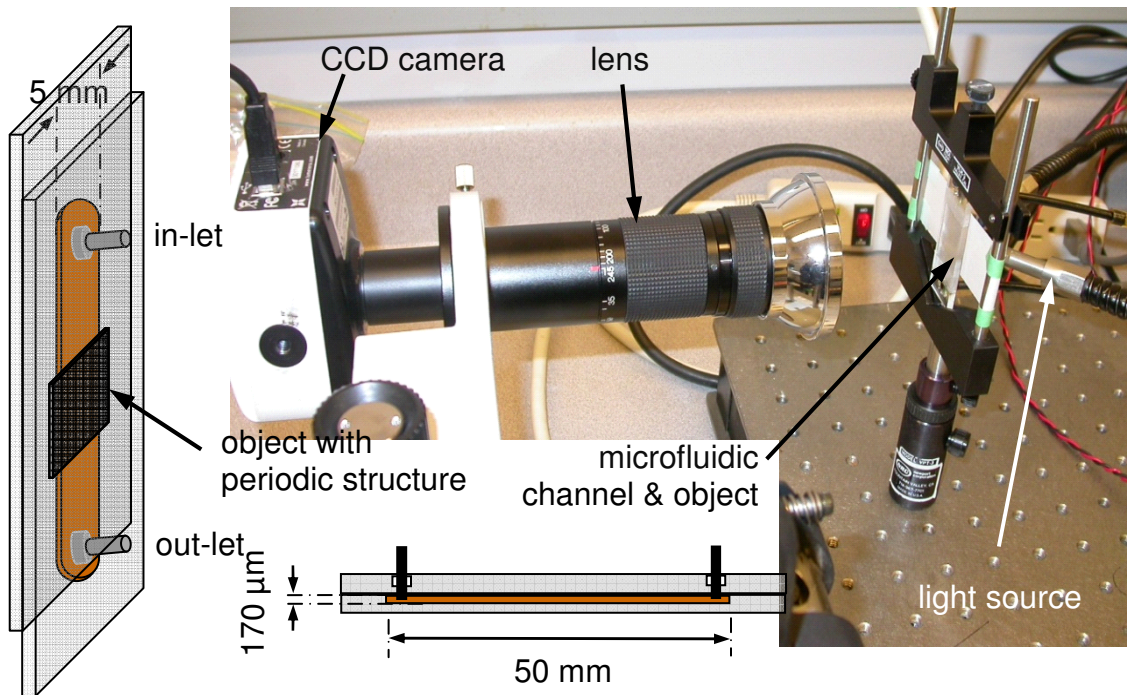


Figure 5.3 Experimental set-up and design of a microfluidic chip

5.5 Preliminary image analysis and experimental methodology

The goal of the preliminary image analysis is to extract, preliminary process, and deliver digital data suitable for further optical analysis. Initially, an optical image of the flowing lubricant and object with periodic structure is acquired as a two-dimensional matrix with respect to the color of each pixel and its X-Y position. In the initially acquired optical

image, the woven cloth provides a square grid represented by dark color having the engine lubricant flowing through within the grid with a constant period T .

During the next step, three image cross-sections at the mid-distance between two horizontal grid lines are selected and extracted to confirm statistically the validity of the measured data. Each image cross-section contains four intersections with vertical grid lines surrounded by lubricant image on each side forming an object shape as a vector of 640 pixels. For better physical understanding of object shape, the pixel values of each image cross section are normalized ranging between 0 (black) to 1 (white). Mapping of pixel color scale (between 0 and 1) vs. pixel position forms the color cross-section. The color cross-section is pre-processed data ready for further analysis of lubricant condition and contaminant presence. Typically this cross-section has a number of peaks and valleys corresponded to the number of vertical lines represented a periodical structure of the object. The peak values (close to white color) correspond to the lubricant color passing through the microfluidic channel without interference with object, while the valleys corresponded to the combined color of the object affected by lubricant. It is necessary to note the normalized image cross-sections should not be averaged into one image cross-section with respect its corresponding location, because in this case the information about deviations of the object shape-based parameters and statistical characteristics will be lost. The preliminary image analysis was done using imaging standard function from MATLAB software (see Appendix A). Figure 5.4 illustrates the schematics of preliminary image analysis.

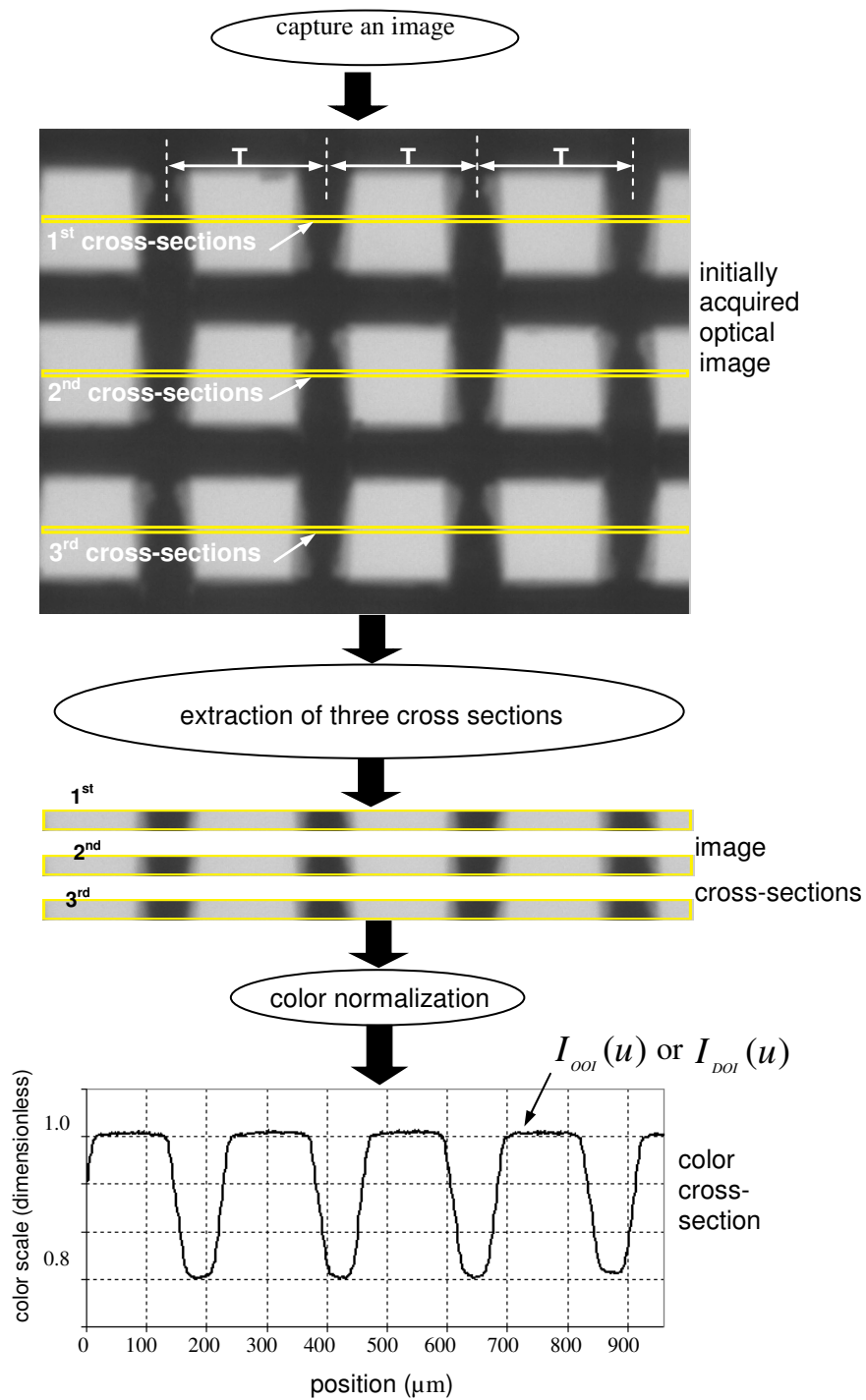


Figure 5.4 Schematic of preliminary image analysis to obtain object's color cross-section

Experimental methodology of object shape-based optical analysis consists in defining object shape parameters and in their measurement and analysis with respect to analysis of lubricant condition and contaminant presence. Typical color optical cross section and object shape parameters are shown in Figure 5.5, where color cross-section, $C(x)$, is a function of pixel color scale (between 0 and 1) vs. pixel position. Several parameters characterising the object shape are proposed and defined below. Within one period of the object structure, T , the amplitude to the highest plateau is defined as the color of lubricant, CL , passing through the microfluidic channel. The amplitude of the lowest plateau is the color of object distorted by the lubricant, CO . These are parameters that characterise the object amplitude. In addition, two parameters that characterize the object width are introduced to fully characterize the object shape. These two additional parameters are the object widths at lubricant level, WL , and the width at object level, WO , where lubricant level was chosen at 90% of lubricant color, $h_{WL} = 0.9CL$, whereas object level was set at 10% above the object color, $h_{WO} = 1.1CO$. Introduction of shape parameters allows representation of color optical cross section as a function of these parameters, $I(u) = f(u, T, CO, CL, WO, WL)$ along cross-section distance, u .

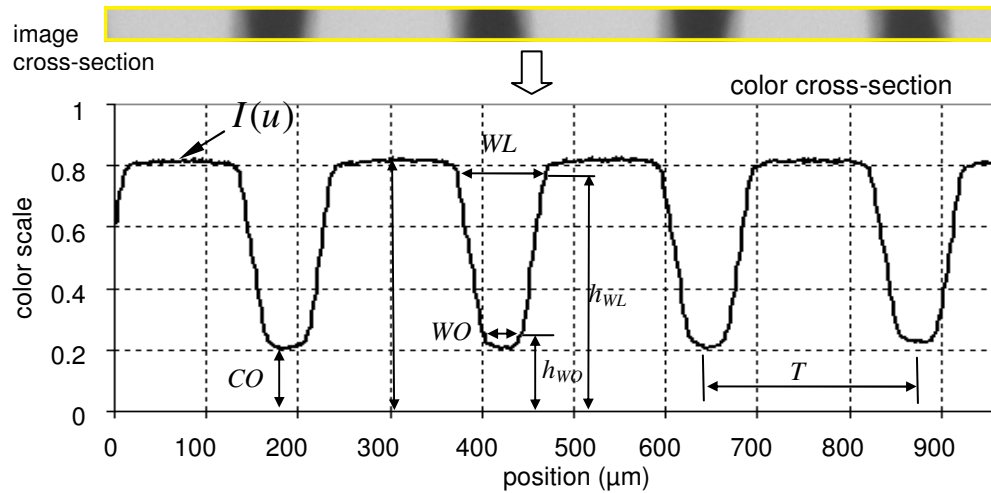


Figure 5.5 Typical image and color cross-sections and object shape parameters

Object shape-based optical analysis methodology is also based on comparison of object shape parameters of fresh and used lubricants as it is shown in Figure 5.6. When

fresh lubricant is introduced, earlier defined shape parameters are considered as constant parameters, $T, CO, CL, WO, WL = const$, to represent an optical medium with no change in its properties. That means the color cross-section of fresh lubricant is a deterministic function of independent variables with no variations in parameter values and it can be reproduced at any position, u , along color cross-section. Color cross section, $I(u)$, changes its character becoming a function with random variables, $I_{doi}(u) = f(u, T_i, CO_i, CL_i, WO_i, WL_i)$, where $T_i, CO_i, CL_i, WO_i, WL_i = var$, and object shape parameters become interdependent with respect to lubricant condition and contaminant presence due to the changes in color, transparency, light absorption, and other optical characteristics.

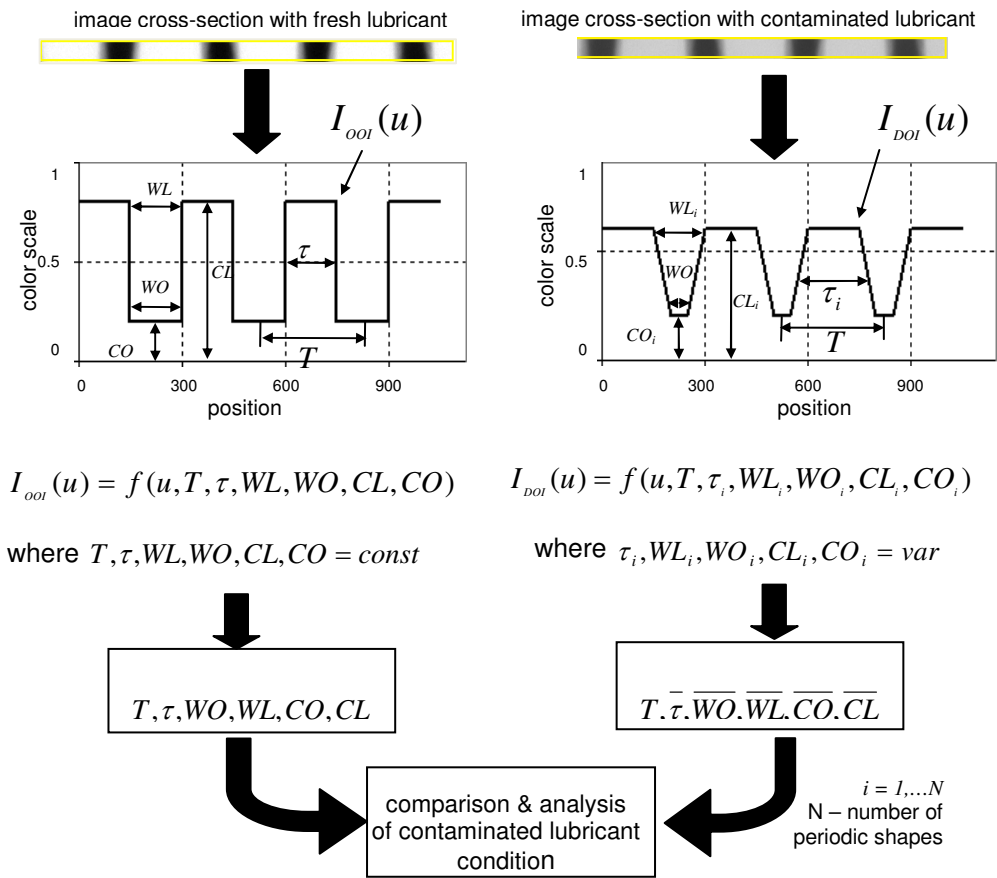


Figure 5.6 Object shape-based optical sensing analysis methodology

In addition to the proposed above parameters, T, CO, CL, WO, WL , two relative object shape parameters are proposed. To gauge the color divergence between lubricant, CL , and lubricant-object combination, CO , the relative lubricant-object color index, ΔC , is introduced and it is defined by the following expression:

$$\Delta C = CO/CL \quad (4)$$

In general, relative lubricant-object color, ΔC , shows how well shape of the object can be recognised at the background of lubricant and it is ranging from 0 to 1 (or from 0% to 100%). Critical limit of 100% optically indicates that object can not be recognised because their colors are identical.

During light propagation through the lubricant, in addition to the object color change represented by ΔC , the object image shape also changes the width of the periodic structure diluting the optical image. This phenomenon can be estimated by introduction of non-uniformity coefficient of object width, ΔW , and defined as the percentage changes in the relative width of object shape by the following expression:

$$\Delta W = (WL - WO)/WL \quad (5)$$

This parameter quantifies the slop of object shape between two levels – at lubricant and object. A non-uniformity coefficient of object width, ΔW , is also ranging from 0 to 1 (or from 0% to 100%), where critical limit of 100% optically indicates that optical image and shape of the object are deteriorating and object totally loses its shape due to lubricant condition and/or contaminant presence and object can not be recognised because their colors become identical.

5.6 Experimental verification

To demonstrate the capability of the proposed sensing system to characterize contaminated and deteriorated lubricant and monitor the change in lubricant optical properties, three separate experiments were carried out. In the first experiment, fresh lubricant (Pennzoil SAE 5W30) was mixed with coolant, gasoline and water at a

concentration of 0%-10%. In the second experiment a combination of coolant (0-5%) and gasoline (0-5%) was added to the fresh lubricant (Pennzoil SAE 5W30) and the change in the lubricant optical properties was studied. In third experiment, a commercially available SAW 5W-20 engine lubricating oil was used for the road test. A set of lubricating oil samples was collected from the engine oil pan through the dip stick tube using flexible tubing and syringe. The collected samples were from a Ford Taurus under general service, with a mixed city and highway driving condition. The road test experiment was performed in real time. During the experiments, samples were pumped through the microfluidic channel, optical images were acquired, and statistical characteristics (ΔC and ΔW) were calculated for each sample.

5.6.1 Analysis of coolant, gasoline and water contamination

The effect of introducing coolant to the engine lubricant and increasing its concentration on color scale graph is illustrated in Figure 5.7. Introduction of 1% coolant into the engine lubricant sample immediately caused a decrease in pick-to-valley (P-to-V) value of the DOI graph from 0.624 to 0.594 (5% reduction). As the coolant concentration was increased to 10%, the P-to-V values showed a non-uniform reduction. The P-to-V value reduction rate was higher between 1%-4% contaminant concentrations. As the concentration increased to 5%, 6%, 7%, 8%, 9%, and 10% the P-to-V values decreased at a slower rate. Overall, introduction of coolant into the engine lubricant from 1% to 10% decreased the P-to-V values of color scale graph from 0.624 to 0.182 (a difference of 0.442). In contrary, addition of gasoline into the lubricant did not make an obvious change in the color cross-section graph. As gasoline concentration was increased from 1% to 10%, the P-to-V values of DOI showed a slight increase from 0.595 to 0.598 (0.5% change in the graph amplitude). Like coolant, addition of water showed an immediate reduction on the P-to-V values of DOI. Introduction of 1% of water lowered the P-to-V value from 0.613 to 0.585 (4.6% reduction). As the water concentration was increased to 10% the P-to-V values of DOI decreased to 0.084. Addition of 10% water to engine lubricant lowered the P-to-V values of DOI from 0.613 to 0.332 (45% reduction).

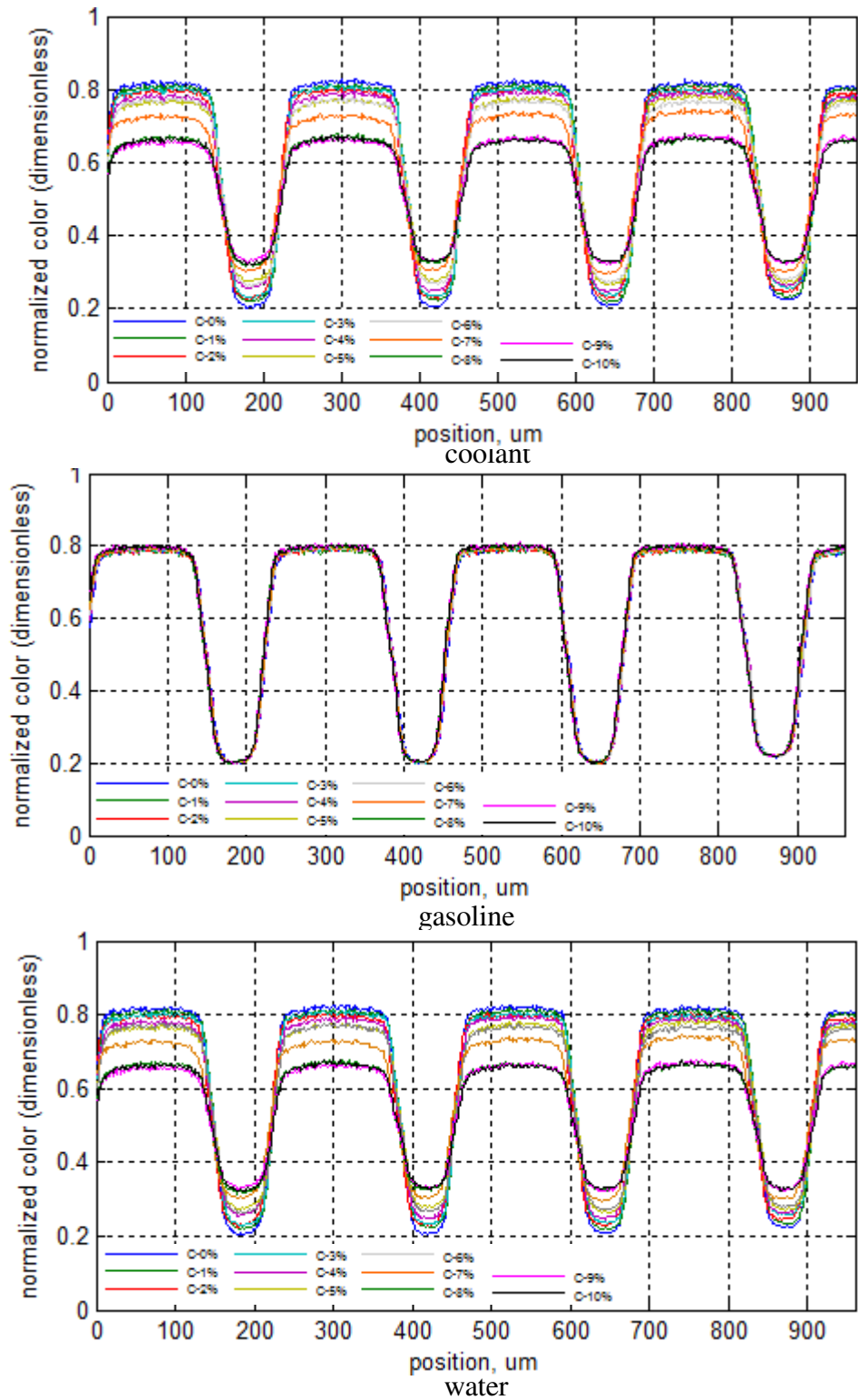


Figure 5.7 Evolution of color cross-sections (OOI and DOI) with respect to coolant, gasoline, and water concentration

The OOI and DOI color cross sections were further used calculating ΔC and ΔW using standard mathematical functions from MATLAB software (see Appendix C). Figure 5.8 shows the evaluation of the relative lubricant-object color index ΔC with respect to coolant, gasoline and water concentration. In particular, Figure 5.8a shows the relative lubricant-object color index and characterization of coolant contamination in the engine lubricant. In general, the change in coolant relative lubricant-object color can be ascribed to the concentration of the coolant. Increase in the concentration of the coolant in the samples provides a decrease in ΔC values. Introduction of coolant into engine lubricant at 1% of concentration showed a decrease in ΔC from 73.9% to 72.02% (difference of 1.87%). As the concentration of the coolant was increased from 1% to 10%, ΔC decreased non-linearly from 72.02% to 27.60%. Overall, the ΔC values showed a reduction of 46.29%.

Introduction of 1% of gasoline into the engine lubricant did not show any change in the relative lubricant-object color index. As the concentration of gasoline was increased from 1% to 10%, ΔC value remained steady 73.8% range (see Figure 5.8b). It was evident addition of gasoline into the engine lubricant did not make any change in lubricant color with respect to object color.

Figure 5.8.c shows the relative lubricant-object color index and characterization of water contamination in the engine lubricant. Introduction of water into engine lubricant at 1% of concentration showed a decrease in ΔC from 73.9% to 71.97% (difference of 1.93%). As the concentration of water was increased from 1% to 10%, the ΔC values decreased from 71.97% to 50.25%. Overall, the ΔC values showed a reduction of 23.65%, and uniform decrease in ΔC values of 5.91% per increments.

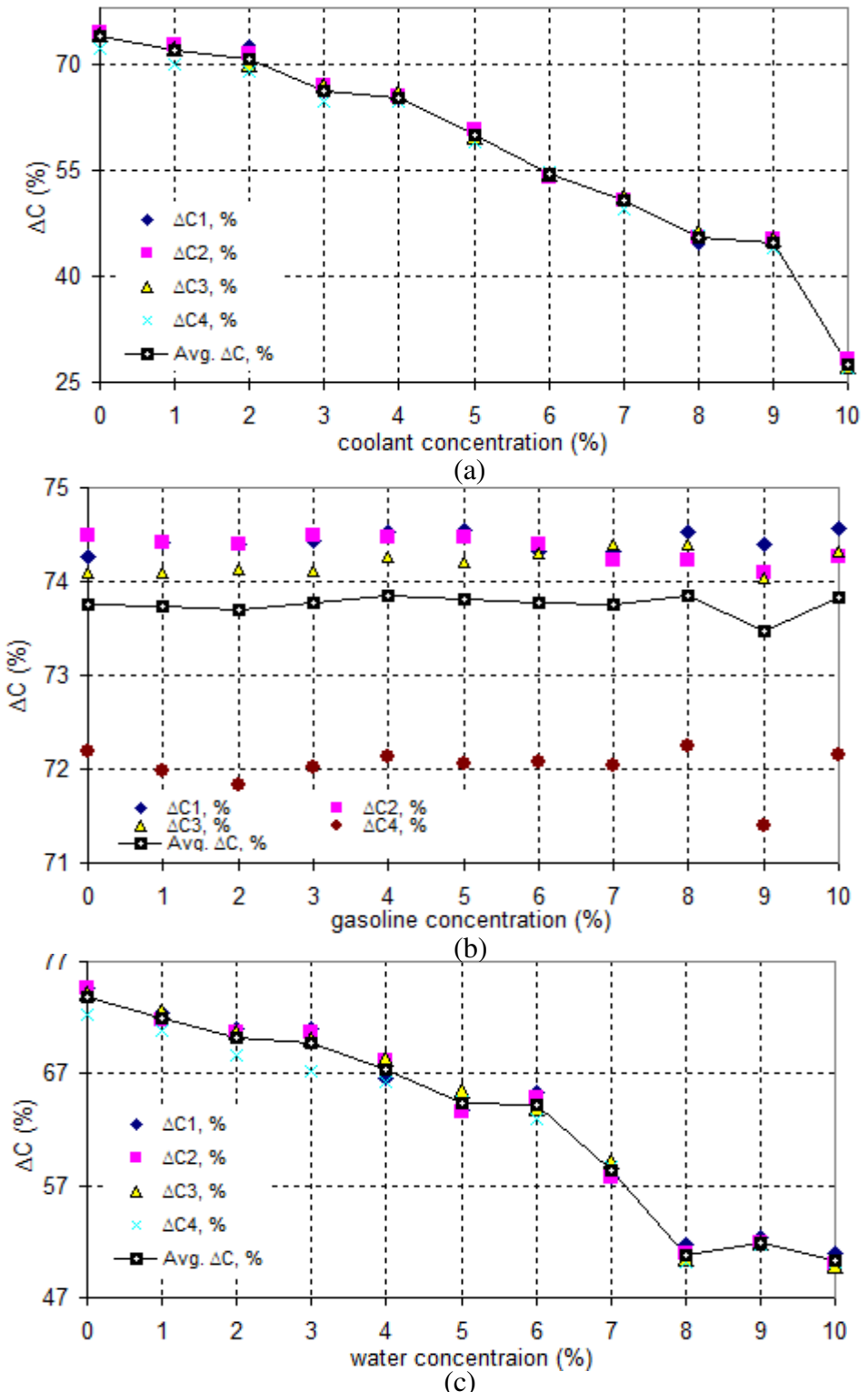


Figure 5.8 Evaluation of relative lubricant-object color index ΔC with respect to coolant, gasoline and water concentration

Non-uniformity coefficient of object width ΔW has also exhibited good correlation with introduction of contaminants into the engine lubricant. Figure 5.9 shows the evaluation of non-uniformity coefficient of object width with respect to coolant, gasoline and water concentration. Introduction of coolant into engine lubricant at 1% of concentration showed a decrease in ΔW from 60.02% to 59.84% (difference of 0.18%). As the concentration of the coolant was increased from 1% to 10%, ΔW decreased non-linearly from 59.84% to 29.06%. Overall, the ΔW values showed a reduction of 30.98% (see Figure 5.9a).

Figure 5.9b shows the non-uniformity of object width and characterization of gasoline contamination in the engine lubricant. Introduction of 1% of gasoline into the engine lubricant lowered the ΔW values from 61.58 to 61.35 (a reduction of 0.23%). As the contaminants concentration was increased from 1% to 10%, the ΔW showed a reduction of 2.28% overall.

As a general trend, introduction of water into lubricant at 1% of concentration lowered the ΔW values from 60.07% to 58.90% (difference of 1.17%). While, the concentration of water was increased to 4%, the ΔW values were decreased to 58.16%. The reduction rate of ΔW was increased dramatically as water concentration was increased from 4% to 8%. The reduction rate showed a slowdown from 8% to 10% of water. Introduction of the water into the lubricant from 1% to 10% caused a shift in the non-uniformity coefficient ΔW values from 60.07% to 48.42% (difference of 11.65%) (see Figure 5.9c).

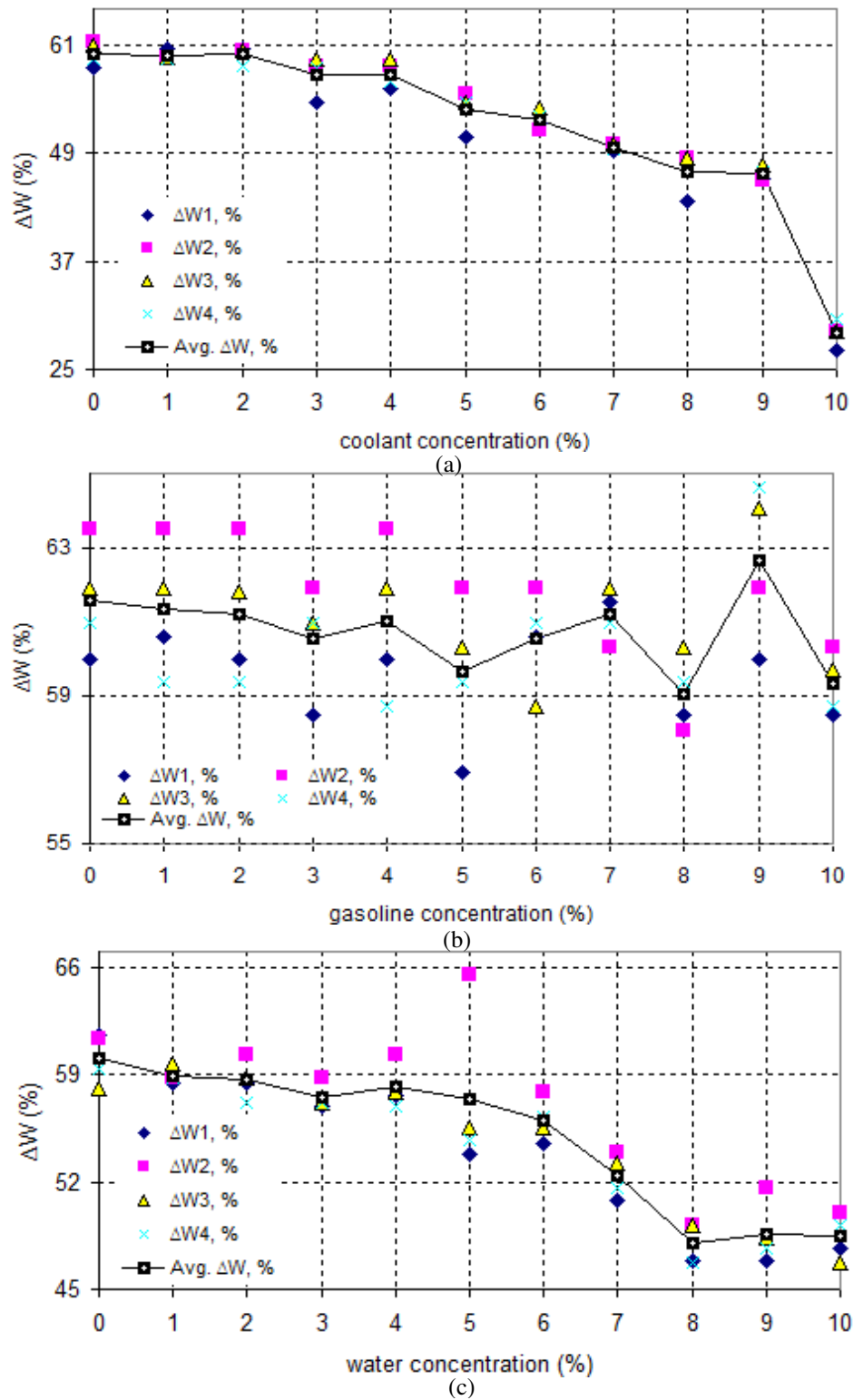


Figure 5.9 Evaluation of the non-uniformity coefficient of object width ΔW with respect to coolant, gasoline, and water concentration

To monitor the changes in the relative lubricant-object color index ΔC and non-uniformity of object width ΔW simultaneously as contaminants concentration changes, the ΔW and ΔC values were plotted creating a 2D informational space for monitoring the condition of lubricant. In general, using one information parameter is not statistically sufficient for reliable on-line monitoring of process condition. Therefore, combining two statistically obtained one-dimensional (1D) information parameters, such as ΔC and ΔW , into one 2-D informational parameters $\{\Delta C, \Delta W\}$ allows evaluation and monitoring of lubricant contamination as a function of two statistical variables in corresponding 2D information plane. Figure 5.10 shows evolution of contaminants in the information space $\{\Delta C, \Delta W\}$. This graph represents the color change and shape deformation during engine lubricant evolution process simultaneously. Figure 5.10a shows that ΔW and ΔC values both decreased as the coolant concentration was increased from 0% to 10%. This shows how these two parameters correlate and statistically dependent with each other as the coolant concentration increased.

Figure 5.10b shows the 2-D informational parameters space $\{\Delta C, \Delta W\}$ for 0% to 10% of gasoline contamination. Since the addition of gasoline into the lubricant had no effect on the ΔC , the $\{\Delta C, \Delta W\}$ plane shows the lack of correlation which implies statistical independency of these two parameters.

The effect of addition of water into the lubricant on ΔW and ΔC is presented in Figure 5.10c. This graph indicates introduction of water into the engine lubricant and increasing its concentration from 1% to 10% lowered the ΔW and ΔC values. ΔW and ΔC show a strong correlation with respect to contaminant concentration.

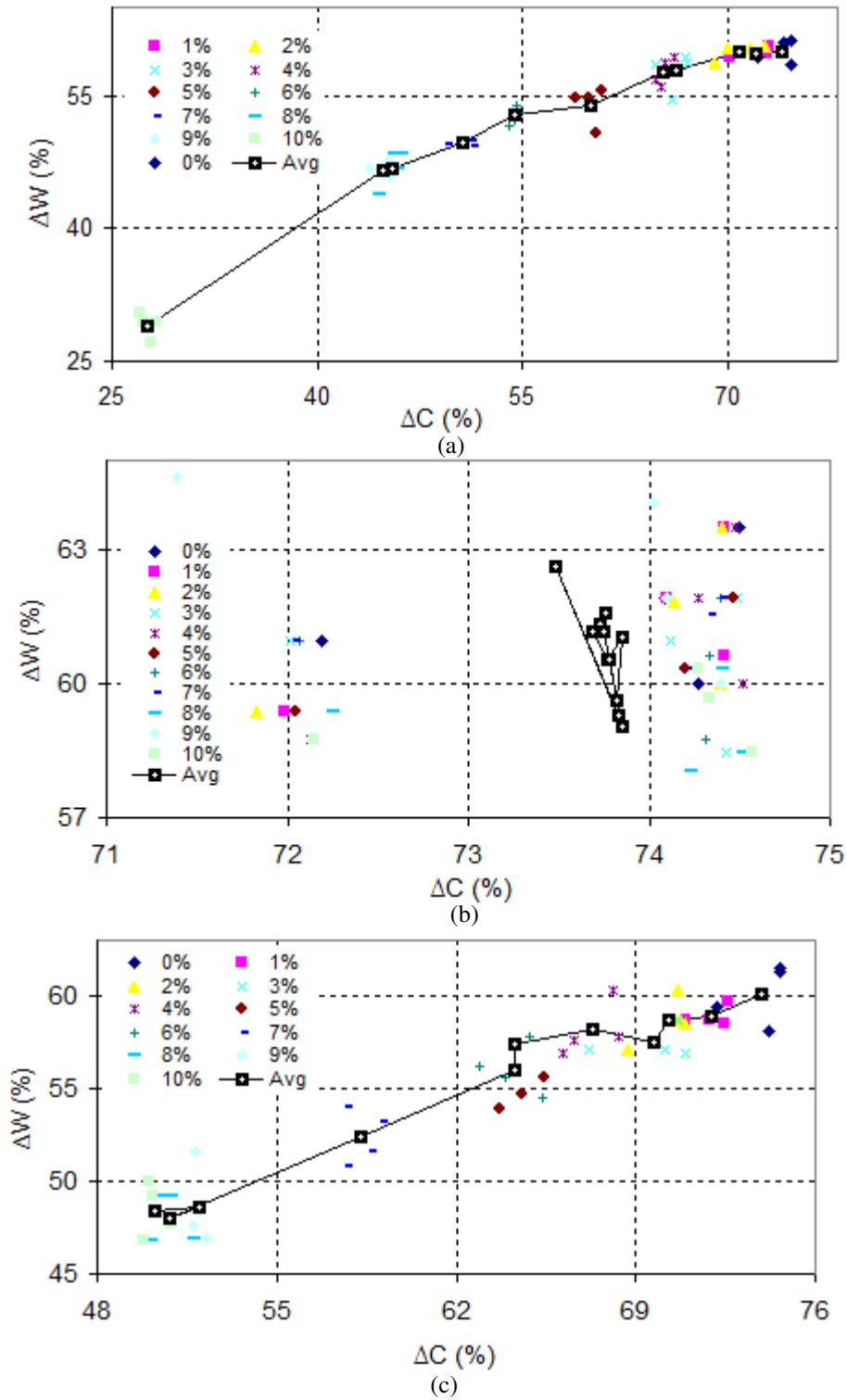


Figure 5.10 $\{\Delta C, \Delta W\}$ information space wrt coolant, gasoline and water concentration

5.6.2 Analysis of combined coolant and gasoline

To demonstrate the capability of object shape-based optical sensing methodology in monitoring the condition of contaminated engine lubricant, a combination of coolant (0-5%) and gasoline (0-5%) was added to the fresh lubricant (Pennzoil SAE 5W30) and the relative lubricant-object color index ΔC and non-uniformity of object width ΔW parameters were studied. Figure 5.11 illustrates the combination of mixture ratio between contaminants and lubricant of all samples. During the experiments, contaminated lubricant samples were pumped through the microfluidic channel, optical images were acquired, and statistical shape parameters ($\Delta W, \Delta C$) were calculated for each sample.

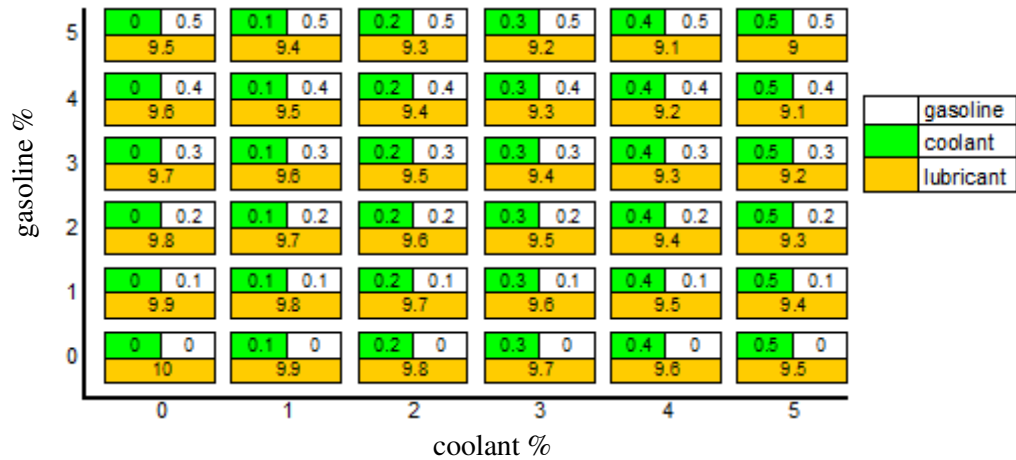


Figure 5.11 Schematic presentation of coolant-gasoline combined contaminated engine lubricant proportional mixture

The effect of introducing coolant-gasoline to the engine lubricant and increasing its concentration on color scale graph is illustrated in Figure 5.12. Introduction of 1% coolant and gasoline into the engine lubricant sample immediately caused a decrease in P-to-V of the graph from 0.6845 to 0.627 (8.4% reduction). From 1% to 2%, 3%, 4% and 5%, these P-to-V values decreased at a rate of 0.0815, 0.0152, 0.054, and 0.0397 respectively. Overall, introduction of coolant-gasoline into the engine lubricant from 1% to 5% decreased the amplitude of color scale graph from 0.6845 to 0.4366 (a difference of 0.2479).

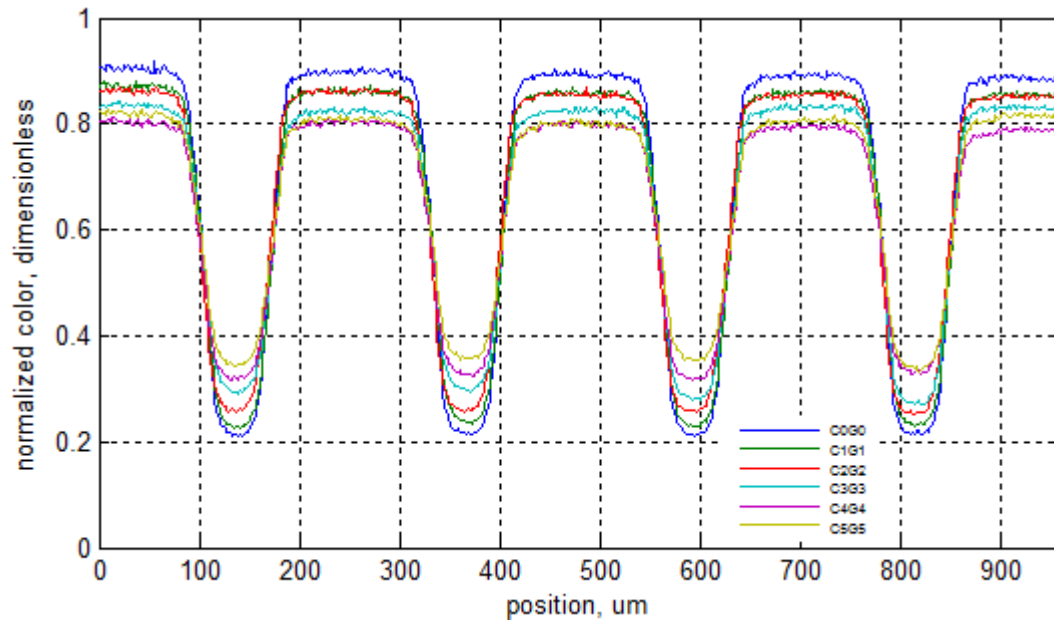


Figure 5.12 OOI and DOI color cross-section graph of coolant-gasoline contaminated engine lubricant

The OOI and DOI color cross sections were used to calculate ΔC and ΔW for each sample using MATLAB software (see Appendix C). Then the calculated parameters were plotted at each combination concentration. Figure 5.13 presents the 2-D informational space of ΔW and ΔC of combined contaminant samples.

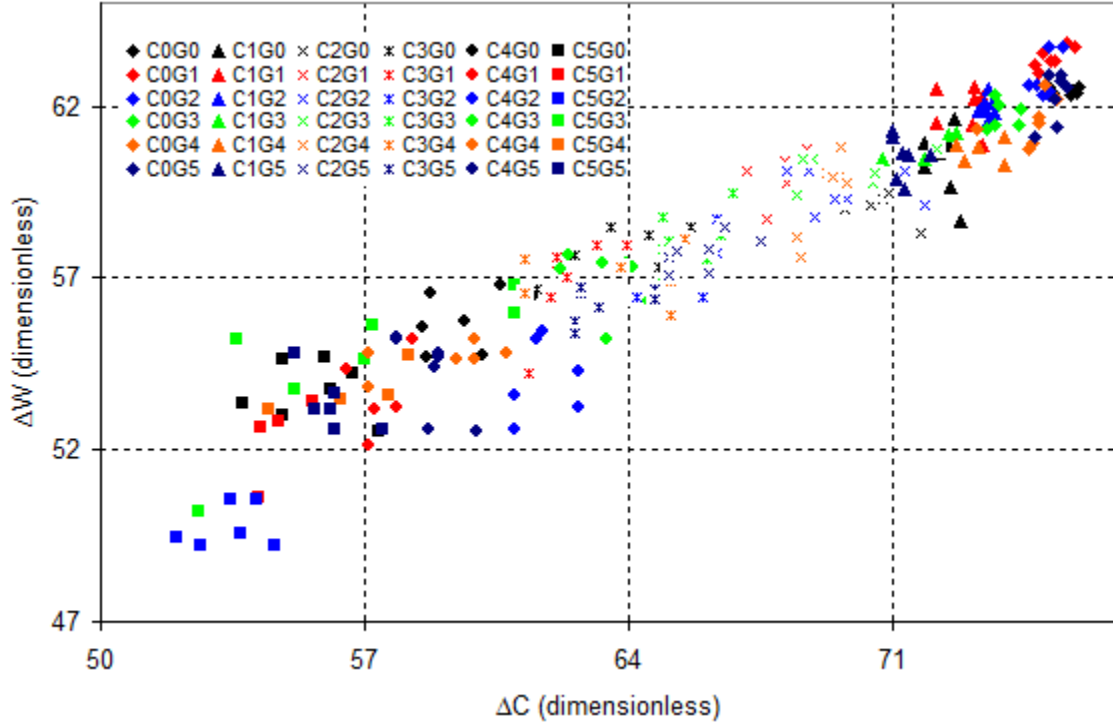


Figure 5.13 Evolution of coolant-gasoline combined contaminant in $\{\Delta C, \Delta W\}$ informational space

In general, addition of combined coolant and gasoline (0%-5%) into engine lubricant decreased the relative lubricant-object color index ΔC and non-uniformity of object width ΔW simultaneously as contaminants concentration was increased. The reduction in the relative lubricant-object color index ΔC values were 27.36%, while the non-uniformity of object width ΔW was lowered by 13.36%. Then for more detailed observation, each series of samples ($C_{0\%-5\%}G_{0\%}$, $C_{0\%-5\%}G_{1\%}$, $C_{0\%-5\%}G_{2\%}$, $C_{0\%-5\%}G_{3\%}$, $C_{0\%-5\%}G_{4\%}$, $C_{0\%-5\%}G_{5\%}$) was studied individually (see Figure 5.14).

It was shown that the addition of combined coolant-gasoline contaminant changed the $\Delta W - \Delta C$ graph in a linear fashion. At any gasoline concentration, increasing the concentration of coolant from 0%- 5% induced a similar variation pattern in $\Delta W - \Delta C$ space. Introduction of 1% of coolant caused an obvious reduction in $\Delta W - \Delta C$ value. In $C_{0\%-5\%}G_{0\%}$ series, introduction of 1% of coolant caused an obvious reduction in $\Delta W -$

ΔC value. From 0% to 2% of contaminants, the reduction was at a higher rate as to compare to 2% to 5%. Overall, addition of combined contaminants into the engine lubricant reduced the ΔC by 16.95%, while ΔW showed a reduction of 7.25%. At 1% gasoline concentration, increasing the concentration of coolant from 0% to 5% decreased the relative lubricant-object color index ΔC values from 75.16% to 545.85% (a 20.31% reduction), when the non-uniformity of object width ΔW values showed a reduction of 11.01%. At 2% gasoline, the ΔC values displayed a decrease of 26.29% as coolant concentration was increased. The ΔW values were lowered by 13.78% from 62.89% to 49.11%. For $C_{0\%-5\%}G_{3\%}$ series, the ΔC values decreased from 74.12% to 55.86% (18.26% increase). The ΔW values also were lowered from 61.83 to 53.27 (8.56% reduction). For $C_{0\%-5\%}G_{4\%}$ series, increase in ΔC values was by 18.13% from 74.89%, while ΔW values decreased by 7.7% from 61.55%. For $C_{0\%-5\%}G_{5\%}$ series, the ΔC values decreased from 75.41% to 56.15 (19.26% increase), when ΔW showed a reduction from 62.34% to 53.54% (8.8% reduction). Overall, it was observed ΔC and ΔW values correlate with each other and they are statistically dependent. Figure 5.14 presents the individual $\{\Delta C, \Delta W\}$ information space of coolant-gasoline combination.

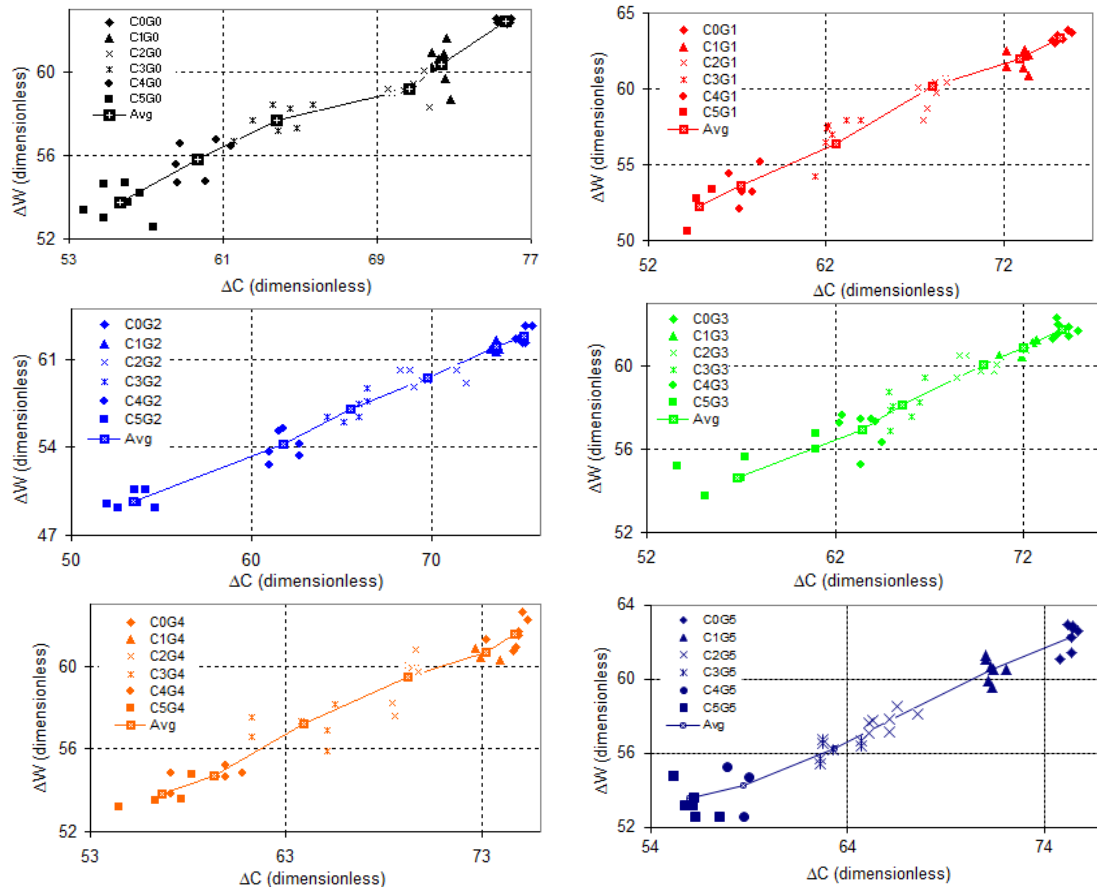


Figure 5.14 $\{\Delta C, \Delta W\}$ informational space of $C_{0\%-5\%}G_{0\%}$, $C_{0\%-5\%}G_{1\%}$, $C_{0\%-5\%}G_{2\%}$, $C_{0\%-5\%}G_{3\%}$, $C_{0\%-5\%}G_{4\%}$, $C_{0\%-5\%}G_{5\%}$

5.6.3 Road test engine lubricant analysis

In this experiment, a commercially available SAW 5W-20 engine lubricating oil was used for the road test. A set of oil samples was collected from the test. The collected samples were from a Ford Taurus under general service, with a mixed city and highway driving condition. The purpose of this test was to see the correlation between the travelled distance and change in the optical properties of the lubricant and also examine the capability of the proposed methodology to monitor the condition of engine lubricant under realistic condition. All the samples went through the similar procedure as described in section 5.3.

Figure 5.15 illustrates the color cross-section graph for travelled distance of 0 Km, 200 Km, 800 Km, 1000 Km, 1200 Km, 1500 Km, 2350 Km, 3450 Km, and 4200 Km samples. It is appear that the amplitude of the color cross-section graph (P-to-V) gradually decreased as the travelled distance increased. This indicates that there is a strong correlation between travelled distance and optical property of the lubricant. This is evidence that the rate at which the P-to-V of the color cross section decreases is directly depends on the travelled distance which is the indication of normal degradation process of the engine lubricant. Overall, from 0 Km to 4200 Km travelled distance, the P-to-V the color cross-section graph decreased from 0.699 to 0.616, a reduction of 0.083 or 11.8%.

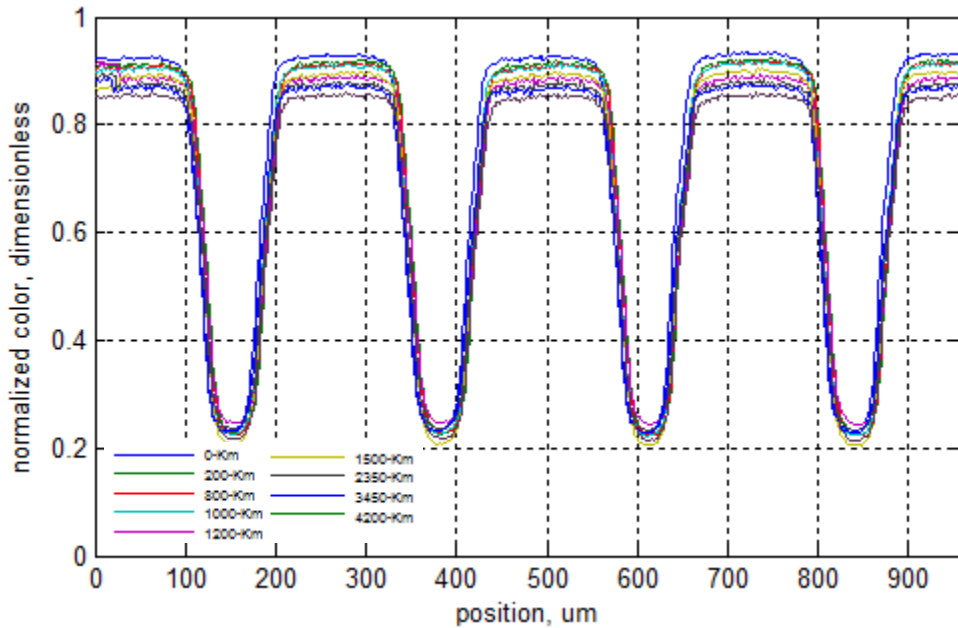


Figure 5.15 Color cross-section graph of road test engine lubricant analysis

Similar to the previous cases, the color cross-sections of fresh lubricant image and used lubricant were used as the experimental data to calculate the relative lubricant-object color index ΔC and non-uniformity coefficient of object width ΔW . Standard mathematical function from MATLAB was used to calculate the ΔC and ΔW (see Appendix C). Effect of accumulated travelled distance on the relative lubricant-object color index ΔC is shown in Figure 5.16. The change in coolant relative lubricant-object

color can be ascribed to the travelled distance. Increase in the travelled distance provides a decrease in ΔC values.

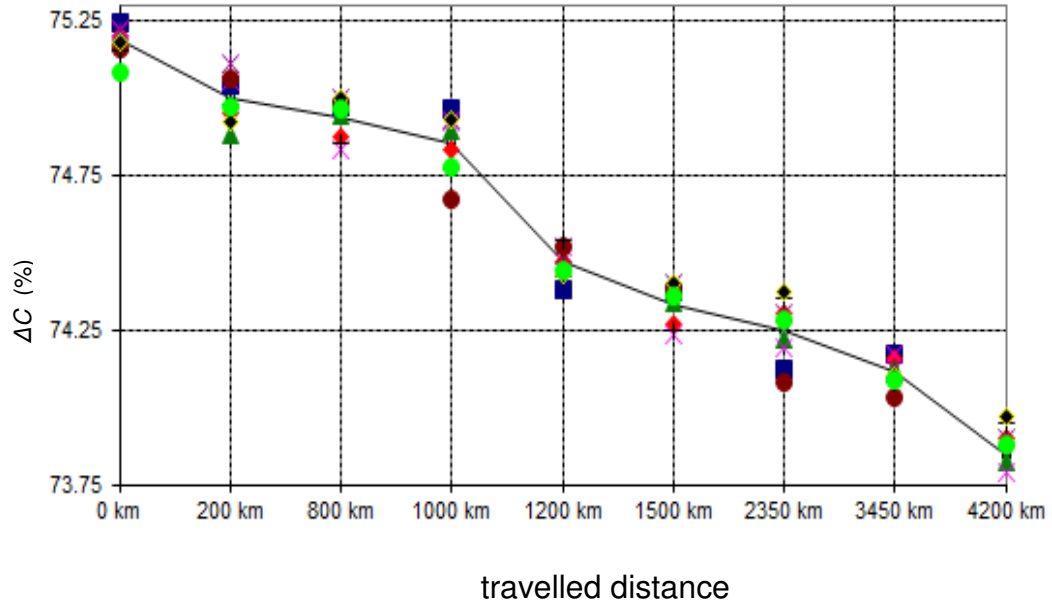


Figure 5.16 Road test engine lubricant ΔC at different travelled distance

In 4200 km travelled distance, ΔC showed a decrease of 4.33% from 75.18 to 73.85.

Non-uniformity coefficient of object width ΔW has also exhibited a good correlation with travelled distance in the road test. Figure 5.17 shows the evaluation of non-uniformity coefficient of object width with respect to travelled distance. Travelling 200 km showed an immediate decrease in ΔW values. As the travelled distance increased up to 4200 km, the ΔW values decreased from 62.85 to 61.46, a decrease of 1.4%.

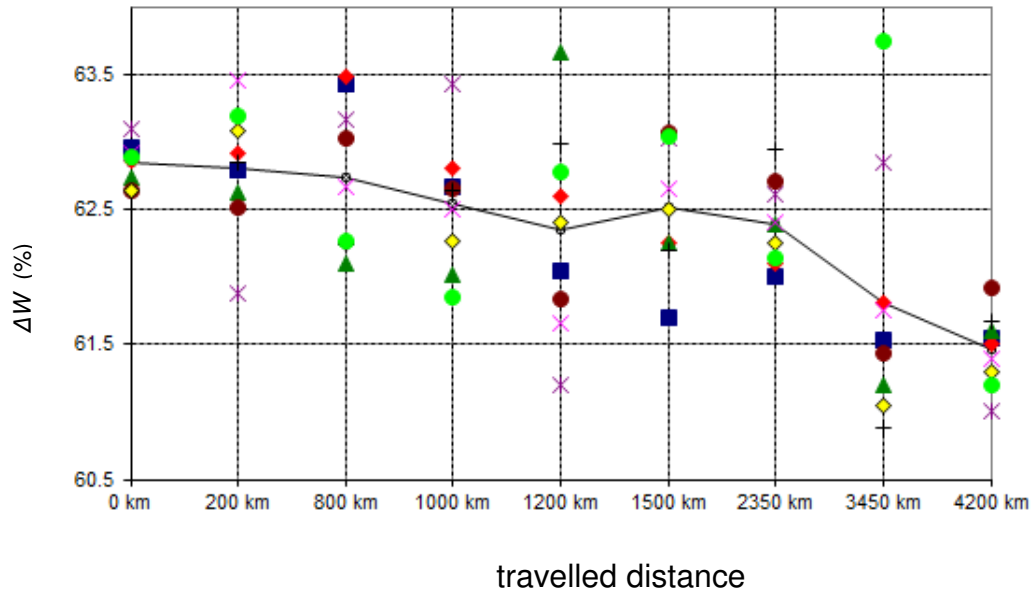


Figure 5.17 Road test engine lubricant ΔW wrt travelled distance

To monitor the changes in the relative lubricant-object color index ΔC and non-uniformity of object width ΔW simultaneously as the accumulated travelled distance increased, the ΔW values were graphed with ΔC at each travelled distance. Figure 5.18 shows the 2-D informational space $\{\Delta C, \Delta W\}$ with respect to travelled distance. Figure 5.18 shows how the ΔW and ΔC values correlated with each other as the accumulated travelled distance increased from 0 km, to 200 km, 800 km, 1000 km, 1200 km, 1500 km, 2350 km, 3450 km, and 4200 km. This is evident that the travelled distance lowered $\Delta W - \Delta C$ values simultaneously and these two parameters correlate with each other in the same direction.

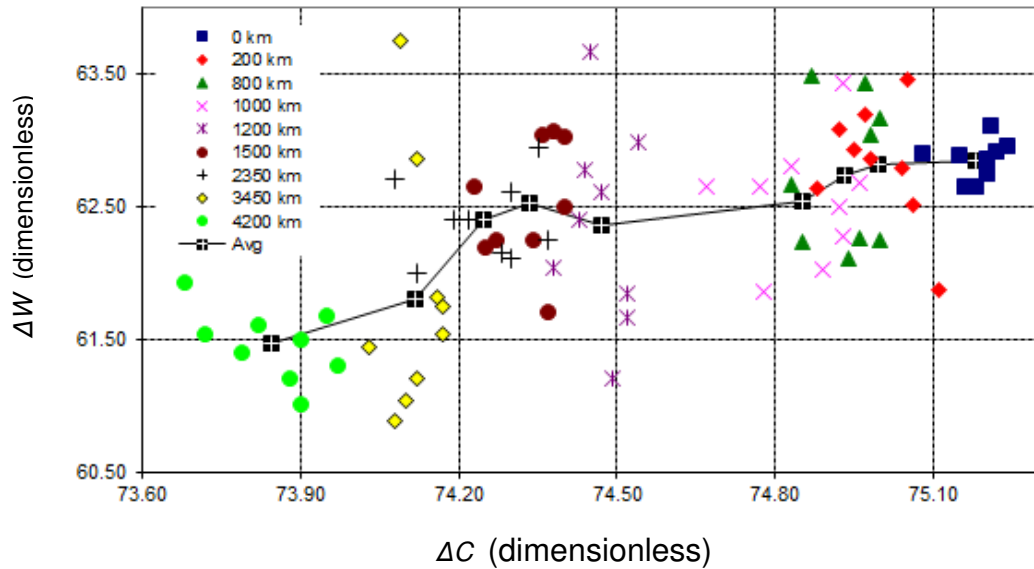


Figure 5.18 $\{\Delta C, \Delta W\}$ information space of road test engine lubricant

5.7 Summary and conclusion

In this chapter a new methodology, object shape based optical sensing methodology for optical analysis of contaminated lubricants was introduced and its applicability was verified by measuring and monitoring of coolant, gasoline and water contaminant concentrations individually, as well as mixed. To demonstrate the capability of the proposed methodology in monitoring the condition of the engine lubricant realistically, a set of oil samples was collected from a Ford Taurus under general service, with a mixed city and highway driving condition. The road test experiment was performed in real time. A novelty of the proposed methodology consists in obtaining and analysis of an optical image that combines an object with known periodic shape and a thin film of the contaminated lubricant. Introduction of an object with *a priori* known periodical structure allowed reduction of 2D into 1D optical analysis. This methodology proposed to measure several parameters of the acquired optical images, such as, color of lubricant and object, object shape width at object and lubricant levels, object relative color, and object width non-uniformity coefficient, for fresh and contaminated lubricants. Estimation of contaminant presence and lubricant condition was performed by comparison of parameters for fresh and contaminated lubricants. The object shape based optical sensing

methodology was verified experimentally showing ability to distinguish lubricant with 1% to 10% coolant, gasoline and water contamination. Also, it was shown that this methodology is capable of monitoring the contaminants concentration in a combined form (coolant-gasoline 0%-5%) as well. Capability of the proposed methodology was extended to establish the linkage between accumulated travelled distance and the change in the optical statistical properties of the engine lubricant.

From the results obtained, the following main conclusions can be drawn:

1. Developed object shape-based optical sensing analysis methodology is a novel approach for analysis of a synergetic effect of combined lubricant-object optical appearance. It opens new opportunities for on-line monitoring, diagnostics and control of engine lubricant condition and engine performance.
2. The engineering contribution of this work is the implementation of opto-microfluidic sensing system for extraction of optical information and monitoring the characteristics of the engine lubricating oil on-line in real time. Opto-microfluidics sensing system represents the use of advanced optical elements to increase the functionality of microfluidic devices and also the use of advanced microfluidic devices to increase the functionality of photonic devices. Such integration represents a novel approach to dynamic manipulation of optical systems with many applications in automotive fluid sensing field.
3. Implementation of systems approach, an intellectual discipline to solve complex problem, to monitor the health of engine through optical analysis of engine lubricant is a new approach in the automotive field for engine performance. This approach brings more insight into importance of engine lubricant and lubricant system and how lubricant can be used as a source of information for engine performance.
4. Addition of 1%-10% of coolant into the engine lubricant decreased the amplitude of color scale graph by almost 62%. Introduction of gasoline at the same concentration rate into the lubricant did produce any change in the amplitude of the color scale graph. Like coolant, addition of water reduced the graph amplitude by 45%.

5. Evaluation of the relative lubricant-object color index ΔC indicated that increase in the concentration of coolant, 1%-10%, provided a 46.3% decrease in ΔC value in a non-linear format. On the contrary, addition of gasoline has no effect on the value of ΔC . Like coolant, water decreased the value of ΔC by 23.65% in a linear fashion as the contaminate concentration was increased up to 10%.
6. Non-uniformity coefficient of object width ΔW has also exhibited good correlation with introduction of contaminants into the engine lubricant. Addition of coolant up to 10% into the engine lubricant lowered the ΔW value by almost 31%. Gasoline exhibited a similar effect on the ΔW , however the reduction rate was 2.3%. Introduction of water into the lubricant had a reduction effect on the ΔW values. This reduction was much higher between 4% to 10% as to compare to 1% to 4%. Overall addition of water reduced the ΔW value by 11.7%.
7. Plotting the relative lubricant-object color index ΔC values with non-uniformity coefficient of object width ΔW at different contamination concentration created a 2-D informational space for monitoring of lubricant condition. Addition of coolant at 1% and increasing to 10% lowered $\Delta W - \Delta C$ values with a strong correlation. Since the addition of gasoline into the lubricant had no effect on the ΔC , the $\{\Delta C, \Delta W\}$ plot showed lack of correlation between these two parameters. Addition of water into the lubricant showed a reduction effect on the $\Delta W - \Delta C$ values. Monitoring the lubricant condition from the $\{\Delta C, \Delta W\}$ informational space indicated a strong correlation and statistical dependency between these values.
8. The developed methodology was also applied for analysis of combinations of coolant and gasoline (0%-5%) contaminants. Addition of combination of coolant-gasoline (0%-5%) lowered the $\Delta W - \Delta C$ values with good correlation. In general, addition of combined coolant and gasoline (0%-5%) into engine lubricant decreased the relative lubricant-object color index ΔC and non-uniformity of object width ΔW simultaneously as contaminants concentration was increased. The reduction in the

relative lubricant-object color index ΔC values were 27.36%, while the non-uniformity of object width ΔW was lowered by 13.36%.

9. Object shape based optical analysis method was also applied for analysis of road test samples with different millage. In this study samples with 0 km, 200 km, 800 km, 1000 km, 1200 km, 1500 km, 2350 km, 3450 km, and 4200 km traveled distance were collected and analyzed in real time. The results indicated that the accumulated travelled distance directly affect the statistical parameters of the lubricant. The relative lubricant-object color index ΔC decreased as the accumulated travelled distance was increased from 75.18% to 73.85. The travelled distanced also decreased the non-uniformity of object width ΔW from 62.85% to 61.46%. The 2-D presentation of ΔC - ΔW indicated that both statistical parameters moved in the same direction as the travelled distance increased.

Chapter 6

6 Statistical Optical Analysis Methodology for Monitoring Contaminated Engine Lubricant

This chapter describes an optical sensing methodology, system and statistical optics analysis applied to qualify and quantify the presence of contaminants in the engine lubricants. The statistical optics analysis is used to determine statistical characteristics of a combined object-lubricant image of a periodically structured object distorted by a thin film of turbid media. Presence of contaminants and their concentration is determined by statistical auto-characteristics and cross-characteristics. The novelty of the proposed methodology consists in introduction of an object with a known periodical structure allowed obtaining and analysis of an optical image that combines an object with known periodic shape and a thin film of the contaminated lubricant. The *priori* known periodical structure allows reduction of 2D into 1D optical analysis for on-line measurement purposes.

6.1 Statistical optics analysis methodology

In optics, imperfect of distorting medium is defined as a thin layer with inhomogeneities of the refractive index of thin medium. The inhomogeneous medium has a devastating effect on the resolution achieved by the optical system. When an object is placed behind a thin film of an inhomogeneous medium (e.g. contaminated lubricant) and an image obtained, the object image will be distorted by the medium acting as a distortion operator. In this case, quality of the distorted object image (DOI) will mainly depend on the actual condition of the turbid medium. Based on the theory of light propagation through the random turbid medium [45], the transformation/distortion operator gains a mathematical notation as an optical transfer function (OTF) that represents a transformation of the original object image (OOI) into DOI.

When OOI and DOI are known, the distortion operator or the actual optical properties of the media (e.g. engine lubricant) can be identified. By knowing the OOI (deterministic object), variations of the distortion operator can be fully described by the

variations of the DOI. In a general sense, by the “removing” known properties of the OOI from the DOI, properties of the distortion operator can be obtained that will fully characterize an actual condition of the engine lubricant.

The acquired image through the random liquid medium (e.g. lubricant) DOI contains a combination of an original object and liquid medium images. Therefore, the acquired combined object-lubricant image and its parameters become functionally depended on interrelated optical parameters of the object shape and media. In this case, analysis of statistical characteristics and parameters of the DOI can be successfully applied to identify a functional interdependence of the known object parameters and unknown parameters of the lubricant as an image-distorting turbid liquid medium.

Based on the discussion above, it is necessary to realize that in order to characterize qualitatively and quantitatively the turbid liquid medium (e.g. engine lubricant), complete statistical analysis of both statistical characteristics of the distorted image DOI and statistical characteristics of the distortion effect is required. In addition, statistical characteristics of OOI are required and they do not depend on the turbid liquid medium and its condition. This is a basis of the methodology for statistical optics analysis of contaminated engine lubricants.

The methodology uses two sources of optical information – images of original and distorted object represented by intensity distributions $I_{OOI}(x, y)$ and $I_{DOI}(x, y)$, respectively, and radiated in a spatially incoherent fashion in the object plane. In this case, two types of statistical optics characteristics can be calculated – auto(self)- and cross- statistical characteristics. The auto-statistical characteristics, such as, auto-correlation function (ACF), auto-spectral function (ASF), *etc.*, describe statistical properties of the random process itself, e.g. of $I_{OOI}(x, y)$ or $I_{DOI}(x, y)$. The cross-statistical characteristics, represented by cross-correlation (CCF), cross-spectral (CSF), transfer (TF) and coherence (CF) functions characterize functional and statistical interdependence between $I_{OOI}(x, y)$ and $I_{DOI}(x, y)$ and correspondingly characterize a distorting effect. In this case, entire distortion effect where $I_{OOI}(x, y)$ is being

transformed into $I_{DOI}(x, y)$ by a distortion operator $h(v, u)$ can be described as a linear time-invariant single-input ($I_{OOI}(x, y)$) single-output ($I_{DOI}(x, y)$) dynamic system. Also, the operator $h(v, u)$ can be described mathematically by a multiplicative amplitude transmittance and it is correspondingly called a modulation transfer function of a random media [121].

In the spatial domain, a transformation of the OOI $I_{OOI}(x, y)$ into a DOI $I_{DOI}(x, y)$ by the distortion operator $h(v, u)$ can be described in general by a 2D convolution integral:

$$I_{DOI}(x, y) = h(v, u) * I_{OOI}(x, y) = \iint h((x, y)_{DOI}, (x, y)_{OOI}) I_{OOI}(x, y) dx_{OOI} dy_{OOI} \quad (1)$$

assuming that all intensity contributions in a point (x, y) add up. In spatial frequency domain, Equation (1) can be expressed as the following after applying a Fourier transform to the convolution integral:

$$S_{DOI}(\omega, \psi) = |H(j\omega, j\psi)|^2 S_{OOI}(\omega, \psi) \quad (2)$$

where $S_{DOI}(\omega, \psi)$, $S_{OOI}(\omega, \psi)$, and $H(j\omega, j\psi)$ are the 2D Fourier transforms of $I_{DOI}(x, y)$, $I_{OOI}(x, y)$ and $h((x, y)_{DOI}, (x, y)_{OOI})$, respectively. $H(j\omega, j\psi)$ is also called as a 2D optical transfer function (OTF) [52,93].

Equation (2) confirms one more time that complete statistical optics analysis of the contaminated lubricants is only possible through statistical characterisation of a combined effect of light propagation through the turbid liquid medium (e.g. engine lubricant) and image distortion by the medium. Therefore, in brief, statistical optics analysis methodology consists in (a) acquiring optical images before and after its distortion by the contaminated lubricant (e.g. $I_{OOI}(x, y)$ and $I_{DOI}(x, y)$), (b) calculation of auto-statistical characteristics of the optical images (e.g. ACF_{OOI} , ACF_{DOI} , ASF_{OOI} , ASF_{DOI} , etc), (c) calculation of cross-statistical characteristics between optical images (e.g. CCF , CSF , TF , CF , etc.). Final step of the methodology (d) consist in the

comparison of statistical optics characteristics of fresh and contaminated lubricant uncovering evolution of optical properties of the combined object images. Variations and differences in parameters of these statistical characteristics give reliable information for condition estimating and monitoring of the contaminated lubricant.

6.2 Opto-microfluidic sensing system, experimental set-up and measurement methodology

When light propagates through the lubricant, due to the complex mixture of different contaminants, additives and wear particles, the optical properties of the lubricant, e.g. color, transparency, refractive index, absorbance, *etc.* are changing in a very complex manner. A thin layer of the lubricant can be considered as a randomly inhomogeneous liquid medium and the theory of statistical optics [45,52] can be applied to fully characterize the statistical optical properties of the combined object-lubricant image. This can be achieved by a system with a functional design where light propagates through an object and medium (e.g. lubricant) and an image of the known (deterministic) object.

Generalized methodology for experimental optical analysis of contaminated lubricants is shown in Figure 6.1. Initially, the light is sent through a lubricant and object with periodic structure and a combined optical image is recorded. According to the proposed logic for further comparison, initially, optical image of a medium without distorting ingredients, e.g. fresh engine lubricant or lubricant right after oil change, will be acquired. Such an image from the undistorted optical medium and object represents the initial state or condition of the optical medium. As engine runs lubricant degradation process occurs leading to breakdown of hydrocarbon chains, depletion of additives, and addition of contaminants. Optical images with operating lubricant and unchanged periodical object are acquired further delivering optical information with respect to degradation of lubricant condition. Optical image analysis for both fresh and used engine lubricants consists of extraction of certain statistical characteristics and their consecutive comparison. The acquired optical data from images requires initial image processing, such as, cross-sectioning, color normalization *etc.* making optical images and data more suitable for further statistical analysis, such as object shape-based and statistical optical

analysis. Final step of the experimental analysis methodology is focused on a quantitative and qualitative analysis of contaminant presence and analysis of lubricant condition evolution using object shape related parameters and statistical characteristics of DOI, e.g. as OTF, autocorrelation functions, power spectrum densities, etc. Comparison of these parameters and characteristics provides accurate and precise estimation of the contaminant presence. In this methodology, the object shape related parameters and statistical characteristics of the OOI for a fresh lubricant (without contaminants) are considered as a benchmark from which the evolution of the object shape related parameters and statistical characteristics of the DOI due to the introduction of contaminants is analysed.

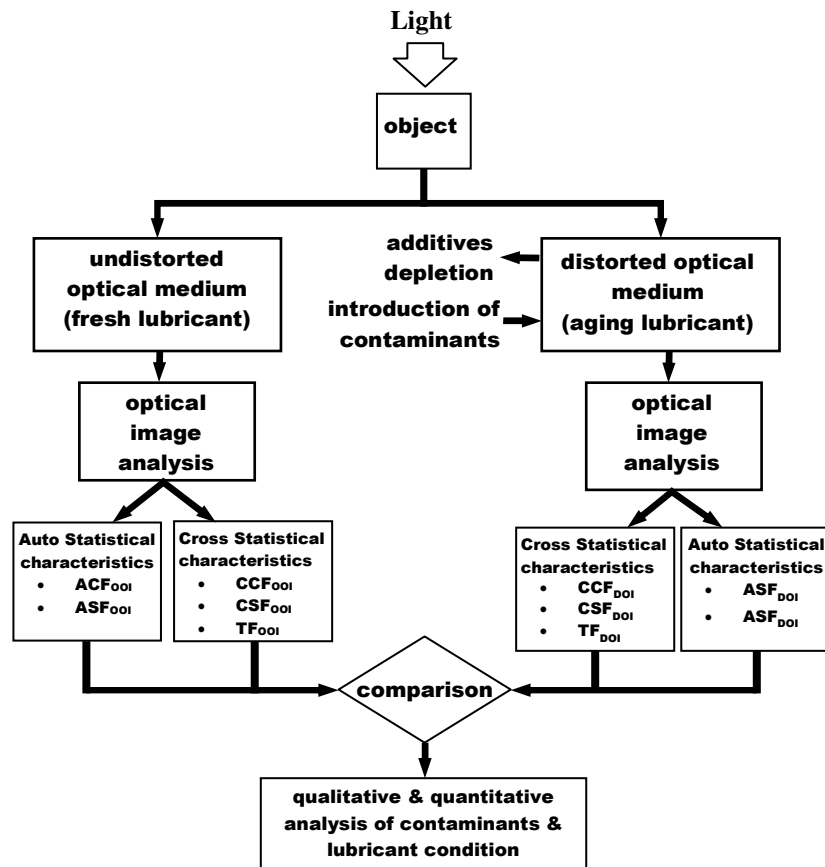


Figure 6.1 Generalized methodology for experimental optical analysis of contaminated lubricant

However, a preliminary image analysis is required in order to obtain a statistically valid color cross-section of the object image. This color cross-section is origin information for statistical optical analysis.

6.2.1 Functional design of opto-micro sensing system

Figure 6.2 represents the functional design of the proposed opto-microfluidic sensing system, where an object located behind of a microfluidic channel with flowing contaminated lubricant and optical image acquisition system. The system has an incoherent light source illuminating the object located in the (ξ, η) plane. The radiation from the object propagates through a sufficiently thin media (e.g. engine lubricant) located in the (u, v) plane and it is represented mathematically by a multiplicative amplitude transmittance (e.g. optical transfer function) $h(u, v)$. A blurred or distorted image of the object is appeared in the (x, y) plane and is described by the intensity distribution function $I(x, y)$. The thin media (e.g. engine lubricant) is acting as a turbid media affecting the performance of the optical system. Such functional design allows applying the concept of an optical imaging through a thin random “screen” as a thin distorting structure [45]. However, the principal difference in applying this concept in this paper is that instead of using classical approach to analyze the effect of thin random screen on the performance of optical imaging system, it is proposed to characterize a thin random screen (i.e. lubricant in the microfluidic channel) from the performance of optical system.

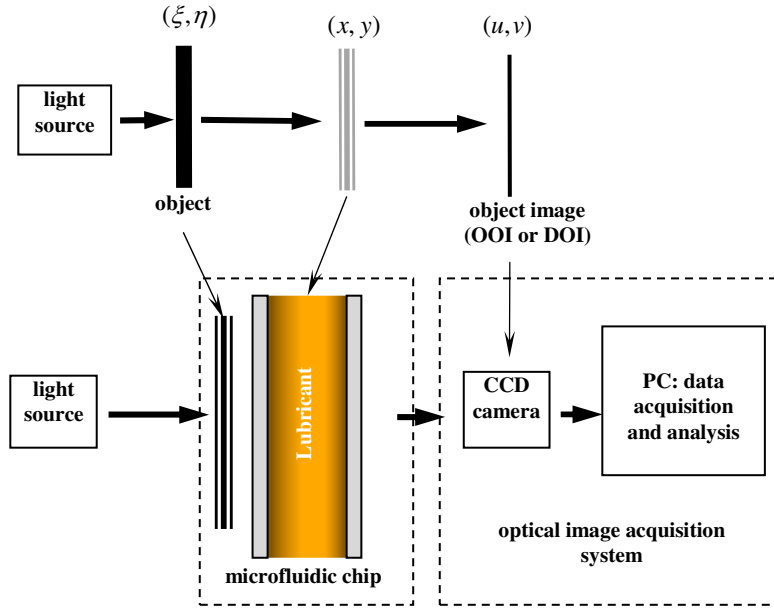


Figure 6.2 Functional design of the opto-microfluidic sensing (measuring) system

Proposed above “thin screen” functional representation of the opto-microfluidic sensing system is based on two assumptions in order to satisfy statistical optics definition [45]. First, it is assumed that the screen is sufficiently thin that rays enter and leave the thin film at essentially the same coordinates (x, y) . This assumption can be physically satisfied by a small depth of the microfluidic channel. Second, it is assumed that all frequency components of the incoming light are equally transmitted. This assumption can be physically satisfied by a specific narrow bandwidth of the light.

The use of Equation (2) for a complete deterministic analysis is not practically feasible because of unknown specific values of $h(u, v)$ at each $\{u, v\}$ point. Therefore, for real time and on-line calculation purposes, it is desirable to reduce the 2D formulation (Equation 1 and/or 2) into 1D case. This can be only possible when the OOI will have distinguished geometrical features along only one coordinate, e.g. x_{OOI} and other dimension will not have significant statistical meaning. Such dimension reduction simplifies Equation (2) as

$$S_{DOI}(\omega) = |H(j\omega)|^2 S_{OOI}(\omega) \quad (3)$$

One of possibilities for such dimension reduction is a use of a deterministic periodic structure, e.g. along u coordinate. Figure 6.3 shows an example of OOI (object with fresh lubricant), its horizontal cross-section and a spectral density of the OOI horizontal cross-section. Mathematically, OOI cross-section can be understood as a periodic sequence of rectangular pulses:

$$I_{OOI}(u) = f(u, T, \tau, A), \text{ where } T, \tau, A = \text{const} \quad (4)$$

where T , τ , and A are the period, duration and amplitude of OOI cross-section, respectively. This deterministic periodical process has a well-defined spectral density along u coordinate as [19]:

$$S_{OOI}(\omega) = \frac{2}{\pi} n \left(\frac{\sin(\tau\omega/2)}{\omega} \right)^2 \quad (5)$$

where n is the number of periodical lines in the OOI and ω is the spatial radial frequency.

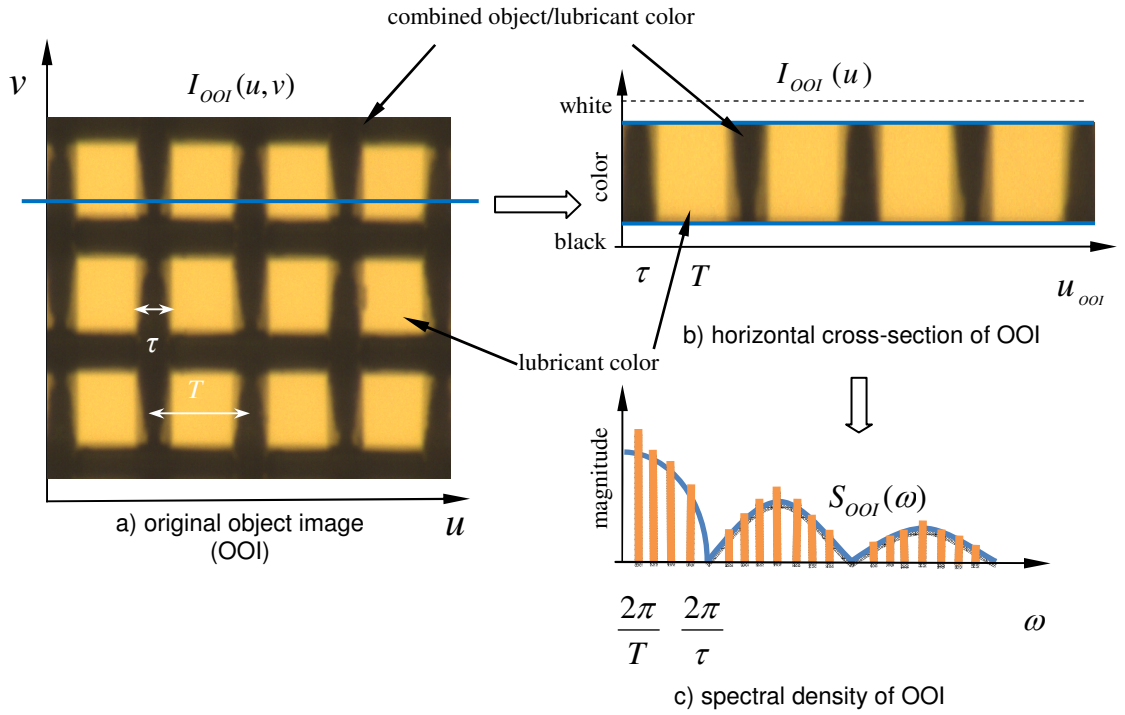


Figure 6.3 Original object image with known periodical structure and its characteristics

That implies properties and characteristics of the OOI to be specific, precisely measurable, and *a priori* known e.g., certain spectral density $S_{OOI}(\omega)$ and auto-correlation function $C_{OOI}(u)$.

In contrast, introduction of contaminants affects DOI (combined contaminated lubricant and object image) properties. Therefore, $I_{DOI}(u)$ becomes a random process with introduction of contaminants due to the changes in the DOI color cross-section parameters as:

$$I_{DOI}(u) = f(u, T, \tau_i, A_i) \quad , \text{ where } \tau_i, A_i = \text{var} \quad (6)$$

Due to a distortion effect and introduction of contaminants, a width of the distorted (blurred) periodical structure $\tau_{DOI} \neq \tau_{OOI}$ and a difference between object and lubricant $A_{DOI} \neq A_{OOI}$ significantly change. As a result, an entire shape curve of the color cross section (as a spatial process) is changed causing variations in auto-statistical

characteristics, such as auto-correlation function $C_{DOI}(u)$, auto spectral density $S_{DOI}(\omega)$, *etc.* Therefore, first part of the statistical optical analysis methodology of the contaminated lubricants consists in analysis and comparison of auto-statistical characteristics calculated from the OOI and DOI color cross-sections, e.g. $C_{OOI}(u)$ vs. $C_{DOI}(u)$ and/or $S_{OOI}(\omega)$ vs. $S_{DOI}(\omega)$. However it should be noted that the period T of the structure remains unchanged with introduction of contaminants because of an original periodic structure. This part of the statistical optical methodology directly deals with the results of lubricant contamination, where difference between characteristics for fresh and contaminated lubricant estimates a contamination value. Therefore, it is more suitable for on-line monitoring of the contaminated lubricants where statistical characteristics of actual lubricant condition are time-by-time (or after certain mileage) compared with statistical characteristics of the fresh lubricant. In practical applications, a maximum difference between statistical characteristics of the fresh and used lubricant can be set to detect a functional limit of the in-use lubricant. In contrast to the first part, second part of the statistical optical methodology is focused on the characterisation and analysis of the distortion effect using an OTF defined in Eq. 3, which can be re-written as:

$$|H(j\omega)|^2 = S_{DOI}(\omega)/S_{OOI}(\omega) \text{ or } H(j\omega) = S_{DOI,OOI}(j\omega)/S_{OOI}(\omega) \quad (7)$$

where $S_{DOI,OOI}(j\omega)$ is the cross-spectrum between DOI and OOI color cross-sections. Since $S_{OOI}(\omega)$ is calculated for a fresh lubricant only, it always remains unchanged, while $S_{DOI}(\omega)$ and $S_{DOI,OOI}(j\omega)$ are always changed with respect to the current lubricant condition and a certain contaminant concentration. Therefore two conclusions are become apparent. Firstly, changes in the amplitude and phase characteristics of $H(j\omega)$ will adequately characterize the evolution of lubricant condition with respect to the introduced contaminant(s). And secondly, $S_{DOI,OOI}(j\omega)$ and $S_{DOI}(\omega)$ fully represent $H(j\omega)$ and $|H(j\omega)|^2$ because $S_{OOI}(\omega)$ is independent from changes in the contaminant condition.

6.2.2 Preliminary image analysis and experimental methodology

Preliminary image analysis is a critical part of the entire experimental procedure because it extracts reliable information on OOI and DOI from raw image data for further advanced statistical optics analysis. A main goal of the preliminary image analysis is to obtain color cross-sections of OOIS and DOIs. The object's color cross-section will be used in the statistical optical analysis to extract corresponding statistical characteristics of the OOI and DOI for their further comparison. A schematic of the preliminary image analysis is shown in Figure 6.4. The goal of the preliminary image analysis is to extract, preliminary process, and deliver digital data suitable for further optical analysis. Initially, an optical image of the lubricant and object with periodic structure is acquired as a two-dimensional matrix array with respect to the color of each pixel and its X-Y position. In the initially acquired optical image, the woven cloth provides a square grid represented by dark color having the engine lubricant flowing through within the grid with a constant period T .

During the next step, three image cross-sections at the mid-distance between two horizontal grid lines are selected and extracted to confirm statistically the validity of the measured data. Each image cross-section contains four intersections with vertical grid lines surrounded by lubricant image on each side forming an object shape as a vector of 640 pixels. For better physical understanding of object shape, the pixel values of each image cross section are normalized ranging between 0 (black) to 1 (white). Mapping pixel color scale (between 0 and 1) vs. pixel position forms the color cross-section. The color cross-section is pre-processed data ready for further analysis of lubricant condition and contaminant presence. Typically this cross-section has a number of peaks and valleys corresponded to the number of vertical lines representing the periodical structure of the object. The peak values (close to white color) correspond to the lubricant color passing through the microfluidic channel without interference with object, while the valleys corresponded to the combined color of the object affected by lubricant. Standard mathematical function from MATLAB software was used to extract this information from the captured images (see Appendix B)

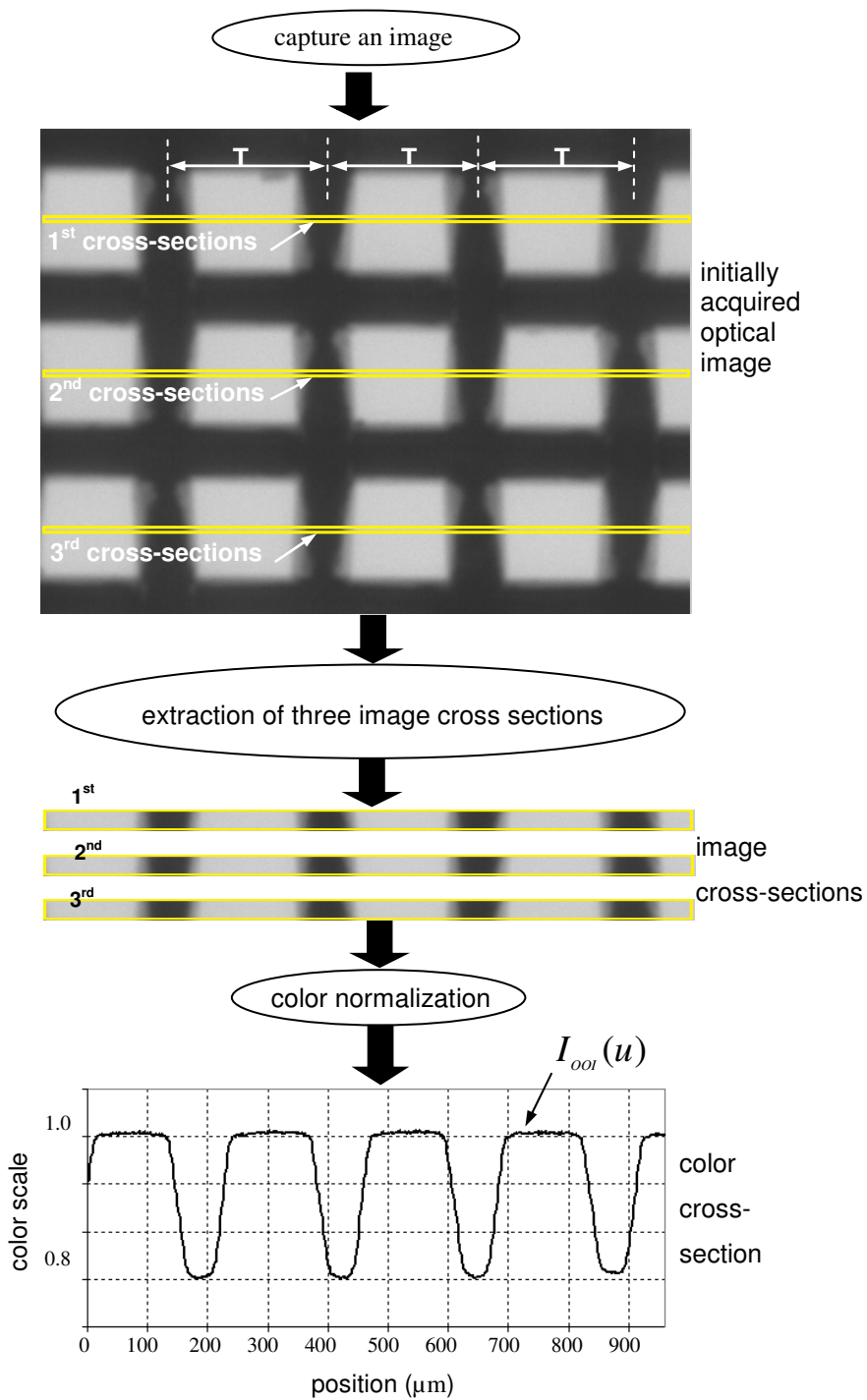


Figure 6.4 Schematic of preliminary image analysis to obtain object's color cross-section

Generalized experimental methodology for statistical optics analysis of contaminated lubricants is shown in Figure 6.5. Initially, the light is sent through a lubricant and object with periodic structure and a combined optical image is recorded. According to the proposed logic for further comparison, initially, optical image of a medium without distorting ingredients, e.g. fresh engine lubricant or lubricant right after oil change, will be acquired. Such an image from the undistorted optical medium and object represents the initial state or condition of the optical medium. As engine runs lubricant degradation process occurs. Optical images with operating lubricant and unchanged periodical object are acquired further delivering optical information with respect to the degradation of lubricant conditions. Optical image analysis for both fresh and used engine lubricants consists of extraction of certain statistical characteristics and their consecutive comparison. The acquired optical data from images requires initial image processing, such as, cross-sectioning, color normalization *etc.* Final step of the experimental analysis methodology is focused on a quantitative analysis of contaminant presence and analysis of lubricant condition evolution using statistical characteristics of DOI, e.g. as OTF, autocorrelation functions, power spectrum densities, etc. Comparison of these parameters and characteristics provides accurate and reliable estimation of the contaminant presence. In this methodology, the statistical characteristics of the OOI for a fresh lubricant (without contaminants) are considered as a benchmark from which the evolution of the statistical characteristics of the DOI due to the introduction of contaminants is analyzed.

In addition to mentioned above statistical optics characteristics, effective width of the OTF at a certain frequency ω_0 was calculated as:

$$\Delta H_{eff}(\omega_0) = \frac{\int_0^{\infty} |H(j\omega)|^2 d\omega}{|H(j\omega_0)|^2 d\omega} \quad (8)$$

A ΔH_{eff} value characterizes a frequency bandwidth where OTF transfers a major part of the optical information, e.g. during transformation of OOI into DOI with

introduction of contaminants. Therefore, the ΔH_{eff} value can be used as an additional informational parameter for monitoring engine lubricant condition.

It is necessary to note in addition that averaging of color cross-sections was not applied during preliminary image analysis and each color cross-section was considered as a unique original measured characteristic. In contrast, the averaging was applied at the final stage of statistical optics analysis only. For example, initially a particular statistical characteristic (e.g. auto-correlation function, auto spectral density, etc.) is calculated from the original color cross-section and only after that all calculated particular statistical characteristics are averaged into one without losing any statistically valid information.

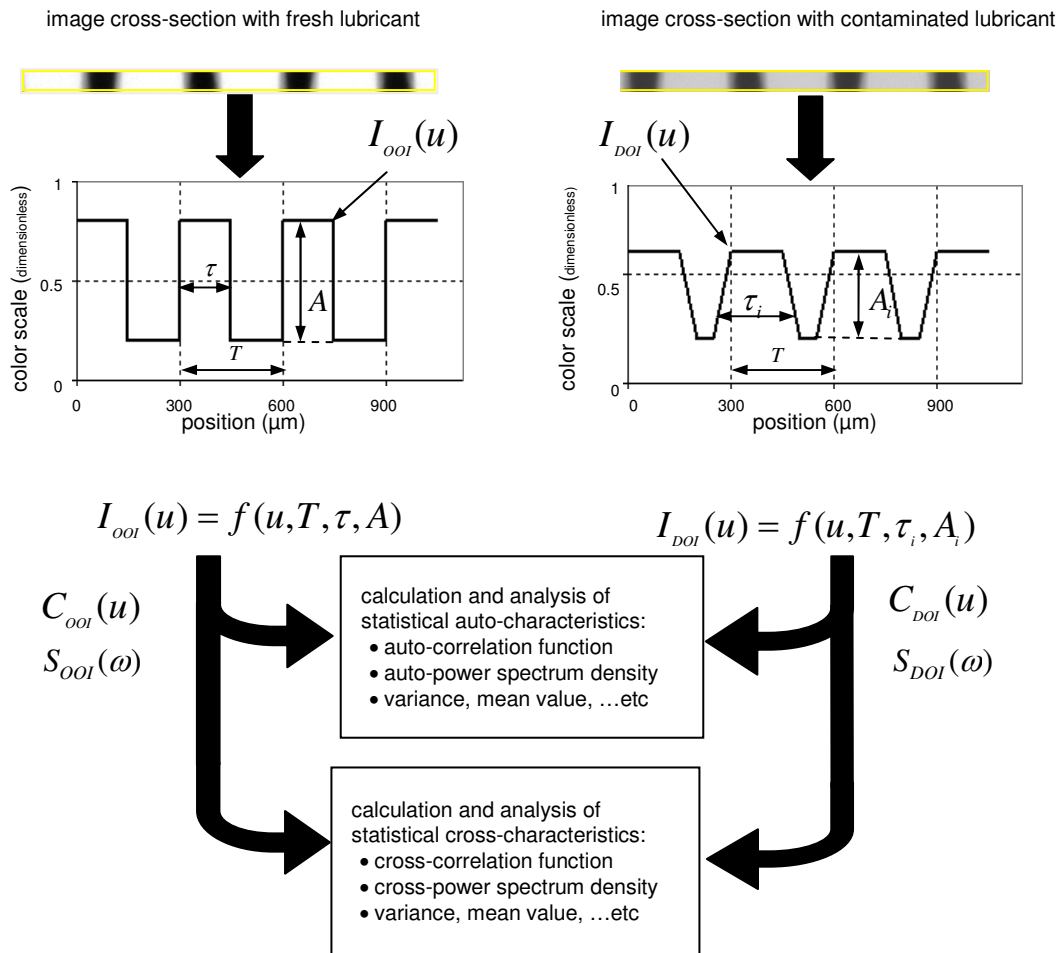


Figure 6.5 Generalized schematic of the statistical optical analysis methodology

6.3 Experimental verification

To illustrate capabilities of the statistical optical analysis methodology and the proposed sensing system three separate experiments were carried out. In the first experiment, fresh lubricant (Pennzoil SAE 5W30) was mixed with coolant, gasoline and water at a concentration of 0% to 10%. In the second experiment a combination of coolant (0-5%) and gasoline (0-5%) was added to the fresh lubricant (Pennzoil SAE 5W30) and the change in the lubricant optical properties was studied. In third experiment, a commercially available SAW 5W-20 engine lubricating oil was used for the road test. A set of engine lubricating oil samples was collected from the vehicle for real time analysis. The collected samples were from a Ford Taurus under general service, with a mixed city and highway driving condition. During the experiments, samples were pumped through the microfluidic channel, optical images were acquired and statistical characteristics such as ACT, ASF, and OTF were calculated for each sample.

6.3.1 Statistical optical analysis of coolant, gasoline, and water contaminated lubricant

The effect of introducing coolant to the engine lubricant and increasing its concentration on color scale graph is illustrated in Figure 6.6. Introduction of 1% coolant into the engine lubricant sample immediately caused a decrease in peak-to-valley (P-to-V) of the graph from 0.624 to 0.594 (5% reduction). From 1% to 2%, 3%, and 4%, the P-to-V decreased at a much higher rate of 0.086 (14.4% reduction). From 4% to 10%, the P-to-V of color cross-section graph decreased at the rate of 0.12. Overall, introduction of coolant into the engine lubricant from 1% to 10% decreased the P-to-V of DOI from 0.624 to 0.182 (a difference of 0.442). In contrary, addition of gasoline into the lubricant did not make an obvious change in the color cross-section graph. As gasoline concentration was increased from 1% to 10%, the P-to-V showed a slight increase from 0.595 to 0.598 (0.5% change). Like coolant, addition of water showed an immediate reduction on the graph P-to-V. Introduction of 1% of water lowered the graph P-to-V from 0.613 to 0.585 (4.6% reduction). From 1% to 10% of water contamination the graph P-to-V decreased at an average rate of 0.048 per increment. Addition of 10% water to engine lubricant lowered the P-to-V of color scale graph from 0.613 to 0.332

(45% reduction). The change in the P-to-V of the color scale graph is studied in details in the following sections.

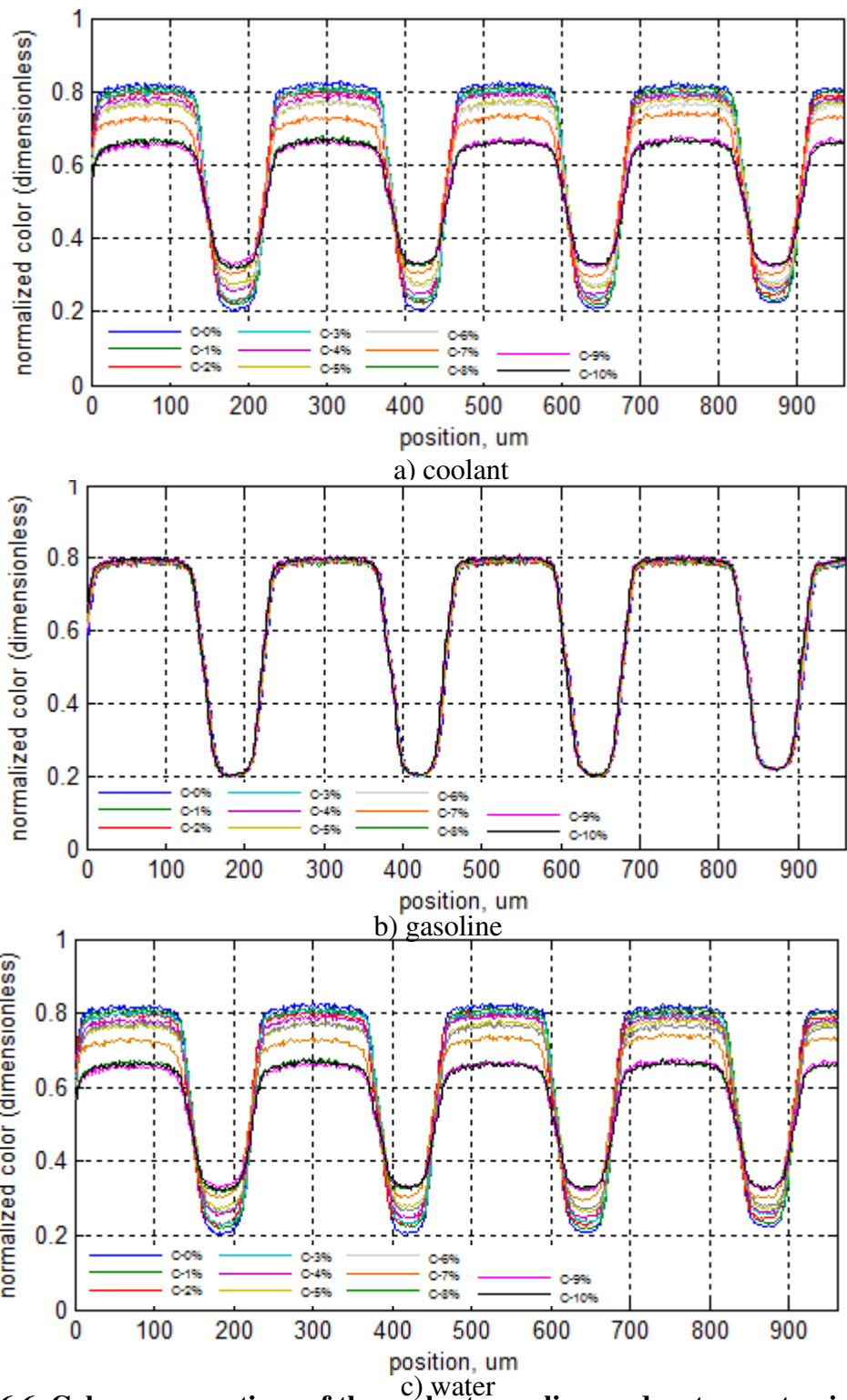


Figure 6.6 Color cross-sections of the coolant, gasoline, and water contaminated lubricant

The OOI and DOI color cross-sections were used as the experimental data to perform statistical auto-correlation function using standard mathematical function from MATLAB software (see Appendix B). Figure 6.7 shows the normalized (divided over a variance value and therefore calculated in normalized units (n.u.)) auto correlation functions of the color scale graph of contaminated lubricant with coolant, gasoline, and water with concentrations of 0% to 10%. As it was expected having a deterministic periodical structure of the object, the correlation graph is a periodic function. Correlations located at $\{0, T, 2T, \dots\}$ have no amplitude variations with respect to the contaminants concentration. All differences in auto-correlation functions $C_{OOI}(u)$ and $C_{DOI}(u)$ are located around coordinates $\{T/2, 3T/2, \dots\}$. Correlation amplitudes around these coordinates contain statistically valid information regarding contaminant concentration. A closer examination of the coolant correlation function graph within 70...150 μm region (around $T/2=110 \mu\text{m}$) shows that while a concentration of the coolant was increased from 0% to 10%, a minimum negative correlation value increased from -0.5245 n.u.² to -0.6215 n.u.² (an increase of 15.6%). Introducing 1% concentration of coolant caused the correlation value to increase by 0.0062 n.u.². Variation in the correlation values was not uniform. At 3%, 5%, 8%, and 10% coolant concentrations the correlation values increased at a higher rate as to compare to the rest. Gasoline correlation function graph showed addition of 1% gasoline into the lubricant increased the correlation value from -0.5193 n.u.² to -0.52096 n.u.². Increasing the gasoline concentration from 1% to 10% increased the correlation value from -0.52096 n.u.² to -0.5278 n.u.², however, the increase rate was not uniform for all the concentrations and slowed down at higher values of contaminant. Overall addition of gasoline to the engine lubricant increased the correlation value by 1.6%. Introduction of 1% of water into lubricant increased the correlation values from -0.5258 n.u.² to -0.5277 n.u.² (an increase of 0.0019 n.u.²). While the water concentration was increased to 1% and 10%, the correlation values increased from -0.5277 n.u.² to -0.5760 n.u.². The rate of increase was more uniform as to compare to coolant and gasoline (an average of 0.0051 n.u.² per increment). In total, addition of 10% water into the engine lubricant increased the correlation values at $T/2$ region by 8.7%.

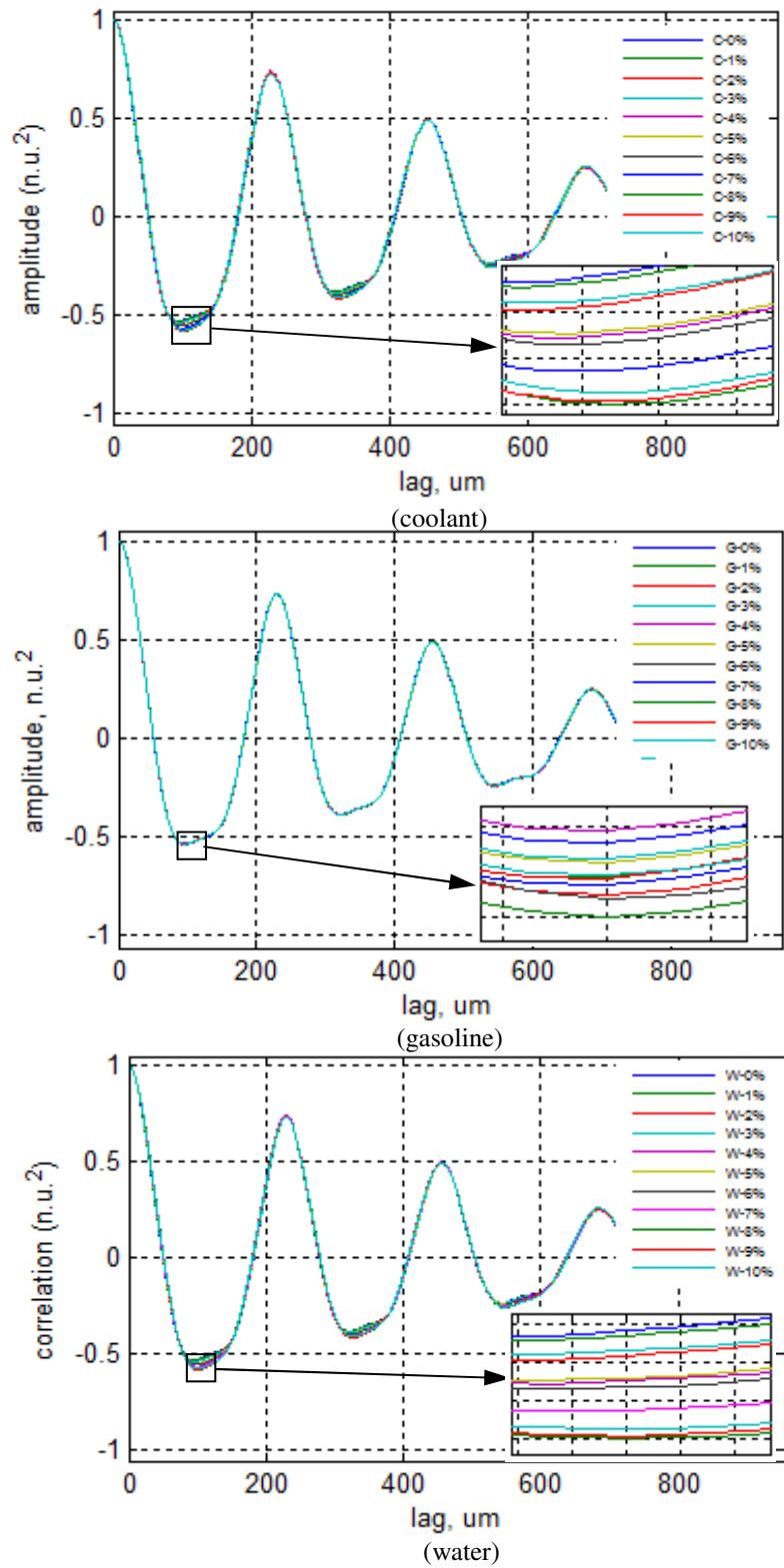


Figure 6.7 Auto correlation function of coolant, gasoline and water contaminated engine lubricant

The color cross-sections were used as the experimental data to perform statistical auto spectral function using standard mathematical function from MATLAB software. Figure 6.8 shows auto spectral functions of the color scale graphs of contaminated lubricant with coolant, gasoline, and water with concentrations of 0% to 10%. The auto spectral function of the color cross-section is sharply peaked at frequency of 0.00651 ($1/\mu\text{m}$), but still continues smoothly. It is necessary to note that as the concentration of the contaminants changes, the amplitude and width of auto spectral functions graph changes. Therefore, the width of auto spectral function graph at half of maximum amplitude (W_{ASF}) was selected for the comparative analysis of ASF_{OOI} and ASF_{DOI} with respect to contaminant concentration.

Introducing 1% coolant into the engine lubricant lowered the W_{ASF} form 0.00320 ($1/\mu\text{m}$) to 0.00319 ($1/\mu\text{m}$) immediately. As the coolant concentration was increased to 10%, the W_{ASF} value changed to 0.00312 ($1/\mu\text{m}$), a 2.5% reduction. Addition of 1% of gasoline into engine lubricant had an increasing effect the W_{ASF} , but overall it did not show an obvious change in the W_{ASF} value. Like coolant, introduction of water into the engine lubricant lowered the W_{ASF} value form 0.00320 ($1/\mu\text{m}$) to 0.00319 ($1/\mu\text{m}$). As the water concentration was increased from 1% to 10%, the W_{ASF} values reduced from 0.00319 ($1/\mu\text{m}$) to 0.00314 ($1/\mu\text{m}$). Overall, introduction of water from 1%-10% effected the W_{ASF} values by 1.9%. (see Figure 6.9)

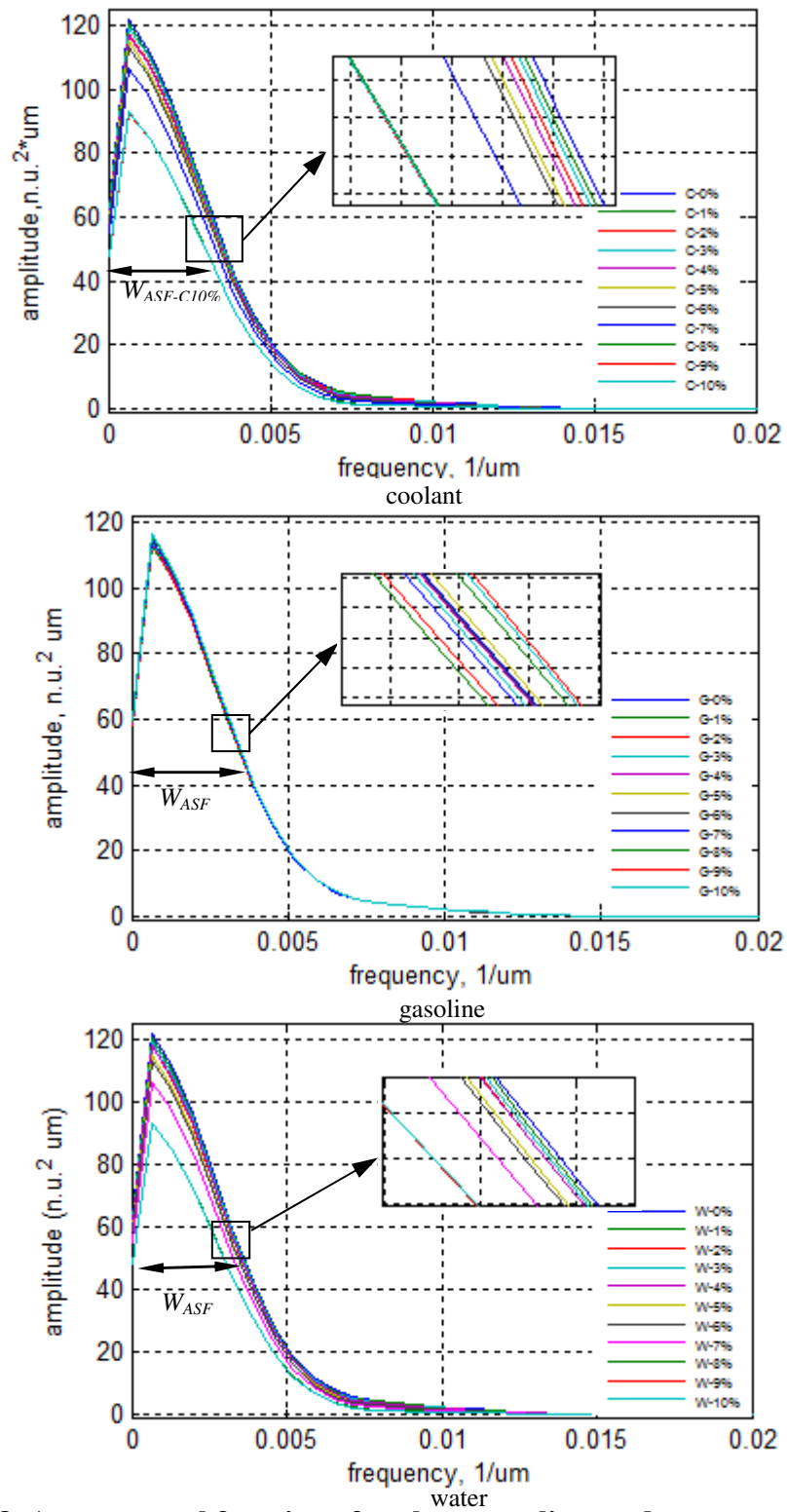


Figure 6.8 Auto spectral function of coolant, gasoline, and water contaminated engine lubricant

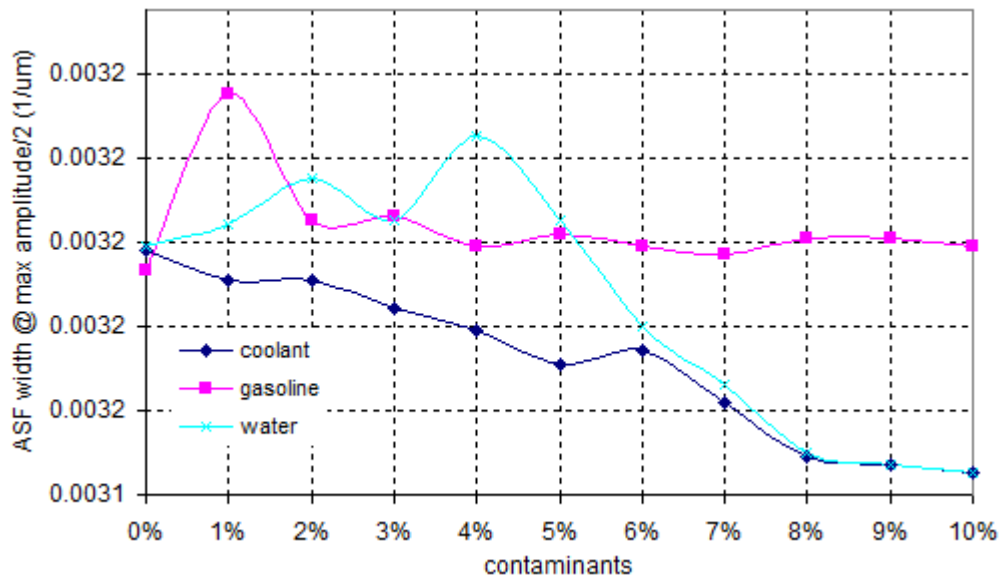


Figure 6.9 Evaluation of change in W_{ASF} graph with respect to contaminants percentage

Optical transfer function OTF is another statistical optics characteristics showing the transformation of OOI represented by $I_{OOI}(u)$ into DOI represented by $I_{DOI}(u)$ due to the introduction of contaminants. Eq. 7 was used to calculate the OTF between $I_{OOI}(u)$ and $I_{DOI}(u)$ for different contaminants concentrations with respect to a fresh lubricant using standard mathematical function from MATLAB software. An OTF value of 1 represents a benchmark level for comparison with the OTF of contaminated lubricant. This value 1 cannot be exceeded due to the physical meaning of the OTF, and therefore, any negative deviation of the OTF calculated for a contaminated lubricant will be due to the degradation of lubricant optical properties leading to a distortion of the object image. It is shown in Figure 6.10, even with the introduction of 1% of coolant or water, $OTF_{1\%}$ lowers significantly below 1 within a frequency range between 0 and $0.025 \mu\text{m}^{-1}$, while 1% of gasoline did not cause any significant effect on the optical transfer function graph. As the coolant and water concentration was increased from 1% to 10%, the negative deviation in transfer function graph was observed. Overall, the introduction

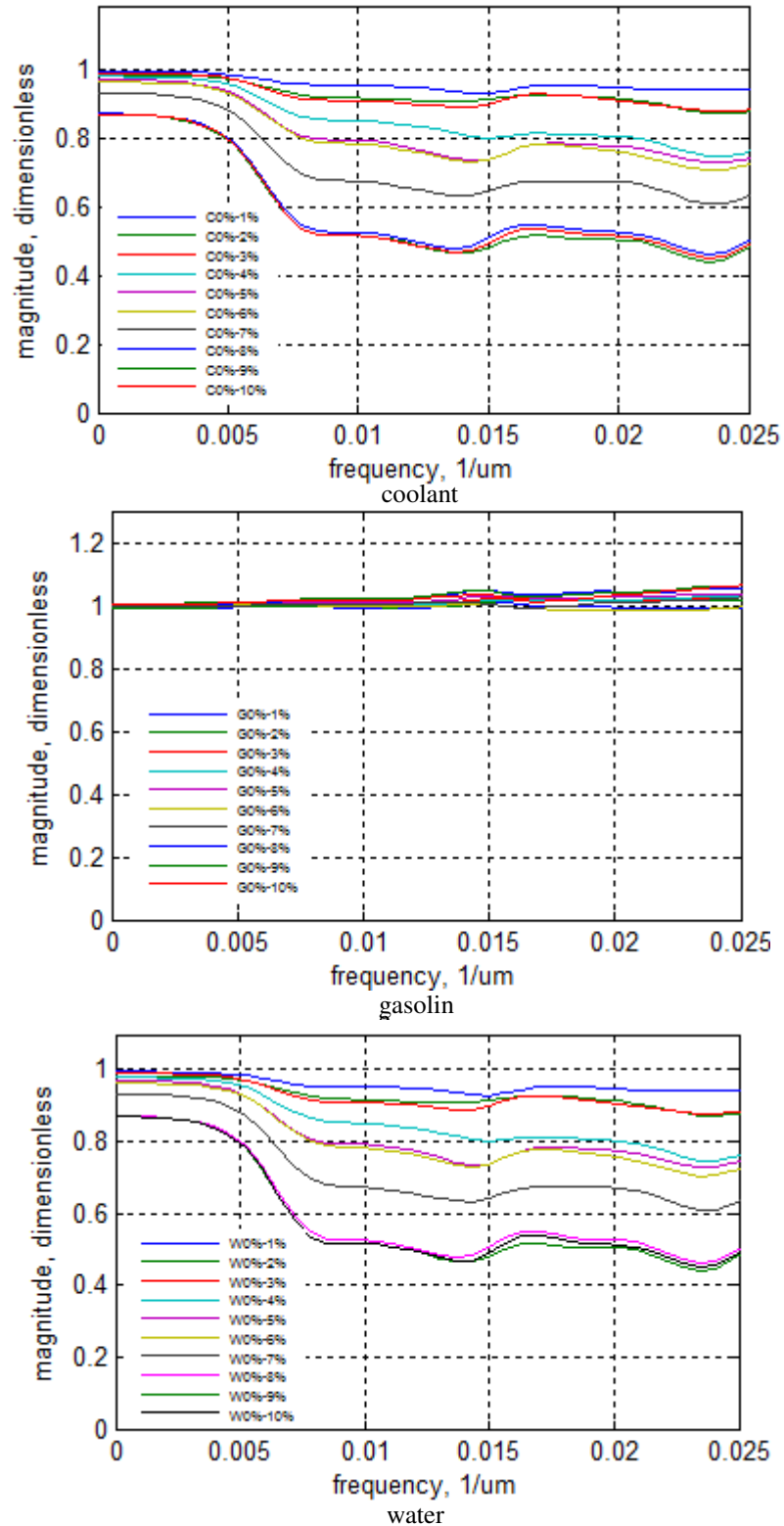


Figure 6.10 Evolution optical transfer function with respect to coolant, gasoline and water concentration

of coolant and water into the engine lubricant significantly weakened the statistical linkage between $I_{OOI}(u)$ and $I_{DOI}(u)$, and the magnitude of the OTF was decreased with the higher contaminant concentration, while addition of gasoline did not cause a similar effect on OTF graph.

To quantify the changes in OTF, Equation 8 was used to calculate the effective width of the transfer function between the ranges of $\omega = 0 \mu\text{m}^{-1}$ to $\omega = 0.025 \mu\text{m}^{-1}$. Addition of 1% of coolant into the lubricant changed the ΔH_{eff} value from $0.025 \mu\text{m}^{-1}$ to $0.02434 \mu\text{m}^{-1}$ (a $0.0007 \mu\text{m}^{-1}$ reduction). As the coolant concentration was increased to 10%, the ΔH_{eff} value decreased to $0.01129 \mu\text{m}^{-1}$. In total, addition of 0%-10% of coolant into the engine lubricant lowered the ΔH_{eff} value by $0.0137 \mu\text{m}^{-1}$. Addition of gasoline did not have any decreasing effect on the ΔH_{eff} value, while addition of 1% of water lowered the ΔH_{eff} values from the $0.025 \mu\text{m}^{-1}$ level to $0.02437 \mu\text{m}^{-1}$ (a $0.0006 \mu\text{m}^{-1}$ reduction). As water concentration was increased from to 10%, the ΔH_{eff} values decreased to $0.0169 \mu\text{m}^{-1}$. Overall, introduction of 0%-10 of water lowered the ΔH_{eff} values from $0.025 \mu\text{m}^{-1}$ to $0.0169 \mu\text{m}^{-1}$ (a $0.0081 \mu\text{m}^{-1}$ reduction). Amongst the three contaminants, coolant had the most effect on the $I_{OOI}(u)$, while water came second and gasoline did not show any effect on the $I_{OOI}(u)$.

In general, using one information parameter is not statistically sufficient for reliable on-line monitoring of process conditions. Therefore, combining two statistically obtained one-dimensional (1D) information parameters, such as $C(T/2)$ and ΔH_{eff} , into one 2D informational parameter $\{C(T/2), \Delta H_{eff}\}$ allows evaluation and monitoring of lubricant contamination as a function of two statistical variables in corresponding 2D information plane.

Figure 6.11 shows evolution of coolant, gasoline and water contamination in the information space $\{C(T/2), \Delta H_{eff}\}$. In general, addition of 1% to 10% of coolant into engine lubricant caused a reduction in the ΔH_{eff} values and an increase in $C(T/2)$ values. Variation of ΔH_{eff} and $C(T/2)$ values in the $\{C(T/2), \Delta H_{eff}\}$ informational space indicate a strong correlation between these values. Addition of gasoline into the lubricant showed an increase in $C(T/2)$ values while ΔH_{eff} values were almost constant. Gasoline $\{C(T/2), \Delta H_{eff}\}$ informational space shows a moderate upward trend on the graph. This was mainly due to a slight increase of in ΔH_{eff} value at higher gasoline concentration. Like coolant, addition of water into the engine lubricant also showed a close correlation between ΔH_{eff} and $C(T/2)$ values as the water concentration was increased. $\{C(T/2), \Delta H_{eff}\}$ plan illustrated this relationship.

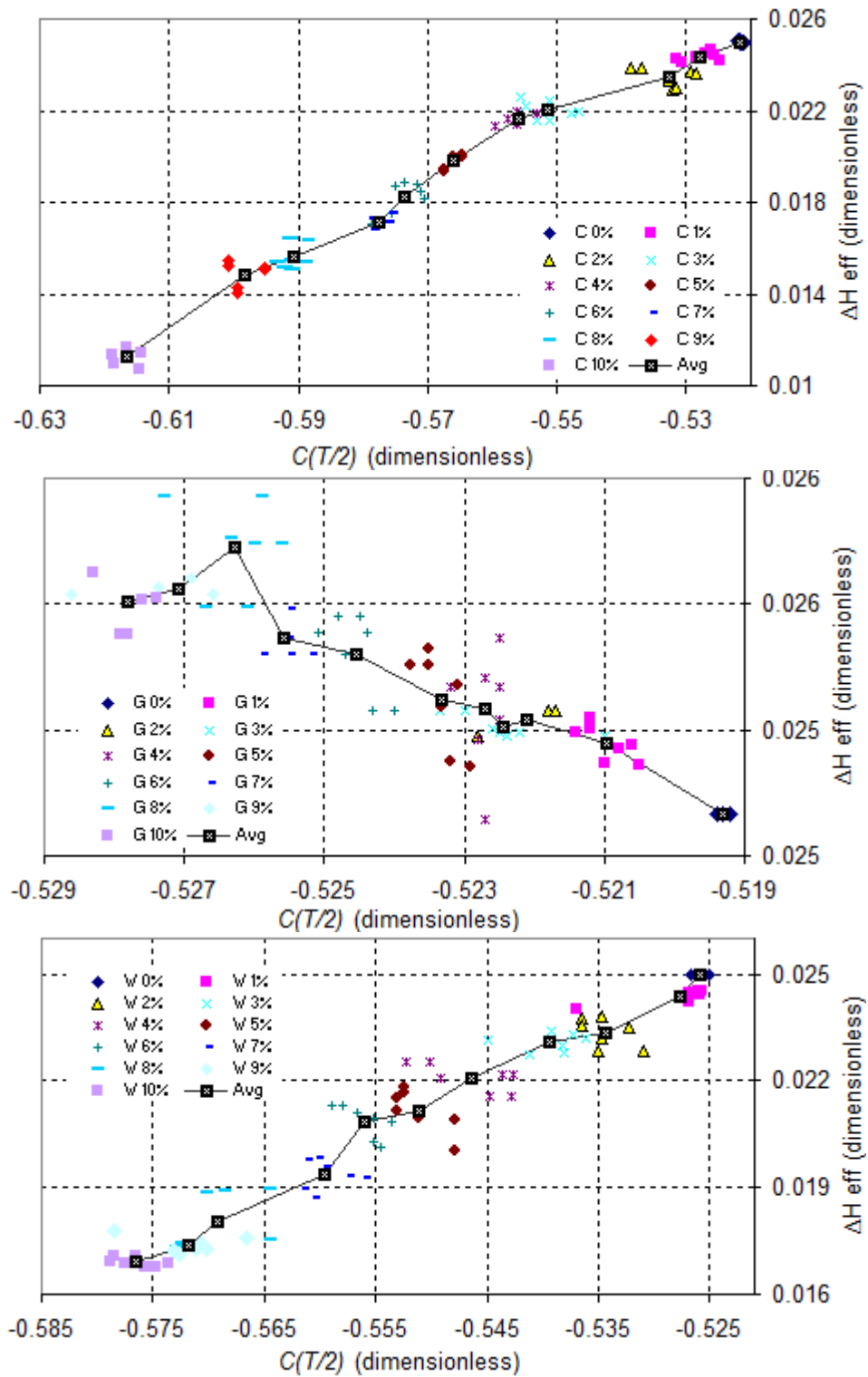


Figure 6.11 $\{C(T/2), \Delta H_{eff}\}$ informational space of coolant, gasoline, and water contaminated engine lubricant

Figure 6.12 illustrates the 2-D informational space $\{\Delta H_{eff}, W_{ASF}\}$ for monitoring lubricant contamination using two statistical variables ΔH_{eff} and W_{ASF} values. Addition of coolant into engine lubricant had a decreasing effect on the values of W_{ASF} and ΔH_{eff} . The changes of these two parameters with respect to the increase in coolant concentration are presented in $\{\Delta H_{eff}, W_{ASF}\}$ space. As coolant concentration increases, the W_{ASF} shows a close correlation with ΔH_{eff} values in a down ward trend. Introduction of gasoline into the engine lubricant did not show any significant effect on the W_{ASF} and ΔH_{eff} values. A 2-D presentation of these statistical parameters also indicates the lack of correlation between W_{ASF} and ΔH_{eff} as gasoline concentration was increased in the lubricant. Addition of water into the engine lubricant also had a decreasing influence on the W_{ASF} and ΔH_{eff} individually. A 2-D presentation of these two parameters with respect to increase in the water concentration indicates a strong correlation between these two parameters in the negative territory with a descending trend. It is noticed that at 5% of water concentration there is a positive shift in the W_{ASF} values.

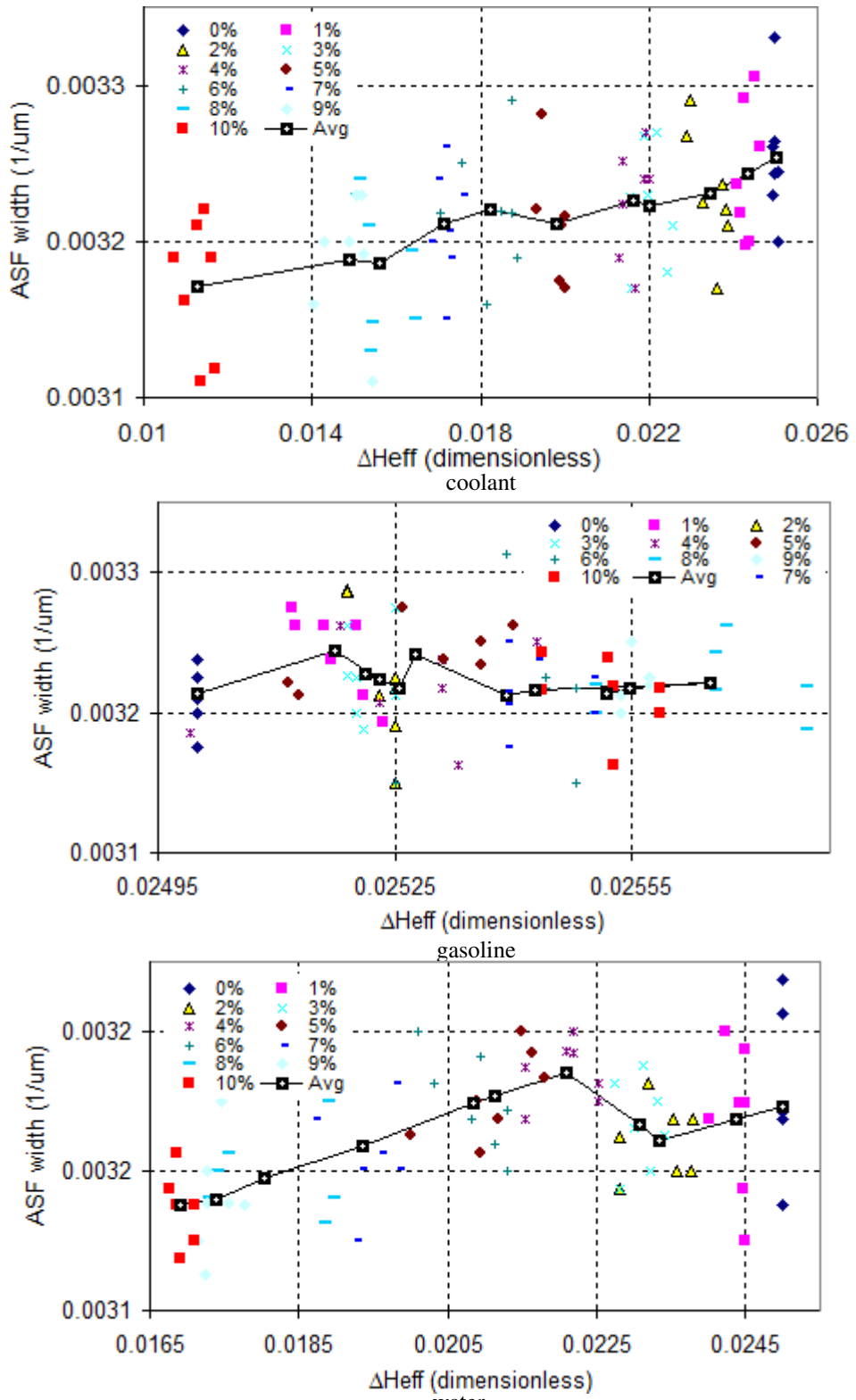


Figure 6.12 Evaluation of $\{\Delta H_{eff}, W_{ASF}\}$ for coolant, gasoline and water

A 2-D scatter plot of W_{ASF} and $C(T/2)$ values are presented in Figure 6.13. Previously it was shown addition of coolant into the engine lubricant increased the $C(T/2)$ values in the negative territory. It was also observed coolant lowered the W_{ASF} values. The 2-dimensional information space $\{C(T/2), W_{ASF}\}$ of these parameters indicates that these values are statistically dependent. Addition of gasoline into the engine lubricant did not influence the W_{ASF} and $C(T/2)$ values significantly. However, a 2 dimensional representation of these parameters indicates a weak or lack of correlation between these parameters. Introduction of water in to engine lubricant showed an increase in the $C(T/2)$ values in the negative territory, while it reduced the W_{ASF} . Plotting these parameters in a 2 dimensional presentation indicates a strong correlation between these two statistical parameters in a declining fashion.

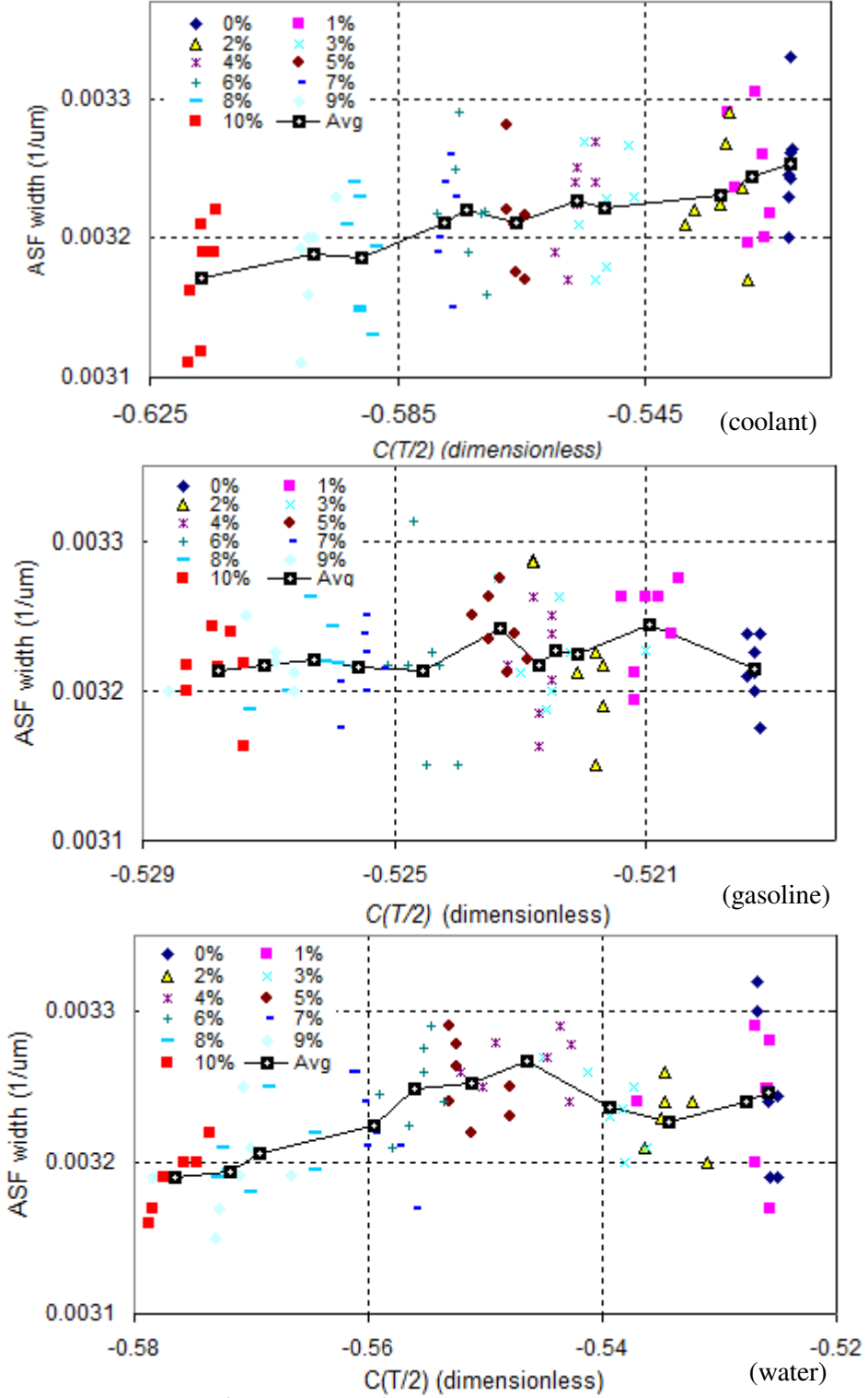


Figure 6.13 Evaluation of $\{C(T/2), W_{ASF}\}$ information space wrt coolant, gasoline and water concentration

6.3.2 Analysis of combined coolant and gasoline contamination

To demonstrate the capability of statistical optical sensing methodology in monitoring the condition of contaminated engine lubricant, a combination of coolant (0-5%) and gasoline (0-5%) was added to the fresh lubricant (Pennzoil SAE 5W30) and the color change and shape deformation of the object was studied. Figure 5.11 illustrates the combination of mixture ratio between contaminants and lubricant of all samples. During the experiment, contaminated lubricant samples were pumped through the microfluidic channel, optical images were acquired, and statistical optical parameters were calculated for each sample.

The effect of introducing coolant-gasoline to the engine lubricant and increasing its concentration on color scale graph is illustrated in Figure 6.14. Introduction of 1% coolant and gasoline into the engine lubricant sample immediately caused a decrease in P-to-V of the graph from 0.6845 to 0.627 (8.4% reduction). From 1% to 2%, 3%, 4% and 5%, these P-to-V values decreased at a rate of 0.0815, 0.0152, 0.054, and 0.0397 respectively. Overall, introduction of coolant-gasoline into the engine lubricant from 1% to 5% decreased the amplitude of color scale graph from 0.6845 to 0.4366 (a difference of 0.2479).

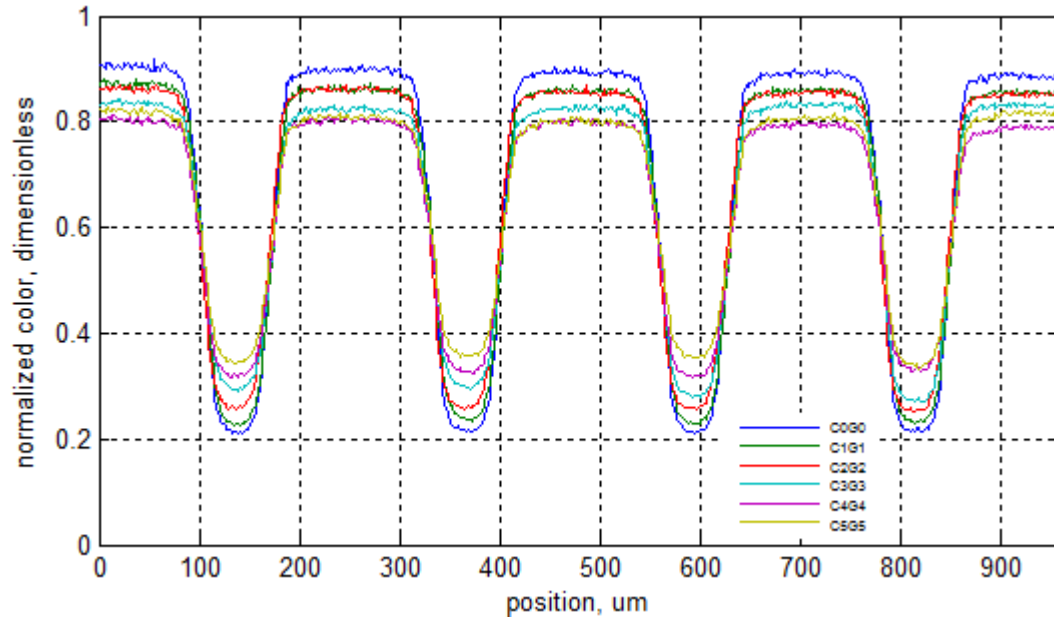


Figure 6.14 Color cross-section graph of coolant-gasoline contaminated engine lubricant

The color cross-sections of fresh lubricant image and contaminated lubricant were used as the experimental data to perform statistical auto-correlation function. Figure 6.15 shows auto correlation functions of contaminated lubricants (0%-5%). All differences in auto-correlation functions $C_{OOI}(u)$ and $C_{DOI}(u)$ are located around coordinates $\{T/2, 3T/2, \dots\}$. A closer examination of the coolant correlation function graph within 70...150 μm region (around $T/2=110 \mu\text{m}$) shows that while a concentration of the contaminants were increased from 0% to 5%, a minimum negative correlation value increased from -0.5694 n.u.^2 to -0.6143 n.u.^2 (an increase of 7.3%).

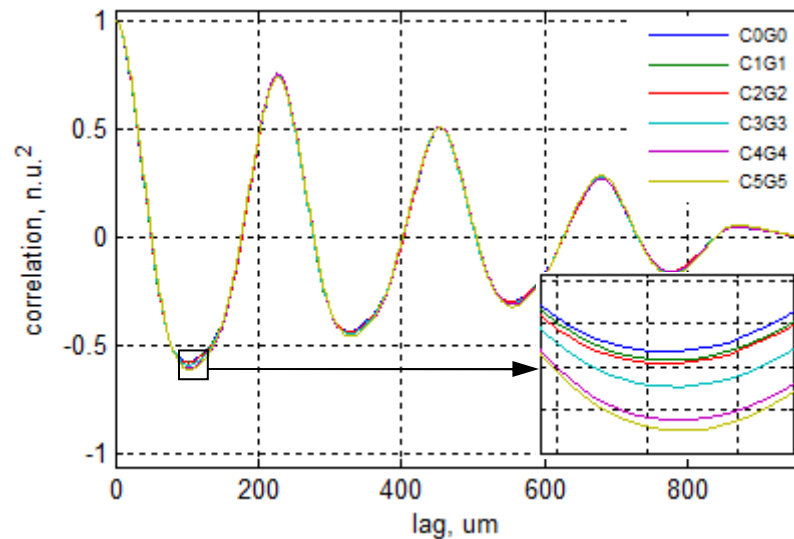


Figure 6.15 Correlation function graph of coolant-gasoline contaminated engine lubricant

The color cross-sections of fresh lubricant image and contaminated lubricant were used as the experimental data to perform auto spectral function analysis. Figure 6.16 shows auto spectral functions of the color scale graph of contaminated lubricant with coolant and gasoline concentrations of 0% to 5%. The auto spectral function of the color cross-section is sharply peaked at frequency of $0.00651 (1/\mu\text{m})$, but still smoothly continuous. Like previous cases, as the concentration of the contaminants were increased, the amplitude and width of auto spectral function graph were reduced.

Addition of coolant-gasoline combined contamination into the engine lubricant induced a reduction effect on the W_{ASF} . However, the magnitude of this effect was directly influenced by the percentage concentration of contaminants. Overall, introducing 1% to 5% of coolant-gasoline into the engine lubricant lowered the W_{ASF} from $0.003431 (1/\mu\text{m})$ to $0.003232 (1/\mu\text{m})$, a 5.8% reduction. Figure 6.16 illustrates the reduction effect of coolant-gasoline contamination on the engine lubricant.

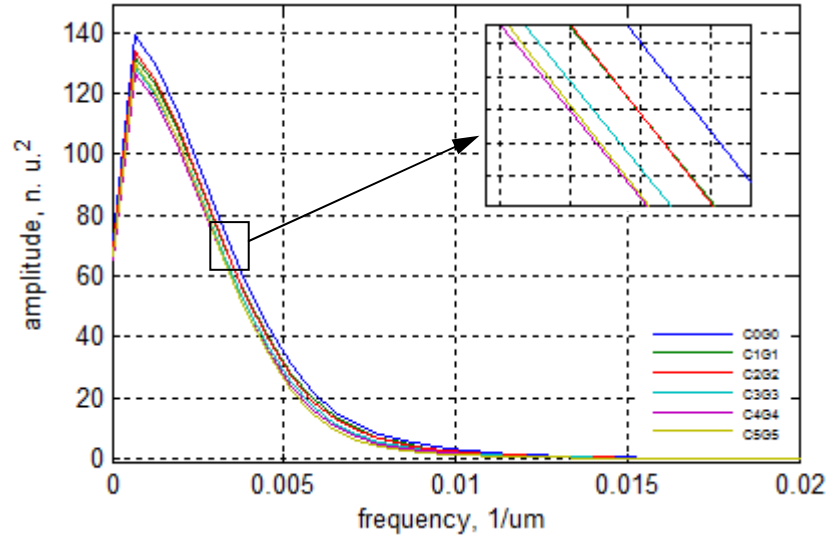


Figure 6.16 Spectrum density function plot of coolant-gasoline contaminated engine lubricant

Similarly, the color cross-sections of fresh and contaminated lubricant images were used as the experimental data to perform optical transfer function. Figure 6.17 shows optical transfer functions of the color scale graph of contaminated lubricant with combined coolant and gasoline concentrations of 0% to 5%.

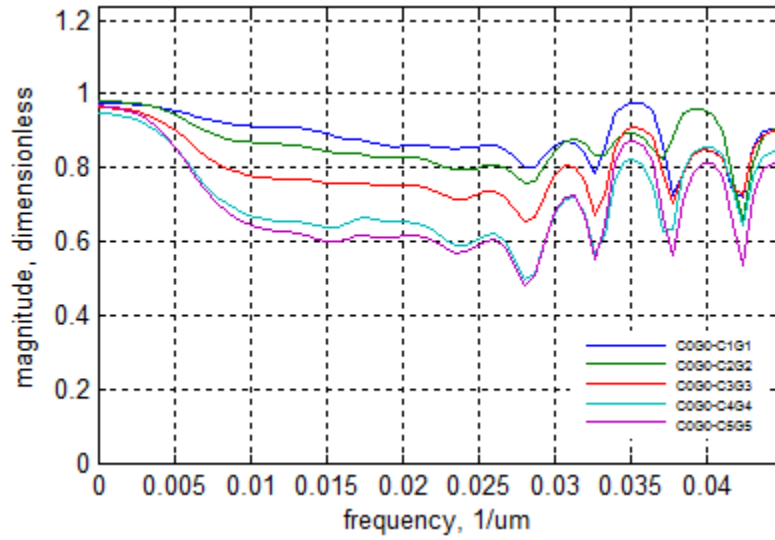


Figure 6.17. Optical transfer function evaluation of coolant-gasoline contaminated engine lubricant

It is noted that introduction of combined contaminant into the engine lubricant had a deterring effect on the optical linkage between input and output images. This effect varies based on the ratio of the combined contamination. However, introduction of combined coolant-gasoline into the engine lubricant and increasing the concentration up to 5% pushed the OTF graph down, and consequently decreased the ΔH_{eff} values from 0.0247 to 0.0171 (a 0.0069 reduction).

Then for each sample, ΔH_{eff} values were plotted against $C(T/2)$ at each combination concentration to form the 2-D information space. Figure 6.18 presents the $\{C(T/2), \Delta H_{eff}\}$ information space of combined contaminants samples.

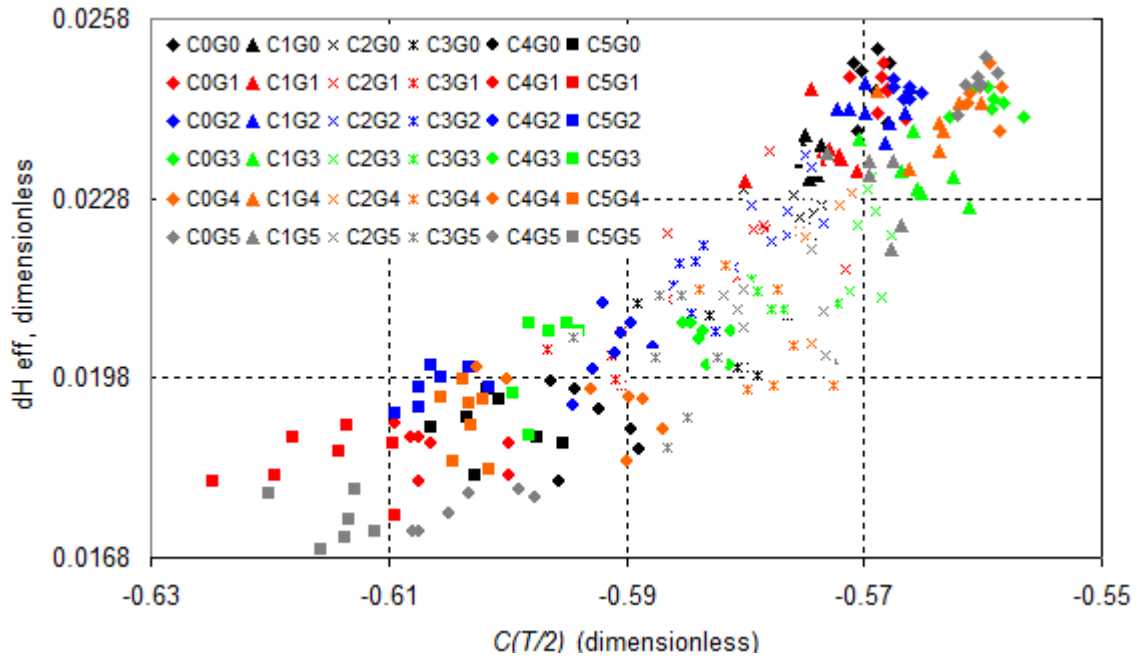


Figure 6.18 $\{C(T/2), \Delta H_{eff}\}$ information space of coolant-gasoline combined contaminated engine lubricant

In general, addition of combined coolant and gasoline (0%-5%) into engine lubricant increased the $C(T/2)$ values from -0.5691 n.u.² to -0.5951 n.u.² (a 0.026 n.u.² increase), however, ΔH_{eff} values decreased from 0.0248 n.u.² to 0.0176 n.u.² (a 0.0072 n.u.² decrease). Then for more detailed observation, each series of samples ($C_{0\%-5\%}G_{0\%}$, $C_{0\%-5\%}G_{1\%}$, $C_{0\%-5\%}G_{2\%}$, $C_{0\%-5\%}G_{3\%}$, $C_{0\%-5\%}G_{4\%}$, $C_{0\%-5\%}G_{5\%}$) was studied individually. It was shown that the addition of combined coolant-gasoline contaminant changed the informational parameters $\{C(T/2), \Delta H_{eff}\}$ plot in a non-linear fashion. At any gasoline concentration, increasing the concentration of coolant from 0%- 5% induced a similar variation pattern in $\{C(T/2), \Delta H_{eff}\}$ plane. Figure 6.18 represents a 2-D scatter plot of ΔH_{eff} and $C(T/2)$ parameters. A closer look at the 2-dimensional plot indicates a strong correlation between $C(T/2)$ and ΔH_{eff} values in the negative territory. Figure 6.19

illustrates the individual 2-D presentation of the $\{C(T/2), \Delta H_{eff}\}$ parameters for 0%-5% of coolant concentration at 0%-5% of gasoline.

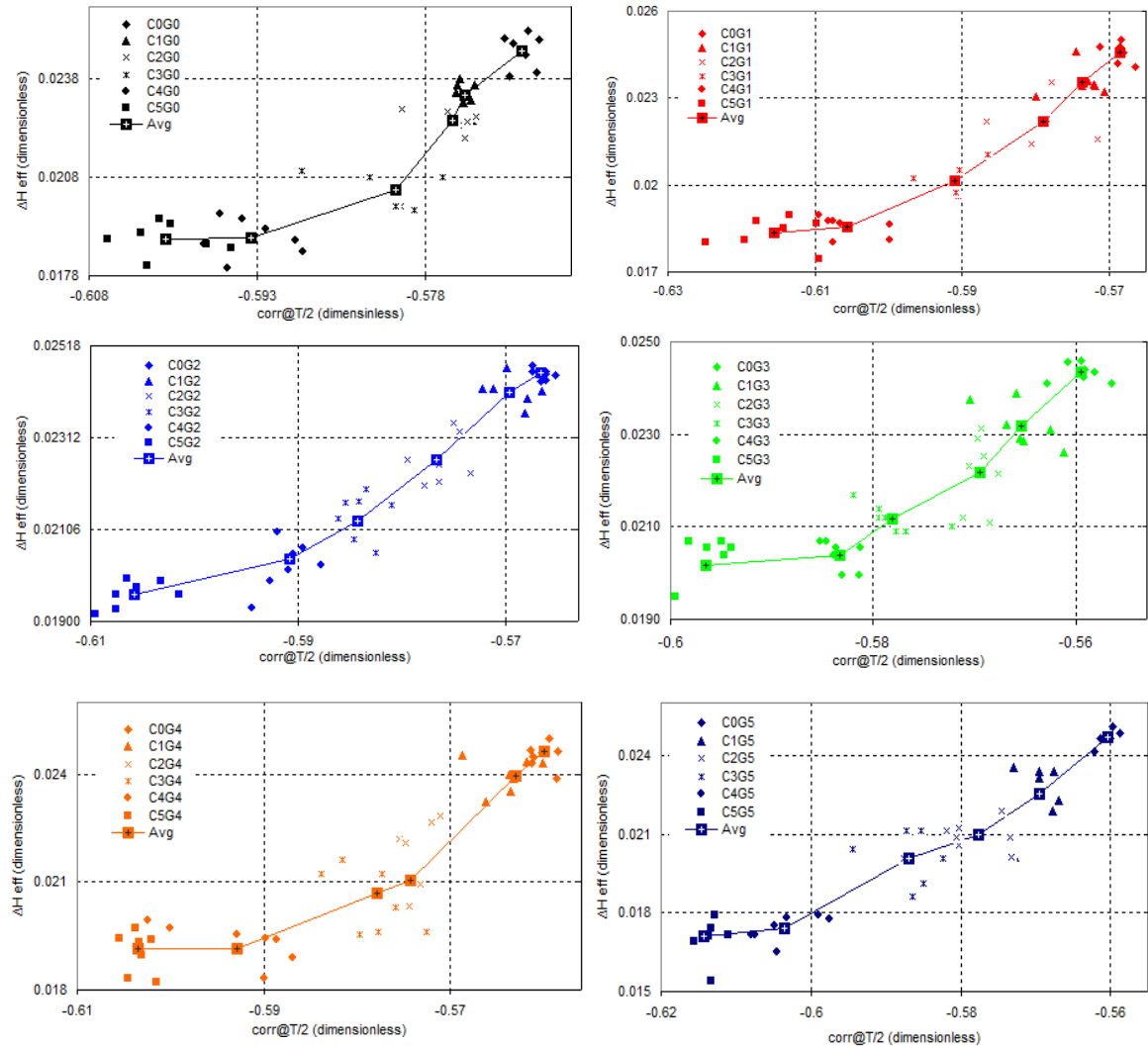


Figure 6.19 2-D information apace $\{C(T/2), \Delta H_{eff}\}$ values for coolant-gasoline concentration (0%-5%)

Figure 6.20 represents the 2-dimensional presentation of parameters W_{ASF} and ΔH_{eff} . In general, addition of combined coolant and gasoline (0%-5%) into engine lubricant decreased the W_{ASF} from 0.003431 (1/ μm) to 0.003232 (1/ μm), similarly

ΔH_{eff} values decreased from 0.0248 n.u.² to 0.0176 n.u.² (a 0.0072 n.u.² decrease). It was shown that the addition of combined coolant-gasoline contaminant changed the $\{\Delta H_{eff}, W_{ASF}\}$ plot in a non-linear fashion for each series of samples (C_{0%-5%}G_{0%}, C_{0%-5%}G_{1%}, C_{0%-5%}G_{2%}, C_{0%-5%}G_{3%}, C_{0%-5%}G_{4%}, C_{0%-5%}G_{5%}). At any gasoline concentration, increasing the concentration of coolant from 0%- 5% influenced a similar variation pattern in $\{\Delta H_{eff}, W_{ASF}\}$ plane. Figure 6.20 represents a 2-D scatter plot of $\{\Delta H_{eff}, W_{ASF}\}$ parameters. A closer look at Figure 6.20 indicates a strong correlation between W_{ASF} and ΔH_{eff} values in the negative territory.

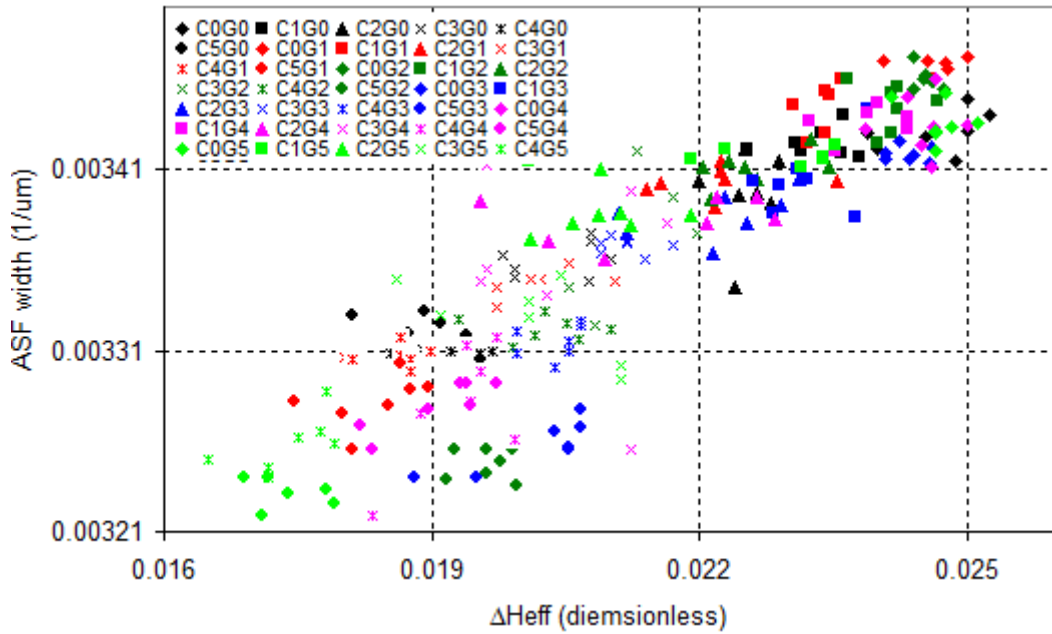


Figure 6.20 $\{\Delta H_{eff}, W_{ASF}\}$ for coolant-gasoline combined contaminated engine lubricant

In section 6.3.1 it was observed addition of coolant and gasoline individually increased the $C(T/2)$ values and decreased the W_{ASF} values. In this section it was noted introduction of combined coolant and gasoline (0%-5%) into engine lubricant also increased the $C(T/2)$ from -0.5691 n.u.² to -0.5951 n.u.², and decreased the W_{ASF}

values from 0.003431 (1/μm) to 0.003232 (1/μm). A closer observation on each series of samples ($C_{0\%-5\%}G_{0\%}$, $C_{0\%-5\%}G_{1\%}$, $C_{0\%-5\%}G_{2\%}$, $C_{0\%-5\%}G_{3\%}$, $C_{0\%-5\%}G_{4\%}$, $C_{0\%-5\%}G_{5\%}$) showed that the addition of combined coolant-gasoline contaminant changed the $\{C(T/2), W_{ASF}\}$ in a non-linear fashion. Figure 6.21 represents a 2-D scatter plot of W_{ASF} and $C(T/2)$ parameters. A closer look at this plot indicates of a strong correlation between $C(T/2)$ and W_{ASF} values.

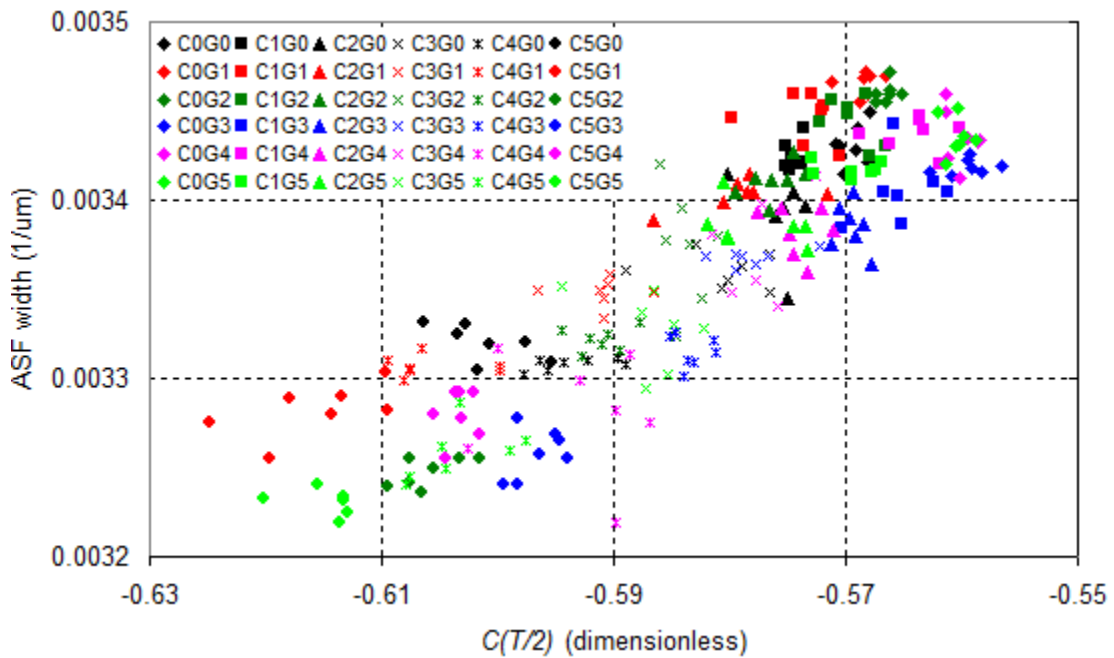


Figure 6.21 $\{C(T/2), W_{ASF}\}$ for coolant-gasoline combined contaminated engine lubricant

6.3.3 Statistical optics analysis of road test

In this experiment, a commercially available SAW 5W-20 engine lubricating oil was used for the road test. A set of oil samples was collected to perform statistical optics analysis in real time. The collected samples were from a Ford Taurus under general service, with a mixed city and highway driving condition. The purpose of this test was to see the correlation between the effect of travelled distance (normal aging process) and change in the optical properties of the lubricant and also examine the capability of the

proposed methodology to monitor the condition of engine lubricant under realistic condition in real time. All the samples went through the similar procedure as described in section 6.2.

Figure 6.22 illustrates the color cross-section graph for travelled distance of 0 km, 200 km, 800 km, 1000 km, 1200 km, 1500 km, 2350 km, 3450 km, and 4200 km. It is appear that the amplitude of the color cross-section graph (P-to-V) gradually decreased as the travelled distance increased. This indicates a correlation between travelled distance (normal aging process) and the P-to-V of the color cross-section graph. This illustrates that variation in the P-to-V of the color cross section is directly related to the travelled distance which is the indication of normal degradation of the engine lubricant. Overall, within the 4200 Km travelled distance, the P-to-V the color cross-section graph decreased from 0.699 to 0.616, a reduction of 0.083 or 11.8%.

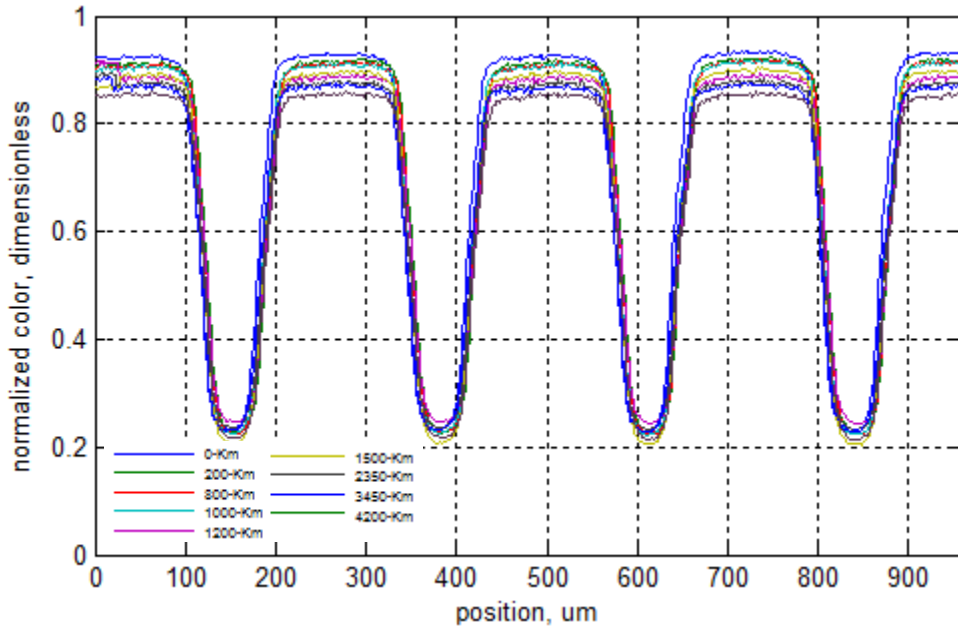


Figure 6.22 Color cross-section graph of Ford Taurus road test analysis

Similar to the previous cases, the color cross-sections of fresh lubricant image and used lubricant were used as the experimental data to perform statistical auto-correlation function. Standard mathematical function from MATLAB was used to calculate the ACF (see Appendix B). Figure 6.23 shows correlation functions of the color cross section

graph of fresh and used lubricant at different kilometres. A closer examination of the fresh and used correlation function graph within 70...150 μm region (around $T/2 = 110\mu\text{m}$) shows that while the travelled distance was increased from 0 to 4200 km, the minimum negative correlation value increased from -0.5574 n.u.² to -0.5433 n.u.² (an increase of 2.6%).

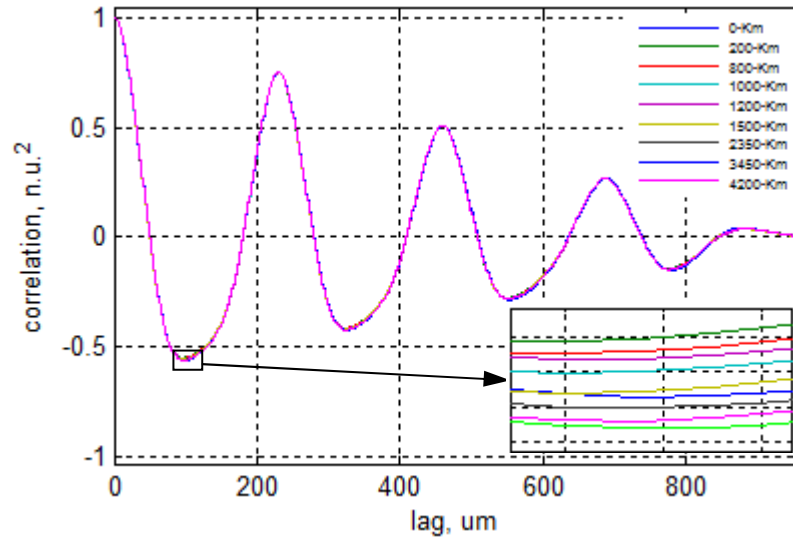


Figure 6.23. Auto correlation of road test analysis

The color cross-sections of fresh lubricant image and used lubricant were used as the experimental data to perform auto spectral function analysis. Figure 6.24 shows auto spectral functions of the color scale graph of fresh and used lubricant at 0 km, 200 km, 800 km, 1000 km, 1200 km, 1500 km, 2350 km, 3450 km, and 4200 km. The auto spectral function of the color cross-section is similar to previous cases with a sharply peak at frequency of 0.00651 ($1/\mu\text{m}$), but smooth and continuous. As the travelled distance increased from 0 km to 4200 km, the amplitude and width of auto spectral function graph (W_{ASF}) changed.

Overall, as the travelled distance increased from 0 km to 4200 km the W_{ASF} was lowered from 0.003343 ($1/\mu\text{m}$) to 0.003292 ($1/\mu\text{m}$), a 1.5% reduction.

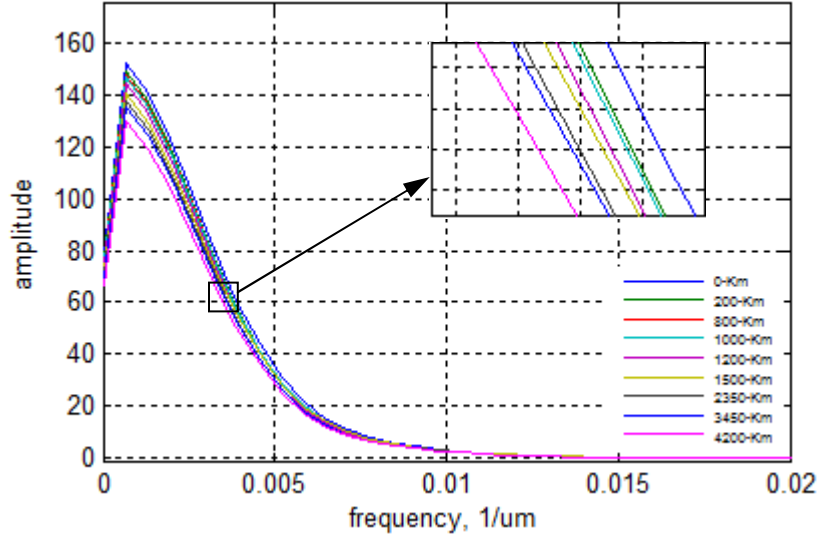


Figure 6.24 Spectrum density function graph of road test analysis

Similarly, the color cross-sections of fresh and used lubricant image were used as the experimental data to perform optical transfer function. Standard mathematical function from MATLAB was used to calculate the OTF. Figure 6.25 shows optical transfer functions of the color scale graphs of travelled distance lubricant with respect to fresh lubricant.

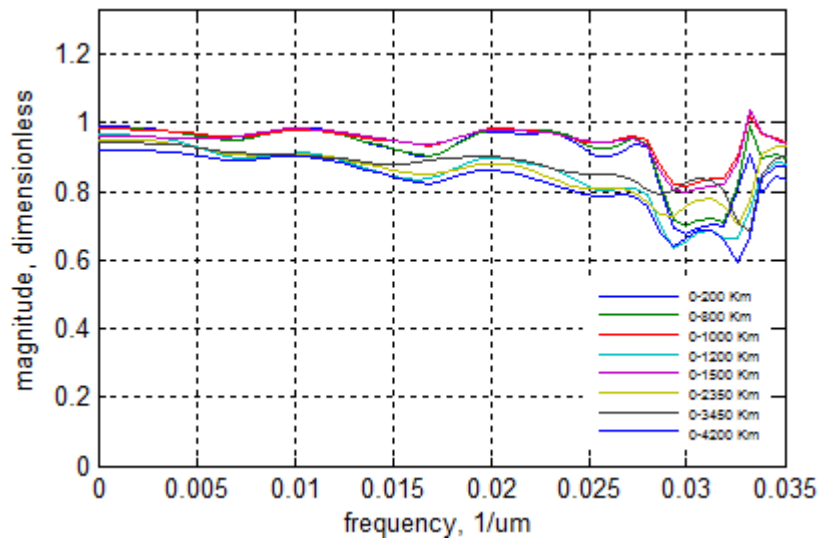


Figure 6.25 Optical transfer function of road test analysis

Travelled distance had a deterring effect on the optical linkage between $I_{OOI}(u)$ and $I_{DOI}(u)$. As the travelled distance accumulated the OTF graph was lowered and ΔH_{eff} showed reduction in its values. Overall, increased in the travelled distance reduced the ΔH_{eff} values from 0.02496 at 0 km to 0.02392 at 4200 km (a 4.2% reduction).

For 2D parameter analysis, ΔH_{eff} and $C(T/2)$ were plotted in a 2-D information space to monitor the engine lubricant condition with respect to the accumulated travelled distance.

Figure 6.26 presents the $\{C(T/2), \Delta H_{eff}\}$ information space for the road test analysis. In general, accumulation of travelled distance from 0 km to 4200 km decreased the $C(T/2)$ values from -0.5574 n.u.² to -0.5433 n.u.² (a 0.0141 n.u.² decrease). ΔH_{eff} values decreased from 0.02496 to 0.02392 (a 0.00104 reduction). Overall, $\{C(T/2), \Delta H_{eff}\}$ informational space showed a strong correlation between $C(T/2)$ and ΔH_{eff} with respect to accumulation of travelled distance. It was noted a shift in value of $C(T/2)$ at 1500 km and 2350 km, but overall the graph showed a downward trend.

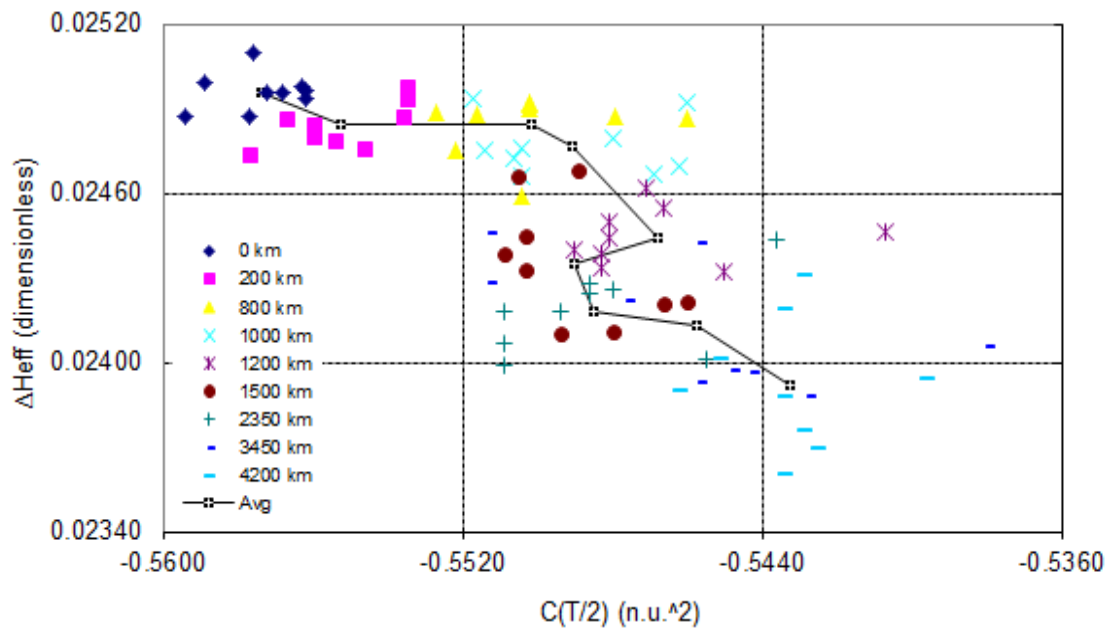


Figure 6.26 $\{C(T/2), \Delta H_{eff}\}$ information space wrt accumulated travelled distance

Relationship between width of auto spectral function width (W_{ASF}) and correlation values at $T/2$ region $C(T/2)$ with respect to the travelled distance was studied in the $\{C(T/2), W_{AFS}\}$ information space (see Figure 6.27). Previously it was observed that accumulated travelled distance reduced the $C(T/2)$ values from -0.5574 n.u.^2 to -0.533 n.u.^2 , a 2.53% reduction. A similar effect was observed on the W_{ASF} values as well. A 2-D presentation of these two parameters with respect to the accumulated travelled distance shows a strong correlation between these two parameters.

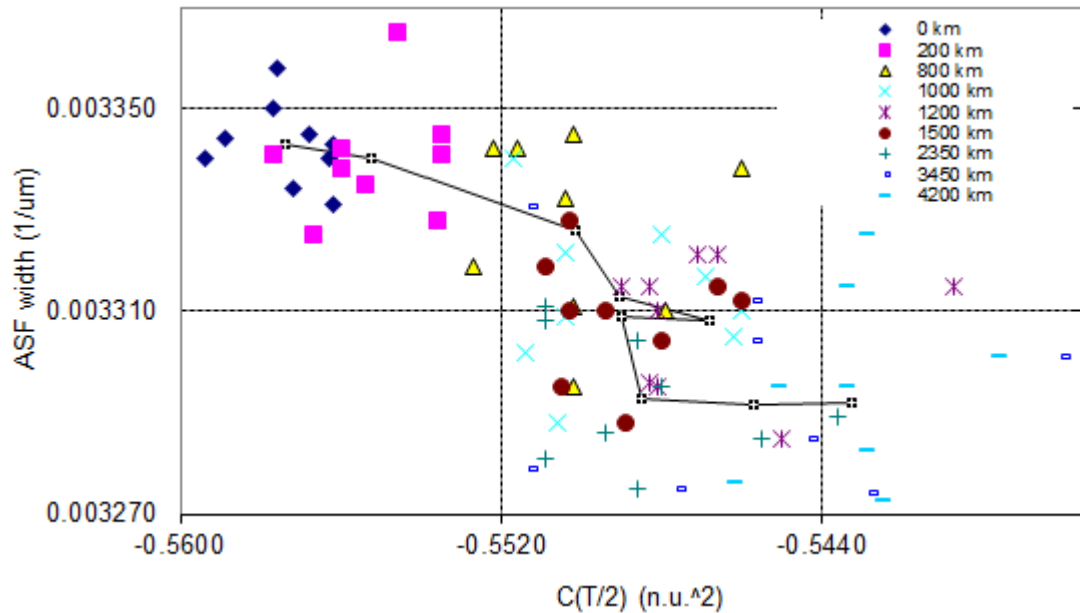


Figure 6.27 $\{C(T/2), W_{ASF}\}$ of road test analysis

Figure 6.28 illustrates how W_{ASF} correlates with ΔH_{eff} in $\{W_{ASF}, \Delta H_{eff}\}$ information space as the accumulated travelled distance increased. The effect of travelled distance on the ΔH_{eff} was decreasing. The accumulated travelled distance reduced the ΔH_{eff} values from 0.02496 to 0.02392 (4.2% reduction). Similarly W_{ASF} values showed a decrease from 0.003343 (1/μm) to 0.00322 (1/μm).

Figure 6.28 illustrates a non-uniform downward trend of W_{ASF} and ΔH_{eff} values with respect to travelled distance. Overall, the 2-D scattered plot of these parameters $\{W_{ASF}, \Delta H_{eff}\}$ indicates there is a negative correlation between these values.

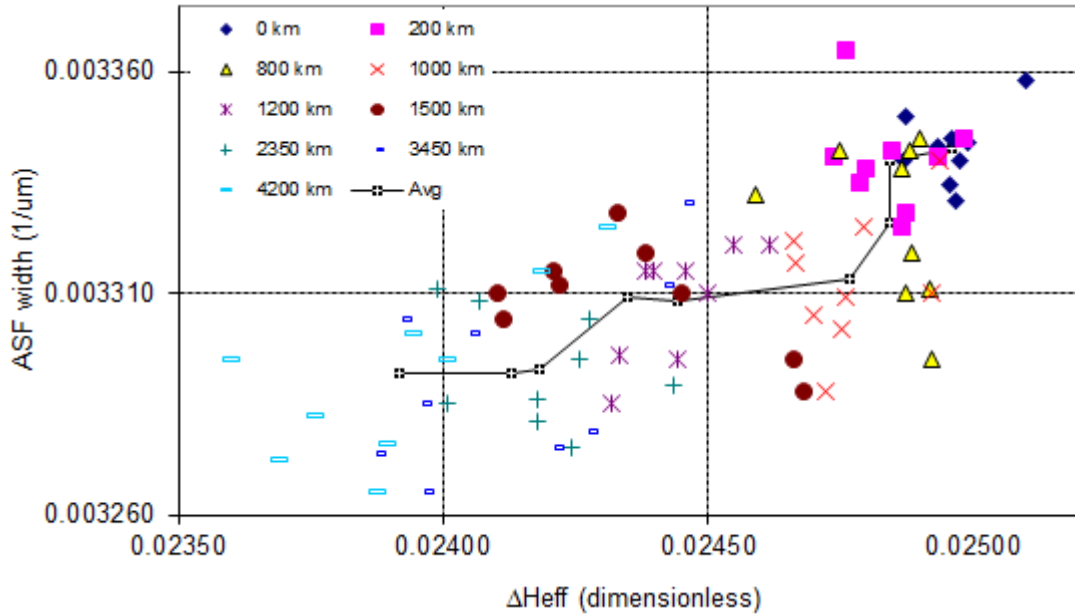


Figure 6.28 $\{W_{AFS}, \Delta H_{eff}\}$ information space wrt accumulated travelled distance

6.4 Summary and conclusion

In this chapter, a new sensing system was introduced to monitor the condition of contaminated and aged lubricants. This sensing system was based on the statistical optical analysis methodology. The applicability of the proposed sensing system was verified by measuring and monitoring of coolant, gasoline and water contaminant concentrations individually, as well as mixed. Also a set of oil samples was collected from a Ford Taurus under general service, with a mixed city and highway driving condition and statistical optical analysis were performed in real time. The originality of the proposed methodology comprises of obtaining and analysis of an optical image that combines an object with known periodic shape and a thin film of the contaminated lubricant. Introduction of an object with *a priori* known periodical structure allowed reduction of 2D into 1D optical analysis, suitable for on-line application. The proposed

sensing system utilizes the comparison of measured parameters and statistical characteristics for fresh and contaminated lubricants.

Statistical analysis was applied at the combined object-lubricant images. Specifically, statistical auto-characteristics, such as auto-correlation function and auto spectral function, and their informational parameters were proposed to characterize optical changes in contaminated/deteriorated lubricants. Statistical cross-characteristics more specifically estimate an optical distortion process of the periodical object image by a thin film of the contaminated lubricant. The utilized methodology in the proposed sensing system was verified experimentally showing ability to distinguish lubricant with 1% to 10% coolant, gasoline, and water contamination. Also, it was shown that this methodology is capable of monitoring the contaminants concentration in a combined form (coolant-gasoline 0%-5%) as well.

From the results obtained, the following main conclusions can be drawn:

1. Developed statistical optical analysis methodology used in the proposed sensing system is a novel approach for analysis of a synergetic effect of combined lubricant-object optical appearance. It opens new opportunities for on-line monitoring, diagnostics and control of engine lubricant condition and engine performance.
2. Implementation of systems approach to monitor the health of engine through optical analysis of engine lubricant is a new approach in the automotive field to manage engine performance and health. This approach realizes the interrelationship between engine health and lubricant condition and by monitoring the properties of the lubricant evaluates the engine health. This new approach provides insight into the importance of engine lubricant and lubricant system and how lubricant can be used as a source of information for engine performance.
3. Application of opto-microfluidic sensing system enables the extraction of optical information from engine lubricant to monitor the characteristics of the lubricating oil on-line and in real time. Opto-microfluidics sensing system represents the use of advanced optical elements to increase the functionality of microfluidic devices and

also the use of advanced microfluidic devices to increase the functionality of photonic devices. Such integration represents a novel approach to dynamic manipulation of optical systems with many applications in automotive fluid sensing field.

4. In statistical auto-characteristics analysis, addition of 0%-10% of coolant, water, and gasoline increased the auto-correlation function values at $T/2$ region by -0.097 n.u.^2 , -0.00684 n.u.^2 and -0.0502 n.u.^2 respectively. These results indicate that value of the auto-correlation function around a half of the structure period is a statistically valid informational parameter for on-line measurement and monitoring of lubricants with different contaminant concentration.
5. Analysis of auto spectral function indicted addition of 0%-10% of coolant, and water decreased the W_{ASF} by $0.00008 \mu\text{m}^{-1}$ and $0.00006 \mu\text{m}^{-1}$. Addition of gasoline into the engine lubricant did not affect the W_{ASF} .
6. In analysis of statistical cross-characteristics, addition of 0%-10% of coolant, and water decreased the effective width of transfer function ΔH_{eff} by 0.0135 and 0.008. Addition of gasoline did not affect ΔH_{eff} .
7. Plotting statistical auto-characteristics parameter i.e. correlation at $T/2$ and cross-characteristics parameters such as effective width of transfer function ΔH_{eff} in a 2-D informational space as contamination concentration changes provided an accurate monitoring tool for condition of lubricant. Addition of coolant, gasoline and water into the engine lubricant shift the $\{C(T/2), \Delta H_{eff}\}$ plot in a linear fashion. For coolant and water variation of ΔH_{eff} and $C(T/2)$ values in the $\{C(T/2), \Delta H_{eff}\}$ informational space indicate a strong correlation between these values. Addition of gasoline into the lubricant showed an increase in $C(T/2)$ values while ΔH_{eff} values were almost constant. Gasoline $\{C(T/2), \Delta H_{eff}\}$ informational space shows a moderate upward trend on the graph. This was mainly due to a slight increase of in ΔH_{eff} value at

higher gasoline concentration. The evolution of $\Delta H_{eff} - W_{ASF}$ in the 2-D informational space with respect to coolant and water concentrations showed as coolant and water concentration were increased, the W_{ASF} shows a close correlation with ΔH_{eff} values in a down ward trend. Introduction of gasoline into the engine lubricant did not show any significant effect on the W_{ASF} and ΔH_{eff} values. A 2-D presentation of these statistical parameters also indicates the lack of correlation between W_{ASF} and ΔH_{eff} as gasoline concentration was increased in the lubricant. A similar relationship was observed between $C(T/2)$ and W_{ASF} . Addition of coolant and water into the engine lubricant showed a close correlation between $C(T/2)$ and W_{ASF} , while addition of gasoline indicated of lack of correlation between these two parameters.

8. The developed methodology was also applied for analysis of combinations of coolant and gasoline (0%-5%) contaminants. Addition of combination of coolant-gasoline (0%-5%) shifted the $\Delta H_{eff} - C(T/2)$ graph non-linearly. While addition of combo contaminants decreased the ΔH_{eff} values from 0.0248 to 0.0176 (a 0.0130 reduction), $C(T/2)$ was increased from -0.5691 to -0.5951 n.u.² (0.026 n.u.² increase). This verifies that the statistical optical analysis is capable of differentiating the combination of contaminants at different concentrations. 2-D presentation of the statistical parameters $\{C(T/2), \Delta H_{eff}\}$, $\{\Delta H_{eff}, W_{ASF}\}$, and $\{C(T/2), W_{ASF}\}$ showed a good correlation between each pairs of parameters as the contaminants concentration was increased.
9. Statistical optical method was also applied for analysis of road test samples with different millage. In this study samples with 0 km, 200 km, 800 km, 1000 km, 1200 km, 1500 km, 2350 km, 3450 km, and 4200 km traveled distance were collected and analyzed. The results indicated that the accumulated travelled distance (lubricant normal aging process) directly affect the statistical parameters of the lubricant. The auto correlation value at $T/2$ region $C(T/2)$ showed reduction from -0.5574 n.u.² to -0.5433 n.u.² as the accumulated travelled distance was increased. The travelled

distanced also decreased the width of auto-spectral function graph from $0.003343 \mu\text{m}^{-1}$ to $0.003292 \mu\text{m}^{-1}$. The effective width of transfer function ΔH_{eff} also decreased from 0.02496 at 0 Km to 0.02392 at 4200 Km as the travelled distance was increased. It is interesting to note that the lubricant degradation process had a decreasing effect on the $C(T/2)$ values different from previous cases. The 2-D presentation of $C(T/2) - \Delta H_{eff}$ and $C(T/2) - W_{ASF}$ indicated that in each cases both statistical parameters moved in the same direction as the travelled distance increased. $\Delta H_{eff} - W_{ASF}$ plot showed both parameters decreased as the travelled distance increased.

Chapter 7

7 On-line Monitoring Engine Lubricant Condition

In this chapter the statistical optics and object shape based optical methodologies proposed in the chapter 5 and 6 will be utilized for on-line, on board monitoring of contaminants in the engine lubricant of a 2005 Ford Taurus. This is to verify the applicability of the proposed sensing system for on-line, on board measurement of contaminants in the lubricating oil. This experiment mimics several realistic circumstances which structural defect of engine part or mismanagement of combustion process or other interrelated causes would lead to the presence of contaminants in the lubricant. These experiments will demonstrate that the two proposed sensing methodologies can measure the presence of coolant, gasoline, and water and consequently provide insight in the state of engine health, combustion management system or other interrelated issues.

7.1 On-line monitoring contaminated engine lubricant

Monitoring automotive fluids have received increasing attention in the recent years. Sensors for automotive liquids, such as engine lubricant, can be used to detect the quality of refilled liquid, increase drain interval, reduce the environmental impact, and evaluate the performance of engine. Monitoring condition of engine lubricant is important since the beginning of a breakdown occurs thousands of miles or hundreds of hours before the breakdown itself and sign of potential breakdown usually appear first in the lubricant.

In all lubricating systems, organic compounds exposed to high temperatures and pressures in the presence of oxygen will partially oxidize. There are a wide variety of by-products produced during the combustion process such as ketones, esters, aldehydes, carbonates and carboxylic acids. Some of these compounds are dissolved by the lubricant or remain suspended owing to the dispersive additives in the oil. The net effect of prolonged oxidation is that chemically the oil becomes acidic causing corrosion whilst physically an increase in viscosity occurs. Besides the oxidation of base oil and depletion of additives, contaminants also change the condition of the lubricant. They enter from

the atmosphere or are generated from within. They reduce the life of mechanical components and lubricant. The most common liquid contaminants are gasoline, coolant and water.

Fuel contamination occurs mostly in crankcase applications. Fuel usually enters the crankcase as the blow-by with combustion gases and from leakage. Fuel contamination reduces the lubricant's performance by promoting early oxidation, thinning viscosity, dilution of the lubricant's additive, and increase the sulfur build-up in the lubricant. Adversely, fuel dilution increases the wear of machine components, and increase corrosion due to formation of sulfuric acid and oxidation-induced organic acids pair up to corrode components surfaces. Hence, the presence of fuel in engine lubricant can lower the viscosity of it and engine lubricant properties can be reduced much faster than any other degradation process, in this way, the contamination by unburned fuel becomes the first and more important causes of degradation of engine oil.

Coolant is a constant threat to leak into the lubricant, especially in crankcase applications. Typically, coolant leaks into the crankcase because of damaged cooler core, defectives seals, and corrosion. When coolant leaks into lubricant it forms gels and emulsions and increases the viscosity of the lubricant. It also increases the oxidation rate and reduces the pH to acidity region. When coolant enters into lubricant, it increases the wear on the machine parts by forming glycol emulsion and starvation of lubricant to the components due to increased viscosity. It increases the corrosion effect on the part due to increase in acidity of the lubricant. Coolant contamination also causes filter failure as well. However, glycol in the lubricating oil can oxidize, polymerize, esterify, evaporate, and be absorbed by lubricant filters.

Water contamination is the second most destructive contaminants. Water can coexist with lubricant in three forms: dissolved, emulsified, and free. Lubricant all can dissolve a small amount of water into their chemistry. The volume of water dissolved in the lubricant depends on the chemistry of the lubricant. In general deteriorated lubricant which contain larger amount of free radical and polar compounds is capable of dissolving larger amount of water before reaching its saturation point.

Inside the engine, where lubricant functions, there exists a harsh environment, high temperature, force and rapid motion. When un-dissolved water is subjected to shearing conditions present in the engine, it is fragmented into small sizes particles and remain suspended in a stable state in the lubricant. The emulsified water creates a hazy, cloudy or milky appearance. Water can also stay free from the lubricant due to insolubility of two liquid and the difference in their specific gravity. The source of water in the lubricant can be from atmosphere, condensation, or the leakage from the coolant.

Water affects the lubricant by forming some chemically aggressive by-products. It also can act as a catalyst to accelerate the oxidation process. Existence of water in the lubricant reservoir can promote growth of biological material and microorganisms which promotes oxidation and cause filter plugging. Water in free or emulsified form interferes with lubricant and weakens the strength of lubricant film. The weakened lubricant film makes the machine more susceptible to abrasive, adhesive and fatigue wear.

Presence of contaminants such as coolant, gasoline, and water in the engine lubricant is a sign of troublesome which directly relates to failure of machinery components. Detecting presence of these elements at an early stage is a crucial task helps to prevent catastrophic failure and cost in any mechanical system with lubrication system. This requires an on-line monitoring system in place to monitor the condition of lubricant and health of engine.

In this chapter the statistical optics and object shape based optical analysis methodologies described in the previous chapters are utilized to sense and monitor the presence of three major contaminants, coolant, gasoline and water in the engine lubricating oil of a 2005 Ford Taurus engine on-line, on board. This experiment mimics a mechanical failure situation in the engine which leads to presence of contaminants in the engine lubricating oil. This experiment will demonstrate the applicability of the proposed sensing systems to measurer the presence of coolant, gasoline, and water on-line and consequently provide critical information and insight in the state of engine health.

7.2 Experimental set up

The experimental set-up used for on-line analysis of engine lubricant consisted of a data acquisition system, micro fluid channel with in-let and out-let connections, detectable object, pumping system, and illumination source. The experimental set-up used in this test was similar with the one described in chapter 5 and 6. The optical data acquisition system was composed of a CCD camera (Lumenera Infinity 1, Canada) with a zoom lens (Keyence, USA) of 35-245 mm focal length, mounted on an optical bench. The camera was connected to a PC equipped with imaging software (Infinity capture software, Lumenera). The CCD camera allowed capturing images from an object placed behind a medium passing through the channel with a magnification of 245x providing an overall optical magnification scale of around 2.25. The images from the camera were acquired as 8-bit 640 x 480 pixel digital bitmap files and they were digitized at 256 grey scale. The microfluidic channel was made of PMMA plastics with thickness of 1.5 mm with dimension of 170 μm deep, 500 μm wide and 50 mm long. The microfluidic channel provided a passage for the contaminated engine lubricant positioned between CCD camera and light source. A micro pump (200 EC-LC-L, Schwarzer Precision, Germany) was used to draw and deliver lubricant to the microfluidic channel from car oil pan directly. A pumping syringe and Teflon tube was used to deliver contaminants into the oil pan through dip stick tube. The detectable object used in this set up was a 10 mm x 10 mm stainless still woven wire cloth (Tech-Met-Canada) with a mesh size of 0.065 mm x 0.065 mm and a circular wire diameter of 0.033 mm. The purpose of stainless steel woven cloth was to introduce a periodic grid into the image suitable for object shape-based and statistical optical analysis. The object was intentionally placed behind the microfluidic channel on opposite side of the CCD camera to avoid distortion of the laminar flow by the periodic structure. The object was fixed to the microfluidic channel wall. The visible light source (Stocker Yale, Model 21AC) with wavelength of 380-750 nm used in this study illuminated the object using two fiber light guides. The opto-microfluidic system was installed on an optical bench stationed near the car. The car used for this experiment was a 2005 Ford Taurus under general service. A commercially available SAW 5W-20 engine lubricating oil was used for the on-line analysis.

7.3 Testing procedure

The objective of this experiment was to introduce 1% to 5% of contaminant into the lubricating oil pan of a 2005 Ford Taurus and measure the statistical optical characteristics of the samples using statistical optics and object shape based optical analysis methodologies to detect the presence of contaminant on-line, on board. Coolant, gasoline, and water were considered as the adding contaminants for this experiment. Each test started with drawing a sample from freshly changed lubricant after allowing engine to run for 20 minutes. Following that contaminant was added into the lubricant using syringe and flexible tube, then let the engine runs for 15-20 minutes (idle and city driving) allowing the contaminant to mix with lubricant properly. As engine was running idle, a sample was withdrawn from the oil pan using micro pump and delivered to the opto-microfluidic sensing system directly. This procedure was repeated for all the contaminants concentrations. After measuring the highest contaminant concentration (5%), the lubricating oil was dumped and engine was filled with fresh oil for the next contaminant measurement. Table 2 shows the steps and details of the testing procedure.

Table 2 On-line on board engine lubricant monitoring procedure

On-line monitoring engine lubricant condition				
Vehicle		Ford Taurus		
Oil Type		SAE 5W-20		
Oil volume		4.3 Liters		
		Contaminants		
		Gasoline	Coolant	Water
step				
1	Oil change	Yes	-	-
2	Odometer reading (km)	141882	141977	142080
3	Preparation	worm up the engine by running idle or city driving 15 min	worm up the engine by running idle or city driving 15 min	worm up the engine by running idle or city driving 15 min
4	Sample 1 (0%)	w ithdraw 30 cc of lubricant, run test and capture images	w ithdraw 30 cc of lubricant, run test and capture images	w ithdraw 30 cc of lubricant, run test and capture images
5	Preparation	add 42.7 cc of gasoline into lubricant via dip stick tube (1% gasoline) and run the engine for 15 min.	add 42.7cc of gasoline into lubricant via dip stick tube (1% gasoline) and run the engine for 15 min.	add 42.7 cc of gasoline into lubricant via dip stick tube (1% gasoline) and run the engine for 15 min.
6	Odometer reading (km)	141907	141992	142100
7	Sample 2 (1%)	w ithdraw 30 cc of lubricant, run test and capture images	w ithdraw 30 cc of lubricant, run test and capture images	w ithdraw 30 cc of lubricant, run test and capture images
8	Preparation	add 85.7 cc of gasoline into lubricant via dip stick tube (2% gasoline) and run the engine for 15 min.	add 85.7 cc of gasoline into lubricant via dip stick tube (2% gasoline) and run the engine for 15 min.	add 85.7 cc of gasoline into lubricant via dip stick tube (2% gasoline) and run the engine for 15 min.
9	Odometer reading (km)	141937	142002	142107
10	Sample 3 (2%)	w ithdraw 30 cc of lubricant, run test and capture images	w ithdraw 30 cc of lubricant, run test and capture images	w ithdraw 30 cc of lubricant, run test and capture images
11	Preparation	add 130 cc of gasoline into lubricant via dip stick tube (3% gasoline) and run the engine for 15 min.	add 130 cc of gasoline into lubricant via dip stick tube (3% gasoline) and run the engine for 15 min.	add 130 cc of gasoline into lubricant via dip stick tube (3% gasoline) and run the engine for 15 min.
12	Odometer reading (km)	141917	142011	142113
13	Sample 4 (3%)	w ithdraw 30 cc of lubricant, run test and capture images	w ithdraw 30 cc of lubricant, run test and capture images	w ithdraw 30 cc of lubricant, run test and capture images
14	Preparation	add 177.5 cc of gasoline into lubricant via dip stick tube (4% gasoline) and run the engine for 15 min.	add 177.5 cc of gasoline into lubricant via dip stick tube (4% gasoline) and run the engine for 15 min.	add 177.5 cc of gasoline into lubricant via dip stick tube (4% gasoline) and run the engine for 15 min.
15	Odometer reading (KM)	141922	142019	142119
16	Sample 5 (4%)	w ithdraw 30 cc of lubricant, run test and capture images	w ithdraw 30 cc of lubricant, run test and capture images	w ithdraw 30 cc of lubricant, run test and capture images
17	Preparation	add 229 cc of gasoline into lubricant via dip stick tube (5% gasoline) and run the engine for 15 min.	add 229 cc of gasoline into lubricant via dip stick tube (5% gasoline) and run the engine for 15 min.	add 229 cc of gasoline into lubricant via dip stick tube (5% gasoline) and run the engine for 15 min.
18	Odometer reading (km)	141927	142025	142127
19	Sample 6 (5%)	w ithdraw 30 cc of lubricant, run test and capture images	w ithdraw 30 cc of lubricant, run test and capture images	w ithdraw 30 cc of lubricant, run test and capture images
20		Oil change	Oil change	Oil change

7.4 Statistical optical analysis and system for on-line monitoring contaminated engine lubricant

The statistical optical analysis performed for on-line monitoring of coolant contaminated engine lubricant was based on the theory of imaging in presence of randomly inhomogeneous medium. Based on this theory, when an object is placed behind a thin film of an inhomogeneous medium i.e. contaminated engine lubricant, the image of the object will be distorted. The medium acts as a distortion operator. In this case, the quality of the distorted object image (DOI) will be mainly depending on the actual condition of the lubricant. Based on the theory of light propagation through the random medium, the transformation/distortion operator mathematically becomes an optical transfer function (OTF) that represents a transformation of original object image (OOI) into the distorted object image (DOI). In a case when OOI and DOI are known, the distortion operator or the actual optical properties of the medium can be identified. This theory and methodology is explained in details in chapter 6.

The sensing system was an optical system consisting optical components and microfluidic device capable of extracting optical information from engine lubricant to monitor the characteristics of the lubricating oil on-line and in real time. The functional design of the sensing system is explained in the previous chapters.

7.4.1 Statistical optical analysis of coolant contaminated engine lubricant

The effect of introducing coolant into the engine lubricant and increasing its concentration on the color scale graph is illustrated in Figure 7.1. Introduction of 1% coolant into the engine lubricating oil pan caused a slight decrease in the pick-to-valley (P-to-V) value of the graph from 0.5124 to 0.5004 (2.3% reduction). As the coolant concentration was increased in the pan to 2%, 3%, 4% and 5%, the color cross section graph P-to-V decreased to 0.4966, 0.4956, 0.5069, and 0.4919. It is noted that the reduction in P-to-V values was not uniform, however, overall addition of 1%-5% of coolant into the engine oil pan lowered the P-to-V values of color cross section graph by 0.0205 (a 4% reduction). This data shows dependency of amplitude characteristics (e.g.

P-to-V, mean values, variance, *etc.*) of the light intensity cross-sections to the contaminant concentration in the oil pan and therefore can be used as informational parameters for condition monitoring of contaminated lubricants.

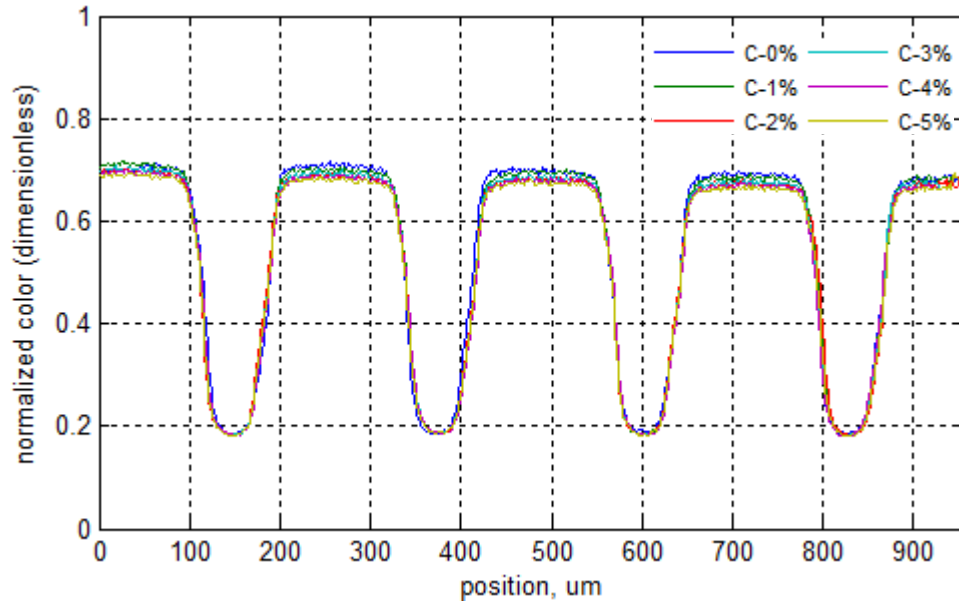


Figure 7.1 Color cross section graph of coolant contaminated engine lubricant

The OOI and DOI color cross-sections of fresh lubricant image and contaminated lubricant were further used as the experimental data performing ACFs, ASFs and OTFs using standard mathematical function from MATLAB software (see Appendix B). Figure 7.2 shows evaluation of normalized ACFs with respect to coolant with concentrations of 0% to 5%. Correlations values located at $\{T/2, 3T/2, \dots\}$ in auto-correlation functions $C_{ooi}(u)$ and $C_{doi}(u)$ are more pronounced as to compare to other locations. A closer examination of the coolant correlation function graph within 70...150 μm region (around $T/2=110 \mu\text{m}$) shows that while a concentration of the coolant was increased from 0% to 5%, a minimum negative correlation value decreased from -0.5226 n.u.² to -0.5172 n.u.². Increase the coolant concentration into the oil pan from 1% to 2%, 3%, 4% and 5% changed the correlation values at $T/2$ region to 0.5204 n.u.², 0.5216 n.u.², 0.5209 n.u.², 0.5193 n.u.² and 0.5172 n.u.².

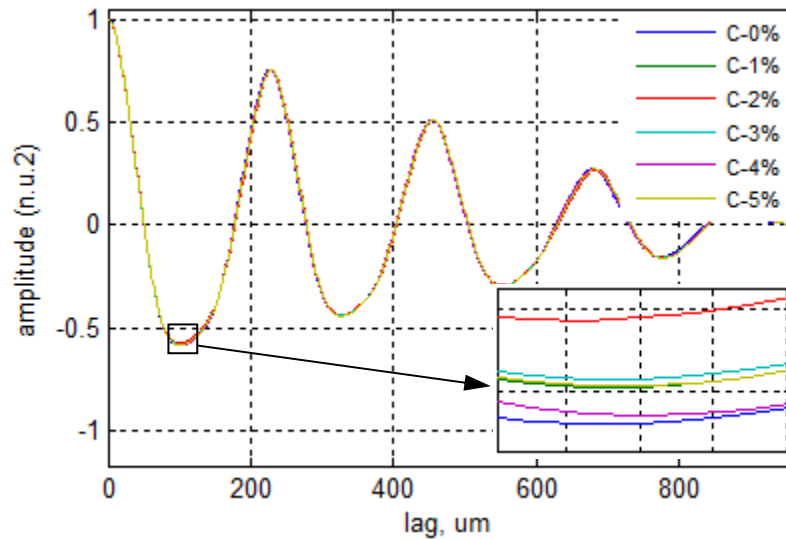


Figure 7.2 Evaluation of auto-correlation function of coolant contaminated engine lubricant with respect to coolant concentration

Auto spectral function is another statistical optics characteristics showing how OOI is transformed into DOI due to introduction of the contaminants. Figure 7.3 shows auto spectral function plots of fresh and 1%-5% coolant contaminated lubricant. From visual observation, auto spectral function plot has a sharp peak at frequency of $0.00651 (1/\mu\text{m})$, but smooth and continuous. As the concentration of the coolant in the oil pan changes, the amplitude and width of spectrum density graph at half maximum height (W_{ASF}) changes too.

As 1% coolant was introduced into the lubricant, the W_{ASF} decreased from $0.003438 (1/\mu\text{m})$ to $0.003424 (1/\mu\text{m})$. From 1% to 5% W_{ASF} showed almost a uniform decrease to $0.003417 (1/\mu\text{m})$. Overall, W_{ASF} showed a decrease of $0.000021 (1/\mu\text{m})$ for addition of 5% coolant into the oil pan.

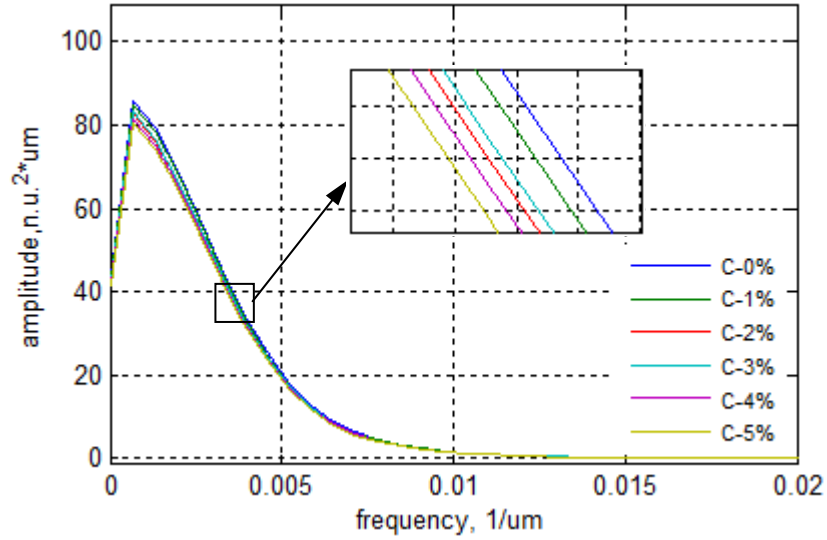


Figure 7.3 Evaluation of spectrum density function of coolant contaminated engine lubricant

The OTF is a statistical cross-characteristics used to monitor transformation of OOI into the DOI caused by introduction of contaminants into the oil pan. The OTFs were calculated for different contaminant concentrations with respect to a fresh lubricant and $S_{OOI}(\omega)$ and $S_{DOI}(\omega)$ and using standard mathematical functions from MATLAB software. An OTF value of 1 represents a benchmark level for comparison with the OTF of contaminated lubricant. Therefore, any value of the OTF below 1 is due to the degradation of lubricant optical properties leading to a distortion of the object image.

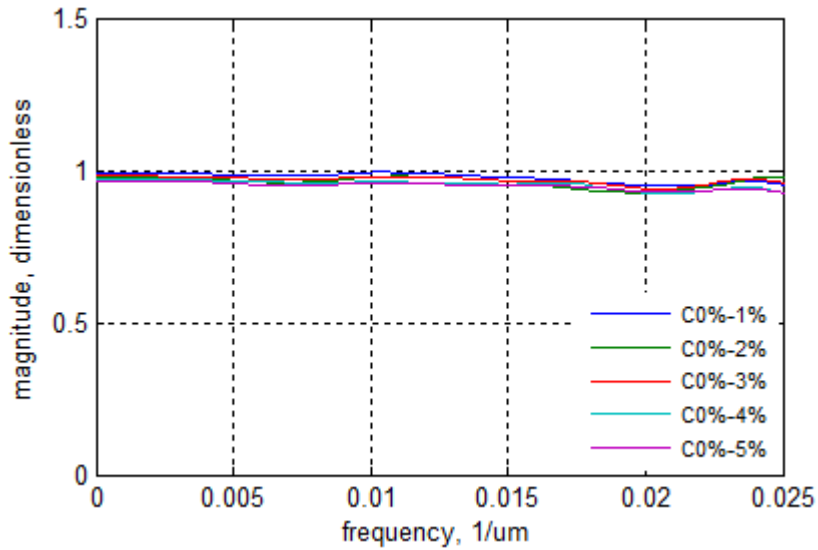


Figure 7.4 Evaluation of optical transfer function of coolant contaminated engine lubricant

Figure 7.4 shows optical transfer functions of the color scale graph of coolant contaminated lubricant with respect to fresh lubricant. From the graph, it is noted that introduction of 1% of coolant into the oil pan and increasing its concentration up to 5% did not affect the optical linkage between $I_{OOI}(u)$ and $I_{DOI}(u)$ significantly. With respect to effective width of optical transfer function, introduction of 1% of coolant into the oil pan caused a reduction in the ΔH_{eff} values from 0.0247 to 0.02466. The reduction was also observed for 1% to 2% of coolant, however, as coolant concentration reached to 3%, the ΔH_{eff} values showed a slight increase from 0.02455 to 0.02457. As the coolant concentration was increased to 4% and 5% in the oil pan, the ΔH_{eff} values decreased to 0.02457 and 0.02456. Overall, introduction of coolant into the oil pan decreased the ΔH_{eff} values by 0.00013.

Figure 7.5 shows the graphical representation of the changes of effective width of transfer function (ΔH_{eff}) and auto correlation function values at $T/2$ region with respect

to coolant concentration. Combination of two statistically obtained one-dimensional (1D) information parameters, such as $C(T/2)$ and ΔH_{eff} , into one 2D informational parameter $\{C(T/2), \Delta H_{eff}\}$ allows evaluation and monitoring of lubricant contamination as a function of two statistical variables in corresponding 2D information plane.

Introduction of coolant into the lubricant and increasing its concentration up to 5% lowered the ΔH_{eff} values from 0.0247 to 0.02456. With respect to $C(T/2)$ values, addition of 1% of coolant into the oil pan and increasing its concentration up to 5% decreased the $C(T/2)$ values from -0.5226 n.u.² to -0.5172 n.u.². Increase in the coolant concentration in the oil pan induced a slight down ward trend in the $\{C(T/2), \Delta H_{eff}\}$ informational space, indication of a weak correlation between these parameters.

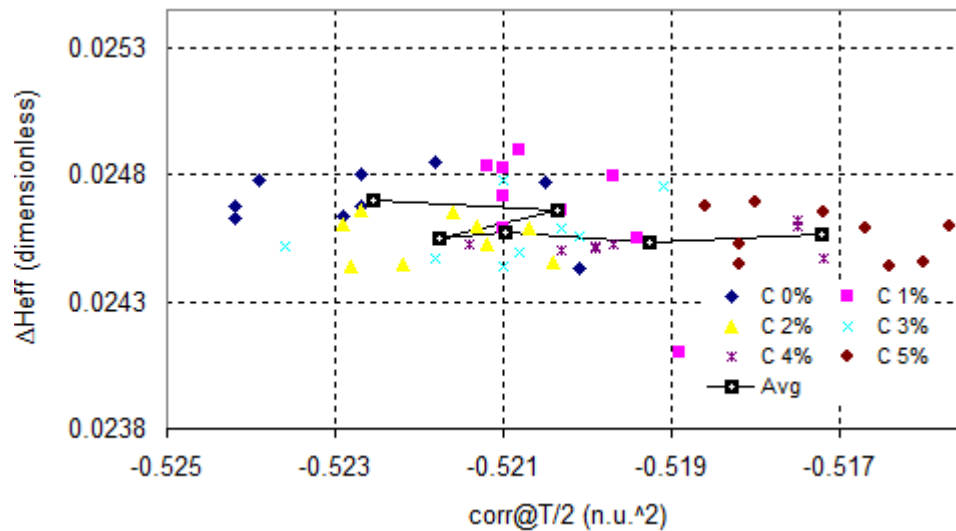


Figure 7.5 Evolution of coolant contaminant in $\{C(T/2), \Delta H_{eff}\}$ information space

Figure 7.6 illustrates the effect of coolant on the W_{ASF} and ΔH_{eff} values. Addition of coolant into engine lubricant had a reduction effect on the W_{ASF} . Introduction of 1% of coolant into the oil pan and increasing its concentration up to 5% lowered the W_{ASF} values. Coolant showed a similar effect on the ΔH_{eff} values as well. The change in values of these two parameters with respect to the increase in coolant concentration is

presented in the 2-D space $\{W_{ASF}, \Delta H_{eff}\}$ plot. As coolant concentration increased, the W_{ASF} and ΔH_{eff} values shifted in a same direction indication of correlation between these two parameters.

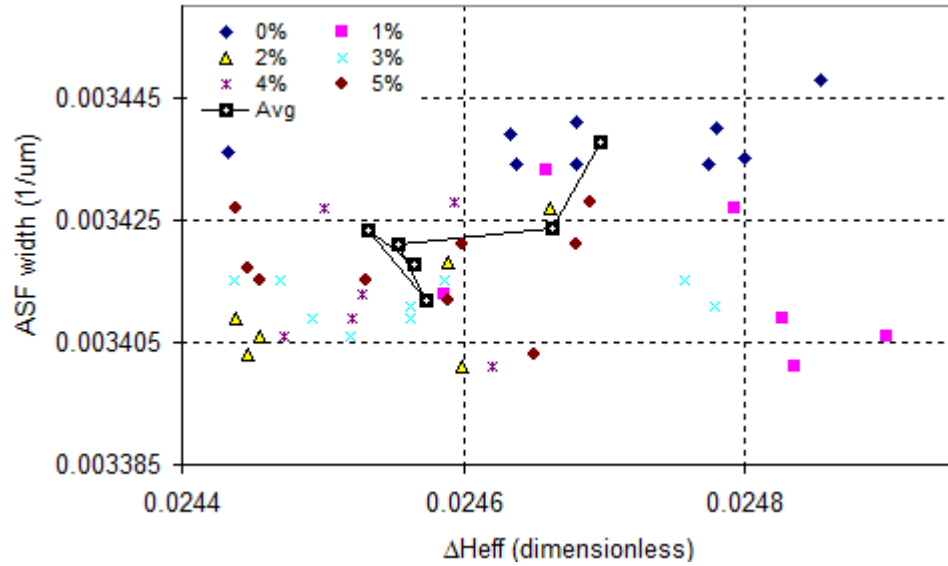


Figure 7.6 Evolution of coolant contaminant in $\{W_{ASF}, \Delta H_{eff}\}$ information space

Figure 7.7 presents the 2-D plane of $\{W_{ASF}, C(T/2)\}$ with respect to increase in the coolant concentration. In general, introduction of coolant into the oil pan had a reduction effect on the $C(T/2)$ and W_{ASF} values. From visual observation, introduction of coolant into the oil pan and increasing its concentration from 1% to 5% caused a slight down ward trend in the $\{W_{ASF}, C(T/2)\}$ space. This downward trend is the indication of weak correlation between these two values.

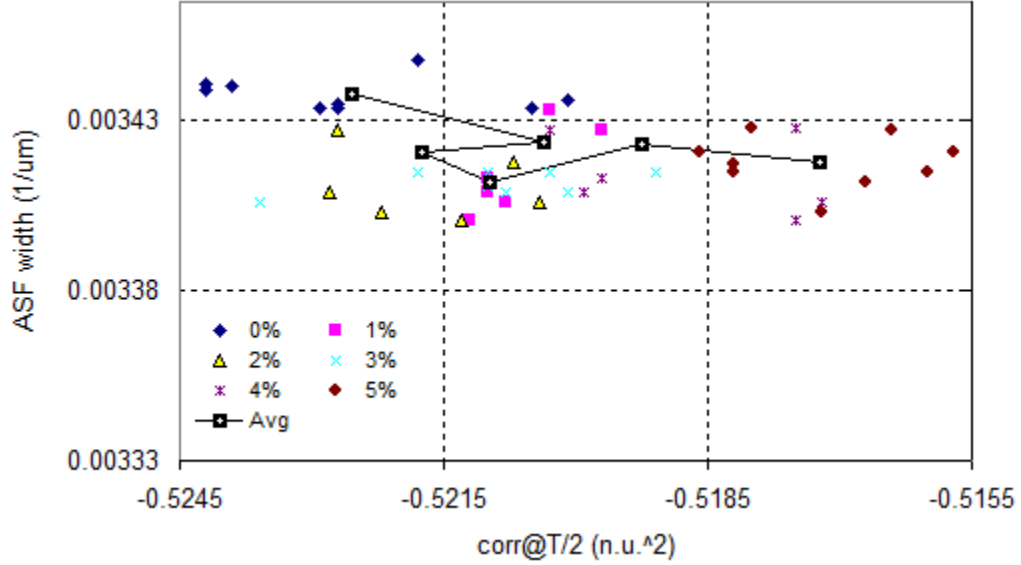


Figure 7.7 Evolution of coolant contaminant in $\{W_{ASF}, C(T/2)\}$ information space

7.4.2 Statistical optical analysis of gasoline contaminated engine lubricant

The effect of introducing gasoline into the engine lubricating oil pan and increasing its concentration on the color scale graph is illustrated in Figure 7.8. Introduction of 1% gasoline into the engine lubricating oil pan caused a decrease in P-to-V values of the graph from 0.5249 to 0.5238 (a reduction of 0.0011). As the gasoline concentration was increased in the oil pan to 2%, 3%, 4% and 5%, the color cross section graph P-to-V values decreased at a non-linear rate to 0.5198, 0.511, 0.4883, and 0.4427. It is noted that the reduction in P-to-V values was not uniform, however, overall addition of 1%-5% of gasoline into the engine oil pan lowered the P-to-V values of color cross section graph by 0.0822 (a 15.7% reduction).

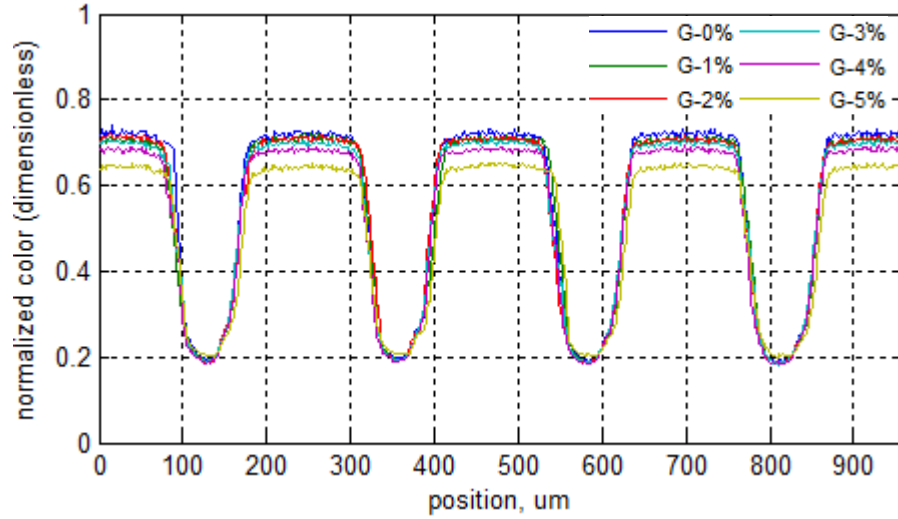


Figure 7.8 Evolution of color-cross-sections (OOI and DOI) wrt gasoline concentration

The OOI and DOI color cross-sections of fresh lubricant image and contaminated lubricant were further used as the experimental data performing ACFs, ASFs and OTFs using standard mathematical function from MATLAB software (see Appendix B). Gasoline auto correlation function graph showed addition of 1% gasoline into the lubricant increased the correlation value at $T/2$ region from -0.5128 n.u.^2 to -0.5168 n.u.^2 . Increasing the gasoline concentration from 1% to 5% increased the $C(T/2)$ value from -0.5218 n.u.^2 to -0.5292 n.u.^2 , however, the increase rate was not uniform for all the concentrations of coolant. Overall addition of gasoline to the engine lubricant increased the $C(T/2)$ values by 3.1%.

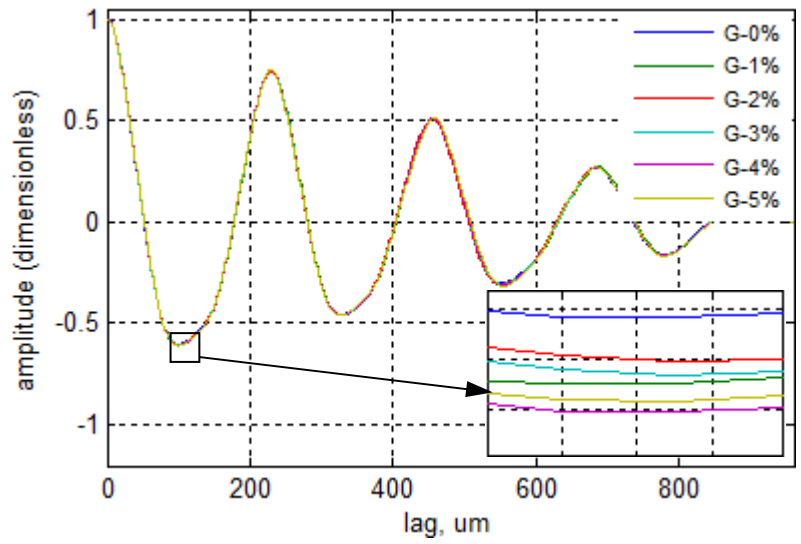


Figure 7.9 Evolution of auto-correlation function wrt gasoline concentration

Evaluation of auto spectral function with respect to concentration of gasoline in the engine lubricating oil pan is illustrated in Figure 7.10. Introduction of 1% of gasoline into the oil pan immediately shifted the auto spectral function plot down ward. As

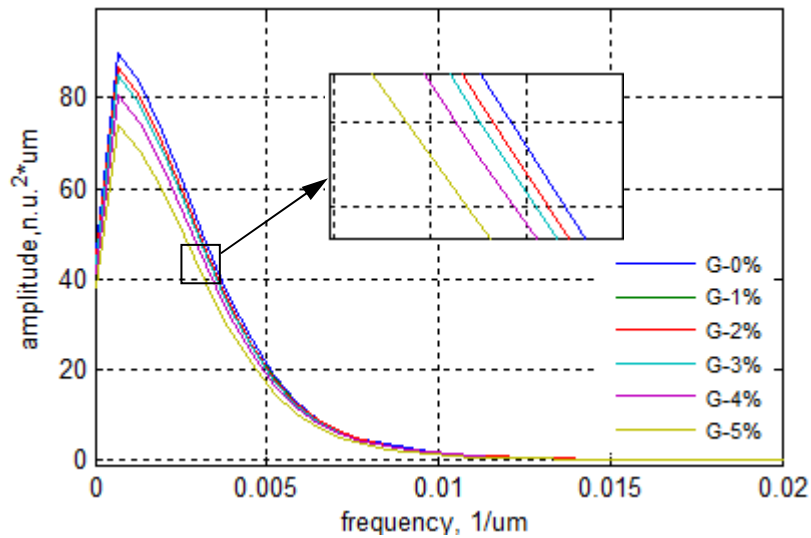


Figure 7.10 Evolution of spectrum density function wrt gasoline concentration

concentration was increased up to 5%, the auto spectral function graph was differentiating further down. Introduction of the gasoline into the lubricant and

increasing its concentration up 5% produced a reduction effect in the W_{ASF} values as well. At 1% of gasoline, the width of auto spectral function graph reduced from .00360 (1/μm) to 0.003347 (1/μm), a reduction of 7%. From 1% to 3% of gasoline, W_{ASF} values did not show any major reduction, however, at 4% the W_{ASF} reduced to 0.003331 (1/μm). As gasoline concentration reaches 5%, the W_{ASF} value reduced further to 0.003285 (1/μm). Overall, introduction of gasoline into the engine lubricating oil pan and increasing its concentration up to 5% reduced the W_{ASF} by 0.000315(1/μm) (8.75% reduction).

Figure 7.11 shows the evolution of optical transfer function with respect to gasoline concentration. A visual observation from the graph indicates addition of gasoline into the engine lubricating oil pan negatively affect the optical linkage between $I_{DOI}(u)$ and $I_{OOI}(u)$. With respect to effective width of optical transfer function ΔH_{eff} , introduction of 1% of gasoline into the lubricant reduced the ΔH_{eff} to 0.02351. As the gasoline concentration was increased to 2%, ΔH_{eff} reduced further down to 0.02322. From 2% to 3% ΔH_{eff} showed a slight increase to 0.02348, and then reduced to 0.02314 at 4% of gasoline. Overall, addition of gasoline into the oil pan from 1% to 5% reduced the ΔH_{eff} by 0.0003 (a 1.2% reduction).

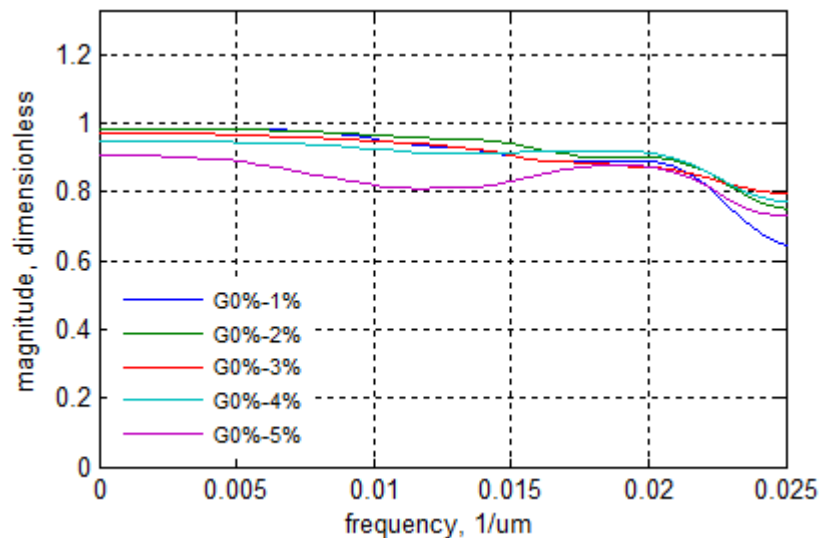


Figure 7.11 Evolution optical transfer function wrt gasoline concentration

Figure 7.12 is the graphical presentation of the changes of effective width of transfer function (ΔH_{eff}) and auto correlation function values at $T/2$ region for with respect gasoline concentrations. In general, introduction of gasoline into the lubricant reduced the ΔH_{eff} values from 0.02444 to 0.02333. $C(T/2)$ values showed an increase in their values from -0.5128 n.u.² to 0.5292 n.u.² as gasoline concentration was increased.

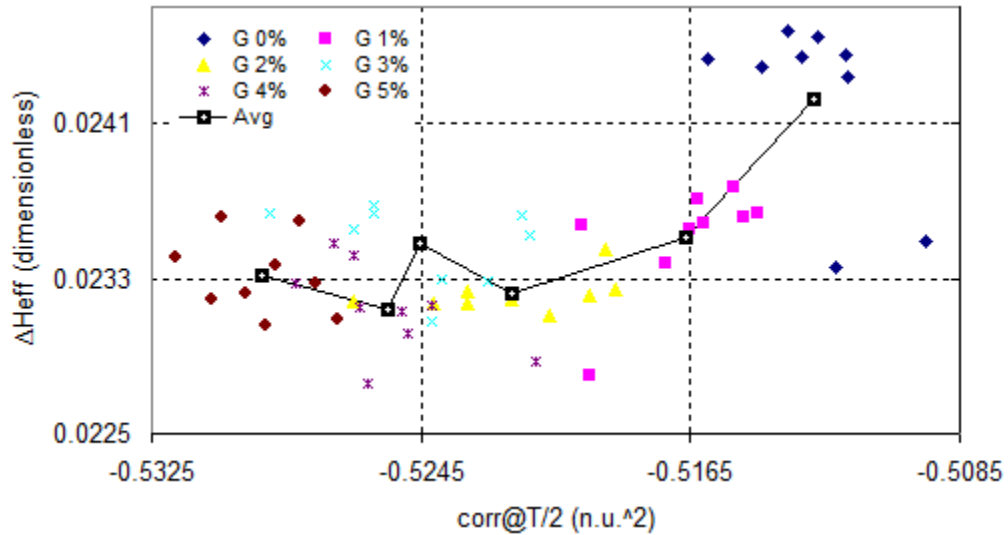


Figure 7.12 Evolution of gasoline contaminant in $\{C(T/2), \Delta H_{eff}\}$ information space

From visual observation, increasing the gasoline concentration in the engine lubricating oil pan induced a down ward trend in the $\{C(T/2), \Delta H_{eff}\}$ informational space, indication of a strong correlation between these parameters.

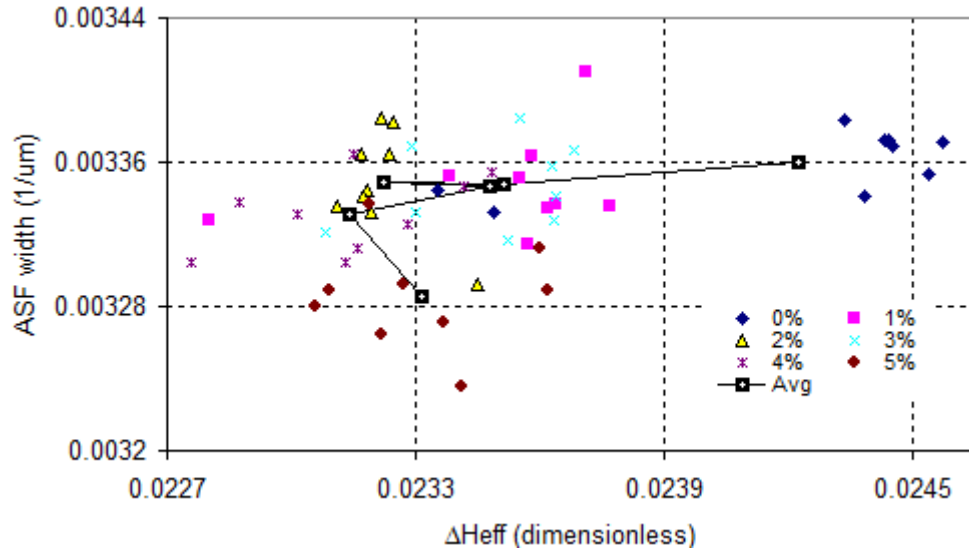


Figure 7.13 Evolution of gasoline contaminant in $\{W_{ASF}, \Delta H_{eff}\}$ information space

Figure 7.4 shows the effect of gasoline on the W_{ASF} and ΔH_{eff} values. Addition of gasoline into engine lubricant had a decreasing effect on the W_{ASF} . Introduction of the gasoline into the lubricant and increasing its concentration up to 5% produced a reduction effect in the W_{ASF} values from 0.003359 (1/μm) to 0.003286 (1/μm). With respect to ΔH_{eff} , addition of 1% -5% of gasoline into the lubricant reduced the ΔH_{eff} from 0.02422 to 0.02331. The changes of these two parameters with respect to the increase in gasoline concentration are presented in $\{W_{ASF}, \Delta H_{eff}\}$ informational plane. Increase in the gasoline concentration pushed both parameters in same direction indicating of statistical correlation between these parameters.

Evolution of gasoline contaminant in $\{W_{ASF}, \Delta H_{eff}\}$ information space is shown in Figure 7.14. Addition of the gasoline into the lubricant and increasing its concentration up to 5% produced a reduction effect in the W_{ASF} values from 0.003359 (1/μm) at 0% to 0.003286 (1/μm) at 5% of gasoline. Meanwhile $C(T/2)$ values showed an increase in their values from -0.5128 n.u.² to 0.5292 n.u.².

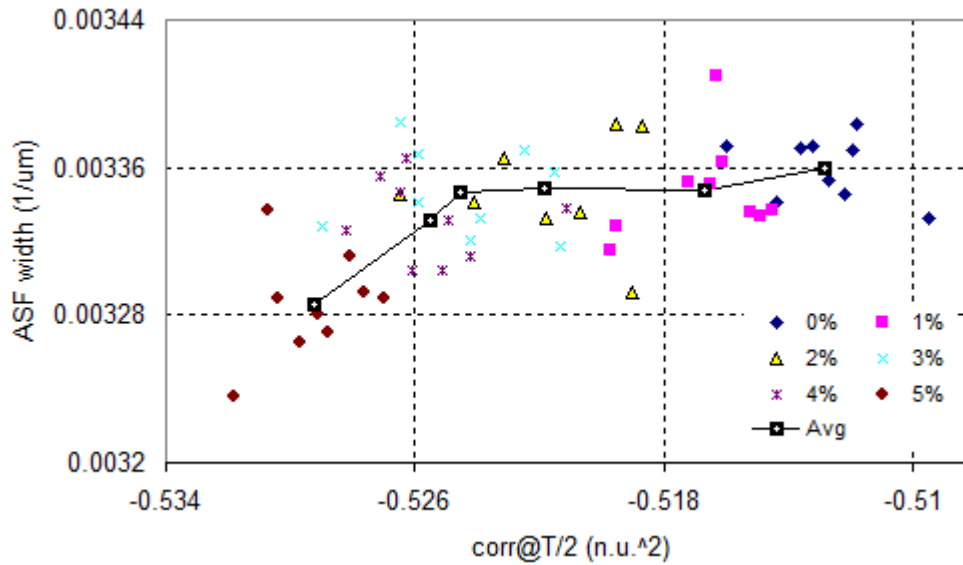


Figure 7.14 Evolution of gasoline contaminant in $\{W_{ASF}, \Delta H_{eff}\}$ information space

Monitoring the lubricant condition using two statistical parameters suggests a correlation between these two parameters. This correlation is stronger as the gasoline concentration increased to 3%, 4% and 5%.

7.4.3 Statistical optical analysis of water contaminated engine lubricant

The effect of introducing water into the engine lubricating oil pan and increasing its concentration on the color scale graph is illustrated in Figure 7.15. Introduction of 1% water into the engine lubricating oil pan caused a decrease in P-to-V values of the graph from 0.4539 to 0.4483 (a reduction of 0.0056). As the water concentration was increased in the oil pan to 2%, 3%, 4% and 5%, the color cross section graph P-to-V values decreased to 0.4319, 0.4266, 0.4257, and 0.4125. It is noted that the reduction in P-to-V values was not uniform, however, overall addition of 1%-5% of water into the engine oil pan lowered the P-to-V values of color cross section graph by 0.0414 (a 9.1% reduction).

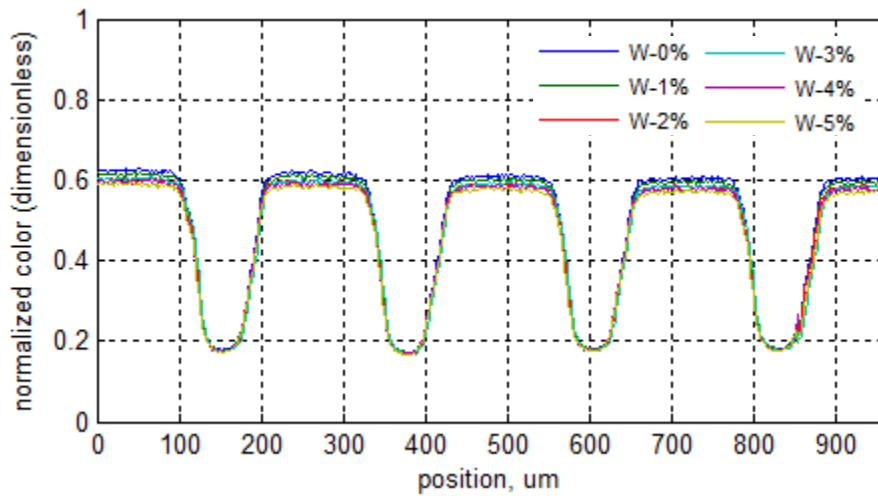


Figure 7.15 Evolution of color-cross-sections (OOI and DOI) with respect to water concentration

The OOI and DOI color cross-sections were used to calculate ACFs, ASFs, and OTFs using standard mathematical function from MATLAB software (see Appendix B).

Figure 7.16 shows the evolution of normalized ACFs with respect to a water concentration of 0% to 5%. Introduction of 1% of water into lubricant increased the $C(T/2)$ values from -0.5225 n.u.^2 to -0.5233 n.u.^2 (an increase of 0.0008 n.u.^2). While the water concentration was increased to 1% and 5%, the correlation values increased from -0.5233 n.u.^2 to -0.5263 n.u.^2 . The rate of increase was uniform at an average of 0.0008 n.u.^2 per increment. In total, addition of 5% water into the engine lubricant increased the $C(T/2)$ values by 0.0038 n.u.^2 .

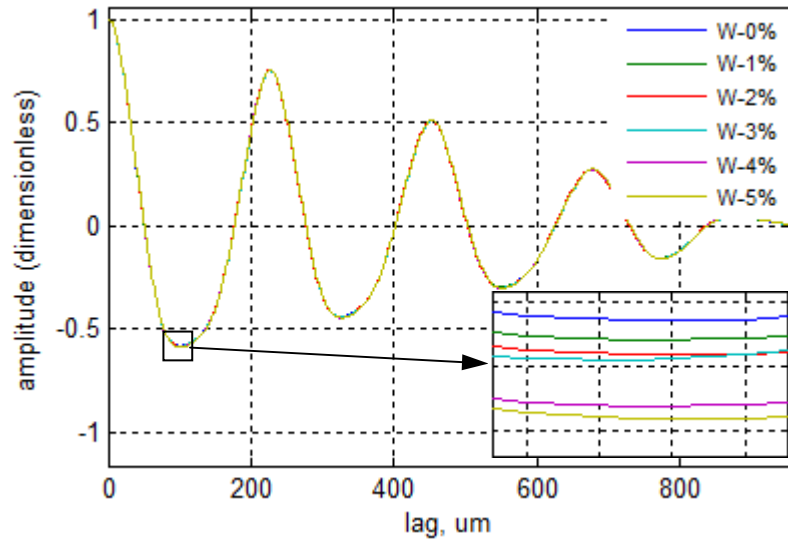


Figure 7.16 Auto-correlation function graph of water contaminated engine lubricant

Evaluation of auto spectral function with respect to concentration of water in the engine lubricating oil pan is illustrated in Figure 7.17. Introduction of 1% of water into the oil pan immediately shifted the auto spectral function graph down ward. As water

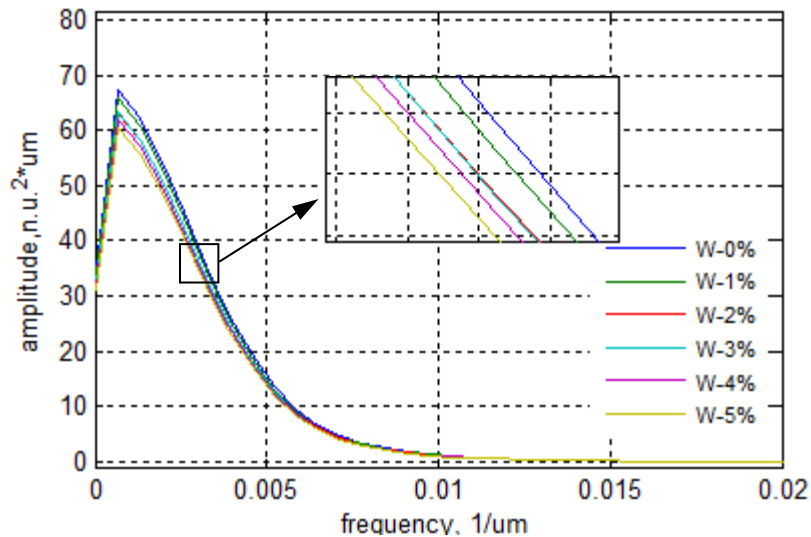


Figure 7.17 Evolution of water contamination on spectrum density function

concentration was increased up to 5%, auto spectral function graph of DOI was differentiating further down as to compare to ASF_{OOI} . Introduction of the water into the lubricant and increasing its concentration up 5% produced a reduction effect in the W_{ASF} values as well. At 1% of water, the width of auto spectral function graph reduced from 0.003486 (1/μm) to 0.003477 (1/μm). From 1% to 3% of water concentration, W_{ASF} values decreased further to 0.003469 (1/μm), 0.003465 (1/μm), 0.003454 (1/μm), and 0.003434 (1/μm). Overall, introduction of water into the engine lubricating oil pan and increasing its concentration up to 5% reduced the W_{ASF} by 0.000052 (1/μm). Figure 7.18 shows the evolution of optical transfer function with respect to water concentration. The visual observation from the graph indicated that addition of the water into the engine lubricating oil pan did not affect the optical linkage between $I_{DOI}(u)$ and $I_{OOI}(u)$ substantially. With respect to effective width of optical transfer function ΔH_{eff} , introduction of 1% of water into the lubricant reduced the ΔH_{eff} value to 0.02482. As the water concentration was increased to 2%, ΔH_{eff} reduced further down to 0.02485. From 2% to 3% ΔH_{eff} showed decreased furthermore to 0.02480. At 4% of water concentration the ΔH_{eff} increased to 0.02460 and then reduced to 0.02450 at 5% of water concentration. Overall, addition of water into the oil pan from 1% to 5% reduced the ΔH_{eff} by 0.00034 (a 1.4% reduction).

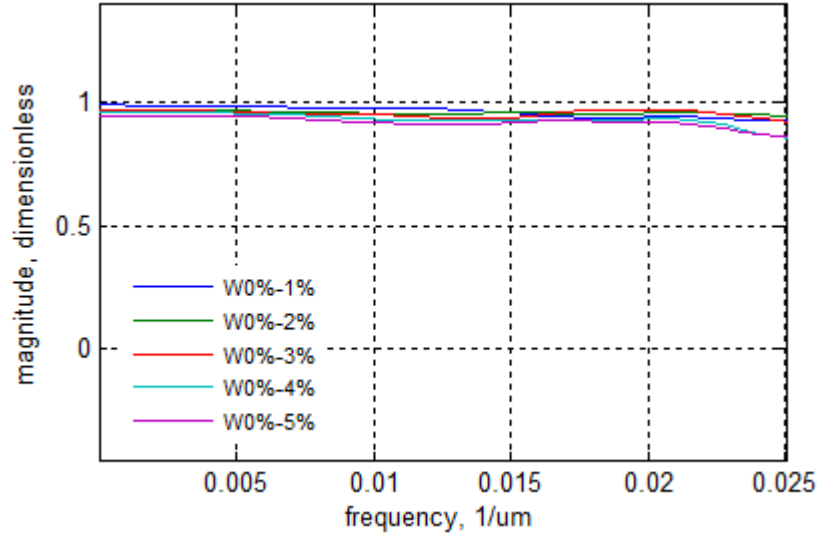


Figure 7.18 Evolution of water concentration on optical transfer function

Figure 7.19 is the graphical presentation of the changes of effective width of transfer function (ΔH_{eff}) and auto correlation function values at $T/2$ region with respect to water concentration. Addition of water into the oil pan from 1% to 5% reduced the ΔH_{eff} by 0.00034, while $C(T/2)$ values increased from -0.5226 n.u.² to -0.5264 n.u.². Visual inspection of the $\{C(T/2), \Delta H_{eff}\}$ informational space indicates from 0 to 2% of water contamination, correlation between these two parameters is weak, however, as contaminant concentration increases to 3%, 4%, and 5% a stronger correlation between these parameters is observed.

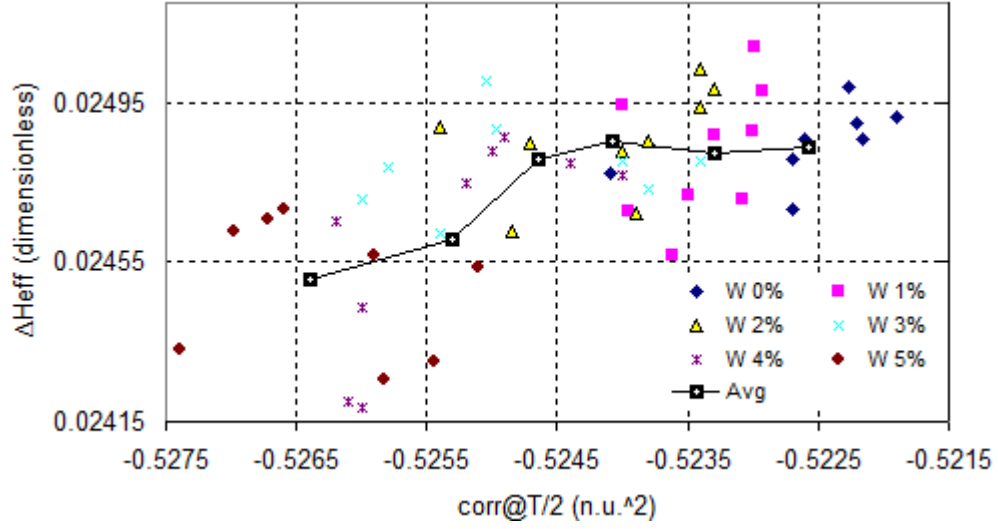


Figure 7.19 Evolution of water contamination in $\{C(T/2), \Delta H_{eff}\}$ information space

Effect of increasing water concentration in the $\{\Delta H_{eff}, W_{ASF}\}$ space is shown in Figure 7.20. Introduction of water into the lubricant and increasing its concentration reduced the W_{ASF} from 0.003486 ($1/\mu\text{m}$) to 0.003434 ($1/\mu\text{m}$). Water had a similar effect on the ΔH_{eff} values. A visual observation from the $\{\Delta H_{eff}, W_{ASF}\}$ space indicates introduction of water into the pan and increasing its concentration led both parameters in

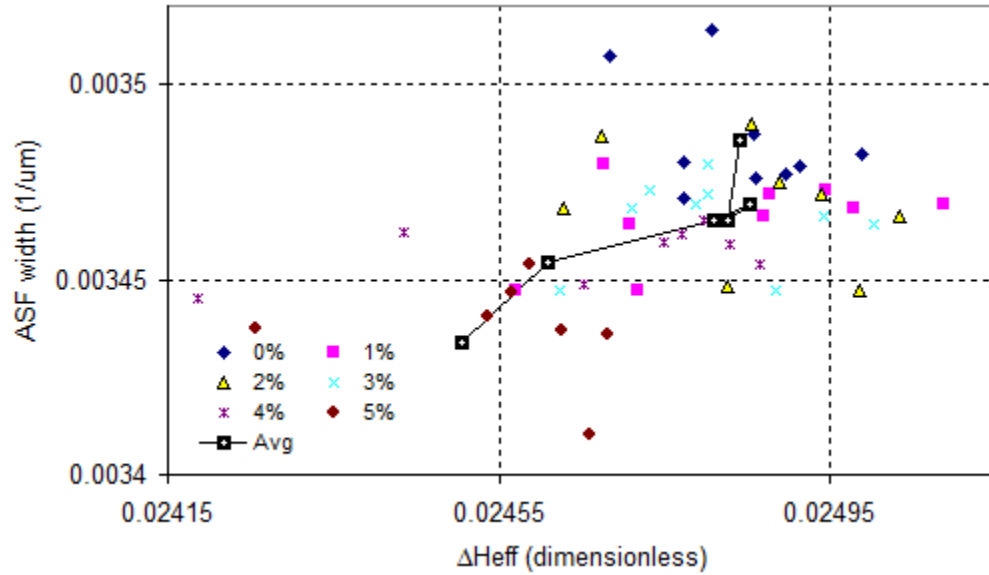


Figure 7.20 Evolution of water concentration on the $\{\Delta H_{eff}, W_{ASF}\}$ in information space

the same direction indicating of a strong correlation between these two parameters. Figure 7.21 illustrates the relationship between $C(T/2)$ and W_{ASF} values in a 2 dimensional space with respect to water concentration. Introduction of water into lubricating oil and increasing its concentration to 5% increased the $C(T/2)$ values from -0.5225 (n.u.²) to -0.5263 (n.u.²). With respect to W_{ASF} , increasing contaminate concentration decreased the W_{ASF} (1/μm) from 0.003486 to 0.003434 (1/μm). The 2-D information space of these two parameters indicates a strong correlation statistical dependency between these parameters.

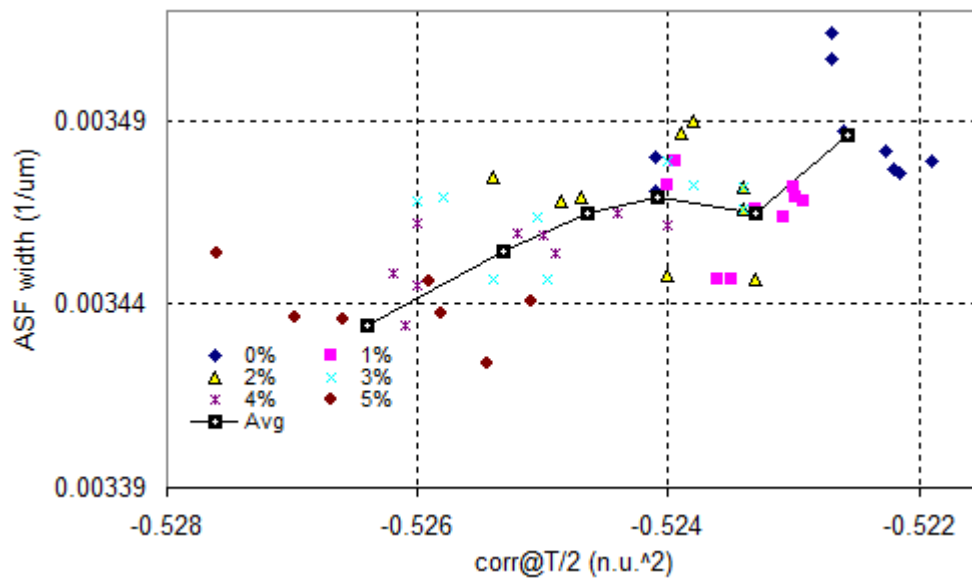


Figure 7.21 Evolution of water contaminant in $\{C(T/2), W_{ASF}\}$ information space

7.5 Object shape based optical analysis for on-line monitoring contaminated engine lubricant

Object shape based analysis methodology is based on the comparison of a set of pre-defined parameters of a priori known object images imbedded in an inhomogeneous medium. The embedded context or the medium which surrounds the shape is considered to be random and responsible for the evolution of the shape. In this condition, the changes in the medium directly influence the object's geometrical properties and study the pattern of change in the shape and comparing to the geometrical properties of the deterministic object enables to monitor and identify the variation in the medium. To differentiate between the original object image (OOI) and distorted object image (DOI), object/lubricant color parameters and shape width related parameters at object and lubricant level were selected as the defining parameters. The described above steps require initial image processing, such as, cross-sectioning, color normalization *etc.* making optical images and data more suitable for further statistical-geometrical analysis.

Performing quantitative and qualitative analysis on the shape parameters (color of lubricant and object, object shape width at object and lubricant levels, object relative color, and object width non-uniformity coefficient) of OOI and DOI provides accurate and precise estimation of medium condition.

Object shape based optical analysis methodology, its sensing system and experimental set-up, image analysis and experimental methodology was described in details in chapter 5. In this chapter the object shape based optical analysis is applied to detect and quantify the presence of coolant, gasoline and water in the engine lubrication oil pan.

7.5.1 Object shape based optical analysis of coolant contaminated engine lubricant

The effect of introducing coolant into the engine lubricant and increasing its concentration on the color scale graph is illustrated in Figure 7.22. Introduction of 1% coolant into the engine lubricating oil pan caused a slight decrease in the pick-to-valley (P-to-V) value of the graph from 0.5124 to 0.5004 (2.3% reduction). As the coolant concentration was increased in the pan to 2%, 3%, 4% and 5%, the color cross section graph P-to-V decreased to 0.4966, 0.4956, 0.5069, and 0.4919. It is noted that the reduction in P-to-V values was not uniform, however, overall addition of 1%-5% of coolant into the engine oil pan lowered the P-to-V values of color cross section graph by 0.0205 (a 4% reduction). This data shows significant dependence of amplitude characteristics (e.g. P-to-V, mean values, variance, *etc.*) of the light intensity cross-sections to the coolant concentration in the oil pan and therefore can be used as informational parameters for condition monitoring of contaminated lubricants.

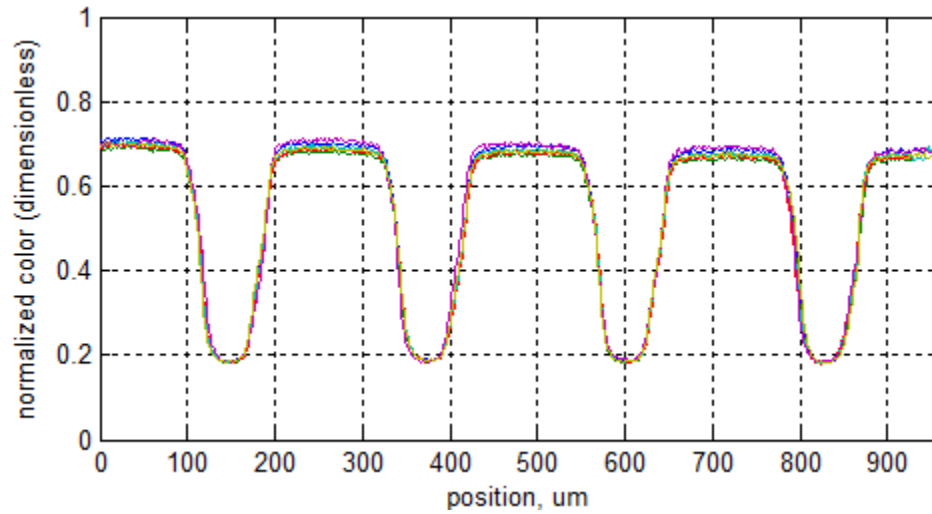


Figure 7.22 Color cross sections (OOI and DOI) of coolant contaminated engine lubricant

The OOI and DOI color cross sections were used to calculate relative lubricant-object color index ΔC and non-uniformity coefficient of object width ΔW . Standard mathematical functions from MATLAB software was used to perform calculate these parameters (see Appendix C).

Figure 7.23 illustrates the change in the ΔC with respect to coolant concentration. Introduction of 1% of coolant into the engine lubricant oil pan immediately reduced the ΔC value from 73.13 to 72.69. As the coolant concentration increased to 2% and 3%, the ΔC values lowered to 72.69, and 72.63. At 4% of coolant, the ΔC showed a slight increase and then reduced to 72.40 at 5% of coolant. Overall, addition of coolant (1%-5%) into the engine lubricating oil pan lowered the ΔC by 0.73.

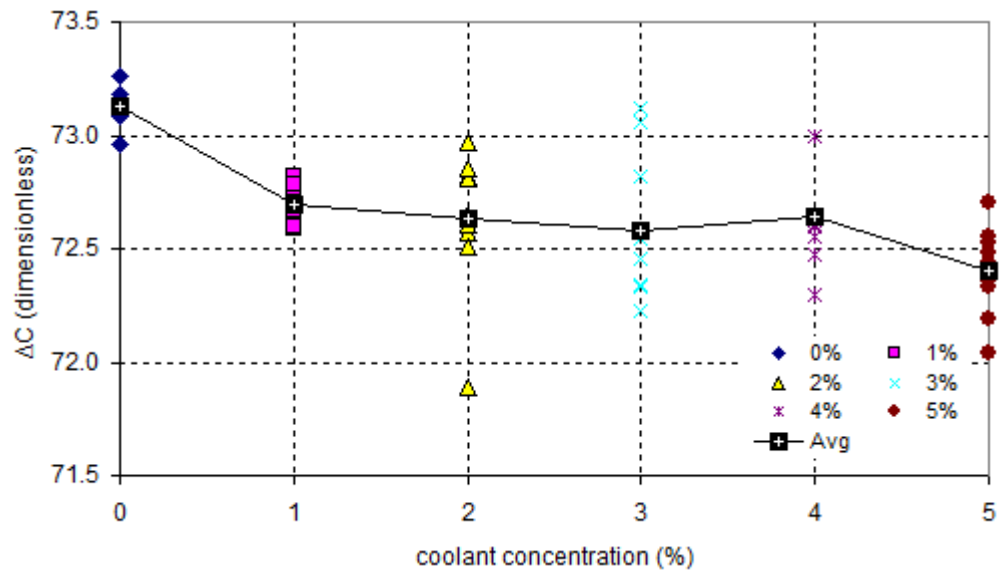


Figure 7.23 Evaluation of relative lubricant-object color index ΔC with respect to coolant concentration

Non-uniformity coefficient of object width ΔW with respect to coolant concentration exhibited a good correlation with coolant concentration (see Figure 7.24).

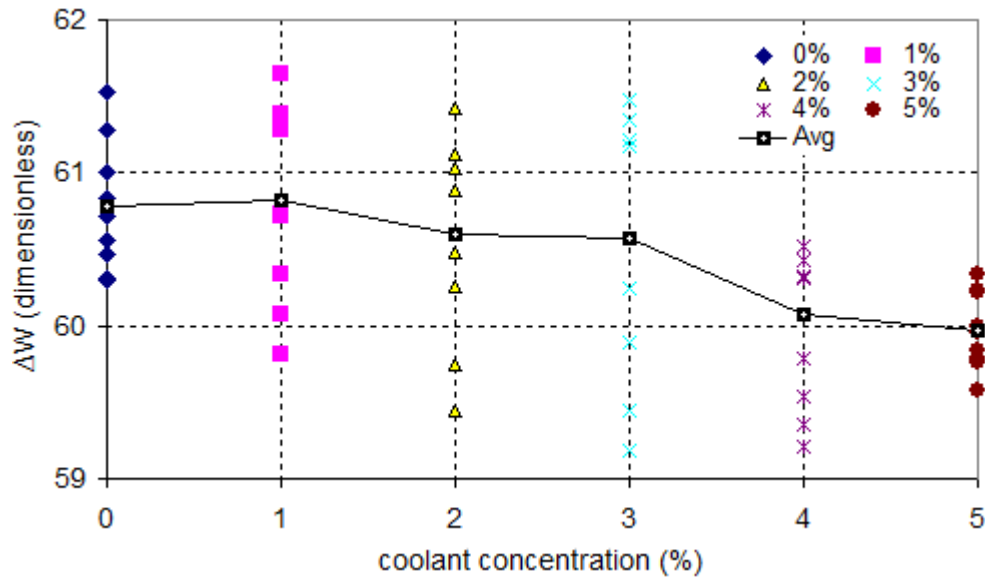


Figure 7.24 Evaluation of relative lubricant-object color index ΔW with respect to coolant concentration

Introduction of 1% of coolant into the engine lubricant oil did not affect the ΔW immediately, however as coolant concentration was increased to 2%, 3%, 4%, and 5%, the ΔW was reduced to 60.60, 60.57, 60.07, and 59.96 respectively. Overall, introduction of coolant into the lubricant oil reduced the ΔW from 60.78 to 59.96 (a 0.82 reduction).

Figure 7.25 presents the $\{\Delta C, \Delta W\}$ 2-D informational space with respect to coolant concentration. This graph illustrates the relationship between these two parameters simultaneously as the contaminant concentration varies. In general, addition of coolant into the engine oil pan had a reduction effect on the ΔC and ΔW values. A visual examination from the $\{\Delta C, \Delta W\}$ space indicates from 0% to 1% of coolant concentration, there is a weak correlation between the ΔC and ΔW values.

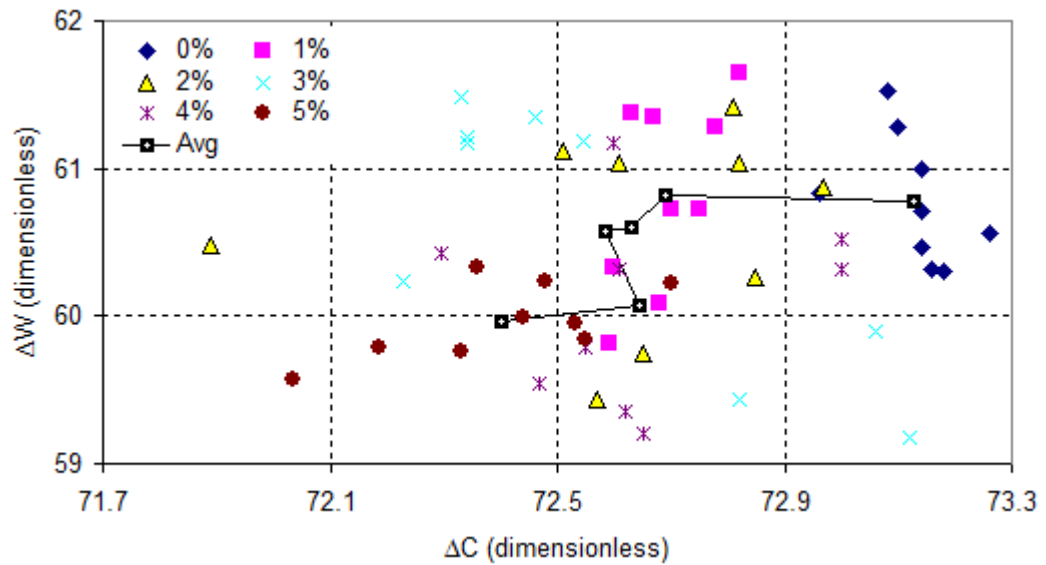


Figure 7.25 Evolution of coolant contamination in $\{\Delta C, \Delta W\}$ information space

As coolant concentration increased from 1% to 2%, 3%, 4 %, and 5% ΔC and ΔW exhibit a stronger correlation. Overall, introduction of coolant into the engine lubricant oil pan and increasing its concentration up to 5% led ΔC and ΔW in the same direction.

7.5.2 Object shape based optical analysis of gasoline contaminated engine lubricant

Figure 7.26 shows the color cross section of fresh and gasoline contaminated (0%-5%) lubricant. Introduction of 1% gasoline into the engine lubricating oil pan caused a decrease in P-to-V values of the graph from 0.5249 to 0.5238 (a reduction of 0.0011). As the gasoline concentration was increased in the oil pan to 2%, 3%, 4% and 5%, the color cross section graph P-to-V values decreased at a non-linear rate to 0.5198, 0.511, 0.4883, and 0.4427. It is noted that the reduction in P-to-V values was not uniform, however, overall addition of 1%-5% of gasoline into the engine oil pan lowered the P-to-V values of color cross section graph by 0.0822 (a 15.7% reduction).

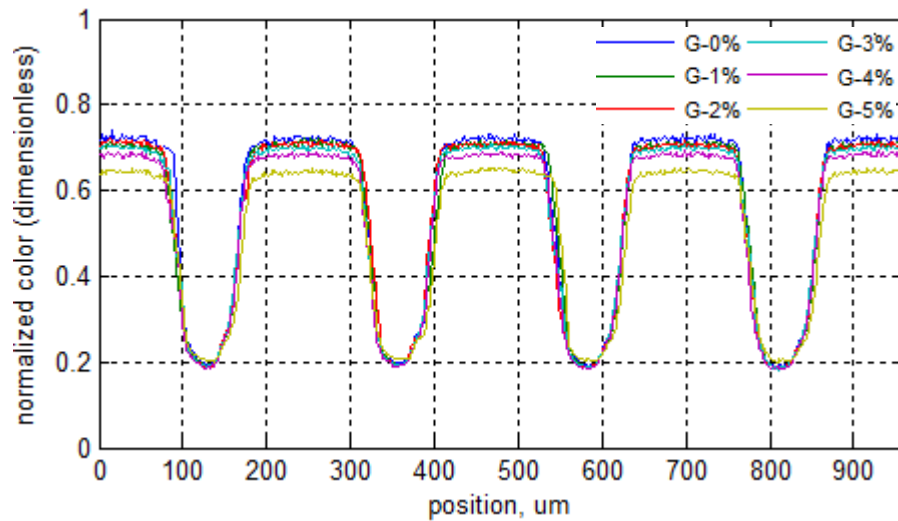


Figure 7.26 Color cross sections (OOI and DOI) of gasoline contaminated engine lubricant

OOI and DOI of color cross-sections were used to calculate the relative lubricant-object color index ΔC and non-uniformity coefficient of object width ΔW .

Figure 7.27 presents the change in the relative lubricant-object color index ΔC of engine lubricant with respect to introduction of water into the engine lubricant oil pan and increasing its concentration from 1% to 5%. Overall, addition of gasoline into the lubricant lowered the relative lubricant-object color index ΔC from 74.66 to 67.20, a 10% reduction. This reduction was not uniform as gasoline concentration was increased by 1% increment. Addition of 1% of gasoline lowered the ΔC value from 74.66 to 74.33. As the concentration was increased to 2%, 3%, 4%, and 5%, the ΔC decreased to 73.53, 70.66, 70.22, and 67.70.

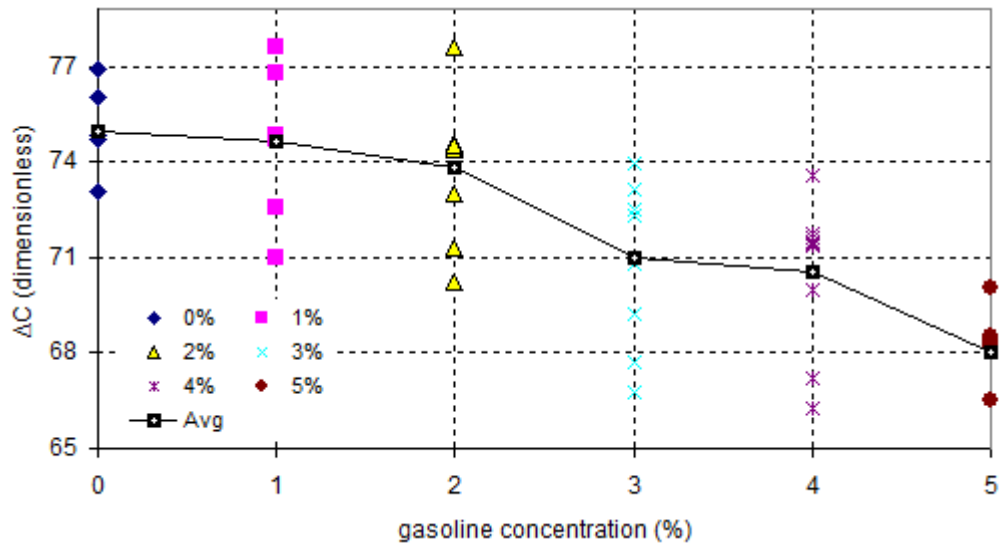


Figure 7.27 Evaluation of relative lubricant-object color index ΔC with respect to gasoline concentration

Figure 7.28 shows the non-uniformity coefficient of object width with respect to contaminant concentration. Introduction of 1% of gasoline into the immediately lowered the ΔW values from 63.53 to 63.38. As gasoline concentration was increased to 1%, the ΔW showed a slight increase to 63.79. Increasing contaminants concentration to 3%, 4% and 5% reduced the ΔW further to 63.27, 62.26, and 58.88. Overall, gasoline reduced the ΔW values from 63.53 to 58.88, a 7.32% reduction.

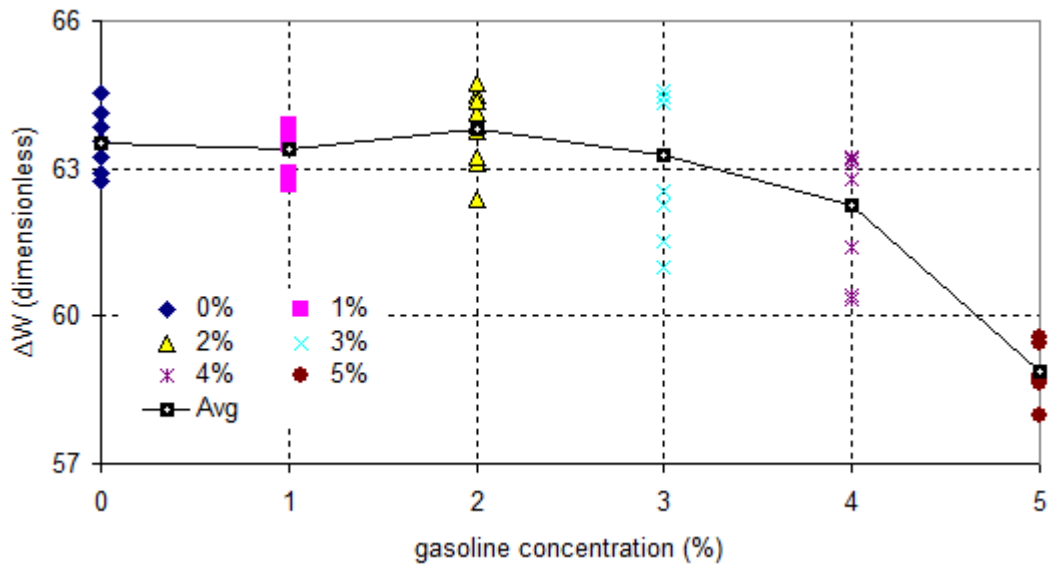


Figure 7.28 Evaluation of non-uniformity coefficient of object width ΔW wrt gasoline concentration

Figure 7.29 represents the 2-D informational space of ΔC and ΔW . $\{\Delta C, \Delta W\}$ shows the relationship between these parameters with respect to variation in the contaminant concentration. From visual observation from 0% to 3% of gasoline concentration, ΔC and ΔW does not exhibit a very strong correlation. From 3% to 5% the correlation between these parameters become stronger and both parameters move in a same direction. Overall, ΔC and ΔW values exhibited a strong correlation as gasoline concentration was increased.

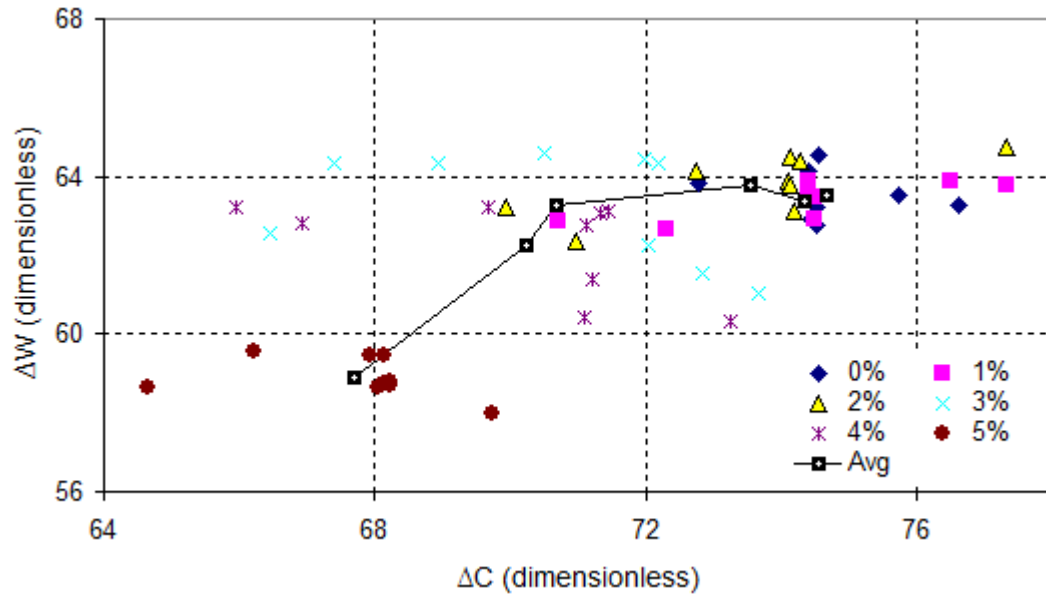


Figure 7.29 Evolution of gasoline concentration in $\{\Delta C, \Delta W\}$ information space

7.5.3 Object shape based optical analysis of water contaminated engine lubricant

Figure 7.30 shows the color cross section of fresh and water contaminated (0%-5%) lubricant. Introduction of 1% water into the engine lubricating oil pan caused a decrease in P-to-V values of the graph from 0.4539 to 0.4483 (a reduction of 0.0056). As the water concentration was increased in the oil pan to 2%, 3%, 4% and 5%, the color cross section graph P-to-V values decreased to 0.4319, 0.4266, 0.4257, and 0.4125. It is noted that the reduction in P-to-V values was not uniform, however, overall addition of 1%-5% of water into the engine oil pan lowered the P-to-V values of color cross section graph by 0.0414 (a 9.1% reduction).

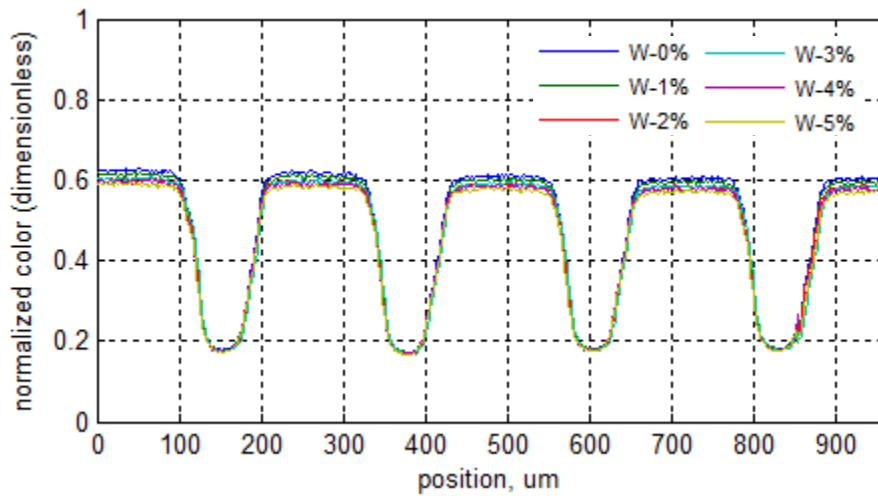


Figure 7.30. Evaluation of color cross section of fresh and water contaminated engine lubricant

OOI and DOI of color cross-sections were further used to calculate the relative lubricant-object color index ΔC and non-uniformity coefficient of object width ΔW using standard mathematical functions from MATLAB software (see Appendix C). Figure 7.31 presents the change in the relative lubricant-object color index ΔC of engine lubricant with respect to introduction of water into the engine lubricant oil pan and increasing its concentration from 1% to 5%. Overall, addition of water into the lubricant lowered the relative lubricant-object color index ΔC from 70.66 to 69.80, a 1.2% reduction. Addition of 1% of gasoline lowered the ΔC value from 70.35 to 70.14. As the concentration was increased to 2%, 3%, 4%, and 5%, the ΔC decreased to 70.21, 69.89 and 69.80.

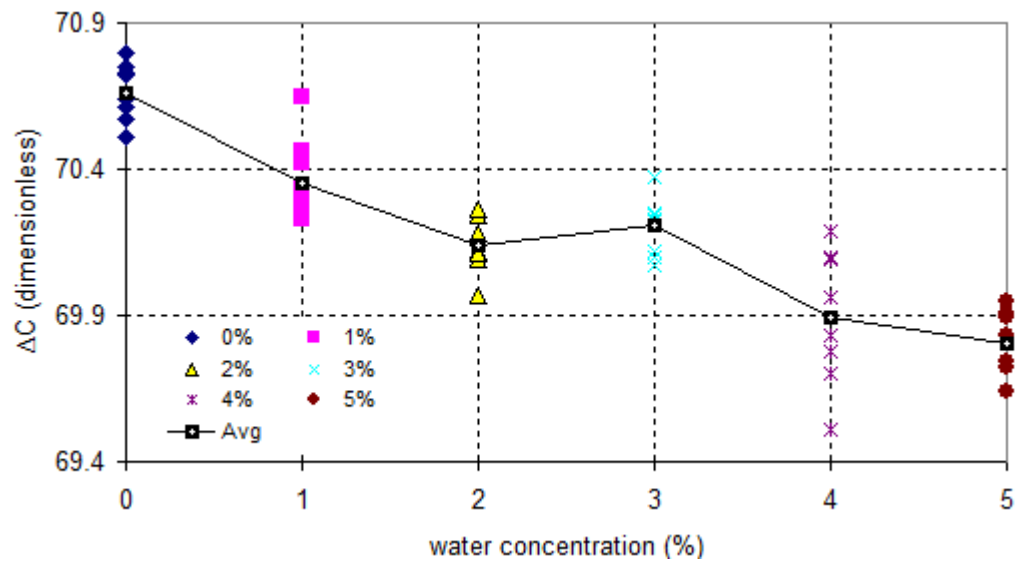


Figure 7.31. Evaluation of relative lubricant-object color index ΔC with respect to water concentration

Figure 7.32 shows the non-uniformity coefficient of object width with respect to contaminant concentration. Introduction of 1% of water immediately lowered the ΔW from 62.16 to 61.99. As water concentration was increased to 2% the ΔW decreased to 60.95. Increasing contaminants concentration to 3%, 4% and 5% changed the ΔW values to 61.50, 60.23, and 59.42. Overall, water reduced the ΔW values from 62.16 to 59.42, a 4.4% reduction.

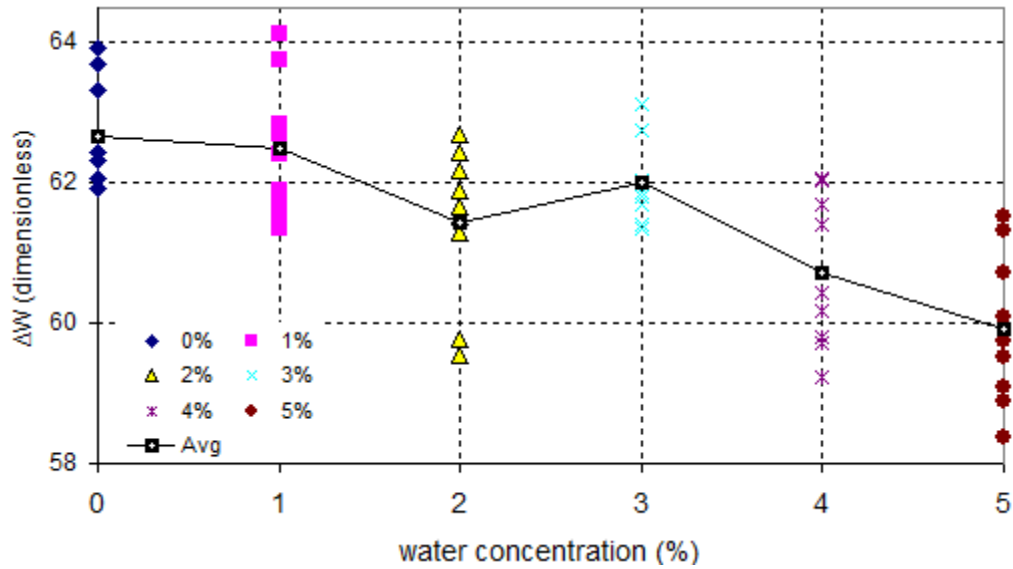


Figure 7.32 Evaluation of non-uniformity coefficient of object width ΔW wrt water concentration

Figure 7.33 represents the relationship between ΔC and ΔW in a 2-D information space. This graph presents the simultaneous changes of these two parameters with

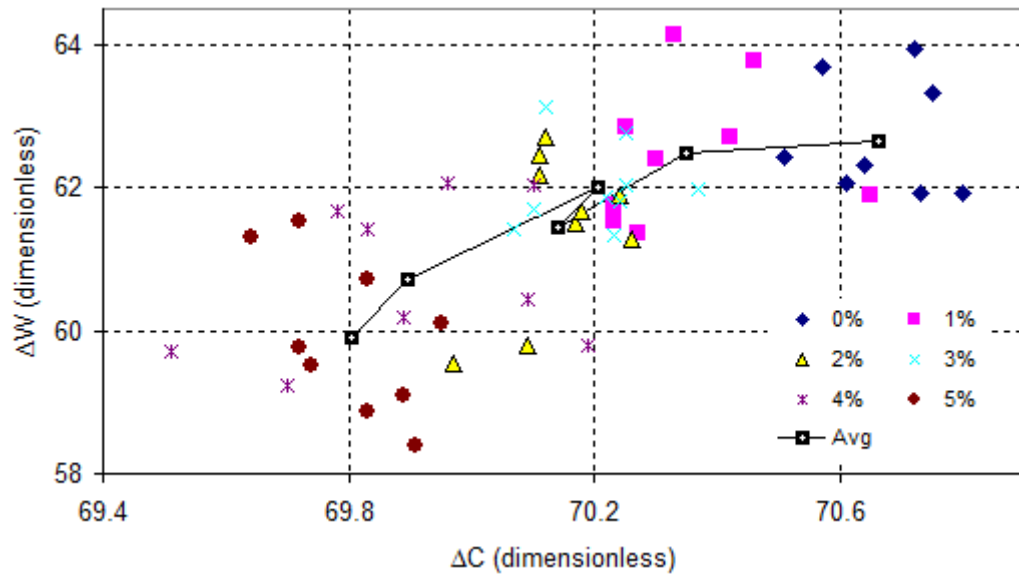


Figure 7.33 Evolution of water concentration in $\{\Delta C, \Delta W\}$ information space

respect to change in water concentration. A visual examination of the graph indicates that as the concentration was increased, ΔC and ΔW values changed in the same direction indicating of a strong correlation between these two parameters.

7.6 Discussion

Engine lubricant is formed from base oil and chemical additives. Depends on the application, lubricants are formulated differently; however the main characteristics of lubricants come from the base oil. Base oil mainly is consisted of hydrocarbons chains. The base oils can be mineral or synthetic. A variety of chemicals are added to the base oil to modify lubricant performance. These chemical are called additives and the most common are anti-oxidation inhibitors, rust inhibitors, dispersant and detergent, anti-wear and extreme pressure additives, viscosity index improvers and etc.

High temperature generated by combustion process and excessive force from the engine moving parts create a very harsh environment for the engine lubricant to work in. The degradation process starts with the breakdown of hydrocarbon compounds into smaller chain and form free radical. The additives also break down and loss their properties, while contaminants accumulate in the lubricant. In general, engine lubricant degradation is the combination of base oil oxidation, additives depletion and addition of contaminants to the lubricant.

In all lubricating systems, organic compounds exposed to high temperatures and pressures in the presence of oxygen will partially oxidize. There are a wide variety of by-products produced during the combustion process. In addition to oxidation products, nitration products are also formed. Presence of oxidation product, NO_x and sulphation SO_x causes lubricant to thicken and form build-up such as varnish or lacquer in the engine. Anytime a too rich fuel/air mixture is burned, soot particulates are formed. Introduction of the contaminants to the engine lubricant increases the lubricant degradation rate.

When engine runs, the normal aging process of engine lubricant is continuously taking place. During this process properties of lubricant changes and lubricant become denser in viscosity and darker in color.

In the experiment conducted in this chapter, as engine runs, there are two different phenomena taking place inside the engine lubricant. The first phenomenon is the normal aging or degradation of the lubricant described above. The second phenomenon is the introduction of contaminants into the oil pan. In chapter 5 and 6, it was observed both of these occurrences deter the optical properties of the lubricant at a different rate in-vitro. However, in-vivo when both of these events take place simultaneously, knowing the contamination rate happens at a much higher rate compare to aging process, the outcome, the degradation rate at which the lubricant deteriorates, may differ. This is due to the choice of contaminants which may increase or decrease the deterioration effect. For instance addition of coolant into the lubricating oil pan did not show a strong deterring effect on the statistical properties of the lubricant, while in chapter 5 and 6 coolant demonstrated the most deterring effect on the lubricant optical properties. This is due to the presence of the lubricant filter which is highly absorbent to coolant. In fact, coolant is known to clog the filter prematurely and causes filter failure. Contrary to the coolant, introduction of gasoline had the most deterring effect on the optical and statistical optical property of the engine lubricant. It is known that the combustion by-product such as nitration NO_x , sulphation SO_x and soot can form residue and sludge inside of engine crankcase lubricant passages. These by-products can be easily dissolved by gasoline and prematurely deteriorate the optical properties of the lubricant. In addition, gasoline molecules can get oxidized more easily than oil molecules promoting oxidation of oil molecules and premature degradation of lubricant.

Addition of water into the oil pan showed a deterring effect on the statistical optical property of the engine lubricant. As engine RPM increases, water molecules become suspended in the lubricant very easily and form lubricant-water emulsion. Emulsified water produces hazy, cloudy or milky appearance easily deterring the optical properties of lubricant.

Overall, gasoline contamination showed the highest deterring effect on the engine lubricant optical properties. Following gasoline, water performed to be s the second most effective contaminant in this experiment. Coolant effect on the engine lubricant statistical optical and shape properties was the least deterring.

7.7 Summary and conclusion

In this chapter the statistical optics and object shape based optical analysis methodologies are utilized to sense and monitor the presence of three major contaminants, coolant, gasoline and water in the lubricating oil of a 2005 Ford Taurus engine on-line. This experiment mimicked several realistic circumstances which structural defect of engine parts or mismanagement of combustion process or other interrelated causes would lead to the presence of contaminants in the engine lubricant. These experiments demonstrated the two proposed sensing methodologies can measure the presence of coolant, gasoline, and water and consequently provide insight in the state of engine health, combustion management system or other interrelated issues.

Statistical analysis was applied at the combined object-lubricant images. Specifically, statistical auto-characteristics, such as auto-correlation function and auto spectral function and statistical cross-characteristics and their informational parameters were applied to characterize optical changes in contaminated/deteriorated lubricants. The utilized methodology in the proposed sensing system was verified experimentally showing ability to distinguish lubricant with 1% to 5% coolant, gasoline, and water contamination.

In the object shape based optical analysis several parameters of the acquired optical images, such as, color of lubricant and object, object shape width at object and lubricant levels, object relative color, and object width non-uniformity coefficient were measured. Estimation of contaminant presence and lubricant condition was performed by comparison of parameters for fresh and contaminated lubricants. The object shape based optical sensing methodology was verified experimentally showing ability to distinguish lubricant with 1% to 5% coolant, gasoline and water contamination.

From the results obtained, the following main conclusions can be drawn:

1. Visual analysis of the OOI (with 0% contaminant concentration) and DOI cross sections showed that addition of 1%-5% of coolant into the engine oil pan lowered the P-to-V values of color cross section graph by 0.0205 (a 4% reduction). Addition of 1%-5% of gasoline lowered the P-to-V values of color cross section graph by 0.0822 (a 15.7% reduction). Introduction of 1%-5% of water reduced the P-to-V values of color cross section graph by 0.0414 (a 9.1% reduction). This data shows significant dependence of amplitude characteristics (e.g. P-to-V, mean values, variance, *etc.*) of the light intensity cross-sections to the contaminants concentrations in the oil pan and therefore can be used as informational parameters for condition monitoring of contaminated lubricants.
2. Addition of 0%-5% of coolant into the lubrication oil pan decreased the auto-correlation function values at $T/2$ region by -0.0053 n.u.². In case of water, and gasoline, the auto-correlation function values at $T/2$ region was increased by -0.01643 n.u.², and -0.00382 n.u.² respectively. These results indicate the $C(T/2)$ values are more sensitive to addition of gasoline and water as to compare to coolant.
3. Analysis of auto spectral function indicted addition of 0%-5% of coolant, gasoline and water decreased W_{ASF} by 0.00002 μm^{-1} , 0.000074 μm^{-1} and 0.000052 μm^{-1} .
4. In analysis of statistical cross-characteristics, addition of 0%-5% of coolant, gasoline and water decreased the effective width of transfer function ΔH_{eff} by 0.0001321, 0.00091 and 0.000335 respectively.
5. Plotting statistical auto-characteristics parameter i.e. $C(T/2)$ and cross-characteristics parameters such as effective width of transfer function ΔH_{eff} at different contamination concentration provided an accurate monitoring tool for condition of lubricant. $\{C(T/2), \Delta H_{eff}\}$ informational space of coolant did not

show a strong correlation between these two parameters. $\{C(T/2), \Delta H_{eff}\}$ of gasoline and water illustrated a strong correlation between these parameters.

6. $\{\Delta H_{eff}, W_{ASF}\}$ information space was also used to monitor the condition of lubricant with respect to addition of coolant, gasoline and water. In general, addition of all contaminants into the oil pan had a reduction effect on ΔH_{eff} and W_{ASF} values. The $\{\Delta H_{eff}, W_{ASF}\}$ informational space of coolant, gasoline and water showed a close correlation between these parameters, however judging by the slope of the plotted values, the gasoline and water provide a stronger correlation between these parameters.
7. $\{C(T/2), W_{ASF}\}$ informational space was used as another indicator for monitoring the lubricant condition. In case of coolant $\{C(T/2), W_{ASF}\}$ indicated a weak relationship between these two parameters, however addition of gasoline and water into the oil pan produced a stronger correlation between these parameters.
8. Evaluation of the relative lubricant-object color index ΔC indicated that increase in the concentration of coolant, gasoline and water, 1%-5%, reduced the ΔC value by 0.73, 6.96, and 0.86 respectively.
9. Non-uniformity coefficient of object width ΔW exhibited a good correlation with introduction of contaminants into the engine lubricant. Addition of coolant, gasoline and water up to 5% into the engine lubricant lowered the ΔW value by 0.81, 4.64, and 2.74 respectively.
10. Plotting the relative lubricant-object color index ΔC and non-uniformity coefficient of object width ΔW at different contamination concentration in a 2-D informational space provided an accurate monitoring tool for condition of lubricant. Addition of coolant at 1% and increasing to 5% shifted both parameters in the same direction however, the rate at which ΔW values changed was different

from ΔC values. $\{\Delta C, \Delta W\}$ informational space of gasoline indicated a strong correlation between these parameters as the gasoline concentration was increased. Similar trend was observed in $\{\Delta C, \Delta W\}$ informational space of water. Introduction of water into the lubricant shifted both parameters in the same direction indicating of a good correlation between the parameters.

11. Obtained results from on-line on board experiment confirm applicability of systems approach to monitor the engine health and performance through the analysis of engine lubricant. Implementation of systems approach to monitor the health of engine through optical analysis of engine lubricant is a new approach in the automotive field to manage engine performance and health. Systems approach realizes the interrelationship between engine health and lubricant condition and by monitoring the properties of the lubricant evaluates the engine health. This new approach provides insight into the importance of engine lubricate and lubricant system and how lubricant can be used as a source of information for engine performance.
12. The success achieved in this study is mainly due to the proper design and appropriate functionality of proposed sensing system. Implementation of opto-microfluidic sensing system enabled the extraction of optical information from engine lubricant to monitor the characteristics of the lubricating oil on-line and in real time. Opto-microfluidics sensing system represents the use of advanced optical elements to increase the functionality of microfluidic devices and also the use of advanced microfluidic devices to increase the functionality of photonic devices. Such integration represents a novel approach to dynamic manipulation of optical systems with many applications in automotive fluid sensing field.

Chapter 8

8 Conclusion

8.1 Summary of results

This thesis mainly investigated the applicability of systems approach for monitoring the health and performance of an internal combustion engine through engine lubricant system. This novel approach is based on the realization of a strong interrelationship between engine performance and lubricant characteristics.

Based on the systems approach, the engine function or performance can be considered as the whole and engine lubricant system and lubricating oil to be decomposed into sub and sub sub-system level for quantitative and objective analysis to extract information related to engine health and performance. The quantitative analysis at the sub sub-system level will provide accurate information on the lubricant characteristics which can be relayed to the state of engine health.

Due to the high accuracy and precision of optical measurement methods, this research selects optical methods to study variation in the engine lubricant characteristics. Since the variations in the lubricant characteristics are unpredictable, lubricant can be modeled as a dynamic optical medium with random characteristics. The random characteristics of medium imply the use of optical transfer function (OTF) analysis for quantitative measurement of optical properties variant in the lubricant based on the changes in input and output optical signals.

Surface plasmon resonance (SPR) measurement, Statistical optical sensing, and object shape-based optical sensing are three optical methodologies used in this research. In all these methodologies lubricant with random properties will affect and transform the characteristics of optical input emitted into the random medium. What causes the transformation of input to output signal is a distortion transformation factor imposed by the lubricant.

In the SPR measurement the effect of changes in the optical properties of engine lubricants caused by the introduction of gasoline, coolant and water on the surface plasmon resonance (SPR) characteristics was analyzed conveying new scientific findings and analysis results which were not available before. It was shown experimentally that attenuation of surface plasmons due to introduction of contaminants to the engine lubricant leads to a noticeable increase in the resonance angle θ_{SPR} and reflectivity minimum R_{min} values due to an increase in the dielectric permittivity ϵ_d .

Developed object shape-based optical sensing analysis methodology is a novel approach for analysis of a synergetic effect of combined lubricant-object optical appearance. This methodology is based on the optical analysis of the distortion effect when an object images is obtained through a thin random optical medium. Several parameters of acquired optical images, such as, color of lubricant and object, object shape width at object and lubricant levels, object relative color, and object width non-uniformity coefficient, are proposed. Measured on-line parameters are used for optical analysis of fresh and contaminated lubricants. Estimation of contaminant presence and lubricant condition is performed by comparison of parameters for fresh and contaminated lubricants.

In statistical optics analysis statistical characteristics of a combined object-lubricant image of a periodically structured object distorted by a thin film of random media (e.g. contaminated engine lubricant) is investigated. Presence of contaminants and their concentration is determined by two types of statistical characteristics. Statistical auto-characteristics (e.g., auto-correlation function) are utilized to estimate a contaminant concentration and its evolution through the comparison of characteristics for fresh and contaminated lubricants. Statistical cross-characteristics (e.g., cross-correlation functions and optical transfer function) are mainly used for the analysis of the distortion effect directly correlated with the presence of contaminants and their concentration.

The functionality of both methodologies was verified in-vitro and in-vivo showing an ability to distinguish the lubricant with coolant, gasoline and water on-line. Obtained results confirm applicability of systems approach to monitor the engine health and performance through the analysis of engine lubricant.

8.2 Thesis contribution

The scientific contribution of this research is the implementation of systems approach, an intellectual discipline method to attack complex problem, for engine health evaluation through analysis of engine lubricant using optical property of engine lubricant. Systems approach encompasses both the holistic and modular views. It grasps the essential features of the whole system, analyzes it into parts with proper interfaces, and synthesizes knowledge about the parts to understand the whole. This approach grasps the system and its details in many levels, decomposes a subsystem into sub-subsystems to simplifying the complexity of the problem and provides focus approach to different levels. Systems approach realizes the interrelationship between engine health and lubricant condition and by monitoring the properties of the lubricant evaluates the engine health. This approach provides insight into the importance of engine lubricate and lubricant system and how lubricant can be used as a source of information for engine performance.

The engineering contribution of this work is the implementation of opto-microfluidic sensing system for extraction of optical information and monitoring the characteristics of the engine lubricating oil on-line in real time. The opto-microfluidics sensing system used in this research represents the use of advanced optical elements to increase the functionality of microfluidic devices and conversely the use of advanced microfluidic devices to increase the functionality of photonic devices. Such integration represents a novel approach to dynamic manipulation of optical systems with many applications in automotive fluid sensing arena.

The originality of the object shape-based optical sensing analysis and statistical optics analysis methodologies comprises of obtaining and analysis of an optical image that combines an object with known periodic shape and a thin film of the contaminated

lubricant. Introduction of an object with *a priori* known periodical structure allowed reduction of 2D into 1D optical analysis, suitable for on-line measurement application.

8.3 Suggestions for future work

As an extension to the present work on the monitoring of the engine performance and health can be integration and reconfigurability of the optical components such as light source, lenses and *etc.* into the microfluidic chip. Capability of 1D image analysis and integration or packaging of the optical components and microfluidic system will make this sensing system a strong candidate for on-line or in-line monitoring of engine performance.

Moving forward, this methodology can be installed on a probe i.e. engine lubricant dipstick to form an optical probe for on-line on board optical analysis of any machinery equipment with lubrication system. This idea requires integration of CCD camera and optical fibers (optical waveguide) for delivering light and image from the lubricant and object to the CCD camera.

Publication

- 1) Aghayan, H., Bordatchev, E V, and Yang, J 2010, Object shape-based methodology for optical analysis of contaminated engine lubricants, *Proc. of the ISOT 2010 International Symposium on Optomechatronic Technologies*, 25-27 October 2010, Toronto, Ontario, Canada, Paper No. OSD-6, 6 p.
- 2) Aghayan H, Bordatchev E V, and Yang J 2011, Monitoring of contaminants in engine lubricants using Surface Plasmon Resonance measurement, *Proc. of the CANCAM 2011 23rd Canadian Congress of Applied Mechanics*, 5-9 June 2011, Vancouver, BC, Canada, Paper No.85, 4 p, accepted for publication on March 7, 2011
- 3) Aghayan H, Bordatchev E V, and Yang J 2011, Opto-micro fluid system for analysis of contaminants in engine lubricants *Proc. of the CANCAM 2011 23rd Canadian Congress of Applied Mechanics*, 5-9 June 2011, Vancouver, BC, Canada, Paper No.98, 4 p, accepted for publication on March 7, 2011
- 4) Aghayan H R, Bordatchev E V, and Yang J 2010, SPR characterization of contaminants in engine lubricants, *Industrial Lubrication and Tribology*, submitted on January 2, 2010, manuscript ID # ILT-01-2011, accepted for publication on March 8, 2011, Article will be published in *Industrial Lubrication and Tribology* journal, issue 1 in 2013.
- 5) Aghayan H R, Bordatchev E V, and Yang J 2011, Two methodologies for optical analysis of contaminated engine lubricant, *Measurement Science and Technology*, Submitted on May 2011, accepted for publication on November 2011
- 6) Aghayan H R, Bordatchev E V, and Yang J 2011, Object shape-based optical sensing methodology and system for condition monitoring of contaminated engine lubricants, *Optics and Lasers in Engineering*, submitted on April 2012, Ms. Ref. No.: OLEN-D-12-00138

References

1. Agoston, A., Dörr, N., and Jakoby, B. (2006), "Online Application of sensors monitoring lubricating lubricant properties in biogas engine", *Proceedings of IEEE Sensors Conference, EXCO, Daegu, Korea*, Oct. 22-25, pp. 1099-102.
2. Agoston, A., Dörr, N., and Jakoby, B. (2007), "Corrosion sensors for engine lubricants — laboratory evaluation and field tests", *Sensors and Actuators B*, Vol. 127, pp. 15–21.
3. Agoston, A., Ötsch, C., and Jakoby, B. (2004), "Application of microacoustic viscosity sensors for online lubricant condition monitoring", *VDI Berichte*, Vol. 1829, pp. 833-36.
4. Agoston, A., Ötsch, C., and Jakoby, B. (2005), "Viscosity sensors for engine lubricant condition monitoring — Application and interpretation of results", *Sensors and Actuators A*, Vol. 121, pp. 327–32.
5. Agoston, A., Ötsch, C., Zhuravleva, J., and Jakoby, B. (2004), "An IR-Absorption Sensor System for the Determination of Engine Lubricant Deterioration", *Proceedings of IEEE Sensors Conference, Vienna, Austria*, 24-27 Oct., pp. 463-6.
6. Agoston, A., Schneidhofer, C., Dörr, N., and Jakoby, B. (2008), "A concept of an infrared sensor system for lubricant condition monitoring", *Elektrotechnik & Informationstechnik*, Vol. 125 No. 3, pp. 71-5.
7. Agoston, C. Ötsch, B. Jakoby: "Application of Sensors for On-line Lubricant Condition Monitoring"; in: "Current Trends in Tribology", K. Vercammen et al. (ed.); Institute for Terotechnology - National Research Institute, Poland, 2004, ISBN: 83-70204-418-X, L.13 - L.16.
8. Albarbar, A. and Gu, F. (2007), "Internal combustion engine lubricating lubricant condition monitoring based on vibro-acoustic measurements", *Insight*, Vol. 49 No. 12, pp. 715-8.
9. Albarbar, A., Gennish, R., Gu, F., and Ball, A. (2004), "Lubricating lubricant condition monitoring using vibration and air-borne acoustic measurements", *Proceedings of 7th Conference on Engineering Systems Design and Analysis, Manchester, UK*, July 19-22, pp. 205-9.
10. Ballari, M., Bonetto, F. and Anardo, E. (2005), "NMR relaxometry analysis of lubricant lubricants degradation", *J. Phys. D: Appl. Phys.*, Vol. 38, pp. 3746-50.
11. Basu, A., Berndorfer, A., Buelna, C., Campbell, J., Ismail, K., Lin, Y., Rodriguez, L., and Wangm, S.S. (2000), "Smart sensing" of Lubricant Degradation and Lubricant Level Measurements in Gasoline Engines, *Proceedings of SAE 2000 World Congress Detroit, Michigan, USA*, March 6-9, 7 p.
12. Basu, A., Ruona, W., Zawacki, G., Gangopadhyay, A., Scholl, D., Visser, J., Dobrinski, H., and Doebrich, M. (2009), "Development and Testing of an Innovative Lubricant Condition Sensor", *SAE paper 2009-01-1466*, 8 p.

13. Bennett, J.W., Matsiev, L., Uhrich, M., Kolosov, O., Bryning, Z., and Lattin, R. (2006), "New solid state condition sensor for real time engine lubricant condition monitoring", Proceedings of SAE World Congress, Detroit, Michigan, USA, Apr. 3-6, SAE Paper 2006-01-1324, 8 p.
14. Bergwerff, A. A., Van Knapen, F. (2006), "Surface plasmon resonance biosensors for detection of pathogenic microorganisms: strategies to secure food and environmental safety", J. AOAC Int., Vol. 89(3), pp. 826-31.
15. Bilyi, O.I., Getman, V.B., Ferensovich, and Ya, P. (2000), "Optical sensor for check-up of content of microparticles in light lubricant products", Proceedings of SPIE, Vol. 4148, pp. 239-41.
16. Bode, B., Auge, J., and Trettin, T. (2004), "Micro-rheometer for inline lubricant quality detection", Proceedings of IEEE Sensors Conference, Vienna, Austria, Oct. 24-27, pp. 802-805.
17. Born M and Wolf E 1997 *Principles of Optics* (Cambridge New York Oakleigh: Cambridge University Press) 6th edition
18. Byington, C., Brewer, R., Nair, V., and Mott, A. (2007), "Experiences and testing of an autonomous on-line lubricant quality monitor for diesel engines", Proceedings of 62nd Annual Meeting of the Society of Tribologists and Lubrication Engineers, pp. 1-23.
19. Caelen, I., Kalman, A., Wahlstrom, L (2004), "Biosensor-based determination of riboflavin in milk samples", Anal. Chem., Vol. 76(1), pp. 137-43.
20. Capone, S., Epifani, M., Francioso, L., Presicce, D.S., Siciliano, P., and Carlucci, P. (2006), "A novel method based on gas microsensors to analyze diesel engine lubricant contaminated by diluent unburned diesel fuel", Proceedings of IEEE Sensors Conference, EXCO, Daegu, Korea, Oct. 22-25, pp. 1377-9.
21. Capone, S., Zuppa, M., Montagna, G., Siciliano, P., Distante, C., Caione, F. and Carlucci, A.P. (2008a), "Application of a gas sensors array to the detection of fuel as contamination defect in engine lubricant", Proceedings of IEEE Sensors Conference, Lecce, Italy, Oct. 26-29, pp. 442-5.
22. Capone, S., Zuppa, M., Presicce, D.S., Francioso, L., Casino, F., and Siciliano, P. (2008b), "Metal oxide gas sensor array for the detection of diesel fuel in engine lubricant", Sensors and Actuators B, Vol. 131, 125-33.
23. Continental Automotive Systems, (2003), "QLT lubricant status sensors: helping protect the environment", available at: http://www.conti-online.com/generator/www/com/en/continental/portal/themes/press_services/press_releases/fairs_events/iaa/pr_2003_09_09_sensorik_en.html (accessed 17 May 2009).
24. Continental Automotive Systems, (2006a), "Lubricant quality sensor protects motorcycle engines against wear and makes lubricant level checks unnecessary", available at: http://www.contionline.com/generator/www/com/en/continental/portal/themes/press_services/press_releases/products/automotive_systems/gt_pr_2006_11_16_motorcycle_qlt_en.html (accessed 17 May 2009).

25. Continental Automotive Systems, (2006b), "QDIS lubricant diagnostic system reduces running costs and lengthens the vehicle's service life", available at: http://www.conti-online.com/generator/www/de/en/cas/cas/themes/press_service/hidden/press_releases/products/sensor_systems/lubricant_condition_sensors/pr_2006_09_19_iaa_cv_qdis/pr_2006_09_19_iaa_cv_qdis_en.html (accessed 17 May 2009).
26. Cootes T F, Taylor C J, Cooper D H, and Graham J 1995 Active Shape Models, Training and Application, *Computer vision and image understanding*, **61** (1) 38-59
27. Dahmani, R., and Gupta, N. (2002), "Spectroscopic analysis of automotive engine lubricant", *Proceedings of SPIE*, Vol. 4574, pp. 179-183.
28. Dephi www.delphi.com | 0027 | **1**
29. Dickert, F.L., Forth, P., Lieberzeit, P.A., and Voigt, G. (2000), "Quality control of automotive engine lubricants with mass-sensitive chemical sensors - QCMs and molecularly imprinted polymers", *Fresenius J. Anal. Chem.*, Vol. 366, pp. 802-6.
30. Dickert, F.L., Greibl, W., Rohrer, A. and Voigt, G. (2001), "Sol-Gel-Coated Quartz Crystal Microbalances for Monitoring Automotive Lubricant Degradation", *Advanced Materials*, Vol. 13 No. 17, pp. 1327-30.
31. Dillon, P. P.; Daly, S. J.; Manning, B. M.; O'Kennedy, R. (2003), "Immunoassay for the determination of morphine-3-glucuronide using a surface plasmon resonance-based biosensor", *Biosens. Bioelectron.*, Vol. 18, pp. 217-27.
32. Dobrinski, H., Buhrdorf, A., Lindemann, M., Lüdtkke, O. (2008), "Combi-sensor for Lubricant Level and Lubricant Quality Management", SAE 2008 World Congress & Exhibition, April 2008, Detroit, MI, USA Proceedings, SAE paper 2008-01-0906, 14 p.
33. Dobrinski, H., Buhrdorf, A., Lüdtkke, O., and Knipper, U. (2007), "Multiparameter Lubricant Condition Sensor Based on the Tuning Fork Principle", *Proceedings of 2007 SAE World Congress*, Detroit, Michigan, USA, April 16-19, SAE paper 2007-01-0392, 10 p.
34. Dryden I L and Mardia K V 1998 *Statistical Shape Analysis* (John Wiley)
35. Duchowski, J.K., and Ringholm, E.C. (2006), "A novel approach to predictive maintenance - a portable, multi-component MEMS sensor for on-line monitoring of fluid condition in hydraulic and lubricating system", *Proceedings of STLE Annual Meeting*, Calgary, Alberta, Canada, May 7-11, Preprint No. AM(NP)-06-12, 12 p.
36. Dupont, D., Muller-Renaud, S. (2006), "Quantification of proteins in dairy products using an optical biosensor", *J. AOAC Int.*, Vol. 89, pp. 843.
37. Durdag, K. (2007), "A solid state of affairs", *Gear Solutions*, No. 10 (October), pp. 32-43.
38. Durdag, K. (2008), "Solid state acoustic wave sensors for real-time in-line measurement of lubricant viscosity", *Sensor Review*, Vol. 28, No. 1, pp. 68-73.

39. Fleming, W.J. (2006), "Automotive electronics", IEEE Vehicular Technology Magazine, September 2006, pp. 49-52.
40. Fleming, W.J. (2008), "New Automotive Sensors — A review", IEEE Sensors Journal, Vol. 8 No. 11, pp. 1900-21.
41. Foster, N.S., Amonette, J.E., Autrey, T., and Ho, J.T. (2001), "Detection of trace levels of water in lubricant by photoacoustic spectroscopy", *Sensors and Actuators B*, Vol. 77, pp. 620-4.
42. Gillis, E. H., Gosling, J. P., Sreenan, J. M., Kane, M. (2002), "Development and validation of a biosensor-based immunoassay for progesterone in bovine milk", *J. Immunol. Methods*, Vol. 267(2), pp. 131-8.
43. Gillis, E. H., Traynor, I., Gosling, J. P., Kane, M. (2006), "Improvements to a surface plasmon resonance-based immunoassay for the steroid hormone progesterone", *J. AOAC Int.*, Vol. 89(3), pp. 838-42.
44. Gobi, K., Tanaka, H., Shoyama, Y., Miura, N. (2004), "Continuous flow immunosensor for highly selective and real-time detection of sub-ppb levels of 2-hydroxybiphenyl by using surface plasmon resonance imaging", *Biosens Bioelectron*, Vol. 20, pp. 350.
45. Goodman J W 2000 *Statistical Optics* (New York: John Wiley and sons)
46. Gotch, R. (2001) "End of black art", *Automotive Engineer*, No. 3 (March), pp. 78-9.
47. Haughey, S. A., Baxter, C. A. (2006), "Biosensor screening for veterinary drug residues in foodstuffs", *J. AOAC Int.*, Vol. 89(3), pp. 862-7.
48. Healy, D. A., Hayes, C. J., Leonard, P., McKenna, L., O'Kennedy, R. (2007), "Biosensor developments: application to prostate-specific antigen detection", *Trends Biotechnol*, Vol. 25(3), pp. 125-31.
49. Hella Technical Information Electronics, oil sensor available at: http://www.hella.com/hella-com-en/assets/media_global/TI_Oelsensorik_GB_TT_05.pdf
50. Homola, J. (2006), *Surface Plasmon Resonance Based Sensors*, Springer Berlin Heidelberg, New York, NY, USA.
51. Homola, J., Yee, S. S. and Gauglitz, G. (1999), "Surface plasmon resonance sensors: review", *Sensors and Actuators B*, Vol. 54, pp. 3-15.
52. Ishimaru A 1999 *Wave propagation and scattering in random media* (Wiley-IEEE Press)
53. Jakoby, B. and Vellekoop, M.J. (2004), "Physical sensors for water-in-lubricant emulsions", *Sensors and Actuators A*, Vol. 110, pp. 28-32.
54. Jakoby, B., Eisenschmid, H., and Herrmann, F. (2002), "The Potential of Microacoustic SAW and BAW-Based Sensors for Automotive Applications — A Review", *IEEE Sensors Journal*, Vol. 2, No. 5, pp. 443-52.

55. Jakoby, B., Eisenschmid, H., and Schatz, O. (2001), "On-board evaluation of engine lubricant using physical sensors", VDI-Berichte, Vol. 1646, pp. 699-707.
56. Jakoby, B., Scherer, M., Buskies, M., and Eisenschmid, H. (2002), "Microacoustic viscosity sensor for automotive applications", Proceedings of IEEE Sensors Conference, Orlando, Florida, USA, Vol. 2, pp. 1587-90.
57. Jakoby, B., Scherer, M., Buskies, M., and Eisenschmid, H. (2003), "An automotive engine lubricant viscosity sensor", IEEE Sensors Journal, Vol. 3 No. 5, pp. 562-8.
58. Kasberger, J. and Jakoby, B. (2007), "Design of a Novel Fully Integrated IR - Absorption Sensor System", Proceedings of IEEE Sensors Conference, Atlanta, Georgia, USA, pp. 515-8.
59. Kasberger, J., Saeed, A., Hilber, W., Hingerl, K., and Jakoby, B. (2008), "Towards an integrated IR-absorption microsensor for the online monitoring of fluids", Elektronik & Informationstechnik, Vol. 125 No. 3, pp. 65-70.
60. Kim, T. J., Cho, H. S., Park, N. Y., Lee, J. I. (2006), "Serodiagnostic comparison between two methods, ELISA and surface plasmon resonance for the detection of antibody titres of Mycoplasma hyopneumoniae", J. Vet. Med. Ser. B: Infect. Dis. Vet. Public Health, Vol. 53(2), pp. 87-90.
61. Kim, W.-T., Choi, M.-Y., and Park, H.- W. (2004), "Development of the Automobile Engine Lubricant Sensor by Measuring the Dielectric Constant of Lubricant", Proceedings of 16th WCNDT 2004 - World Conference on Nondestructive Testing, Aug 30 - Sep 3, 2004 - Montreal, Canada, paper #771, 6 p.
62. Kolomenskii, A.A., Gershon, P.D. and Schuessler, H.A. (2000), "Surface-plasmon resonance spectrometry and characterization of absorbing liquids", *Applied Optics*, Vol. 39, No. 19, pp. 3314-3320.
63. Kretschmann, E. (1971), "Die Bestimmung Optischer Konstanten von Metallen durch Anregung von Oberflaechenplasmaschwingungen", *Zeitschrift für Physik A Hadrons and Nuclei*, Vol. 241, pp. 313–324.
64. Kudlaty, K., Purde, A., and Koch, A.W. (2003), "Development of an infrared sensor for on-line analysis of lubricant deterioration", Proceedings of IEEE Sensors Conference, Toronto, Ontario, Canada, October 22-24, pp. 903-8.
65. Kumar, S. and Mukherjee, P.S. (2005), "Online condition monitoring of engine lubricant," *Industrial Lubrication and Tribology*, 57(6), pp. 260–267.
66. Ladd, J., Boozer, C., Yu, Q., Chen, S., Homola, J., Jiang (2004), "DNA-directed protein immobilization on mixed self-assembled monolayers via a streptavidin bridge", *S. Langmuir*, Vol. 20(19), pp. 8090-5.
67. Lee, H.-S., Wang, S.S., Smolenski, D.J., Viola, M.B., and Klusendorf, E.E. (1994), "In situ monitoring of high-temperature degraded engine lubricant condition with microsensors", *Sensor and Actuators B*, Vol. 20, pp. 49-54.
68. Li, J. (2005), "Development of microfabricated sensor array for lubricant evaluation", PhD Dissertation, Department of Chemical Engineering, Case Western Reserve University, 159 p.

69. Lieberzeit, P.A. Glanznig, G., Leidl, A., Voigt, G., and Dickert, F.L. (2006), "Nanostructured Polymers for Detecting Chemical Changes During Engine Lubricant Degradation", *IEEE Sensors Journal*, Vol. 6 No. 3, pp. 529-35.
70. Lieberzeit, P.A., Afzal, A., Glanzing, G. and Dickert, F.L. (2007c), "Molecularly imprinted sol-gel nanoparticles for mass-sensitive engine lubricant degradation sensing", *Anal. Bioanal. Chem.*, Vol. 389, pp. 441-6.
71. Lieberzeit, P.A., Afzal, A., Rehman, A., and Dickert, F.L. (2007a), "Nanoparticles for detecting pollutants and degradation processes with mass-sensitive sensors", *Sensors and Actuators B*, Vol. 127, pp. 132-136.
72. Lubricant Condition and Lubricant Level Sensor SGM110, Product information, Robert Bosch GmbH, 2004, 2 p.
73. Lvovich, V. F. and Smiechowski, M.F. (2006), "Impedance characterization of industrial lubricants", *Electrochimica Acta*, Vol. 51, pp. 1487-96.
74. Lvovich, V. F., Liu, C.C. and Smiechowski, M.F. (2006), "Optimization and fabrication of planar interdigitated impedance sensors for highly resistive non-aqueous industrial fluids," *Sensors and Actuators B*, 119, pp. 490-6.
75. Manz, D. and Cheng, W.K. (2007), "On-Line Measurements of Engine Lubricant Aeration by X-Ray Absorption", *ASME J. of Engineering for Gas Turbines & Power*, Vol. 129, pp. 287-93.
76. Marek, J., Trah, H.-P., Suzuki, Y., and Yokomori, I. (Ed's) (2003), *Sensors for Automotive Applications*, Wiley-VCH GmbH & Co. KGaA, Weinheim.
77. Martin, S.J., Frye, G.C., and Wessendorf, K.O. (1994), "Sensing liquid properties with thickness-shear mode resonators," *Sensors and Actuators A*, vol. 44, pp. 209-18.
78. Michael, P.W., Wanke, T.S., and McCambridge, M.A. (2007), "Additive and Base Lubricant Effects in Automatic Particle Counters", *Journal of ASTM International*, Vol. 4 No. 4, Paper ID JAI100941, 7 p.
79. Minunni, M., Mascini (1993), "Detection of Pesticide in Drinking Water Using Real-Time Biospecific Interaction Analysis (BIA)", *M. Anal. Lett.* , Vol. 26, pp. 1441-59.
80. Mohammed, I., Mullett, W. M., Lai, E. P. C., Yeung, J. M. (2001), "Is biosensor a viable method for food allergen detection?" *Anal. Chim. Acta*, Vol. 444, pp. 97-102.
81. Moon, S.-I., Paek, K.-K., Lee, Y.-H., Kim, J.-K., Kim, S.-W., and Ju, B.-K. (2006), "Multiwall carbon nanotube sensor for monitoring engine lubricant degradation", *Electrochemical and Solid-State Letters*, Vol. 9 No. 8, pp. H78-H80.
82. Na, D., Kim, S., and Park, S. (2002), "Capacitive microsensor for monitoring the deterioration of automobile engine lubricant", *Proceedings of SPIE*, Vol. 4936, pp. 387-93.

83. Nedelkov, D., Nelson, R. W. (2003), "Detection of Staphylococcal Enterotoxin B via Biomolecular Interaction Analysis Mass Spectrometry", *Appl. Environ. Microbiol.*, Vol. 69, pp. 5212.
84. Nedelkov, D., Rasooly, A., Nelson, R. W. (2000), "Multitoxin biosensor-mass spectrometry analysis: a new approach for rapid, real-time, sensitive analysis of staphylococcal toxins in food", *Int. J. Food Microbiol.*, Vol. 60(1), pp. 1-13.
85. Ock, K., Jang, G., Roh, Y., Kim, S., Kim, J., Koh, K. (2001), "Optical detection of Cu²⁺ ion using a SQ-dye containing polymeric thin-film on Au surface", *Microchem. J.*, Vol. 70(3), pp. 301-5.
86. Physical and Chemical Properties of Engine Lubricants, SAE Information Report SAE J357, 13 p.
87. Podeszwa, T., Jaroszewicz, L.R., and Cyran, K. (2003), "Fiberscope based engine condition monitoring system", *Proceedings of SPIE*, Vol. 5124, pp. 299-303.
88. Prosser, S. (2007), "Automotive sensors: past, present and future", *Journal of Physics: Conference series*, Vol. 76, paper # 012001, 6 p.
89. Raadnui, S. and Kleesuwat, S. (2005), "Low-cost condition monitoring sensor for used lubricant analysis", *Wear*, Vol. 259, pp. 1502-6.
90. Raether, H. (1988), *Surface Plasmons on Smooth and Rough Surfaces and on Gratings*, Vol. 111 of Springer Tracts in Modern Physics, Springer, Heidelberg, Germany.
91. Ramo, S., St.Clair, R. K. (1998), "The Systems Approach Fresh Solution to Complex Problems Through Combining Science and Practical Sense", available @: www.incose.org/productspubs/doc/systemsapproach.pdf
92. Rojo, N.; Ercilla, G.; Haro, I. (2003), "GB virus C (GBV-C) / hepatitis G virus (HGV): towards the design of synthetic peptides-based biosensors for immunodiagnosis of GBV-C/HGV infection", *Curr. Protein Pept. Sci.*, 4(4), 291-8.
93. Rytov S M, Kravtsov Yu A, and Tatarskii V I 1998 Principles of Statistical Radiophysics (Berlin: Springer-Verlag) Vols. 1-4
94. Saloka, G.S. and Meitzler, A.H. (1991), "A capacitive lubricant deterioration sensor", *Proceedings of SAE International Congress, Detroit, Michigan, USA, Feb. 25 – March 1, SAE paper 910497*, pp. 137-46.
95. Samsonova, J. V., Uskova, N. A., Andresyuk, A. N., Franek, M., Elliott, C. T. (2004), "Biacore biosensor immunoassay for 4-nonylphenols: assay optimization and applicability for shellfish analysis", *Chemosphere*, Vol. 57, pp. 975.
96. Schasfoort, R.B.M. and Tudos, A.J. (2008), *Handbook of Surface Plasmon Resonance*, RSCPublishing, Cambridge, UK.
97. Scherer, M., Arndt, M., Bertrand, P., and Jakoby, B. (2004), "Fluid condition monitoring sensors for diesel engine control", *Proceedings of IEEE Sensors Conference, Vienna, Austria, Oct. 24-27*, pp. 459-62.

98. Scott, A. J., Mabesa, J. R. Jr., Gorsich, D., Rathgeb, B., Said, A.A., Dugan, M., Haddock, T.F., and Bado, Ph. (2004), "Optical microsystem for analyzing engine lubricants", *Proceedings of SPIE*, Vol. 5590, pp. 122-7.
99. Sepcic, K., Josowicz, M., Janata, J., and Selby, T., (2004), "Diagnosis of used engine lubricant based on gas phase analysis", *Analyst*, Vol. 129, pp. 1070-5.
100. Shimomura, M., Nomura, Y., Zhang, W., Sakino, M., Lee, K. H., Ikebukuro, K., Karube, I. (2001), "Simple and rapid detection method using surface plasmon resonance for dioxins, polychlorinated biphenyls and atrazine", *Anal. Chim. Acta*, Vol. 434, pp. 223-30.
101. Slavík, R., Homola, J. and Brynda, E. (2002), "A miniature fiber optic surface plasmon resonance sensor for fast detection of staphylococcal enterotoxin B", *Biosensors and Bioelectronics*, Vol. 17 No. 6-7, pp. 591-5.
102. Smiechowski, M. F. and Lvovich, V. F (2002), "Electrochemical monitoring of water-surfactant interactions in industrial lubricant", *Journal of Electroanalytical Chemistry*, Vol. 534, pp. 171-80.
103. Smiechowski, M.F. and Lvovich, V.F. (2003), "Iridium oxide sensors for acidity and basicity detection in industrial lubricants", *Sensors and Actuators B*, Vol. 96, pp. 261-7.
104. Smolenski, D.J. and Schwartz, S.E. (1994), "Automotive engine-lubricant condition monitoring", *CRC Handbook of Lubrication and Tribology*, pp. 17-32.
105. Soh, N., Tokuda, T., Watanabe, T., Mishima, K., Imato, T., Masadome, T., Asano, Y., Okutani, S., Niwa, O., Brown, S. (2003), "A surface plasmon resonance immunosensor for detecting a dioxin precursor using a gold binding polypeptide", *Talanta*, Vol. 60(4), pp. 733-45.
106. Soh, N., Watanabe, T., Asano, Y., Imato, T. (2003), "Indirect Competitive Immunoassay for Bisphenol A, Based on a Surface Plasmon Resonance Sensor", *Sensor Mater.*, Vol. 15(8), pp. 423-38.
107. Tou, J.T. and Gonzalez, R.C. (1974), *Pattern Recognition Principles*, Addison-Wesley, Reading, MA.
108. Troyer, D. and Fitch, J. (2001), *Oil analysis basic*, Nora Corporation, Tulsa, Oklahoma, USA
109. Turner, J.D., and Austin, L. (2003), "Electrical techniques for monitoring the condition of lubrication lubricant", *Measurement Science and Technology*, Vol. 14, pp. 1794-800.
110. Ulrich, C., Petersson, H., Sungren, H., Bjorefors, F., and Krantz-Rulcker, C. (2007), "Simultaneous estimation of soot and diesel contamination in engine lubricant using electrochemical impedance spectroscopy", *Sensors and Actuators B*, Vol. 127, pp. 613-8.
111. Vaisocherova, H., Mrkvova, K., Piliarik, M., Jinoch, P., Steinbachova, M., Homola (2007), "Surface plasmon resonance biosensor for direct detection of

- antibody against Epstein-Barr virus”, *J. Biosens. Bioelectron*, Vol. 22(19), pp. 1020-5.
112. Wang, S. and Lee, H.-S. (1994), “The development of in situ electrochemical lubricant-condition sensors”, *Sensors and Actuators B*, Vol. 17, pp. 179-85.
 113. Wang, S. and Lee, H.-S. (1997a), “The application of a.c. impedance technique for detecting glycol contamination in engine lubricant”, *Sensors and Actuators B*, 40, pp. 193-197.
 114. Wang, S. and Lee, H.-S. (1997b), “An electrochemical sensor for distinguishing two-stroke-engine lubricants”, *Sensors and Actuators B*, Vol. 40, pp. 199-203.
 115. Wang, S. (2001), “Road test of lubricant condition sensor and sensing technique”, *Sensors and Actuators B*, 73, pp. 106-111.
 116. Wang, S.S. (2001a), “A physical model for the engine lubricant condition sensor”, *Tribology Transactions*, Vol. 44 No. 3, pp. 411-6.
 117. Wang, S.S. (2002), “Engine lubricant condition sensor: method for establishing correlation with total acid number”, *Sensors and Actuators B*, Vol. 86, pp. 122-6.
 118. Wang, S.S. and Lin, Y. (2003), “A new technique for detecting antifreeze in engine lubricant during early stage of leakage”, *Sensors and Actuators B*, Vol. 96, pp. 157-64.
 119. Wei, J., Mu, Y., Song, D., Fang, X., Liu, X., Bu, L., Zhang, H., Zhang, G., Ding, J., Wang, W., Jin, Q., Luo (2003), “A novel sandwich immunosensing method for measuring cardiac troponin I in sera”, *G. Anal. Biochem.*, Vol. 321(2), pp. 209-16.
 120. Yonghui, Y., Weihua, W., Xinpin, Y., Hanliang X., and Chengtao, W. (2003), "An Integrated On-line lubricant Analysis Method for Condition Monitoring", *Measurement Science and Technology*, Vol. 14, pp. 1973-7.
 121. Young I T, Gerbrands J J, and Van Vliet L J 1998 *Fundamentals of image processing* (The Netherlands: The Delft University of Technology)
 122. Zhang, C., George, H., Soukup, B., Kornbrekke, R., Boyle, F.P., and Goolive, S.A. (2004), “Chemical sensor development for measuring soot caused lubricant thickening”, *Proceedings of IEEE International Ultrasonics, Ferroelectrics, and Frequency Control Conference*, Montréal, Quebec, Canada, Aug. 24-27, pp. 200-205.

Appendices

Appendix A: RGB gray scale MATLAB programming

```
clc;
clear all;
I = imread('5G-9.bmp');
J = rgb2gray(I);
figure, imshow(I), figure, imshow(J);
imtool(J)

x=[1 640];
y1=[110 110];
y2=[265 265];
y3=[420 420];

improfile(J,x,y1,640);
hold on;
improfile(J,x,y2,640);
hold on;
improfile(J,x,y3,640);
hold on;
[cx, cy1, cz1]=improfile(J,x,y1,640);
[cx, cy2, cz2]=improfile(J,x,y2,640);
[cx, cy3, cz3]=improfile(J,x,y3,640);

A=[ cz1 cz2 cz3];
B=[(cz1+cz2+cz3)/3];
C=B/255
```

Appendix B: Statistical optics analysis MATLAB programming

```
function coolant2()
%
% comparative analysis of optical data from fresh and contaminated
automotive oils
%
%reading of data file
file_name = 'C 0-10.dat';
fid = fopen(file_name, 'r' );
dX = 1.5; % pixel resolution, um
% spectral parameters
SpF_um = 1/dX; % sampling frequency, 1/um
SpF_um_Nyquist = SpF_um/2; % Nyquist frequency, 1/um
SpF_mm_Nyquist = 1000*SpF_um_Nyquist; % Nyquist frequency, 1/mm
clc
disp( '===== ' );
disp( file_name );
% number of columns
N_columns = fscanf( fid, '%i', 1 );
% number of rows
N_rows = fscanf( fid, '%f', 1 );
% data
for i = 1:N_rows
    z(i,:) = fscanf( fid, '%f\t', [1,N_columns] );
end
fclose( fid );
Z1 = z(:,1);
Z2 = z(:,2);
Z3 = z(:,3);
Z4 = z(:,4);
Z5 = z(:,5);
Z6 = z(:,6);
Z7 = z(:,7);
Z8 = z(:,8);
Z9 = z(:,9);
Z10 = z(:,10);
Z11 = z(:,11);
clear z
clf reset
figure( 1 )
plot( dX*(1:N_rows), [Z1 Z2 Z3 Z4 Z5 Z6 Z7 Z8 Z9 Z10 Z11] );
title( 'Cross-sections of optical images - fresh engine lubricant &
coolant1%-10%' );
xlabel( 'position, um' );
ylabel( 'normalized color (dimensionless)' );
grid on
axis( [0 dX*640 0 1] ); axis on
```

```

legend('C-0%', 'C-1%', 'C-2%', 'C-3%', 'C-4%', 'C-5%', 'C-6%', 'C-7%', 'C-
8%', 'C-9%', 'C-10%')
% remove linear trend (mean value)
A1 = detrend( Z1 );
A2 = detrend( Z2 );
A3 = detrend( Z3 );
A4 = detrend( Z4 );
A5 = detrend( Z5 );
A6 = detrend( Z6 );
A7 = detrend( Z7 );
A8 = detrend( Z8 );
A9 = detrend( Z9 );
A10 = detrend( Z10 );
A11 = detrend( Z11 );
% Cfresh autocorrelation function
CA1 = xcorr( A1, 'biased' );
BA1 = CA1( 640:1279);
RA1 = BA1/BA1(1:1);
clear CA1
CA2 = xcorr( A2, 'biased' );
BA2 = CA2( 640:1279);
RA2 = BA2/BA2(1:1); ;
clear CA2
CA3 = xcorr( A3, 'biased' );
BA3 = CA3( 640:1279);
RA3 = BA3/BA3(1:1);
clear CA3
CA4 = xcorr( A4, 'biased' );
BA4 = CA4( 640:1279);
RA4 = BA4/BA4(1:1);
clear CA4
CA5 = xcorr( A5, 'biased' );
BA5 = CA5( 640:1279);
RA5 = BA5/BA5(1:1);
clear CA5
CA6 = xcorr( A6, 'biased' );
BA6 = CA6( 640:1279);
RA6 = BA6/BA6(1:1);
clear CA6
CA7 = xcorr( A7, 'biased' );
BA7 = CA7( 640:1279);
RA7 = BA7/BA7(1:1);
clear CA7
CA8 = xcorr( A8, 'biased' );
BA8 = CA8( 640:1279);
RA8 = BA8/BA8(1:1);
clear CA8
CA9 = xcorr( A9, 'biased' );
BA9 = CA9( 640:1279);
RA9 = BA9/BA9(1:1);
clear CA9
CA10 = xcorr( A10, 'biased' );
BA10 = CA10( 640:1279);
RA10 = BA10/BA10(1:1);
clear CA10
CA11 = xcorr( A11, 'biased' );

```

```

BA11 = CA11( 640:1279);
RA11 = BA11/BA11(1:1);
clear CA11
NFFT = 2^( nextpow2( N_rows ) ); % length of FFT data
% FRESH auto-spectrum density
%Pxx = abs(fft(x,nfft)).^2/length(x)/Fs;
[PA1, w] = cpsd( Z1, Z1, [], [], NFFT, SpF_um );
[PA2, w] = cpsd( Z2, Z2, [], [], NFFT, SpF_um );
[PA3, w] = cpsd( Z3, Z3, [], [], NFFT, SpF_um );
[PA4, w] = cpsd( Z4, Z4, [], [], NFFT, SpF_um );
[PA5, w] = cpsd( Z5, Z5, [], [], NFFT, SpF_um );
[PA6, w] = cpsd( Z6, Z6, [], [], NFFT, SpF_um );
[PA7, w] = cpsd( Z7, Z7, [], [], NFFT, SpF_um );
[PA8, w] = cpsd( Z8, Z8, [], [], NFFT, SpF_um );
[PA9, w] = cpsd( Z9, Z9, [], [], NFFT, SpF_um );
[PA10, w] = cpsd( Z10, Z10, [], [], NFFT, SpF_um );
[PA11, w] = cpsd( Z11, Z11, [], [], NFFT, SpF_um );
% cross-spectrum density
[Pxy1, w] = cpsd(Z1,Z2,[],[], NFFT, SpF_um);
[Pxy2, w] = cpsd(Z1,Z3,[],[], NFFT, SpF_um);
[Pxy3, w] = cpsd(Z1,Z4,[],[], NFFT, SpF_um);
[Pxy4, w] = cpsd(Z1,Z5,[],[], NFFT, SpF_um);
[Pxy5, w] = cpsd(Z1,Z6,[],[], NFFT, SpF_um);
[Pxy6, w] = cpsd(Z1,Z7,[],[], NFFT, SpF_um);
[Pxy7, w] = cpsd(Z1,Z8,[],[], NFFT, SpF_um);
[Pxy8, w] = cpsd(Z1,Z9,[],[], NFFT, SpF_um);
[Pxy9, w] = cpsd(Z1,Z10,[],[], NFFT, SpF_um);
[Pxy10,w] = cpsd(Z1,Z11,[],[], NFFT, SpF_um);
% transfer function

W1 = Pxy1 ./ PA1;
W2 = Pxy2 ./ PA1;
W3 = Pxy3 ./ PA1;
W4 = Pxy4 ./ PA1;
W5 = Pxy5 ./ PA1;
W6 = Pxy6 ./ PA1;
W7 = Pxy7 ./ PA1;
W8 = Pxy8 ./ PA1;
W9 = Pxy9 ./ PA1;
W10 = Pxy10 ./ PA1;
W1abs = abs( W1 );
W2abs = abs( W2 );
W3abs = abs( W3 );
W4abs = abs( W4 );
W5abs = abs( W5 );
W6abs = abs( W6 );
W7abs = abs( W7 );
W8abs = abs( W8 );
W9abs = abs( W9 );
W10abs = abs( W10 );

figure( 2 )
% Rfresh and Rused autocorrelation function
subplot( 2,2,1 )
% plot( dX*(1:N_rows), [RA1 RA6 RA11] );
plot( dX*(1:N_rows), [RA1 RA2 RA3 RA4 RA5 RA6 RA7 RA8 RA9 RA10 RA11] );

```



```

title( 'Normilized autocorrelation functions' );
xlabel( 'lag, um' );
ylabel( 'amplitude (n.u.^2)' );
axis( [0 dX*640 2.0*min( RA1 ) 1.05*max( RA11)] ); axis on
grid on
% legend('0%Coolant','5%Coolant','10%Coolant')
legend('C-0%', 'C-1%', 'C-2%', 'C-3%', 'C-4%', 'C-5%', 'C-6%', 'C-7%', 'C-
8%', 'C-9%', 'C-10%')
% Pfresh and Pused auto-spectrum densities
subplot( 2,2,2 )
plot( w, [PA1 PA2 PA3 PA4 PA5 PA6 PA7 PA8 PA9 PA10 PA11] );
title( 'Auto-spectrum densities' );
xlabel( 'frequency, 1/um' );
ylabel( 'amplitude,n.u.^2*um' );
axis( [0 0.02 -1 1.35*max( (PA11) )] ); axis on
grid on
legend('C-0%', 'C-1%', 'C-2%', 'C-3%', 'C-4%', 'C-5%', 'C-6%', 'C-7%', 'C-
8%', 'C-9%', 'C-10%')
%module of transfer function
subplot( 2,2,3 )
plot( w, [W1abs W2abs W3abs W4abs W5abs W6abs W7abs W8abs W9abs W10abs]
);
title( 'Module of transfer function' );
xlabel( 'frequency, 1/um' );
ylabel( 'magnititude, dimensionless' );
axis( [0 0.025 0.0 0.95*max( W4abs)] ); axis on
grid on
legend('C0%-1%', 'C0%-2%', 'C0%-3%', 'C0%-4%', 'C0%-5%', 'C0%-6%', 'C0%-
7%', 'C0%-8%', 'C0%-9%', 'C0%-10%')

```

Appendix C: Object shape based optical analysis MATLAB programming

```

function analysis_TaurusShape()
%
% N is a column to analyze

% read data file
fid_dat = fopen( 'comboshape.dat', 'r' );
if( fid_dat == -1 )
    S = sprintf( 'Can not find combo.dat file!' ) ;
    disp( S );
end

%clc
disp(
'*****
*****' );
disp( 'Reading "combo.dat" file!' );
disp( '===== ' );
% number of collums
N_col = fscanf( fid_dat, '%i', 1 );
% number of rows
N_row = fscanf( fid_dat, '%i', 1 );
% sampling interval, um
dX = fscanf( fid_dat, '%f', 1 );
S = sprintf( '          Sampling interval, um: %4.2f', dX ); disp( S );
% Nyquist frequency
SpF_um = 1/dX;          % sampling frequency, 1/um
SpF_um_Nyquist = SpF_um/2;      % Nyquist frequency, 1/um
S = sprintf( '          Nyquist frequency, 1/um: %4.2f', SpF_um_Nyquist
); disp( S );
disp( '===== ' );

% data
H = zeros( N_row, N_col, 'double' );
for i = 1:N_row
    H(i,:) = fscanf( fid_dat, '%f\t', [1,N_col] );
end
fclose( fid_dat );

% read only required collumn
I = H(:,108);
clear H

% =====
figure( 1 )

clf( 'reset' )
% =====
hold on
plot( (0:(N_row-1)), I, 'color', 'blue', 'LineWidth', 1 );
title( 'object cross-section' );
xlabel( 'number' );

```

```

ylabel( 'intencity, dimensionless' );
axis( [0 (N_row-1) 0 1] ); axis on
grid on
hold off

% cut off first data
switch 108
    case 108
        N_cut_off = 21;

        otherwise
            N_cut_off = 55;
end
I = I( (N_cut_off+1):N_row );
N_row = N_row - N_cut_off;

% separate into 4 objects
switch 108
    case 108
        dT = 150;

        otherwise
            dT = 0;
end
N1 = dT;
N2 = dT;
N3 = dT;
N4 = N_row - 3*dT;
I1 = I( 1:dT );
I2 = I( (dT+1):2*dT );
I3 = I( (2*dT+1):3*dT );
I4 = I( (3*dT+1):N_row );

% calculate A1 for each I1-I4
N_A1 = 21;
A1_I1 = mean( I1(1:N_A1) );
A1_I2 = mean( I2(1:N_A1) );
A1_I3 = mean( I3(1:N_A1) );
A1_I4 = mean( I4(1:N_A1) );

% calculate B1_left for each I1-I4
N_B1 = 0.9;
B1_I1_left = 0;
for i=2:N1
    if (I1(i-1) >= N_B1*A1_I1) && (I1(i) < N_B1*A1_I1)
        B1_I1_left = dX*(i-1);
        break;
    end
end
B1_I2_left = 0;
for i=2:N2
    if (I2(i-1) >= N_B1*A1_I2) && (I2(i) < N_B1*A1_I2)
        B1_I2_left = dX*(i-1);
        break;
    end
end

```

```

end
B1_I3_left= 0;
for i=2:N3
    if (I3(i-1) >= N_B1*A1_I3) && (I3(i) < N_B1*A1_I3)
        B1_I3_left= dX*(i-1);
        break;
    end
end
B1_I4_left = 0;
for i=2:N4
    if (I4(i-1) >= N_B1*A1_I4) && (I4(i) < N_B1*A1_I4)
        B1_I4_left = dX*(i-1);
        break;
    end
end

% calculate B1_right for each I1-I4
B1_I1_right = 0;
for i=(dT/2):N1
    if (I1(i-1) < N_B1*A1_I1) && (I1(i) >= N_B1*A1_I1)
        B1_I1_right = dX*i;
        break;
    end
end
B1_I2_right = 0;
for i=(dT/2):N2
    if (I2(i-1) < N_B1*A1_I2) && (I2(i) >= N_B1*A1_I2)
        B1_I2_right = dX*i;
        break;
    end
end
B1_I3_right = 0;
for i=(dT/2):N3
    if (I3(i-1) < N_B1*A1_I3) && (I3(i) >= N_B1*A1_I3)
        B1_I3_right = dX*i;
        break;
    end
end
B1_I4_right = 0;
for i=(dT/2):N4
    if (I4(i-1) < N_B1*A1_I4) && (I4(i) >= N_B1*A1_I4)
        B1_I4_right = dX*i;
        break;
    end
end

% calculate B1 for each I1-I4
B1_I1 = B1_I1_right - B1_I1_left;
B1_I2 = B1_I2_right - B1_I2_left;
B1_I3 = B1_I3_right - B1_I3_left;
B1_I4 = B1_I4_right - B1_I4_left;

dT1 = round( (B1_I1_left + B1_I1/2)/dX );
dT2 = round( (B1_I2_left + B1_I2/2)/dX );
dT3 = round( (B1_I3_left + B1_I3/2)/dX );
dT4 = round( (B1_I4_left + B1_I4/2)/dX );

```

```

% calculate A2 for each I1-I4
N_A2 = 7;
A2_I1 = mean( I1( (dT1-N_A2):(dT1+N_A2)) );
A2_I2 = mean( I2( (dT2-N_A2):(dT2+N_A2)) );
A2_I3 = mean( I3( (dT3-N_A2):(dT3+N_A2)) );
A2_I4 = mean( I4( (dT4-N_A2):(dT4+N_A2)) );

% calculate dA for each I1-I4
dA_I1 = 100*(A1_I1 - A2_I1)/A1_I1;
dA_I2 = 100*(A1_I2 - A2_I2)/A1_I2;
dA_I3 = 100*(A1_I3 - A2_I3)/A1_I3;
dA_I4 = 100*(A1_I4 - A2_I4)/A1_I4;

% calculate B2_left for each I1-I4
N_B2 = 1.1;
B2_I1_left = 0;
for i=2:N1
    if (I1(i-1) >= N_B2*A2_I1) && (I1(i) < N_B2*A2_I1)
        B2_I1_left = dX*(i-1);
        break;
    end
end
B2_I2_left = 0;
for i=2:N2
    if (I2(i-1) >= N_B2*A2_I2) && (I2(i) < N_B2*A2_I2)
        B2_I2_left = dX*(i-1);
        break;
    end
end
B2_I3_left= 0;
for i=2:N3
    if (I3(i-1) >= N_B2*A2_I3) && (I3(i) < N_B2*A2_I3)
        B2_I3_left= dX*(i-1);
        break;
    end
end
B2_I4_left = 0;
for i=2:N4
    if (I4(i-1) >= N_B2*A2_I4) && (I4(i) < N_B2*A2_I4)
        B2_I4_left = dX*(i-1);
        break;
    end
end

% calculate B2_right for each I1-I4
B2_I1_right = 0;
for i=(dT/2):N1
    if (I1(i-1) < N_B2*A2_I1) && (I1(i) >= N_B2*A2_I1)
        B2_I1_right = dX*i;
        break;
    end
end
B2_I2_right = 0;
for i=(dT/2):N2
    if (I2(i-1) < N_B2*A2_I2) && (I2(i) >= N_B2*A2_I2)

```

```

        B2_I2_right = dX*i;
        break;
    end
end
B2_I3_right = 0;
for i=(dT/2):N3
    if (I3(i-1) < N_B2*A2_I3) && (I3(i) >= N_B2*A2_I3)
        B2_I3_right = dX*i;
        break;
    end
end
B2_I4_right = 0;
for i=(dT/2):N4
    if (I4(i-1) < N_B2*A2_I4) && (I4(i) >= N_B2*A2_I4)
        B2_I4_right = dX*i;
        break;
    end
end

% calculate B2 for each I1-I4
B2_I1 = B2_I1_right - B2_I1_left;
B2_I2 = B2_I2_right - B2_I2_left;
B2_I3 = B2_I3_right - B2_I3_left;
B2_I4 = B2_I4_right - B2_I4_left;

% calculate dB for each I1-I4
dB_I1 = 100*(B1_I1 - B2_I1)/B1_I1;
dB_I2 = 100*(B1_I2 - B2_I2)/B1_I2;
dB_I3 = 100*(B1_I3 - B2_I3)/B1_I3;
dB_I4 = 100*(B1_I4 - B2_I4)/B1_I4;

disp( '1st object' );
S = sprintf( '          A1, dimensionless: %5.3f', A1_I1 ); disp( S );
S = sprintf( '          A2, dimensionless: %5.3f', A2_I1 ); disp( S );
S = sprintf( '          dA, %: %5.2f', dA_I1 ); disp( S );
S = sprintf( '          B1_left, um: %5.2f', B1_I1_left ); disp( S
);
S = sprintf( '          B1_right, um: %5.2f', B1_I1_right ); disp( S
);
S = sprintf( '          B1, um: %5.2f', B1_I1 ); disp( S );
S = sprintf( '          B2_left, um: %5.2f', B2_I1_left ); disp( S
);
S = sprintf( '          B2_right, um: %5.2f', B2_I1_right ); disp( S
);
S = sprintf( '          B2, um: %5.2f', B2_I1 ); disp( S );
S = sprintf( '          dB, %: %5.2f', dB_I1 ); disp( S );
disp( '2nd object' );
S = sprintf( '          A1, dimensionless: %5.3f', A1_I2 ); disp( S );
S = sprintf( '          A2, dimensionless: %5.3f', A2_I2 ); disp( S );
S = sprintf( '          dA, %: %5.2f', dA_I2 ); disp( S );
S = sprintf( '          B1_left, um: %5.2f', B1_I2_left ); disp( S
);
S = sprintf( '          B1_right, um: %5.2f', B1_I2_right ); disp( S
);
S = sprintf( '          B1, um: %5.2f', B1_I2 ); disp( S );

```

```

S = sprintf( '                B2_left, um: %5.2f', B2_I2_left ); disp( S
);
S = sprintf( '                B2_right, um: %5.2f', B2_I2_right ); disp( S
);
S = sprintf( '                B2, um: %5.2f', B2_I2 ); disp( S );
S = sprintf( '                dB, %: %5.2f', dB_I2 ); disp( S );
disp( '3rd object' );
S = sprintf( '                A1, dimensionless: %5.3f', A1_I3 ); disp( S );
S = sprintf( '                A2, dimensionless: %5.3f', A2_I3 ); disp( S );
S = sprintf( '                dA, %: %5.2f', dA_I3 ); disp( S );
S = sprintf( '                B1_left, um: %5.2f', B1_I3_left ); disp( S
);
S = sprintf( '                B1_right, um: %5.2f', B1_I3_right ); disp( S
);
S = sprintf( '                B1, um: %5.2f', B1_I3 ); disp( S );
S = sprintf( '                B2_left, um: %5.2f', B2_I3_left ); disp( S
);
S = sprintf( '                B2_right, um: %5.2f', B2_I3_right ); disp( S
);
S = sprintf( '                B2, um: %5.2f', B2_I3 ); disp( S );
S = sprintf( '                dB, %: %5.2f', dB_I3 ); disp( S );
disp( '4th object' );
S = sprintf( '                A1, dimensionless: %5.3f', A1_I4 ); disp( S );
S = sprintf( '                A2, dimensionless: %5.3f', A2_I4 ); disp( S );
S = sprintf( '                dA, %: %5.2f', dA_I4 ); disp( S );
S = sprintf( '                B1_left, um: %5.2f', B1_I4_left ); disp( S
);
S = sprintf( '                B1_right, um: %5.2f', B1_I4_right ); disp( S
);
S = sprintf( '                B1, um: %5.2f', B1_I4 ); disp( S );
S = sprintf( '                B2_left, um: %5.2f', B2_I4_left ); disp( S
);
S = sprintf( '                B2_right, um: %5.2f', B2_I4_right ); disp( S
);
S = sprintf( '                B2, um: %5.2f', B2_I4 ); disp( S );
S = sprintf( '                dB, %: %5.2f', dB_I4 ); disp( S );
disp( '=====');
S = sprintf( '                averaged dA, %: %5.2f',
(dA_I1+dA_I2+dA_I3+dA_I4)/4 ); disp( S );
S = sprintf( '                averaged dB, %: %5.2f',
(dB_I1+dB_I2+dB_I3+dB_I4)/4 ); disp( S );
disp( '=====');

% =====
figure( 2 )
clf( 'reset' )
% =====
subplot(2,2,1)
% =====
hold on
plot( dx*(0:(N1-1)), I1, 'color', 'blue', 'LineWidth', 1 );
title( 'object cross-section (object 1)' );
xlabel( 'position, um' );
ylabel( 'intensity, dimensionless' );
axis( [0 250 0 1] ); axis on

```

```

;axis( [0 dX*(N1-1) 0 1] ); axis on
grid on
hold off

% =====
subplot(2,2,2)
% =====
hold on
plot( dX*(0:(N2-1)), I2, 'color', 'blue', 'LineWidth', 1 );
title( 'object cross-section (object 2)' );
xlabel( 'position, um' );
ylabel( 'intensity, dimensionless' );
axis( [0 250 0 1] ); axis on
;axis( [0 dX*(N2-1) 0 1] ); axis on
grid on
hold off

% =====
subplot(2,2,3)
% =====
hold on
plot( dX*(0:(N3-1)), I3, 'color', 'blue', 'LineWidth', 1 );
title( 'object cross-section (object 3)' );
xlabel( 'position, um' );
ylabel( 'intensity, dimensionless' );
axis( [0 250 0 1] ); axis on
;axis( [0 dX*(N3-1) 0 1] ); axis on
grid on
hold off

% =====
subplot(2,2,4)
% =====
hold on
plot( dX*(0:(N4-1)), I4, 'color', 'blue', 'LineWidth', 1 );
title( 'object cross-section (object 4)' );
xlabel( 'position, um' );
ylabel( 'intensity, dimensionless' );
axis( [0 250 0 1] ); axis on
;axis( [0 dX*(N4-1) 0 1] ); axis on
grid on
hold off

% =====
figure( 3 )
clf( 'reset' )
% =====
subplot(2,2,1)
% =====
hold on
plot( (0:(N1-1)), I1, 'color', 'blue', 'LineWidth', 1 );
title( 'object cross-section (object 1)' );
xlabel( 'number' );
ylabel( 'intensity, dimensionless' );

```



```

axis( [0 160 0 1] ); axis on
grid on
hold off

% =====
subplot(2,2,2)
% =====
hold on
plot( (0:(N2-1)), I2, 'color', 'blue', 'LineWidth', 1 );
title( 'object cross-section (object 2)' );
xlabel( 'number' );
ylabel( 'intensity, dimensionless' );
axis( [0 160 0 1] ); axis on
grid on
hold off

% =====
subplot(2,2,3)
% =====
hold on
plot( (0:(N3-1)), I3, 'color', 'blue', 'LineWidth', 1 );
title( 'object cross-section (object 3)' );
xlabel( 'position, um' );
ylabel( 'intensity, dimensionless' );
axis( [0 160 0 1] ); axis on
grid on
hold off

% =====
subplot(2,2,4)
% =====
hold on
plot( (0:(N4-1)), I4, 'color', 'blue', 'LineWidth', 1 );
title( 'object cross-section (object 4)' );
xlabel( 'number' );
ylabel( 'intensity, dimensionless' );
axis( [0 160 0 1] ); axis on
grid on
hold off

```

Curriculum vitae

Hamid (Harry) Aghayan (P.Eng)

Education

2007-2012 University of Western Ontario, London, ON
Degree: Ph.D. in Mechanical Engineering

2006- 2007 University of Western Ontario, London, ON
Degree: Master of Mechanical Engineering

1995 - 1999 University of Windsor, Windsor, ON
Degree: Bachelor of Applied Science
Program: Mechanical Engineering

Work experience

2008- 2011 Center of Automotive Materials & Manufacturing
Industrial Materials Institutes, National Research Council of Canada, London Ontario

Research and develop optical/lighting sensors for monitoring engine performance through engine lubricant

2004 – 2007 Premier MSS

Global Engine Manufacturing Alliance (GEMA), a joint venture of Chrysler, Hyundai and Mitsubishi Motors

Quality and manufacturing engineering

2001- 2004 East West Industrial Engineering, Windsor, Ontario

Resident engineer at Ford Motor Company, Windsor Engine Plant

1999-2001 Aerotek- Full Time Contract at Ford Motor Company

Powertrain operations, M&PE, production engineering, Livonia Transmission Plant
36200 Plymouth Rd. Box 20, Livonia, MI 48150 USA